

# ACNS 2004

*American Conference on Neutron Scattering*



SPONSORED BY THE NEUTRON SCATTERING SOCIETY OF AMERICA  
HOSTED BY THE NIST CENTER FOR NEUTRON RESEARCH

College Park, Maryland • June 6-10, 2004



# ACNS 2004

*American Conference on Neutron Scattering*

---

SPONSORED BY THE NEUTRON SCATTERING SOCIETY OF AMERICA  
HOSTED BY THE NIST CENTER FOR NEUTRON RESEARCH

**College Park, Maryland • June 6-10, 2004**

## **General Information**

The Second *American Conference on Neutron Scattering* is hosted by the NIST Center for Neutron Research, and will be held in the Inn and Conference Center for the University of Maryland University College in College Park, MD June 6-10, 2004. The conference is being organized under the auspices of the *Neutron Scattering Society of America (NSSA)* and is sponsored by the North American neutron centers. It is planned to be hosted by one of the centers every other year, in years that do not coincide with either the International Conference on Neutron Scattering or the European Conferences on Neutron Scattering. The first conference was a resounding success, being hosted by the Spallation Neutron Source-High Flux Isotope Reactor User Group at Oak Ridge National Laboratory in Knoxville, Tennessee, in June 2002.

The conference is intended to showcase recent scientific results in neutron science in a wide range of fields, including soft and hard condensed matter, biology, engineering materials and applications, chemistry and materials, fundamental physics, and developments in neutron instrumentation. This will be accomplished through a combination of invited talks (30 minutes), contributed talks (15 minutes), and poster sessions. The conference will feature the presentation of the first Cliff Shull Prize for Neutron Science to Dr. J. Michael Rowe of NIST.

The conference is also intended to fulfill many of the objectives of facility "users' meetings" but on a national scale. Presentations will be featured that highlight the present and planned capabilities of the instrumentation for users at the major neutron centers in North America and will provide a forum for users to ask questions and raise issues that relate to using these facilities.

The conference particularly encourages the participation of graduate students, postdocs, and new faculty, as well as established researchers in neutron scattering and allied disciplines. For the former groups, funds will be available to help defray travel expenses.

Additional information about the conference is available on the ACNS website at [www.ncnr.nist.gov/acns/](http://www.ncnr.nist.gov/acns/)

## **NSSA Information**

The Neutron Scattering Society of America (NSSA) was formed in 1992 and is an organization of persons who have an interest in neutron scattering research in a wide spectrum of disciplines. Membership in the society is open to individuals in academia, industry, and government. Graduate students and recent Ph.D.s are especially encouraged to join. There is no cost to be a member, and all members receive a complementary copy of *Neutron News*. The NSSA website is <http://www.neutronsattering.org>. We encourage all conference attendees to stop by the NSSA booth in the Main Concourse during the ACNS meeting.

## **NSSA Executive Committee**

President	Robert M. Briber, University of Maryland
Vice President	James D. Jorgensen, Argonne National Laboratory
Secretary	Simon Billinge, Michigan State University
Treasurer	David Belanger, University of California—Santa Cruz
Membership Secretary	Gregory Smith, Oak Ridge National Laboratory
Members at Large	Shenda Baker, Harvey Mudd College
	Susan Krueger, NIST
	Franz Trouw, Los Alamos National Laboratory

# Welcome

Welcome to the second *American Conference on Neutron Scattering!* Your enthusiastic response reflects the strength of the neutron scattering community in the U.S. and Canada. A total of 389 abstracts were received, a 40% increase over the very successful first ACNS held two years ago in Knoxville, TN. Many of these abstracts represent the research work of young scientists, including over 50 abstracts from graduate students who are competing for the first *Neutron Scattering Society of America Prize for Outstanding Student Research*, foretelling a very bright future for the field.

The papers presented in this conference show the diversity in science that is directly impacted by the use of neutron scattering including: biology, chemistry and materials, engineering/applications, instrumentation, soft matter, condensed matter physics and fundamental physics.

At this meeting, the first *Clifford G. Shull Prize in Neutron Science* will be awarded to Dr. J. Michael Rowe "for his seminal vision, leadership, and contributions to the field of neutron scattering." The NSSA is extremely pleased to be able to honor achievements in neutron scattering with both the Shull Prize and the NSSA Student Research Prize at the 2004 ACNS and we hope to continue this tradition in the future.

Organizing a meeting like this takes an enormous amount of work. We especially wish to express appreciation to the NIST Center for Neutron Research for hosting the conference. Jeff Lynn and Shenda Baker have done an outstanding job in organizing the program, Dave Belanger has handled all of the finances, and Julie Borchers has acted as the local contact for the conference. They have contributed countless hours to the myriad of details that must be gotten right to make a successful meeting. We also express appreciation to the Intense Pulsed Neutron Source at Argonne National Laboratory, the High Flux Isotope Reactor and the Spallation Neutron Source Project at Oak Ridge National Laboratory, the Manuel Lujan Center at Los Alamos National Laboratory, the Neutron Scattering Group at Brookhaven National Laboratory, the Department of Energy - Basic Energy Sciences, the Canadian National Research Council and Institute for Neutron Scattering, the University of Maryland and the National Science Foundation for generous financial support.

Most importantly, we express our appreciation to all of you for contributing such a large number of abstracts for oral presentations and posters. The presentation of great science is what makes a great meeting. There will certainly be a lot of good science presented at ACNS-2004. Enjoy the meeting!

Robert M. Briber  
President  
Neutron Scattering Society of America

Jim Jorgensen  
Vice President  
Neutron Scattering Society of America  
2004 ACNS General Chair

# Contents

1	Conference Organization
2	Transportation
2	Satellite Meetings
4	Lodging
5	Registration
5	Travel Reimbursements
5	Internet Café
6	Breakfast, Lunch and Breaks
6	Receptions and Conference Banquet
7	Neutron Scattering Tutorials
9	Awards
10	User Group Meetings
11	Breakout Sessions
11	Tour of the NIST Center for Neutron Research
11	Neutron Scattering Facilities Displays
12	Conference Exhibitors
13	Information for Presenters
14	Invited Speakers
15	Conference Overview
16	Room Layout
17	Epitome
21	Program
147	Author Index
168	Advertisements

# Conference Organization

## **Sponsors**

The ACNS has received generous support from the following sponsors:

National Science Foundation  
Department of Energy  
Argonne Intense Pulsed Neutron Source  
Brookhaven National Laboratory  
Los Alamos Manuel Lujan Neutron Scattering Center  
NIST Center for Neutron Research  
Oak Ridge High Flux Isotope Reactor  
Oak Ridge Spallation Neutron Source  
University of Maryland

## **Organizing Committee**

General Chair

James Jorgensen, Argonne National Laboratory

Co-Program Chairs

Jeffrey Lynn, National Institute of Standards and Technology  
Shenda Baker, Harvey Mudd College

NSSA President

Robert Briber, University of Maryland

NSSA Treasurer

David Belanger, University of California—Santa Cruz

*Local Contacts:*

Julie Borchers, National Institute of Standards and Technology

Robert Briber, University of Maryland

## **Program Subcommittees**

*Biology*

Joanna Krueger, University of North Carolina  
Dean Myles, Oak Ridge National Laboratory

*Chemistry and Materials*

John Larese, University of Tennessee  
Mike Crawford, Dupont  
Thomas Proffen, Los Alamos National Laboratory

*Engineering/Applications*

Aaron Krawitz, University of Missouri  
Cam Hubbard, Oak Ridge National Laboratory

*Instrumentation*

Roger Pynn, Los Alamos National Laboratory  
Kent Crawford, Oak Ridge National Laboratory  
Dan Neumann, National Institute of Standards and Technology

*Soft Matter*

Mike Kent, Oak Ridge National Laboratory  
Lee Magid, University of Tennessee  
Jyotsana Lal, Argonne National Laboratory

*Condensed Matter Physics*

Steve Nagler, Oak Ridge National Laboratory  
John Tranquada, Brookhaven National Laboratory  
Peter Gehring, National Institute of Standards and Technology

*Fundamental Physics*

John Doyle, Harvard University



# Special Thanks

The program committee, and in particular the program co-chairs, thank Alan Munter and Ronald Cappelletti for their invaluable assistance in the electronic organization of the program—abstract submission, electronic scheduling, and converting and editing the abstracts (much of which was done by suitably written macros), and editing the final program. We are grateful to Kristina Nixon for aesthetically organizing the ACNS website and keeping it up-to-date. We appreciate the prompt assistance of Jill Wessner and Tim Altenberg from the Inn and Conference Center, and we also thank Lisa Press and Sue Warren from the University of Maryland Conference Planning Office.

# Satellite Meetings

## **Conference on Polarized Neutrons in Condensed Matter Investigations (PNCMI 2004)**

<http://www.sns.gov/pncmi2004/>

*June 1 - 4, 2004* at the Renaissance Hotel in Washington, DC

This workshop is being organized by Frank Klose (SNS) with program chairs Hal Lee (SNS) and Georg Ehlers (SNS).

## **Workshop on Applications of Neutron Scattering to Energy Production and Storage**

<http://www.sns.gov/jins/nmi3/>

*June 4-5, 2004* at the Renaissance Hotel in Washington, DC

This workshop is jointly organized by the UT/ORNL Joint Institute for Neutron Sciences and the European NMI3 program, with an international scientific organizing committee coordinated by Lee Magid (University of Tennessee), Al Ekkebus (SNS) and Flavio Carsughi (University of Ancona).

# Transportation

The ACNS conference is served by three major airports, BWI, DCA and IAD. The Supershuttle (<http://www.supershuttle.com>) provides transportation to and from all major airports. **Call 1-800-BLUE VAN (258-3826) for fares and to schedule pick-up and departure times.**

Following are specific suggestions for travel to campus from these airport locations:

**Baltimore-Washington International Airport (BWI)** is located approximately 25 miles north of the university. Driving time is approximately 35 minutes. Ground transportation to College Park is available by van or taxi.

Airport Connection provides van service for about \$18.00 (discounts for more than one person traveling together). Call 1-800-284-6066 or stop at their location at the airport. Taxi service costs approximately \$35.00. Alternately, Metrobus express route B30 runs between the Greenbelt station of the Metrorail and BWI Airport. (See B30 timetable.)

**Reagan National Airport (DCA)** is located in Arlington, Virginia and about 15 miles from College Park. Travel can be slow through downtown



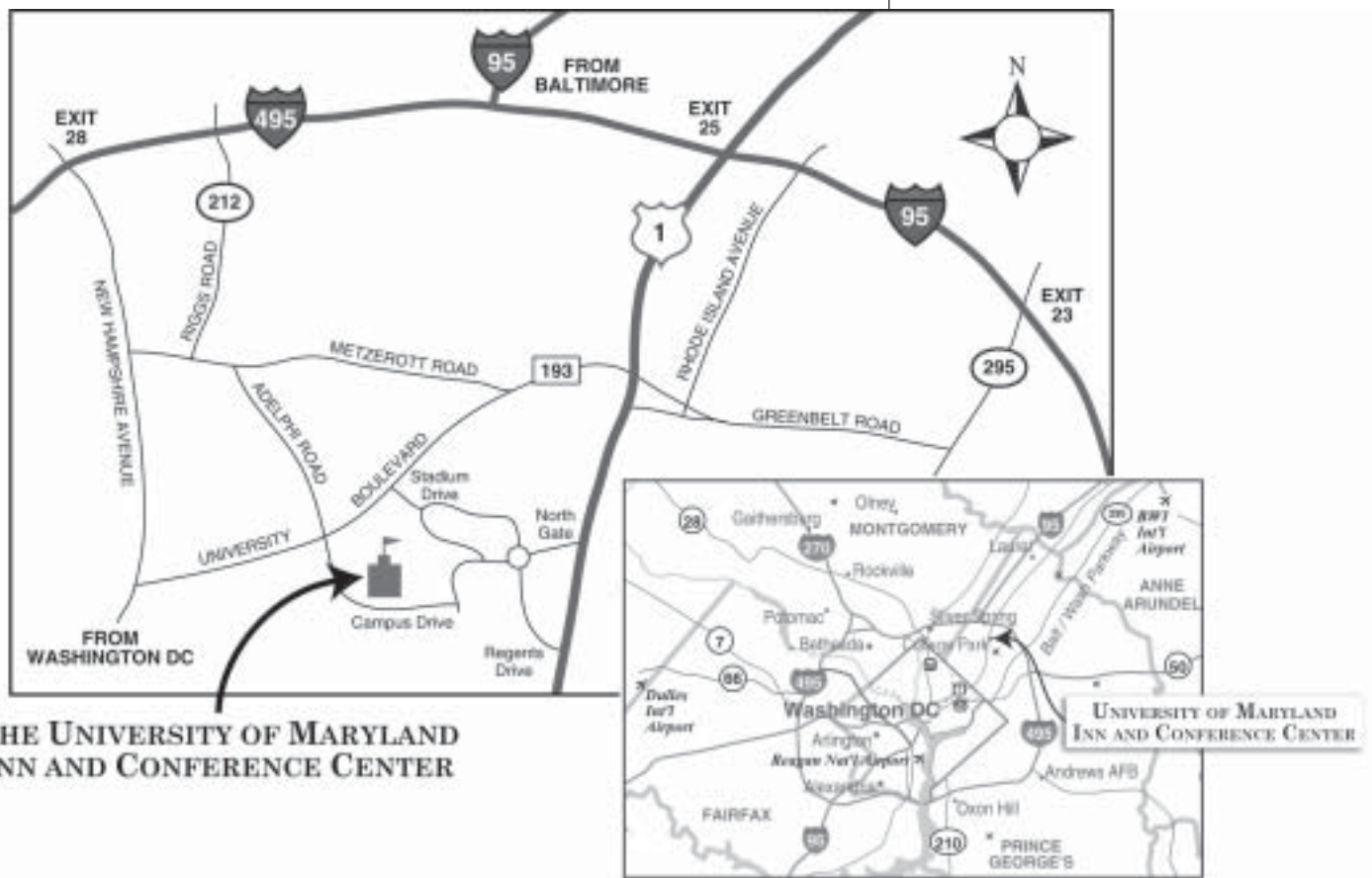
Washington, D.C. during rush hours; approximate driving time is 40 minutes.

You can take the Metrorail from Reagan airport to College Park. Taxi service directly from the airport is approximately \$40.00 one way.

**Dulles International Airport (IAD)** is located near Herndon, Virginia and is about 35 miles from College Park. Driving time is approximately one hour.

Taxi service costs approximately \$55.00 one way. Washington Flyer Taxicabs serve Dulles International Airport exclusively with 24-hour service to and from the airport. Taxicab Dispatchers are on duty 24 hours a day at the East and West ramps on the lower level of the Main Terminal. For information or to arrange transportation for your return trip, call 703-661-6655.

Washington Flyer Coach service is available to take you to the West Falls Church Metrorail station.



# Lodging

## **Inn and Conference Center**

All technical sessions will be held in the Inn and Conference Center for the University of Maryland University College in College Park, Maryland. The Center has spacious meeting facilities located in a campus setting, and includes The Garden Restaurant, Oracle Lounge, and Starbucks Coffee Shop in the Facility. A room rate of \$119/night for single or double is available at the Inn for conference attendees. All rooms are equipped with high speed internet access and other amenities. Parking is free in the garage for all conference attendees. Please tell the parking attendant that you are with the ACNS conference upon leaving the garage.

To book your stay online, follow the Hotel Accommodations link on the main webpage, click on the **Lodging at the Inn and Conference Center** webpage at [www.ncnr.nist.gov/acns/](http://www.ncnr.nist.gov/acns/), and then click on the preferred room type and select the dates of stay. To make reservations by phone, please call 1-800-228-9290 and ask for the special rate for the American Conference on Neutron Scattering (group code "ACNACNA") at the University of Maryland University College Marriott Conference Hotel.

## **On-Campus Lodging for Students only**

Located in a residence hall on-campus at the University of Maryland. Walking distance to Inn and Conference Center of 15 minutes or greater. Room occupancy ranges from 1-4 people (of the same gender) in single and double rooms and 4-8 people in suites. Roommate requests and additional nights are available upon request. Maximum of 50 students. (For additional information regarding on-campus lodging, view the Summer Guest Guide on-line at [www.umd.edu/cvs/guestguide](http://www.umd.edu/cvs/guestguide).)

Options include:

Package A: Includes 5 nights lodging (check-in Saturday, June 5th, check-out Thursday, June 10th ) Single bedroom: \$236.00, Shared double bedroom: \$200.00

Package B: (Includes 4 nights lodging (check-in Sunday, June 6th, check-out Thursday, June 10th) Single bedroom: \$189.00, Shared double bedroom: \$160.00

Campus Meal Plan: Dinner in the on-campus diner on Sunday, Monday and Wednesday. The diner is a 15-20 minute walk from residence halls. Total cost of \$33.00.

Register for On-Campus lodging by using the On-Campus On-line registration\_or by filling out the **On Campus Lodging Form (PDF)** mailing or faxing it to Conferences and Visitor Services - ACNS, University of Maryland

# Registration

Registration is available on-line at the conference website ([www.ncnr.nist.gov/acns/](http://www.ncnr.nist.gov/acns/)). On-site registration is also available. All conference attendees must register and wear their badges during the meeting. The conference registration desk is located in the Main Concourse of the Inn and Conference Center. The registration desk will be open on Sunday, June 6 from 12:00 – 19:00. On Monday through Wednesday, June 7 – 9, the desk will be open from 7:30 – 17:00. On-line registration fees are:

	On or before April 25, 2004	After April 25, 2004*
<b>Full Registration</b>	\$250.00	\$300.00
<b>Student</b>	\$100.00	\$150.00

\*On-line Registration ends May 31, 2004. After 5/31 you must register on-site – \$25 additional fee will apply.

Cancellations received on or before May 14, 2004 are fully refundable, less a \$50.00 processing fee.

- No refunds after May 14, 2004.
- All cancellations must be in writing.

All registrants will receive a badge, a copy of the program book, a complimentary copy of *Neutron News*, a list of participants, a bag with the ACNS logo, continental breakfast on Monday through Thursday, lunch on Monday through Wednesday and continuous daily refreshments.

The ACNS anticipates being able to partially support the travel expenses of some conference participants. Preference will be given to graduate students, postdocs, and junior faculty in the U.S, but others will be considered as funding permits. If you wish to request travel support, please fill out an application on the webpage. Support decisions for registrants applying by April 30 will be conveyed to applicants by May 14. Later applications will be considered as time and funds permit.

Reimbursement checks will be available during the conference at the NSSA booth in the Main Concourse. Please note that the registration fee must be paid in advance; support requests may include the registration fee.

Questions concerning travel support may be directed to Professor David Belanger at [dave@dave.ucsc.edu](mailto:dave@dave.ucsc.edu)

# Travel Reimbursements

## Internet Café

Several computers and internet connections will be available in the Main Concourse for attendees to use. In addition, wireless access (802.11b) to the internet will also be available in the main concourse.

High speed internet connections are also available in each room, and wireless access is available in Starbucks and the Oracle Lounge.

## Breakfast, Lunch and Breaks

A continental breakfast will be available in the Main Concourse each day (Monday-Thursday) of the conference starting at 7:30. Lunch will be available in the Grand Ballroom on Monday at 12:30 and in the Fort McHenry/Founders rooms on Tuesday and Wednesday at 12:30. Refreshments and snacks will be available continuously all day outside of the session rooms during the scientific sessions (Monday-Wednesday).

## Receptions and Conference Banquet

### **Sunday Evening (June 6)**

An *Evening Welcome Reception* will be held Sunday evening from 19:00–20:30 in the Founders room.

### **Monday Evening (June 7)**

A reception will be held Monday evening starting at 19:00 in the Fort McHenry/Chesapeake rooms, in tandem with the Facilities User Meetings, and will extend into the NSSA Student Research Award Poster Session. The reception will end at 21:00.

### **Tuesday Evening (June 8)**

The conference banquet will be held at the College Park Aviation Museum, an affiliate of the Smithsonian Institution, starting at 19:00. The museum is located on the grounds of the world's oldest continuously operating airport, in College Park, Maryland. Additional information about this historic site can be found at <http://www.pgparcs.com/places/historic/cpam/>

The banquet will feature several food stations with Caesar salad, penne pasta, grilled tenderloin of beef, petite pastries and other fare. Wine and beer will be served. The ticket price for the banquet is \$50.00. Tickets can be purchased online at the ACNS website or at the Registration Desk on Sunday and Monday. Buses will be available for transportation to and from the banquet. Buses will depart from the main lobby of the Inn and Conference Center beginning at 18:30.

The Museum is located at 1985 Corporal Frank Scott Drive in College Park, Maryland near the University of Maryland, between US Route 1 & Kenilworth Avenue (Route 201). To drive from the Inn and Conference Center to the Museum:

1. Start out going East on MD-193 E/UNIVERSITY BLVD E toward ADELPHI RD – 1.8 miles
2. Take the US-1 S ramp toward COLLEGE PK. – 0.1 miles
3. Turn SLIGHT RIGHT onto BALTIMORE AVE/US-1 – 0.8 miles

4. Turn LEFT onto PAINT BRANCH PKWY – 1.0 miles
5. Turn LEFT onto CORPORAL FRANK SCOTT DR.



The conference has organized three different tutorials on neutron scattering, the *NCNR Summer School Lectures*, a tutorial on *Residual Stress and Mechanical Behavior*, and a tutorial on *Pair Distribution Function (PDF) Analysis of Diffraction Data*. These sessions will start at 13:00 Sunday afternoon (June 6) and will run in parallel. The NCNR Summer School Lectures will be held in Room 2101/3/5, the tutorial on Residual Stress will be held in Room 2110 and the tutorial on Pair Distribution Function Analysis will be held in Room 2129. There is no charge for attendance, but please indicate your interest on the registration form if you want to attend one so that we will know how many people to expect. Please also note that the NCNR Summer School Lectures are required for people who are accepted into the hands-on part of the training that immediately follows the conference.

Conference registration is mandatory to attend the tutorials.

### **NCNR Summer School Lectures**

A series of introductory lectures in neutron scattering techniques and applications will be presented as part of the NIST 10<sup>th</sup> annual Summer School on Neutron Scattering. These lectures will cover fundamental concepts underlying the theory and practice of neutron scattering and are intended for those with little or no experience with the technique. They are open to anyone attending the ACNS meeting.

Topics to be covered in the Sunday tutorial lectures include:

- Fundamentals of Small-Angle Neutron Scattering  
*Charles Glinka, NIST*
- Neutron Reflectometry: Theory and Practice  
*Chuck Majkrzak, NIST*
- Methods and Applications of Neutron Spectroscopy  
*Dan Neumann, NIST*
- Membrane Diffraction  
*David Worcester, University of Missouri*

In addition to the Sunday lectures, there will be reserved space for approximately 32 participants who will continue with the hands-on part of the NCNR summer school in Gaithersburg on June 10-12, which will

# Neutron Scattering Tutorials

focus this year on SANS and Reflectometry. The summer school is organized by the Center for High Resolution Neutron Scattering that is jointly funded by the NIST Center for Neutron Research and the National Science Foundation. Travel and subsistence support is available for those attending the full summer school.

### **Introduction to Neutron Diffraction Studies of Residual Stress and Mechanical Behaviors**

Mechanical behavior and residual strain mapping have become major fields of study at nearly every neutron source. Dedicated instruments are available or under construction at most facilities. Mechanical behavior studies incorporate use of load frames and optionally furnaces on the neutron diffractometer to study the grain to grain interactions of materials as a function of load and temperature. These studies have expanded rapidly in recent years with the establishment of 2nd generation facilities such as SMARTS at Los Alamos. Engineering studies based on strain mapping are becoming more widely used by industry and academic engineers and will likely expand as international standards for such measurements are established. The tutorial aims to provide the essential information for an interested scientist or engineer to use these techniques and to understand the interrelationship between them.

Topics to be covered include:

- Introduction to the study of residual strains and mechanical behavior by neutron diffraction
- Data analysis approaches and demonstrations for handling data from reactor and spallation sources
- Role of modeling in interpreting the experimental data

Audience:

The tutorial is intended for students, faculty, and industrial scientists who are considering using neutron scattering for residual strain mapping and mechanical behavior studies. The tutorial is sponsored by the University of Tennessee's International Materials Institute (IMI) program . Advanced Neutron Scattering netWorking Education and Research (IMI-ANSWER) sponsored by NSF. Students from US institutions who need travel assistance to attend can request support by contacting Dr. Hahn Choo (hchoo@utk.edu).

### **Local Atomic Structure Using Neutron Pair Distribution Function (PDF) Analysis**

This tutorial will cover theory and practice of the study of disorder in crystals and the study of nanocrystalline materials using real-space atomic pair distribution function (PDF) techniques, with the emphasis being on PDFs obtained from neutron diffraction data. Lectures will include overview and fundamentals, experimental methods, methods of data analysis and modeling. We intend that the latter lectures will include a "walk-through" of a typical data analysis and modeling. CD's of the software and examples will be given to participants who can follow the walk-through on a laptop if available.

The tutorial will be at a level appropriate for a research-active graduate student or more senior researcher new to the subject. Please contact Simon Billinge (billinge@pa.msu.edu) or Thomas Proffen (tproffen@lanl.gov) for more information.



## NSSA Clifford G. Shull Prize in Neutron Science

The NSSA established the *Clifford G. Shull* Prize in Neutron Science to recognize outstanding research in neutron science and leadership promoting the North American neutron scattering community. The prize is named in honor of Professor Clifford G. Shull, who received the 1994 Nobel Prize in Physics with Professor Bertram Brockhouse for their seminal developments in the field of neutron science. The establishment of the prize was announced at the inaugural American Conference on Neutron Scattering in 2002.

**Purpose:** To recognize outstanding research in neutron science and leadership promoting the North American neutron scattering community.

**Nature:** The prize will consist of a plaque and an honorarium of \$5,000 to be presented at the American Conference on Neutron Scattering typically held every two years. The recipient is expected to present an address at the conference. A stipend towards travel expenses to the conference will be paid in addition to the honorarium.

**Establishment and Support:** The prize was established in 2002 and will be administered by the Neutron Scattering Society of America (NSSA.) The NSSA is currently soliciting funds from members and industrial sources toward the endowment of the prize. *Individuals or organizations wishing to contribute to the prize endowment fund should contact Prof. Dave Belanger, NSSA Treasurer, Physics Dept., University of California, Santa Cruz, CA 95064 (e-mail: dave@dave.ucsc.edu)*



Dr. J. Michael Rowe

The 2004 Clifford G. Shull Prize will be awarded to *Dr. J. Michael Rowe* at the banquet Tuesday evening, and his Lecture will be in the Monday morning plenary session in the Auditorium. He is cited "*For his seminal vision, leadership, and contributions to the field of neutron scattering.*"

Early in his career, Mike Rowe was at the forefront of research on the dynamics, structure and fundamental properties of materials, including influential work on hydrogen in metals, orientationally disordered solids and monatomic liquids. In addition, he has made significant contributions to the development of inelastic spectrometers and other instruments that utilize cold neutrons and is a leader in the design of the latest generation cold neutron sources, including the most efficient hydrogen cold



Mike Rowe (left) and Cliff Shull in 1995.

## User Group Meetings

source currently operating in the world at the NCNR. Dr. Rowe's talents and his profound impact on American neutron science go far beyond his individual contributions to research and instrumentation. Through his leadership and engineering creativity over the past 15 years, the NCNR has become the most important and widely used neutron facility thus far developed in the United States. Dr. Rowe received his PhD in 1966 from McMaster University where he worked with Nobel Laureate B.N. Brockhouse. From 1966-72 he worked at Argonne National Lab before joining the National Bureau of Standards (now NIST) in 1973.

### **NSSA Prize for Outstanding Student Research**

An NSSA Prize for Outstanding Student Research has been established by a generous private donation, and will be awarded at each ACNS meeting starting with the 2004 meeting in College Park. To qualify for the award, the student presenting their work at the ACNS must be no later than two years past their graduation date, and the work submitted for consideration must come from their thesis research. The student does not have to be a graduate.

The work must be presented in poster format at the meeting. Students should indicate during the abstract submission to the conference that they are requesting that their poster presentation be considered for the award. This will allow the student posters to be grouped together during the same poster session (scheduled for Monday Evening, June 7, in the Main Concourse).

The candidate will be asked to certify that they performed the majority of the actual neutron scattering work, and will be asked to provide contact information for their advisor. A subcommittee of the overall conference programming committee will judge the work and decide the winner. The winner will be announced during the conference banquet.

The award consists of a certificate, plaque, and \$500 cash.

The user groups from Chalk River, LANSCE, HFIR, IPNS, NCNR, and SNS will host a combined meeting in the Fort McHenry/Chesapeake rooms on Monday evening (June 7) beginning at 19:00. The user group meetings will coincide with the beginning of the Monday evening reception, which will continue into the NSSA Student Research Award Poster Session.

The goals of the user reception are to obtain feedback from neutron users on issues regarding the neutron sources and to inform users of the capabilities of various sources and actions they can take to help these sources in carrying out their mission. The reception format has been chosen to provide a more informal forum for discussions and to promote participation of the users.

The meeting will be divided into four separate groups in different areas of the Fort McHenry/Chesapeake rooms. Each group will have a different focus area for discussion:

1. Facilities – description of facilities and planned upgrades
2. Instruments – description of new and upgraded instruments

3. User Support – covering issues such as sample environment, data acquisition and analysis.
4. Administrative Issues – lobbying and user support for sources. The first three areas will be staffed by members of the participating sources while the final area will be staffed by members of the user groups.

The afternoon of Wednesday, June 9 is being set aside to accommodate Breakout Sessions requested and organized by groups that want to plan, organize and discuss specific projects such as the development of a specific neutron instrument, data collection or analysis systems, etc. The topics of the Breakout Sessions are listed in the program, and the agendas will be distributed by the session organizers. All Breakout sessions will run in parallel beginning at 15:45 in the designated rooms.

A tour of the neutron facilities of the NCNR is being organized for Thursday morning, June 10. Buses will leave the Inn and Conference Center at 8:30, after breakfast. It is about a 30 minute drive to NIST. Transportation returning to the Inn and Conference Center will be available around noon.

If you wish to visit the NCNR, please fill out the form on the ACNS webpage, as visitor clearance must be accomplished in advance of your visit. The transportation to the NCNR can also be used for those who are participating in the NCNR summer school, and if you wish to ride the bus to NIST you should sign up for the tour.

Displays from each of the neutron scattering facilities in North America will be located in the Main Concourse and available Monday-Wednesday. These facilities are the Oak Ridge National Laboratory Spallation Neutron Source and High Flux Isotope Reactor, the NIST Center for Neutron

## **Breakout Sessions**

## **Tour of the NIST Center for Neutron Research**

## **Neutron Scattering Facilities Displays**

# Conference Exhibitors

Research, Los Alamos Manuel Lujan Neutron Scattering Center, Neutron Program for Materials Research at Chalk River Laboratories, and the Argonne Intense Pulsed Neutron Source.

The ACNS will feature eleven exhibitors in the Main Concourse. Hours for the exhibits will be Monday – Wednesday (June 7–9) from 8:00 to 17:30.

Exhibitors are:

**LND, Inc.**

3230 Lawson Blvd.  
1 Oceanside, New York 11572  
<http://www.lndinc.com>

**Advanced Research Systems, Inc.**

905 Harrison St.  
Allentown PA 18103  
<http://www.arscryo.com>

**Ordela, Inc.**

Oak Ridge Detector Laboratory  
1009 Alvin Weinberg Drive  
Oak Ridge, TN 37830  
<http://www.ordela.com>

**GE Quartz and GE Advanced Ceramics**

22557 W. Lunn Road  
Strongsville, OH 44149  
<http://www.gequartz.com>  
<http://www.advceramics.com>

**CAEN and WIENER**

**WIENER, Plein and Baus, Ltd.**

300 E. Auburn Avenue  
Springfield, OH 45505  
937-324-2420  
<http://www.wiener-us.com>

**Kurt J. Lesker Co.**

1515 Worthington Avenue  
Clairton, PA 15025  
1-800-245-1656  
e-mail: [neutron@lesker.com](mailto:neutron@lesker.com)  
<http://www.lesker.com>

**SwissNeutronics  
Neutron Optical Components**

Oberes Zelgli 6  
CH-5313 Klingnau  
Switzerland  
phone: 41 56 245 0202  
fax: 41 56 245 0204  
e-mail: [tech@swissneutronics.ch](mailto:tech@swissneutronics.ch)  
<http://www.swissneutronics.ch>

**Oxford Instruments**

130A Baker Avenue Ext.  
Concord, MA 01742  
Direct: 978-369-7407 ext. 103  
Fax: 978-369-6616  
e-mail: [lonergan@ma.oxinst.com](mailto:lonergan@ma.oxinst.com)  
<http://www.oxford-instruments.com>

**CILAS / GMI**

8 avenue Buffon  
BP 6319  
45063 Orlans Cedex  
FRANCE  
<http://www.cilas.com>

**Del Mar Ventures**

4119 Twilight Ridge  
San Diego, CA 92130  
<http://www.sciner.com/>

# Information for Presenters

## Oral Presentations

Contributed oral presentations are 12 minutes with 3 minutes for questions. Invited presentations are 25 minutes with 5 minutes for questions.

Overhead projectors and LCD projectors with a switch box will be available in each room. We encourage speakers to use the LCD projectors. Speakers should bring their own laptop if possible. Each room will be equipped with a laptop with a CD-ROM and USB port and the following software installed:

- Windows 2000
- Microsoft Office 2000
- Adobe Acrobat Reader
- Windows Media Player

We prefer that all computer-based presentations be in Microsoft PowerPoint 2000 format. During the question-and-answer period of each talk, the next speaker should hook the laptop with their presentation up to the LCD switch box in preparation to begin speaking immediately. Speakers that choose to use the laptop provided by the ACNS should load their presentation onto the computer prior to the beginning of the session.

If presenters have additional technical requests, they should contact Jeff Lynn ([jeff.lynn@nist.gov](mailto:jeff.lynn@nist.gov)) or Shenda Baker ([shenda\\_baker@HMC.edu](mailto:shenda_baker@HMC.edu)) before the conference. The laptop computers available on the PC Cart in the Main Concourse will have similar software to those in the Conference areas, and will be available for speakers to check compatibility of the speaker's presentation with the available software.

## Posters

Poster sessions will be in the Main Concourse, and poster spaces will be identified by number. Posters should be available for viewing in the morning prior to the start of the oral sessions so that they are available for viewing during the entire day. The presenter should stand by the poster throughout the Poster session. Posters should be attached with push pins, which will be provided. Dimensions of the usable poster display area are about 46 inches high by 94 inches wide.

Set-up times for the posters.

**Monday evening session:** Set up no later than lunchtime on Monday

**Tuesday morning session:** Set up during breakfast time on Tuesday

**Wednesday morning session:** Set up during breakfast time on Wednesday

Posters should be taken down in the evening so that poster boards are available before the first session of the following morning.

# Invited Speakers

## Plenary Speakers:

Michael Rowe, NIST  
Robert Briber, University of Maryland  
Joel Mesot, PSI  
Thomas Mason, SNS

## Invited Speakers:

Kent Blasie, University of Pennsylvania  
Susan Krueger, NIST  
Juergen Eckert, LANL  
Raul Lobo, University of Delaware  
Simon Moss, University of Houston  
Jorge Iniguez, University of Maryland/NIST  
Jim Martin, North Carolina State University  
Alexander Kolesnikov, ANL  
Patrick Woodward, Ohio State University  
John Root, Chalk River  
Ersan Ustundag, California Institute of Technology  
Russ Hemley, Geophysical Laboratory  
Barbara Wyslouzil, Ohio State University  
Ray Osborn, ANL  
Nitash Balsara, University of California—Berkeley  
William Hamilton, ORNL  
Vivek Prabhu, NIST  
Dobrin Bossev, University of Maryland/NIST  
Janna Maranas, Pennsylvania State University  
Michel Kenzelmann, Johns Hopkins University/NIST  
Igor Zaliznyak, BNL  
Georg Ehlers, ORNL  
Yumi Ijiri, Oberlin College  
Brooks Harris, University of Pennsylvania  
Ying Chen, LANL  
Young Lee, Massachusetts Institute of Technology  
Robert McQueeney, Iowa State University/Ames Lab  
Brian Maple, University of California—San Diego  
Jack Carpenter, ANL  
Herb Mook, ORNL  
Kazu Yamada, Tohoku University  
Christopher Stock, University of Toronto  
Sergei Dzhosyuk, Harvard University  
William Hersman, University of New Hampshire  
Paul Langan, LANL

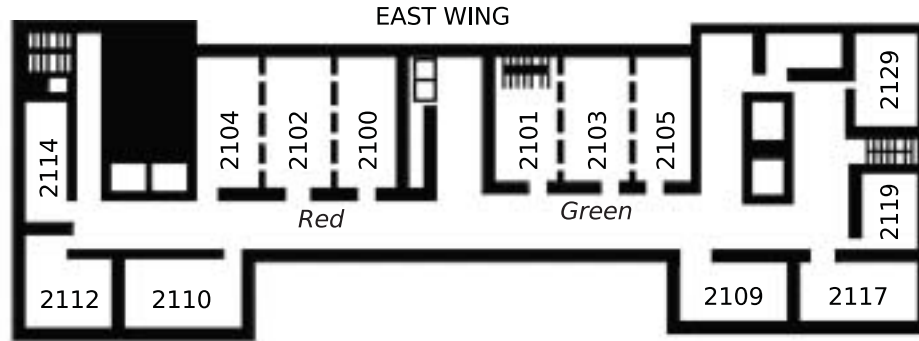


# Conference Overview

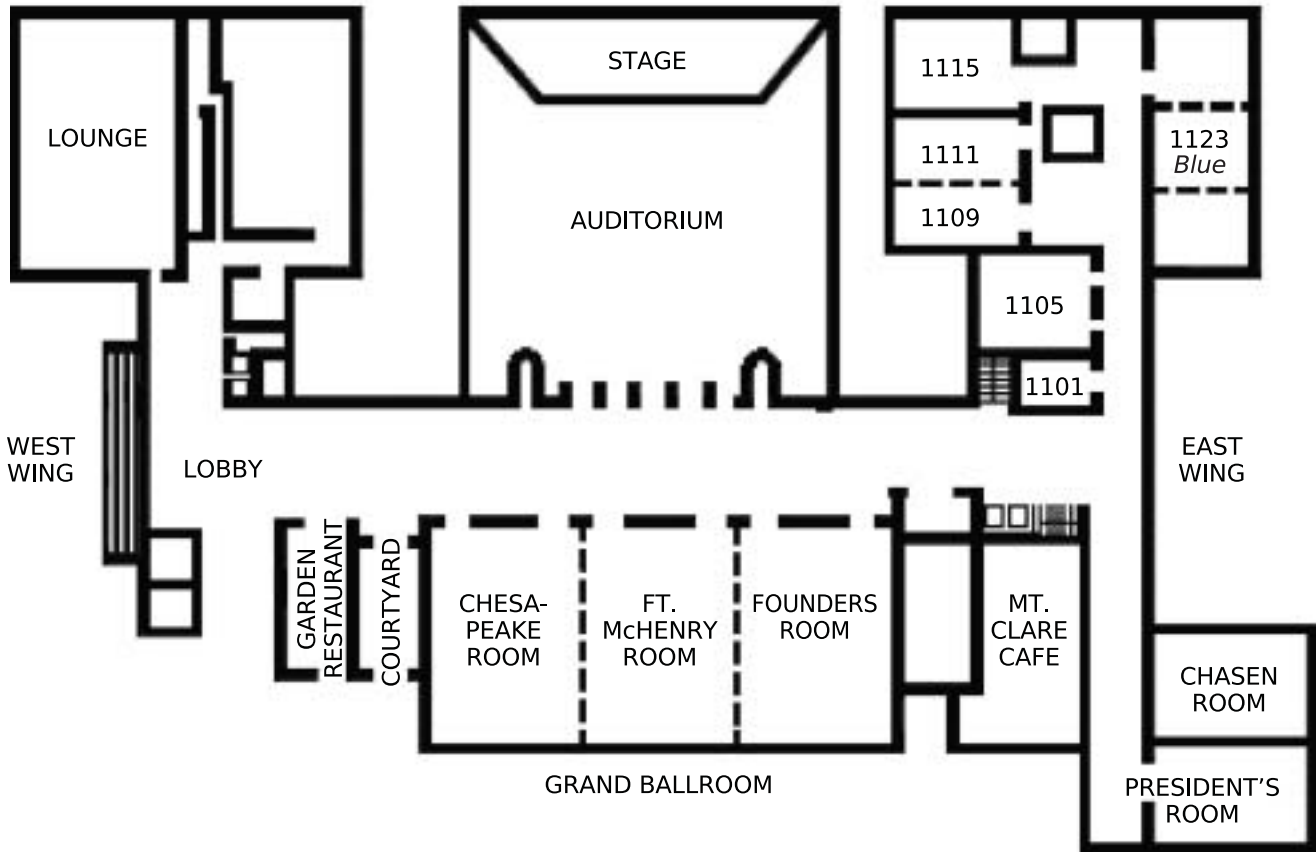
	SUNDAY	MONDAY	TUESDAY	WEDNESDAY	THURSDAY
<b>MORNINGS</b>		Continental Breakfast  Welcome and Introductions  Clifford Shull Prize Lecture  Break  Parallel Scientific Session	Continental Breakfast  Parallel Scientific Sessions  Break  Poster Session	Continental Breakfast  Neutron Plenary Session  Break  Poster Session	Continental Breakfast  Tour of the NIST Center for Neutron Research  Buses Return to Conference Center
<b>AFTERNOONS</b>	Neutron Scattering Tutorials  Conference Registration	LUNCH  Parallel Scientific Sessions  BREAK  Parallel Scientific Sessions	LUNCH  Parallel Scientific Sessions  BREAK  Parallel Scientific Sessions	LUNCH  Parallel Scientific Sessions  BREAK  Breakout Sessions	
<b>EVENINGS</b>	Welcome Reception	User Facility Meetings and Reception  Student Research Award  Poster Session	Conference Banquet	Open	

# Room Layout

SECOND FLOOR



FIRST FLOOR



## Sunday, June 6

12:00 – 19:00 **Registration** (Main Concourse)

13:00 **Neutron Scattering Tutorials**

NCNR Summer School Lectures (Room 2101/3/5 Green)

Residual Stress and Mechanical Behavior (Room 2110)

Pair Distribution Function (PDF) Analysis (Room 2129)

19:00 – 20:30 **Evening Welcome Reception** (Founders Room)

## Monday, June 7

8:30 **M1-B, Opening Session**, Chair: Robert Briber

(Auditorium)

Welcomes

Shull Prize Lecture, J. M. Rowe

10:30 **M2-A, Thin Film Magnetism**, Chair: Charles Majkrzak,

NIST (Room 2101/3/5 Green)

*Ijiri, Lee, Soriano, Kepa, O'Donovan*

10:30 **M2-B, Polymers and Surfactants**, Chair: Kent Blasie, U.

Pennsylvania (Room 2100/2/4 Red)

*Balsara, Hjelm, Mehta, Wang, Hu, Tirumala*

10:30 **M2-C, Instrumentation**, Chair: Kent Crawford, ORNL

(Auditorium)

*Osborn, Glinka, Bleuel, Barker, Ankner*

10:30 **M2-D, Zeolites and Clathrates**, Chair: Thomas Proffen,

LANL (Room 1123 Blue)

*Lobo, Nair, Hemley, Jones, Lokshin*

12:30 **Lunch** (Grand Ballroom)

13:30 **M3-A, Alloys**, Chair: Stephen Shapiro, BNL (Auditorium)

*Moss, Zarestky, Delaire, Wagner, Benson*

13:30 **M3-B, Proteins and Membranes**, Chair: Joanna Krueger,

U. North Carolina (Room 2100/2/4 Red)

*Krueger, Holt, Mihailescu, Caliskan, Bossev*

13:30 **M3-C, Ferroelectrics**, Chair: Takeshi Egami, U.

Tennessee/ORNL (Room 2101/3/5 Green)

*Stock, Ratcliff, Gehring, Vajk, Xu, Yong, Jeong*

13:30 **M3-D, Dynamics in Chemical Systems**, Chair: Dan

Neumann, NIST (Room 1123 Blue)

*Eckert, Reiter, Yildirim, Hartl, Ramirez-Cuesta, Iniguez*

15:45 **M4-A, Cuprate Superconductors**, Chair: Young Lee, MIT

(Auditorium)

*Mook, Tranquada, Mesot, Chen, Yethiraj, Yamada*

15:45 **M4-B, Neutron Properties and Interactions**, Chair:

Mohammed Arif, NIST (Room 2101/3/5 Green)

*Hersman, Fisher, Black, Gudkov, Dzhosyuk*

15:45 **M4-C, Confinement**, Chair: Paul Sokol, Penn State

(Room 1123 Blue)

*Chen, Melnichenko, Kolesnikov, Georgiev, Narehood,*

*Kintzel*

15:45 **M4-D, Polymers and Colloids**, Chair: Michael Kent,

Sandia (Room 2100/2/4 Red)

*Prabhu, Kamath, Krishnamurthy, Wang, Gopalakrishnan*

19:00 **MU, User Meetings and Reception** (McHenry/

Chesapeake Rooms)

20:00 MP, Poster Session: Student Research Award (Main Concourse) (Reception Continues)

## Tuesday, June 8

- 8:30 T1-A, Chemical Applications of SANS, Chair: Charles Glinka, NIST (Room 2101/3/5 Green)  
*Wyslouzil, Prud'homme, Krishnamurthy, Kramer*
- 8:30 T1-B, Thin Films and Membranes, Chair: Lee Magid, U. Tennessee (Room 2100/2/4 Red)  
*Blasie, Pencer, Smith, Kent*
- 8:30 T1-C, Magnetic Structures, Chair: Taner Yildirim, NIST (Room 1123 Blue)  
*Harris, Vaknin, Garlea, Arrott*
- 8:30 T1-D, Neutron Sources, Chair: Roger Pynn, LANL (Auditorium)  
*Baxter, Robinson, Greene, Russina, Carpenter*
- 10:30 TP, Poster Session II (Main Concourse)
- 12:30 Lunch (Fort McHenry/Founders)
- 13:30 T2-A, Proteins: Structure and Hydration, Chair: Dean Myles, ORNL (Room 2100/2/4 Red)  
*Langan, Gregurick, Pivovar, Russo*
- 13:30 T2-B, Materials Chemistry, Chair: John Larese, U. Tennessee (Room 1123 Blue)  
*Livingston, Allen, Hartman, Martin, Williams, Schultz*
- 13:30 T2-C, Instrumentation, Chair: Kenneth Herwig, ORNL (Auditorium)  
*Chen, Gibson, Krist, Kampmann, Weber, Kim, Peters*
- 13:30 T2-D, Heavy Fermion Systems, Chair: Raymond Osborn, ANL (Room 2101/3/5 Green)  
*Maple, Llobet, Christianson, Nakotte, McQueeney*
- 15:45 T3-A, Charge, Orbital, and Spin Ordering in Oxides, Chair: Michael Crawford, Dupont (Auditorium)  
*Woodward, Greedan, Ye, Chatterji, James, Rosenkranz*
- 15:45 T3-B, Polymer Dynamics, Chair: Jyotsana Lal, ANL (Room 2100/2/4 Red)  
*Maranas, Soles, Sung, Taub, Yardimci*
- 15:45 T3-C, Mechanical Behavior and Residual Stress, Chair: Camden Hubbard, ORNL (Room 1123 Blue)  
*Ustundag, Saleh, Gnaeupel-Herold, Wang, Kulkarni, McDaniel*
- 19:00 TB, Banquet at College Park Aviation Museum (Buses depart Inn starting at 18:30)

## Wednesday, June 9

- 8:30 W1-A, Neutron Sources (Plenary), Chair: Michael Rowe, NIST (Auditorium)  
*Briber, Mesot, Mason*
- 10:30 WP, Poster Session III (Main Concourse)
- 12:30 Lunch (Fort McHenry/Founders)

- 13:30 W2-A, Mechanical Behavior and Residual Stress**, Chair: Henry Prask, NIST (Room 1123 Blue)  
*Root, Brown, Ruiz-Hervias, Wagner*
- 13:30 W2-B, Lipids and Micelles**, Chair: Shenda Baker, Harvey Mudd (Room 2100/2/4 Red)  
*Hamilton, Gerber, Doshi, Prud'homme*
- 13:30 W2-C, Cobaltates**, Chair: James Jorgensen, ANL (Auditorium)  
*Lee, Huang, Avdeev, Zaliznyak*
- 13:30 W2-D, Low Dimensional Magnetism**, Chair: Stephen Nagler, ORNL (Room 2101/3/5 Green)  
*Ehlers, Matan, Zhang, Masuda, Zheludev, Kenzelmann*
- 15:45 W3-A, Breakout Sessions**, Chair: Shenda Baker, Harvey Mudd
- W3-A1, Perspectives for Neutron Scattering of Biomembrane Systems** (Auditorium)  
*Organizers: Loesche, White, Tobias, Blaise*
- W3-A2, Use of Depleted U Targets at Low and Medium Power Spallation Source** (Auditorium)  
*Organizers: Rhyne, Teller*
- W3-A3, SNS Magnetism Reflectometer** (Room 2100 Red)  
Organizer: Klose (SNS)
- W3-A4, Portable Software for Neutron Scattering** (Room 1123 Blue)  
*Organizers: Worlton, Mikkelson, Peterson*
- W3-A5, Doing Science with Neutron Scattering Data** (Room 1123 Blue)  
*Organizers: Fultz, Wang*
- W3-A6, Sample Environment at Neutron Scattering Facilities** (Room 2102 Red)  
*Organizers: Volin, Dender, J. S. Fieramosca, Santodonato*
- W3-A7, Fermi Chopper spectrometers for the SNS** (Room 2104 Red)  
*Organizers: Abernathy, Fultz, Granroth, Nagler*
- W3-A8, VISION, A Neutron Vibrational Spectrometer for SNS** (Room 2101 Green)  
*Organizers: Larese, Hudson, Daemen*
- W3-A9, Detectors and SCD for SNS** (Room 2103 Green)  
*Organizers: Hoffmann, Bau, Koetzle, Schultz*
- W3-A10, HYSPEC: A Novel Direct Geometry Polarized Beam Inelastic Instrument for the SNS** (Room 2105 Green)  
*Organizers: Hagen, Shapiro, Zaliznyak*

## Thursday, June 10

**Morning Visit to the NIST Center for Neutron Research**  
(Buses depart the Inn at 8:30)



# Program



# Sunday

12:00 – 19:00, **Registration** (Main Concourse)

## 13:00, Neutron Scattering Tutorials

NCNR Summer School Lectures (Room 2101/3/5)  
Residual Stress and Mechanical Behavior (Room 2110)  
Pair Distribution Function (PDF) Analysis (Room 2129)

19:00 – 20:30, **Evening Welcome Reception**  
(Founders Room)

# Monday

## M1-B, Shull Prize Lecture, Chair: Robert Briber (U. Maryland), Auditorium

M1-B1 (08:30) **Welcome**  
TBA

## M1-B2 (09:00) Forty Years of Neutron Scattering – a Personal View (Plenary)

*J. M. Rowe (NIST Center for Neutron Research; Clifford G. Shull Prize Lecture)*

This talk will present a personal view of the trends in neutron research over the past 40 years, illustrated by examples from the author's own research interests and management activities. It will include a brief history of neutron source development in the USA, as seen by an inveterate committee member. The development of the NIST Center for Neutron Research will be discussed in some detail, particularly as it relates to new science opportunities and user activity.

## M2-A, Thin Film Magnetism, Chair: Charles Majkrzak (NIST), Room 2101/3/5 Green

M2-A1 (10:30) **Neutron scattering studies of exchange bias in  $\text{Fe}_3\text{O}_4/\text{CoO}$  epitaxial thin films (Invited)**

*Y. Ijiri (Department of Physics and Astronomy, Oberlin College, Oberlin, OH 44074)*

In recent years, there has been much interest in understanding and manipulating two-component magnetic systems that exhibit the phenomenon of *exchange biasing*. First discovered in the 1950s, the effect typically refers to the *biasing* or shift of the hysteresis loop of a ferromagnetic (F) material due to *exchange* interactions with an antiferromagnetic (AF)

material. Despite extensive work and its technological importance in data storage, many questions remain concerning the microscopic mechanisms, and as a result, there is a significant need for experiments designed to characterize the nature of the interfacial spins (F and AF) in buried interfaces.

Neutron scattering work in this area has provided important insights into exchange bias. In particular, in this talk, I will describe our results in investigating the spin structures in a series of exchange-biased  $\text{Fe}_3\text{O}_4/\text{CoO}$  epitaxial thin films. Focusing on the AF CoO spins, we have observed new easy axes distinct from bulk behavior and in addition, an increase in the effective ordering temperature ( $\sim T_N$ ) for decreasing CoO thickness. At the same time, we have also found an unusual perpendicular coupling of the AF and F spins in this system. The field and temperature dependencies of the spin structures exhibit strong correlations to the macroscopic biasing phenomenon. In particular, the perpendicular coupling arrangement of the AF and F spins *freezes in* at the blocking temperature ( $T_b$ ) below which exchange biasing is observed. These results are interpreted with a model for biasing that highlights the role of anisotropic exchange, as first proposed by Dzyaloshinsky and Moriya.

This work has been done in collaboration with J.A. Borchers and R.W. Erwin (NIST), P.J. van der Zaag (Philips), and T.C. Schulthess (Oak Ridge National Laboratory).

## M2-A2 (11:00) Magnetic coupling across antiferromagnetic layer in exchange-bias Co/FeMn/Py trilayer

*W.T. Lee (Spallation Neutron Source, Oak Ridge National Laboratory), G.P. Felcher (Materials Science Division, Argonne National Laboratory), F.Y. Yang (Department of Physics, Ohio State University), F. Zhu, C.L. Chien (Department of Physics & Astronomy, Johns Hopkins University)*

Polarized neutron reflectometry (PNR) and magnetization measurements were used to study an unusual magnetic behavior found in trilayers of Co/FeMn/Py, where the soft ferromagnet permalloy and the hard magnet Co were separated by an antiferromagnet (AF) FeMn layer of thickness  $t$ . Each sample was studied for the effects of two different field-cooling procedures: The trilayer was initially subjected to a magnetic history at 425K, which is above the FeMn Neel temperature  $T_N$ , such that the Co and Py magnetization were either (1) parallel or (2) opposite to each other in the field-cooling field. After field-cooled the sample below  $T_N$  to room temperature, the measure-

ment field was applied along the field-cooling axis. We found the hysteresis loop for a film depended on its field-cooling history. In films with  $t > 90 \text{ \AA}$ , PNR studies showed that the Py and Co were magnetized collinearly to H as two independent films. The exchange-bias induced hysteresis loop shifts of the Py and Co can be individually identified. In contrast, in films with  $t < 90 \text{ \AA}$ , the Py and Co magnetic vectors formed an angle that depended on both  $t$  and  $H$ . Such angular dependence was found regardless of the field-cooling history of the trilayer. We therefore concluded that the angular dependence arose not as a result of the field-cooling procedure, or a “freezing in” of the magnetic configuration below  $T_N$ , but rather from a magnetic coupling of the Py and Co.

### M2-A3 (11:15) Magnetic behavior of epitaxial Europium thin films

*S. Soriano, K. Dumesnil, C. Dufour, T. Gourieux (L.P.M. (UMR-CNRS 7556) Universite H. Poincare, BP 239, 54506 Vandoeuvre Cedex, France), A. Stunault (Institut Laue Langevin), M. Hennion (Laboratoire Léon Brillouin, C.E.A Saclay, 91191 Gif-sur-Yvette Cedex), J. Borchers (NIST Center for Neutron Research), Ph. Mangin (L.P.M. (UMR-CNRS 7556) Universite H. Poincare, BP 239, 54506 Vandoeuvre Cedex, France; NIST Center for Neutron Research)*

We present the magnetic behavior of thin films of a very atypical rare earth, Europium, which has only recently been grown by molecular beam epitaxy along the [110] direction to form a bcc single-domain crystal[1]. In these (110) Eu films, the [001] axis lies in the growth plane, whereas the two others cubic axes ([100] and [010]) are out of the plane at  $45^\circ$  from the growth direction. Below a temperature  $T_{cl}$ , the sample is clamped to the (sapphire + niobium) substrate, which gives rise to strains  $\epsilon(T)$ .  $T_{cl}$  decreases and  $\epsilon(T)$  lowers as the europium thickness is increased. The magnetic structures have been determined using Resonant x-ray Magnetic Scattering at ESRF and neutron scattering at LLB and at the NIST Center for Neutron Research. As in bulk europium the thin films exhibit a helical magnetic ordering at  $T_N = 90 \text{ K}$  with magnetic propagation vectors along the cubic axes [100], [010] (out of the plane of the sample) and [001] (in the plane of the sample), which gives rise to three kinds of magnetic domains D1, D2 and D3 respectively. However, as the temperature is lowered two phenomena are observed:

- i) The wave vectors of the D1 and D2 domains leave the cubic directions and move closer to the [110] growth direction. They rotate of an angle  $\beta(T)$ .
- ii) The D3 domains vanish at a temperature  $T_1$  and

are only restored (and even, as in the bulk, fill then the whole sample) if a critical field  $H_c(T)$  is applied along [001].  $\beta(T)$ ,  $T_1$  and  $H_c(T)$  are shown to be correlated to the strain components  $\epsilon(T)$ , themselves related to the thicknesses of the samples. The role of the shear deformations is shown to be of prime importance. In addition, unlike in the bulk [2], it seems the magnetic transition is no longer of first order. To explain these evolutions, several mechanisms are discussed. They are based on surface dipolar effects, exchange anisotropy induced by the deformations and on magnetoelastic contributions.

[1] S. Soriano, K. Dumesnil, C. Dufour, D. Pierre (in press) Crystal Growth (2004)

[2] A.H. Milhouse, and K.A. McEwen, Solid State Com., **13**, 339-345 (1973)

### M2-A4 (11:30) Neutron scattering studies of the spin structure and magnetic domains in semiconductor superlattices

*H. Kepa (Department of Physics, Oregon State University, Corvallis, OR 97331, USA; Institute of Experimental Physics, Warsaw University, ul. Hoza 69, Warsaw, Poland), A.Yu. Sipatov (Kharkov State Polytechnic University, 21 Frunze St., Kharkov 310002, Ukraine), P. Sankowski, P. Kacman (Institute of Physics PA S and ERATO Spintronics Project, Al. Lotnikow 32/46, 02-668 Warsaw, Poland), C. F. Majkrzak (NIST Center for Neutron Research), T. M. Giebultowicz (Department of Physics, Oregon State University, Corvallis, OR 97331, USA)*

Neutron diffraction and reflectivity experiments performed on a number of magnetic semiconductor superlattices (SL), in search for interlayer coupling (IC), are reported. Antiferromagnetic (AFM) EuTe/PbTe SL and ferromagnetic (FM) EuS-based multilayers, with narrow-gap semiconductor (PbS) as well as insulating (YbSe) diamagnetic spacers, were studied. Pronounced interlayer magnetic correlations have been revealed in EuTe/PbTe by neutron diffraction, the only tool which enables such observation in AFM systems. In the FM multilayers it was proven by neutron reflectivity experiments that consecutive EuS layers are antiferromagnetically coupled. In order to determine the strength of the AFM IC in EuS-based systems, the intensity of the first magnetic SL Bragg peak vs. applied external magnetic field was measured. Finally, the in-plane anisotropy and the domain structure were studied by polarized neutron reflectivity. Despite the fourfold symmetry of the growth plane, a preferred orientation of domain magnetization directions along one of the two

possible in-plane axes ([210] and [110] for EuS/PbS and EuS/YbSe, respectively) was found.

The IC strength  $J$  and the anisotropy constant  $K$  were obtained by least-square fitting of the peak intensity vs. magnetic field experimental data to model data. The model is based on minimizing the total magnetic energy of the SL as a function of the magnetization directions. To obtain a good fit, it was necessary to take into account the interfacial roughness by assuming a Gaussian spread of  $J$ . For both EuS/PbS and EuS/YbSe SL, the best fit was obtained for the directions of the in-plane easy axes, which agree with those determined by polarized neutron reflectivity. A tight-binding theoretical model was proposed, which explains the IC phenomena in both, AFM and FM, IV-VI semiconductor SLs in terms of electronic band structure effects. This is the only model which predicts the AFM IC between EuS layers, as seen in the experiment. The model also predicts smaller strength and shorter range of IC when the EuS layers are separated by YbSe instead of PbS, in qualitative agreement with the fitted  $J$  values.

#### **M2-A5 (11:45) Polarized neutron reflectivity on CoFeO<sub>x</sub> exchange springs for spin valve applications**

*K. V. O'Donovan (NIST Center for Neutron Research; University of Maryland, College Park and University of California, Irvine), J. A. Borchers (NIST Center for Neutron Research), S. Maat, M. J. Carey, B. A. Gurney (Hitachi Global Storage Technologies)*

Modern hard disk reading heads employ spin valves, which are multicomponent magnetic films with two independent ferromagnetic layers. Most spin valves use a metallic antiferromagnet, such as PtMn, to pin one of the ferromagnetic layers. Use of an insulating biasing layer can be advantageous because it pins without shunting the current, which leads to higher giant magnetoresistance (GMR) values, thus providing greater readback sensitivity to the recorded data. One promising candidate is ferrimagnetic cobalt ferrite (CoFe<sub>2</sub>O<sub>4</sub>), which pins the neighboring ferromagnetic layer through an exchange-spring mechanism.<sup>1</sup> Recently, we grew a CoFe<sub>2</sub>O<sub>4</sub>/Co/Cu/Co/NiFe spin valve that shows high GMR, excellent pinning and good free-layer properties. To optimize the performance of this structure, we have examined the field-dependent switching of the individual layers using polarized neutron reflectometry (PNR). Measurements of the reflectivity from the front and back of these films can be used to discern noncollinear magnetism, in which the direction of magnetization changes by several degrees over a depth of a few nanometers. Our measurements on a CoFe<sub>2</sub>O<sub>4</sub>(50.0

nm)/CoFe<sub>10</sub>(6.0 nm)/Ta(10.0 nm) sample confirm that the hard ferrimagnetic CoFe<sub>2</sub>O<sub>4</sub> layer and the soft ferromagnetic CoFe layer are coupled together in applied fields ranging from 0 to 900 mT. In intermediate field ranges near 54 mT, fits to the data indicate that a twist is evident in the exchange-spring as expected and it is confined mostly to the CoFe<sub>2</sub>O<sub>4</sub> layer. This surprising result contrasts with the usual expectation that the magnetic twist reside in the hard layer in the field region of reversibility. Fits suggest that the twist gradually collapses as the field is increased.

<sup>1</sup> E.F. Kneller and R. Hawig, *IEEE Trans. Magn.*, **27**, 3588 (1991).

#### **M2-B, Polymers and Surfactants, Chair: Kent Blasie (U. Pennsylvania), Room 2100/2/4 Red**

##### **M2-B1 (10:30) Searching for the Critical Nucleus in Phase Separating Polymer Blends (Invited)**

*N.P. Balsara (University of California, Berkeley; Lawrence Berkeley National Laboratory), T.J. Rappl (University of California, Berkeley)*

The initial stage of liquid-liquid phase separation in metastable blends of high molecular weight polymers was studied by time-resolved small angle neutron scattering. The large size of the polymer molecules used in this study causes chain entanglement to occur, leading to extremely slow dynamics. This enables direct examination of the initial clustering of molecules prior to macroscopic phase separation. We find that the scattering profiles are time-independent for scattering vectors ( $q$ ) larger than a critical scattering vector ( $q_c$ ). We demonstrate the relationship between the critical nucleus size ( $R_c$ ) and the critical scattering vector. The dependence of  $R_c$  on quench depth is in qualitative disagreement with all available theories on phase separation kinetics.

##### **M2-B2 (11:00) Volume transition and internal structures of small poly(N-isopropylacrylamide) microgels**

*R. P. Hjelm (Los Alamos Neutron Science Center, Los Alamos National Laboratory), X. Xia (Department of Physics, University of North Texas, Denton, TX), L. Arleth (Los Alamos Neutron Science Center, Los Alamos National Laboratory), J. Wu (Department of Chemical and Environmental Engineering, University of California, Riverside, CA), Z. Hu (Department of Physics, University of North Texas, Denton, TX)*

Monodispersed poly(N-isopropylacrylamide) (PNIPAM) nanoparticles, with the hydrodynamic radius  $R_h$  less than 50 nm at room temperature (about two orders of magnitude smaller than those



reported previously), have been synthesized in the presence of a large amount of emulsifiers. These microgel particles undergo a swollen-collapsed volume transition in an aqueous solution when the temperature is raised to around 34°C. The volume transition and structure changes of the microgel particles as a function of temperature are probed using laser light scattering and small angle neutron scattering (SANS) with the objective of determining the small particle internal structure, particle-particle and particle-solvent interactions. We find that, within the resolution of the experiments, these particles have a uniform radial cross-linker density on either side of the transition temperature, in contrast to previous reports on the heterogeneous structures of larger PNIPAM microgel particles, but in good agreement with recent reports based on computer simulations of smaller microgels. Furthermore, the particle interactions change across the transition temperature: at temperatures below the transition, the interactions appear to be described by a hard sphere contact potential, although there is evidence for a strong hard-sphere-like repulsive particle interaction; above the volume transition temperature, the potential is best described by an attractive interaction.

#### **M2-B3 (11:15) The Impact of the Molecular Structure of a Compatibilizer on the Interfacial Structure of Compatibilized Polymeric Interfaces**

*R. Mehta, S. Kamath, C.P. O'Brien, M. Lay, M.D. Dadmun (University of Tennessee)*

This talk will discuss results by our group that has centered on understanding the optimal modification of polymeric biphasic interfaces to improve their strength. Monte Carlo simulation and experimental studies indicate that copolymeric interfacial modifiers that are blocky copolymers improve the strength of polymer/polymer interfaces most effectively. This result is interpreted to indicate that these copolymers most effectively entangle with the homopolymers by the formation of doubly bound loops at the soft interface.

Additionally, neutron reflectivity has been completed to correlate this mechanical data to the structure of the copolymer/homopolymer interfaces. More specifically, the depth profiles of trilayer thin films that consist of a layer of deuterated poly(methyl methacrylate), a layer of a protonated styrene/methyl methacrylate copolymer, and a top layer of deuterated polystyrene were determined using neutron reflectivity for various copolymer architectures, ranging from alternating to random to diblock copolymers. The depth profile and interfacial characteristics of this trilayer indicate that the specific

sequence distribution of the copolymer dramatically impacts the ability of that copolymer to extend into the polymer and entangle. The data demonstrate that, for a given molecular weight and copolymer composition, the pentablock and triblock copolymers create the broadest interfaces between the copolymer and homopolymer, while random and alternating copolymers produce the narrowest. This trend agrees with the mechanical testing data and will be discussed.

#### **M2-B4 (11:30) Dispersing Single-Walled Carbon Nanotubes with Surfactants**

*H. Wang (Department of Materials Science and Engineering, Michigan Technological University, Houghton, MI 49931), W. Zhou, K. I. Winey, J. E. Fischer (Department of Materials Science and Engineering, University of Pennsylvania, Philadelphia PA 19104), D. L. Ho, E. K. Hobbie, C. Glinka (National Institute of Standards and Technology)*

We have investigated the dispersion of single walled carbon nanotubes (SWNTs) in heavy water with the surfactant Triton X-100 using primarily small angle neutron scattering. The data show that the SWNTs in this study have a large incoherent scattering cross-section, implying that they may be heavily hydrogenated due to acid treatment. The hydrogenation of SWNTs may play an important role in their dispersion with amphiphilic surfactants. The data also suggest an optimal surfactant concentration for dispersion, which we suggest results from competition between maximization of surfactant adsorption onto SWNT surfaces and a depletion interaction between SWNT bundles due to surfactant micelles. The latter effect drives SWNT reaggregation above a critical micellar volume fraction, leading to the general conclusion that the amount of surfactant, rather than its SWNT mass ratio, is the more relevant parameter in controlling dispersion. At optimal dispersion, the surfactant adsorption ratio is ca. 0.004 mol/g, comparable to previous findings.

#### **M2-B5 (11:45) Photoacid reaction-diffusion path in a chemically amplified photoresist**

*Tengjiao Hu, Ronald Jones, Eric Lin, Wen-li Wu, Dario Goldfarb, Marie Angelopoulos (NIST Polymer Division)*

Photo-generated acid molecules act as a catalyst in the deprotection of chemically amplified photoresists. The initial locations of the acid molecules provide reaction centers and the subsequent movement of these small acid molecules during a heating step defines the physical reaction paths. The spatial evolution of the reaction paths is closely related to

the overall shape of the latent image. Acid reaction-diffusion paths near the imaging edges play an important role in the line-edge roughness control, which is approaching to only a couple of nanometers in patterns created from photoresist. A few preliminary works have focused on measuring the acid diffusion coefficient in photoresists. The movement of the interface between acid feeding layer and photoresist layer has been used to indirectly infer the acid diffusion because the results are coupled with a further development process. Ion conductivity measurement overcomes this complication but still assumes a Fickian model for acid diffusion. However, there is no such a proof yet. Identifying the relationship between the evolution of microscopic reaction-diffusion paths to a macroscopic latent image is critical information for industrial applications.

A model photoresist polymer with only side groups deuterated was used in our experiment. Deprotection cleaves the deuterated parts and causes a large contrast change in neutron scattering, which can be followed in a standard small angle neutron scattering experiment. At extremely low acid concentration, the scattering provides the form factor of the diffusion path of a single acid molecule in the photoresist. Our results indicate that the acid molecules diffuse randomly in the photoresist. The overlapping and merging of several deprotection paths was studied by varying reaction time at a constant acid concentration. Our result shows a gradual merging of different deprotection paths as determined from the effective fractal dimensions of the observed deprotection volume. The fractal growth of the deprotection volume is closely related to the distribution of the deprotected monomer units and the subsequent final pattern formation after development.

**M2-B6 (12:00) USANS Investigation of Poly (N-isopropylacrylamide) Gels Prepared from Synchrotron-Radiation-Induced Polymerization in a Retrograde-Precipitation Environment**

*V. R. Tirumala (Advanced Photon Source, Argonne National Laboratory, Argonne, IL), L. Guo (Intense Pulsed Neutron Source, Argonne National Lab), G. T. Caneba (Department of Chemical Engineering, Michigan Technological University, Houghton MI 49931), D. C. Mancini (Advanced Photon Source, Argonne National Laboratory, Argonne, IL), P. Thiyagarajan (Intense Pulsed Neutron Source, Argonne National Lab), J. G. Barker (National Institute of Standards and Technology)*

Poly (N-isopropylacrylamide) belongs to the class of thermoreversible hydrogels that can respond to a change in ambient temperature with a change in

their physical characteristics. Due to their reversible response and hydrophilic behavior, hydrogels based on poly (N-isopropylacrylamide) are widely researched for applications ranging from controlled drug delivery to microfluidic valves and actuators. The stimuli-response behavior of these gels, which depends on their synthesis route, is therefore, of utmost importance. Conventional synthesis of hydrogels results in a nanoporous morphology that decreases the permeability of water and, therefore, their response rates. Gel response can thus be improved by introducing macropores into the polymer network. The morphology of the gel networks can be characterized by neutron scattering in the presence of a deuterated solvent.

We have recently prepared poly (N-isopropylacrylamide) hydrogels by a novel synchrotron-radiation-induced polymerization. The monomers were solution polymerized by exposing to x-rays from 2-BM-B bending magnet, at the Advanced Photon Source. The time of exposure affects the crosslinking density, since monomer crosslinking and polymer chain scission occur simultaneously during irradiation. The gels were also prepared above their lower critical solution temperature in water, which results in a microporous morphology that is evident only when the gels are swollen. Such unique morphology of these gels should enable them to be ultrafast in their stimuli-response. The inherent pore structure of the gels was characterized below and above their phase transition temperature by ultra-small-angle neutron scattering. The correlation length of the gel network was observed to be power-law dependent on the absorbed dose. The average pore size of the gels was also found to reversibly change by  $\sim 200 \text{ \AA}$ , depending on the monomer concentration and the absorbed dose.

*Acknowledgments:* Work at the Advanced Photon Source was supported by the Department of Energy, Office of Science, BES, under contract No. W-31-109-ENG-38. The U.S. Government retains for itself, and others acting on its behalf, a paid-up, nonexclusive, irrevocable worldwide license in said article to reproduce, prepare derivative works, distribute copies to the public, and perform publicly and display publicly, by or on behalf of the Government.

**M2-C, Instrumentation, Chair: Kent Crawford (ORNL), Auditorium**

**M2-C1 (10:30) Prospects for Single Crystal Diffuse Scattering with Elastic Discrimination (Invited)**

*R. Osborn, S. Rosenkranz (Materials Science Division, Argonne National Laboratory)*

There is growing interest in understanding complex materials in which disorder, and the nanoscale self-organization associated with it, plays an important role in their bulk properties. Examples of disorder in crystalline matrices include polaronic disorder in magnetoresistive oxides, stripe disorder in superconducting cuprates, nanodomains in ferroelectric relaxors, defect correlations in fast-ion conductors, rotational disorder in molecular solids and intercalation compounds, adsorption in microporous frameworks, and quasicrystals. Coherent diffuse scattering from single crystals, using either neutrons or x-rays, is the most powerful probe of such complex disorder. It is the only technique that can be used to determine both the local distortions around a point defect and the length scale and morphology of defect-defect correlations, i.e., the tendency for defects to cluster or self-assemble into nanoscale structures. Nevertheless, there are formidable technical difficulties both in obtaining reliable diffuse scattering data and in using it to construct models of defect structures. White-beam pulsed neutron instruments provide efficient access to the large volumes of reciprocal space that are required to model disorder accurately. However, they accomplish this without energy analysis so that static diffuse scattering is contaminated by inelastic scattering from vibrational and other dynamic processes in the sample. At present, there is no way to eliminate this inelastic signal without monochromating the incident or scattered beams, which results in a substantial loss of intensity. A proposed instrument, named Corelli, solves this problem by combining the high-efficiency of white-beam Laue diffraction with energy discrimination produced by the use of statistical choppers. The limitations of the cross-correlation method, by which the intrinsic scattering law is reconstructed from the modulated data, and the reasons for its effectiveness in this context will be discussed.

This work was performed under the support of the US Department of Energy, Office of Science, under contract no. W-31-109-ENG-38.

#### **M2-C2 (11:00) Sub-Millisecond Time-Resolved Small-Angle Neutron Scattering**

*Charles J. Glinka (NIST Center for Neutron Research), Stephan Polachowski, J. Raebiger (FZ-Juelich)*

A time-of-flight (TOF) technique at a steady state source proposed by Roland Gähler for time-resolved SANS measurements with sub-millisecond time resolution is currently being implemented on one of the 30-m SANS instruments at NIST's Center for Neutron Research. The technique, labeled TISANE by

Gähler, requires a high-speed disk chopper, preceding the instrument's pinhole collimation, to pulse the beam at a frequency that is linearly related to the frequency (10 to 1000 Hz) of an applied field at the sample. In TOF terminology, the instrument operates in the far frame-overlap regime such that neutrons from several successive pulses arrive at the detector at a particular time corresponding to a definite (sub-millisecond) time interval within the period of the applied field at the sample.

The plan for implementing TISANE on the NIST/NSF 30-m SANS instrument on guide NG-3 at the NCNR and its current status will be described along with estimates of the attainable time-resolution ( $\sim 50$   $\mu$ sec). Possible applications for the technique in macromolecular systems and structured fluids will be discussed.

#### **M2-C3 (11:15) Modulated Intensity Small Angle Neutron Scattering - MISANS**

*M. Bleuel, J. Lal, K. C. Littrell (Intense Pulsed Neutron Source, Argonne National Lab), R. Gähler (Institut Laue Langevin)*

We present MISANS, a new design of an instrument, which combines the properties of an existing Small Angle Neutron Scattering (SANS)-spectrometer at a pulsed source (SAD@IPNS) with a MIEZE-type neutron resonance spin echo (NRSE)-spectrometer. Thus the new instrument features the high NSE energy resolution for quasi-elastic measurements with a SANS q-resolution. Furthermore the MIEZE-technique allows the measurement of magnetic and spin-incoherent scattering samples as well as the use of an area detector.

The spectrometer will also take full advantage of using a pulsed source, both the spatial and the time domain will be completely scanned within one pulse, without moving parts inside the instrument. In order to archive all provided information, the planned area detector consists of time resolving scintillation photo multipliers.

#### **M2-C4 (11:30) Performance of a Thermal-Neutron Double-Crystal Diffractometer for USANS at NIST**

*J. G. Barker, C. J. Glinka, J. Moyer, M-H. Kim (NIST Center for Neutron Research), A. R. Drews (Ford Motor Company, Dearborn, MI), M. Agamalian (Spallation Neutron Source, Oak Ridge National Laboratory)*

An ultra-high-resolution, small-angle neutron-scattering (USANS) double crystal diffractometer (DCD) has been constructed at the NIST Center for Neutron Research (NCNR). The instrument uses multiple reflections from perfect single crystal silicon (220),

before and after the sample, to produce a low instrument background suitable for small angle scattering measurements. The minimum detector background to beam intensity ratio is  $5 \times 10^{-7}$ . The instrument is located on a dedicated thermal neutron beam port, utilizing 2.38 Å wavelength neutrons, producing a  $17,000 \text{ cm}^{-2}\text{s}^{-1}$  peak neutron flux at the sample. The measurement range of the instrument extends from  $3 \times 10^{-4} \text{ nm}^{-1}$  to  $0.2 \text{ nm}^{-1}$  in scattering wavevector ( $q$ ), corresponding to structure size information in materials ranging from 30 nm to 20,000 nm. If the capability of the DCD is combined with the NCNR's 30 m long pinhole type instruments covering  $0.01 \text{ nm}^{-1}$  to  $6.0 \text{ nm}^{-1}$  in  $q$ , structure in materials from 1.0 nm to 20,000 nm can be measured. The design and characteristics of the instrument, and the mode of operation, are described, and data are presented which demonstrate the instrument performance.

#### **M2-C5 (11:45) Instrument Design via Envelope Back and Spreadsheet**

*J.F. Ankner, Ch. Rehm (Spallation Neutron Source, Oak Ridge National Laboratory)*

All too often, the first recourse of the neutron instrument designer is to some sort of stochastic or Monte Carlo (MC) simulation. While very efficient at generating results, MC simulation can suffer from a deficiency of insight, failing to provide clear criteria to direct instrument design choices. This state of affairs is as unnecessary as it is unfortunate, since the modules used in MC simulation must, by definition, contain analytical descriptions of the components simulated. By abstracting out the analytical formalism, thinking a bit about the relevant phase space, and developing common-sense metrics, one can provide a framework for understanding simulation results. Further, since these computations generally consume far less time than full-blown MC, one can model phenomena, such as background scattering, that simply cannot practically be addressed via MC. We will describe our application of acceptance-diagram techniques to primary neutron optical design (including disk choppers) and present a set of phase-space simulation metrics for evaluating results. In addition, we will consider the optical characteristics of neutron scattering/emission from interior beamline surfaces, a type of secondary-source problem difficult to treat using MC. Ultimately, the surest designs arise from judicious use of both analytical and stochastic methods, the former providing a framework for understanding the latter, as well as the means for circumventing their computational limitations.

#### **M2-D, Zeolites and Clathrates, Chair: Thomas Proffen (LANL), Room 1123 Blue**

##### **M2-D1 (10:30) Structural Refinement of Disordered Zeolites Using the Pair-Distribution Function Method (Invited)**

*I. Peral (Department of Chemical Engineering, University of Delaware, Newark, DE 19716; NIST Center for Neutron Research), M.M. Martínez-Iñesta, R.F. Lobo (Department of Chemical Engineering, University of Delaware, Newark, DE 19716), T. Proffen (Los Alamos Neutron Science Center, Los Alamos National Laboratory)*

Structural disorder is a common fact in zeolite materials and the methods commonly used for the refinement of zeolite structures (Rietveld refinements and single crystal structures) are unsuitable to obtain detailed atomic information of the disordered counterparts. To address this need, we have applied the Pair Distribution Function Method (PDF), an experimental function that describes the distribution of the atomic distances of a material, to zeolite beta, an important zeolite catalyst in the petrochemical industry. Zeolite beta is a high-silica 12-ring pore zeolite containing a three-dimensional pore system. The structure of beta was conceived as an intergrowth of two crystalline (hypothetical) polytypes A and B. The pores in polytype A are arranged in an ABABAB... type configuration and in polytype B they are arranged in an ABCABC... type configuration. We were able to refine the structure of both polytypes of zeolite beta by combining refinements with the neutron and synchrotron pair distribution functions. Comparing the calculated neutron PDFs, we observe a large general improvement in the fit of the experimental neutron-PDF from the accepted structural model to our refined model as seen in the difference curves. It is, however, necessary to refine both neutron and x-ray PDFs sequentially to obtain reasonable models of the zeolite structures.

##### **M2-D2 (11:00) Methyl Rotational Tunneling Dynamics of p-xylene confined in a crystalline zeolite host**

*S. Nair (School of Chemical & Biomolecular Engineering, Georgia Tech), R. M. Dimeo, D. A. Neumann (NIST Center for Neutron Research), A. J. Horsewill (Department of Physics & Astronomy, University of Nottingham)*

The rotational tunneling of molecules, functional groups or ions is known to be a sensitive and quantitative probe of the local energetics and structure of a material. Crystalline nanoporous aluminosilicates (zeolites) are used in organic separations owing to their shape- and size-selectivity for various types of



organic sorbate molecules. This behavior is influenced by the framework-sorbate and sorbate-sorbate interactions, which determine the molecular adsorption and transport processes in the porous material. The methyl rotational tunneling spectrum of p-xylene confined in nanoporous zeolite crystals has been measured by inelastic neutron scattering (INS) and proton nuclear magnetic resonance (NMR), and analyzed to extract the rotational potential energy surfaces characteristic of the methyl groups in the host-guest complex. The number and relative intensities of the tunneling peaks observed by INS indicate the presence of methyl-methyl coupling interactions in addition to the methyl-zeolite interactions. The INS tunneling spectra from the crystals (space group  $P2_12_12_1$  with four crystallographically inequivalent methyl rotors) are quantitatively interpreted as a combination of transitions involving two coupled methyl rotors as well as a transition involving single-particle tunneling of a third inequivalent rotor, in a manner consistent with the observed tunneling energies and relative intensities. Together, the crystal structure and the absence of additional peaks in the INS spectra suggest that the tunneling of the fourth inequivalent rotor is strongly hindered and inaccessible to INS measurements. This is verified by proton NMR measurements of the spin-lattice relaxation time which reveal the tunneling characteristics of the fourth inequivalent rotor.

#### **M2-D3 (11:15) High-Pressure Neutron Scattering and the SNAP Instrument at the SNS (Invited)**

**R. J. Hemley** (*Geophysical Laboratory, Carnegie Institution of Washington, Washington, DC 20015, USA*), **John Parise** (*Departments of Geosciences and Chemistry, State University of New York, Stony Brook, NY 11794*) **Chris Tulk** (*Spallation Neutron Source and Chemical Sciences Division, Oak Ridge National Laboratory, Oak Ridge, TN 37831*) and **Hokwang Mao** (*Geophysical Laboratory*)

Research on materials under pressure is experiencing impressive growth in a number of new areas. The SNAP (Spallation Neutrons And Pressure) facility, the high-pressure instrument at the Spallation Neutron Source (SNS), is poised to capitalize on the many recent developments in the study of materials under pressure. The project involves the creation of a unique instrument that will utilize the high neutron flux of the SNS together with state-of-the-art high-pressure devices and advance the current pressure range of neutron studies well beyond present limits (tens of GPa), making possible many new classes of experiments. The facility will enable studies of a wide variety of new scientific problems involving matter under a broad range of pressures and spanning

physics, chemistry, geoscience, planetary science, materials science, and bioscience. The instrument will be designed for single-crystal and powder diffraction measurements, with a flexible detector system and space for focusing optics, ancillary on-line measurements, and sufficient area downstream for a second station. An important recent advance is the development of new K-B focusing optics for neutrons that can now produce beam sizes down to  $100 \times 100 \mu\text{m}$ . Moreover, the creation of the SNS is taking place just at a time when radically new pressure cell designs will vastly broaden the number of techniques available for routine studies of materials over a broad P-T range, to well above megabar ( $> 100 \text{ GPa}$ ) pressures, while allowing unprecedented resolution, accuracy, and sensitivity at all conditions. A new generation of large volume gem-anvil devices based on moissanite (SiC) and single crystal diamond, including new single crystal diamonds produced by chemical vapor deposition, is becoming available. In the intermediate pressure range ( $< 30 \text{ GPa}$ ), devices such as the Paris-Edinburgh and ZAP cells will be used, and high-precision measurements at lower pressures ( $\sim 1 \text{ GPa}$  range) will be done with gas apparatus. These high-pressure devices will be coupled with the high-pressure instrument to give maximum performance, with the high-pressure facility also providing core support for high-pressure activities at other instruments at the SNS.

#### **M2-D4 (11:45) Structural Distortions and Guest Dynamics of Clathrate Hydrates**

**C. Y. Jones** (*NIST Center for Neutron Research*), **I. Peral** (*NIST Center for Neutron Research; Department of Materials Science and Engineering, University of Maryland*)

Gas hydrates are water-based, natural gas-containing inclusion compounds that occur in nature in vast deposits under the ocean floor and in the arctic permafrost. (1) They belong to a larger family of inclusion compounds known as clathrate hydrates. The structure of a clathrate hydrate (CH) comprises water molecules held together by hydrogen bonds in a three-dimensional "host" network of spherical polyhedra, or cages, which contain a small "guest" molecules. Neutron powder diffraction studies of a CH ( $\text{C}_4\text{H}_8\text{O} \cdot 17\text{D}_2\text{O}$ ) with the guest tetrahydrofuran (THF) in the range (7-165) K have shown that distortions occur in the host as a function of temperature (T). (2) In particular, distortions at low T brings D atoms closer than the O atoms to the center of the cage, and indicate that changes in the specific configuration of O and D may be important in the determination of the guest-host interactions and the resulting CH properties. An explanation for the

distortions is suggested in the findings from quasielastic neutron scattering studies (QENS) of trimethylene oxide (TMO) CH, chemical formula  $C_3H_6O \cdot 17D_2O$ . (3) The QENS results show distinct regions of high-T and low-T rotational dynamics, and an activation energy for guest rotation which is higher in the high-T regime than at low T. This presentation describes recent neutron diffraction and QENS results in the range (5-260) K on the CHs of the cyclic ethers THF, TMO, and propylene oxide. A relationship between the host structural distortions and the changes in the guest dynamics is proposed.

[1] Makagon, Y. F.; Trebin, F. A.; Trofimuk, A. A.; Tsarev, V. P.; Chersky, N. V.; Dokl. Acad. Sci. USSR — Earch Sci. Sect. 1972, 196, 197-200.

[2] Jones, C. Y.; Marshall, S. L.; Chakoumakos, B. C.; Rawn, C. J.; Ishii, Y. "Structure and Thermal Expansivity of Tetrahydrofuran Deuterate Determined by Neutron Powder Diffraction." J. Phys. Chem. B 2003, 107(25), 6026-6031.

[3] Jones, C. Y.; Peral, I. "Dynamics of Trimethylene Oxide in a Structure II Clathrate Hydrate." Submitted to The American Mineralogist.

#### M2-D5 (12:00) Crystal structure of hydrogen clathrate hydrate by *in situ* high-pressure neutron diffraction

*K. A. Lokshin, Y. Zhao, D. He (Los Alamos Neutron Science Center, Los Alamos National Laboratory), W. L. Mao (Department of the Geophysical Sciences, University of Chicago, Chicago, IL 60637, USA; Geophysical Laboratory, Carnegie Institution of Washington, Washington, DC 20015, USA), H.-K. Mao, R. J. Hemley (Geophysical Laboratory, Carnegie Institution of Washington, Washington, DC 20015, USA), M. V. Lobanov, M. Greenblatt (Department of Chemistry and Chemical Biology, Rutgers University, Piscataway, NJ 08854, USA)*

New experimental setup for neutron diffraction at high hydrostatic pressure (up to 10 kbar) and in the 10-300 K temperature range was developed at LANSCE, LANL. The detailed crystal structure information was determined for hydrogen clathrate hydrate as a function of temperature and pressure for the first time. We found that hydrogen occupancy in the  $(32 + x)H_2 \cdot 136H_2O$ ,  $x = 0-12$  clathrate can be reversibly varied by changing the large (hexakaidecahedral) cage occupancy between 2 and 4 molecules, but keeping single occupancy of the small (dodecahedral) cage. Above 130-160 K the guest hydrogen molecules were found in the delocalized state, rotating around the centres of the cages. Decrease of temperature results in the rotation freezing followed by a complete localization below 50 K.

#### M3-A, Alloys, Chair: Stephen Shapiro (BNL), Auditorium

##### M3-A1 (13:30) NIST-DCS Neutron Measurements of Lattice Disorder in a dilute Ge-Si Crystal and in a Null-matrix Ni(62)-Pt Alloy Crystal (Invited)

*J.A. Rodriguez, S.C. Moss (Physics Department, University of Houston), J.L. Robertson (Oak Ridge National Laboratory), J.R.D. Copley, D.A. Neumann (NIST Center for Neutron Research), J. Major, V. Bugaev, H. Reichert, H. Dosch (Max Planck Institute fuer Metallforschung, Stuttgart)*

Using the disk chopper spectrometer (DCS) at NIST in an elastic scattering mode, we have investigated two alloy crystals: 1) a dilute alloy of Ge in Si ( $\sim 10\%$ ) and 2) a null-matrix crystal of  $0.52^{62}\text{Ni}-0.48\text{Pt}$ , so chosen ( $^{62}\text{Ni}$  has a negative scattering length) that all effects depending on the average lattice scattering (Bragg peaks and Huang diffuse scattering (HDS—due to displacement-displacement correlations) vanishes while the short-range order (SRO) and cross correlation between concentration and displacements, often called the size effect scattering (SE), are now given by the sum of the absolute values of the scattering lengths of the two components.

The Si-Ge crystal was initially studied in the (-110) plane in reciprocal space. After removing the can scattering and normalizing the data, the planar plot from this (previously determined) random alloy showed pronounced fans of diffuse scattering emanating strongly on the low angle side of the Bragg peaks. Selected asymmetric line scans confirmed our earlier SE and HDS scan (1) along  $\langle 110 \rangle$ , a sure sign that the size of Ge is larger than Si and its displacement field extends to distant neighbors. This data is currently being analysed in Stuttgart by Prof. Bugaev and his students and additional scans in the (001) plane are underway.

The null-matrix data are truly extraordinary. There are only tiny specks of Bragg peaks (useful for alignment) and absolutely no HDS about the Bragg positions. The SRO and SE scattering are quite prominent and are being analysed in real space by Rodriguez and Robertson to extract both SRO and individual species-dependent displacements for each coordination shell, and in k-space by Prof. Bugaev and his colleagues.

The results as they come out will be discussed in the context of the electronic theory of alloy phase stability, determined from data above  $T_c$ , the first order phase transition temperature.

[1] D. LeBolloc'h et al., Phys. Rev. B 63, 035204 (2001)

Research supported in Houston by the NSF on DMR-0099573

### **M3-A2 (14:00) Compositional variation of the phonon dispersion curves of bcc Fe-Ga alloys**

*J.L. Zarestky, O. Garlea (Ames Laboratory and Department of Physics and Astronomy, Iowa State University, Ames, Iowa 50011), T.A. Lograsso (Ames Laboratory, Metal and Ceramic Sciences, Iowa State University, Ames, IA 50011), C. Stassis (Ames Laboratory and Department of Physics and Astronomy, Iowa State University, Ames, Iowa 50011)*

The Fe-Ga system is of considerable scientific and technological importance<sup>(1)</sup> because it is a unique example of a ductile polycrystalline magnetostrictive alloy. Motivated by elastic constant measurements<sup>(1)</sup> which indicate that the shear elastic constant  $1/2(C_{11} - C_{12})$  decreases with increasing Gallium concentration and extrapolates to zero at approximately 26 at. % Ga, we began a systematic study of the phonon dispersion curves of these alloys as a function of concentration. The  $TA_2[110]$  transverse phonons, with polarization in the  $[1-10]$  direction, show considerable softening as the composition is varied from 10.8 to 22.5 at. % Ga. This softening occurs not only at low wave vectors ( $q$ 's) (elastic wave region) but at  $q$ 's extending to the zone boundary and is greater than expected from the difference in Fe and Ga masses. It is correlated with the large increase in magnetostriction observed in this range of compositions. The softening of the dispersion curves in other symmetry directions will also be discussed.

[1] M. Wuttig et al. - Applied Physics Letters, Vol. 80, No. 7, 1135, 2002

### **M3-A3 (14:15) Vibrational Entropy of Dilute Alloying in Vanadium Studied by Inelastic Neutron Scattering**

*O. Delaire, T. L. Swan-Wood, M. G. Kresch, B. T. Fultz (California Institute of Technology)*

Inelastic neutron scattering spectra were measured at room temperature on the LRMECS spectrometer for the dilute random substitutional alloys V(X) with X = Ni, Pd, Pt and Co, at impurity concentrations of 6 % to 7 %, and compared to that of pure vanadium. These spectra show a large stiffening of the phonon DOS when these impurities are introduced into the V host, even at these low concentrations. The experimental neutron-weighted DOS curves were inverted using a supercell Born-von Karman model coupled to an algorithm for optimizing the force-constants. From these calculations we obtained inter-atomic force-constants and DOS curves de-weighted from the

different neutron cross-sections of V and impurities. The vibrational entropy of substitutional alloying in vanadium was calculated using these inverted DOS curves. We estimate the phonon entropy of alloying in vanadium for 6.25 % Ni, Pd, or Pt, and 7 % Co respectively to be:  $-0.093 \pm 0.001 k_B/\text{atom}$ ,  $-0.136 \pm 0.001 k_B/\text{atom}$ ,  $-0.188 \pm 0.001 k_B/\text{atom}$ , and  $-0.305 \pm 0.003 k_B/\text{atom}$ . The large negative vibrational entropy of alloying observed for the V-Pt and V-Co systems is comparable to or larger than the gain in configurational entropy for a 6 % to 7 % solute concentration. The source of this stiffening is primarily an increase in the 1NN longitudinal force-constants between the impurities and the host atoms. We show that the magnitude of this effect is in good agreement with the Rose universal equation of state and elastic relaxation theories. We expect to present additional results on V(Fe, Ti, Zr) alloys of similar compositions.

### **M3-A4 (14:30) SANS Investigation and Model Description of Micromagnetism in a nano-precipitated two-phase Alloy**

*W. Wagner, J. Kohlbrecher (Paul Scherrer Institut, 5232 Villigen-PSI, Switzerland)*

Small-Angle Neutron Scattering (SANS) was applied to investigate the micromagnetic properties of an alloy with nanometer sized ferromagnetic clusters embedded in a nonmagnetic (or paramagnetic) crystalline bulk matrix. Such kind of structure establishes in the two-phase alloy of composition Cu-24at. % Ni-8at. % Fe, upon annealing segregating precipitates of a ferromagnetic Fe/Ni-rich phase embedded in a paramagnetic Cu-rich matrix. The precipitate array is governed by a pronounced  $\{100\} <110>$  rolling texture in combination with a preferential pile-up along the  $<100>$  directions, resulting in a fourfold peak-structure in the two-dimensional, nuclear and magnetic SANS pattern.

For a detailed interpretation of the magnetic SANS pattern and their response to an external field, a computer-assisted model reconstruction was performed, considering a regular three-dimensional array of magnetic clusters with variable orientation of the magnetic alignment in a thermally activated environment. These simulations prove that the magnetic moments of the precipitates are tightly bound to the easy directions, i.e. to  $<100>$ . At zero field, they are randomly distributed to all possible easy axes, whereas an external field of intermediate strength switches them into the easy axes with field parallel component, before they are forced into field-parallel alignment by a very strong field. The data are interpreted in terms of a model balancing the



magnetic anisotropy, magnetic coupling across the interfacial matrix, potential energy in an external field and thermal activation.

### **M3-A5 (14:45) Fatigue-Induced Martensitic Phase Formation and Its Deformation Behavior in a Cobalt-Based Superalloy**

*M. L. Benson, T. A. Saleh, P. K. Liaw, H. Choo (Department of Materials Science and Engineering, The University of Tennessee, Knoxville, TN 37996, USA.), M. R. Daymond (ISIS, Rutherford Appleton Laboratory), D. W. Brown (Spallation Neutron Source, Oak Ridge National Laboratory), X.-L. Wang, A. D. Stoica (Los Alamos Neutron Science Center, Los Alamos National Laboratory), R. A. Buchanan (Department of Materials Science and Engineering, The University of Tennessee, Knoxville, TN 37996, USA.), D. L. Klarstrom (Haynes International, Inc., Kokomo, IN 46904, USA.)*

ULTIMET®, a cobalt-based superalloy, is known to go through a martensitic phase transformation from a metastable face centered cubic (fcc) phase to a stable hexagonal close packed (hcp) phase during deformation at ambient temperature. *In situ* neutron diffraction measurements were performed to study the deformation behavior of ULTIMET® alloys during two types of cyclic loading tests, i.e. stress-controlled tension/tension and strain-controlled tension/compression fatigue tests. The relationship between the magnitude and sign of the applied stress (or strain), development of intergranular strains, and the evolution of deformation-induced hcp phase fractions during the fatigue testing will be discussed. Furthermore, differences in mechanical behavior between the two different types of fatigue experiments will be presented. The data obtained from these experiments will be used to explain the evolution of lattice strain in the two crystallographic orientations and in different phases during fatigue. A goal of this work is to use the information obtained to improve lifetime modeling techniques of this alloy.

*Acknowledgements:* The author acknowledges the financial support of the National Science Foundation, the Combined Research-Curriculum Development (CRCD) Programs, under EEC-9527527 and EEC-0203415, the Integrative Graduate Education and Research Training (IGERT) Program, under DGE-9987548, and the International Materials Institutes (IMI), under DMR-0231320, to the University of Tennessee, Knoxville, with Ms. M. Poats, Dr. W. Jennings, Dr. L. Goldberg, and Dr. C. Huber as contract monitors, respectively. In addition, the financial support of the Tennessee Advanced Materi-

als Laboratory (TAML), with Prof. E. W. Plummer as director, is recognized.

### **M3-B, Proteins and Membranes, Chair: Joanna Krueger (U. North Carolina), Room 2100/2/4 Red**

#### **M3-B1 (13:30) SANS Characterization of Standard Virus Particles for Clinical Diagnostic Assays (Invited)**

*S. Krueger (NIST Center for Neutron Research), I. Elashvili, C. Wick (Edgewood Chemical Biological Center, 5183 Blackhawk Road, Aberdeen Proving Ground, MD 21010-5424), C. O'Connell (Biotechnology Division, NIST, 100 Bureau Drive, Stop 8311, Gaithersburg, MD 20899-8311), D.A. Kuzmanovic (Biotechnology Division, NIST, 100 Bureau Drive, Stop 8311, Gaithersburg, MD 20899-8311; Geo-Centers, Inc, P.O. Box 68, Aberdeen Proving Ground, MD 21010-5242)*

Small angle neutron scattering (SANS) has been used to characterize the structure of wild-type and genetically modified MS2 bacterial virus (phage) by examining its physical characteristics in solution. This research was initiated in response to scientific needs from the biomedical community. Technical advances in molecular biology have made the synthesis of proteins for basic or biomedical research routine. Although artificially produced, many of these proteins are enzymatically active. In the case of some virus proteins, they also retain the ability to self-assemble into complete virus-like particles (VLPs). The inability of modern molecular biological techniques alone to identify or physically characterize these VLPs has hampered their use in vaccine development and as standards in commercially available clinical diagnostic assays.

Presently, noninfectious, genetically modified forms of the MS2 phage are commercially available for use in basic research diagnostic assays for the HIV, Ebola, Borna, Hepatitis A, C, and G, Dengue, Enterovirus, West Nile, and Norwalk viruses, among others. However these standard virus particles are not commercially available for human biomedical diagnostic assays because their physical characteristics in solution have not been measured. In this work, SANS has been coupled with a novel virus counting instrument, the Integrated Virus Detection System (IVDS) to address the scientific analytical challenges associated with this new generation of biological standards and potential vaccine carrying agents. Specifically, IVDS and the SANS contrast variation technique were employed to determine the molecular weight of the individual components of the MS2

virion (protein shell and genomic RNA) and the spatial relationship of the genomic RNA to its protein shell. Results will be shown for wild-type MS2 particles, recombinant MS2 particles containing RNA of different sizes and from different sources, and for RNA-free reconstituted MS2 capsids.

### **M3-B2 (14:00) Self Assembly of Membrane Protein Arrays**

*Stephen A. Holt (ISIS, Rutherford Appleton Laboratory), Jeremy H. Lakey, Neil Keegan (School of Cell and Molecular Biosciences, The Medical School, The University of Newcastle-upon-Tyne, NE2 4HH, United Kingdom), Sofian M. Daud (Institute for Nanoscale Science and Technology, The University of Newcastle-upon-Tyne, NE2 4HH, United Kingdom)*

High density protein arrays on solid surfaces are becoming an increasingly important component of post-genomic technologies where there is a need for protein recognition interfaces in physical devices. Uses for these layers range from protein array technology for screening of the proteome through diagnostic “point of care” devices aimed at specific protein or metabolite targets to biocompatible surfaces for nanoscale design of implant surfaces or cell culture environments. DNA arrays have become well established in the marketplace, however DNA recognition is only a one-dimensional interaction. Protein-protein recognition usually relies upon the three-dimensional fold of both components. The maintenance of tertiary structure with the correct orientation relative to the substrate is essential for a well defined protein array. The outer membrane pore forming protein OmpF from *Escherichia coli* has been used to produce protein arrays on silicon blocks that have been coated with titanium and gold. The protein has been mutated by the addition of a single cysteine residue which enables it to chemisorb to the gold substrate with the required orientation. A thiolipid is then added to the sample cell to complete the self assembling membrane mimetic at the interface. We have applied neutron reflectometry to this system to validate our models which incorporate the relative distribution of the lipids and proteins, the exclusion of water from regions of the bilayer and the overall thickness of the lipid layers and the protein. Initial modelling of the data demonstrates that the protein array has self assembled with the expected physical dimensions. Further detailed analysis of the data is currently underway.

### **M3-B3 (14:15) Determining lipid structure by neutron reflection**

*M. Mihailescu, S. White (University of California at*

*Irvine), N. Berk, C. Majkrzak (NIST Center for Neutron Research)*

Multilamellar lipid membranes from the Glycero-Phosphocholine category, deposited on solid substrate were analyzed in reflection geometry, under low hydration conditions, i.e. 0 to 95% relative humidity. The new Advanced Neutron Diffractometer/Reflectometer built and operated since September 2003, under the “Cold Neutrons for Biology and Technology” project, was employed for these investigations. The high quality of the data permitted reconstruction of the scattering length density profile of the lipid along the normal to the multi-bilayer plane, and allowed for a direct comparison with models published previously [King & White 1986]. Contrast variation by replacing H<sub>2</sub>O vapor with D<sub>2</sub>O, in the sample ambient chamber, allows for the determination of the water distribution around the lipid head-group [Wiener & White 1991]. Moreover, the degree of lipid packing order is explored, by varying number of double bonds per lipid acyl chain. The position and extensions of the double bonds are assessed. Functional data analysis methods can be used to assess statistical uncertainties of the measured profiles.

[1] G. I. King and S. H. White, *Biophys. J.* 49 : 1047 (1986)

[2] M. C. Wiener, G. I. King and S. H. White, *Biophys. J.* 60 : 568 (1991)

*Acknowledgments:* Research supported through Grant No. NIH-RR14812 from the National Center for Research and Resources, and the University of California at Irvine

### **M3-B4 (14:30) Dominant effect of solvent on protein dynamics**

*G. H. Caliskan (The University of Akron, Polymer Science Department), M. T. Cicerone (NIST Polymer Division), M. Gangoda, R. B. Gregory (Kent State University, Department of Chemistry), A. Kisliuk (The University of Akron, Polymer Science Department), I. Peral (University of Maryland, College Park), J. H. Roh, A. P. Sokolov (The University of Akron, Polymer Science Department)*

Dynamic transition in proteins and DNA is observed as a sharp increase in mean-squared displacement (MSD) of atoms at the transition temperature ( $T_D$ ). This transition is closely related to the activation of protein's functions. However, due to MSD being an integrated quantity, the origin of this transition is still not clear. Analysis of energy resolved spectra would shed light on to the origin of the dynamic transition in biological macromolecules.

We measured dynamics of protein lysozyme in various solvents, (water, glycerol, trehalose and dry state) in a broad temperature (150K to 320K) range. High Flux Back-Scattering Spectrometer, in combination with the Time-of-Flight Spectrometer at the National Institute of Standards and Technology Center for Neutron Research have been used for measurements of the spectra in a broad energy range from  $\sim 1 \mu\text{eV}$  up to  $\sim 65 \text{ meV}$ . Our measurements revealed two different relaxation processes in the accessible energy window. The fast process with the width  $\sim 2 \text{ meV}$  and is rather independent of temperature, except for the amplitude. The slow process is strongly temperature dependent, and is observed below  $\sim 0.5 \text{ meV}$ . Our results unambiguously show that the dynamic transition is caused by the slow relaxation process that moves in to  $\mu\text{eV}$  energy window. This leads to a sharp increase in the measured MSD. The slow process of the protein is strongly affected by the solvent, and it is possible to shift the  $T_D$ , by changing the solvent. Moreover,  $T_D$  observed for lysozyme in water and in glycerol appears to be close to the dynamic crossover temperatures of bulk water and bulk glycerol, respectively. No dynamic transition is observed for protein in trehalose, at least below the glass transition of trehalose. This proves the earlier idea formulated in the field that the solvents control the protein dynamics and activity. It opens a new perspective to control the bioactivity of proteins.

### **M3-B5 (14:45) Bending Rigidity of Bio-Membranes Studied by Neutron Spin-Echo Technique (Invited)**

**D. Bossev** (*University of Maryland, College Park; National Institute of Standards and Technology*), **N. Rosov** (*National Institute of Standards and Technology*)

The dynamics of multilamellar vesicles made of 1,2-Dimyristoyl-sn-Glycero-3-Phosphocholine (DMPC), is studied in the presence of cholesterol, addition of electrolyte, and as a function of temperature using Neutron Spin Echo (NSE) technique. NSE is the most direct method to monitor the thermal undulations of the lipid bilayers in solution because it is a unique scattering technique that covers the time scale of 0.01 ns to 100 ns, characteristic of these motions. We have used the Zilman-Granek approach to interpret the decay of the intermediate scattering function and to evaluate the bending modulus of elasticity,  $\kappa$ , of the lipid bilayers. To elucidate temperature effect on  $\kappa$  we have done measurements in a crystalline state of the bilayers ( $T < T_c$ ,  $T_c = 24 \text{ }^\circ\text{C}$  for DMPC) and in the liquid state ( $T > T_c$ ). The bending modulus of elasticity in a crystalline state is one order of magnitude higher than that in the liquid state whereas in a

liquid state  $\kappa$  is found to be independent of temperature. The presence of 30 % to 50 % cholesterol increases the bending modulus of elasticity of DMPC bilayers in a liquid state by a factor of 4 to 7. Presence of electrolyte (NaCl at  $0.05 \text{ mol L}^{-1}$ ) also stiffens the DMPC bilayers by a factor of 1.5 in a liquid state. Both, cholesterol and NaCl electrolyte, have a negligible effect on  $\kappa$  in a crystalline state. The results are compared to those obtained by other methods. The possible mechanisms of these effects are also discussed in the scope of DMPC bilayers structure.

### **M3-C, Ferroelectrics, Chair: Takeshi Egami (U. Tennessee/ORNL), Room 2101/3/5 Green**

#### **M3-C1 (13:30) Dynamic Properties of the Relaxors $\text{Pb}(\text{Mg}_{1/3}\text{Nb}_{2/3})\text{O}_3$ and $\text{Pb}(\text{Zn}_{1/3}\text{Nb}_{2/3})\text{O}_3$ (Invited)**

**C. Stock**, *R. J. Birgeneau, S. Wakimoto (Physics Department, University of Toronto, Toronto, Ontario, Canada), G. Shirane (Physics Department, Brookhaven National Laboratory)*

The relaxors  $\text{Pb}(\text{Mg}_{1/3}\text{Nb}_{2/3})\text{O}_3$  (PMN) and  $\text{Pb}(\text{Zn}_{1/3}\text{Nb}_{2/3})\text{O}_3$  (PZN) both exhibit a very similar dielectric response around the critical temperature  $T_c$ . Recent neutron inelastic scattering results have found a recovery of the transverse optic mode below  $T_c$  in both materials, indicating that a ferroelectric distortion exists in the unpoled state. It was widely believed that these two materials were very different based on x-ray diffraction results, which pointed to PZN as being rhombohedral at low temperatures while PMN remained cubic. Recent high-energy x-ray experiments have suggested, however, that the bulk low-temperature unit cells in both PMN and PZN are nearly cubic, and have found that the near-surface unit cell in PZN is rhombohedral. Because of this outcome, a detailed comparison of the dynamic and static properties of PMN and PZN is required in order to reveal their similarities and differences.

We present a review of neutron scattering results showing that the static and dynamic properties of PMN and PZN are very similar. We define the similarity through a comparison of the low-frequency phonons and the diffuse scattering observed in both systems. Based on these similarities we propose that these materials belong to the same universality class. We argue that the three-dimensional Heisenberg model, with cubic anisotropy, in a random field may explain many of the unusual properties observed in PMN and PZN and compare the static and dynamic properties to those of  $\text{Mn}_{0.5}\text{Zn}_{0.5}\text{F}_2$ . We also discuss results suggesting that the diffuse scattering and the anomalous damping of the optic mode can be consistently understood, and are not simply artifacts of coupling between the acoustic and optic modes.



### M3-C2 (14:00) Elucidation of a Magnetoelectric Switch

*W. Ratcliff II, S.-H Lee (NIST Center for Neutron Research), V. Kiryukhin (Department of Physics and Astronomy, Rutgers University, Piscataway, New Jersey 08854, USA), R. Erwin (NIST Center for Neutron Research), N. Hur, S.Y. Park, S.-W. Cheong (Department of Physics and Astronomy, Rutgers University, Piscataway, New Jersey 08854, USA)*

It has been recently found that a Mn based magneto-electric material develops a spontaneous electric polarization below the Neel ordering temperature. Furthermore, this spontaneous polarization can be switched through the application of a magnetic field. Several anomalies were also observed in the dielectric constant. We have performed neutron diffraction measurements on a single crystal, and have found that anomalies in the dielectric constant and the polarization are correlated with magnetic transitions induced by field or temperature. During this talk, I will present the magnetic phase diagram of this system and show how it corresponds to the spontaneous polarization and anomalies in the dielectric constant.

### M3-C3 (14:15) Neutron Diffuse Scattering from Relaxor Ferroelectrics

*P. M. Gehring (National Institute of Standards and Technology), K. Ohwada (Japan Atomic Energy Research Institute, Synchrotron Radiation Research Center (at SPring 8)), H. Hiraka (Tohoku University, Institute for Materials Research; Physics Department, Brookhaven National Laboratory), G. Y. Xu (Physics Department, Brookhaven National Laboratory), S. H. Lee (National Institute of Standards and Technology), G. Shirane (Physics Department, Brookhaven National Laboratory)*

We report measurements of the neutron diffuse scattering from a single crystal of the relaxor ferroelectric  $\text{PbZn}_{1/3}\text{Nb}_{2/3}\text{O}_5$  doped with 8%  $\text{PbTiO}_3$  (PZN-8%PT) for temperatures  $100 \text{ K} < T < 530 \text{ K}$  and electric fields  $0 \text{ kV/cm} < E < 10 \text{ kV/cm}$ . The diffuse scattering transverse to the (003) Bragg peak is strongly suppressed in the tetragonal phase at 400K for  $E = 2 \text{ kV/cm}$  applied along the [001] direction. Surprisingly, no change is observed in the diffuse scattering measured transverse to (300), even for field strengths up to 10 kV/cm. Thus the application of an external electric field in the tetragonal (ferroelectric) phase of PZN-8%PT does not produce a uniformly polarized state. This result can be understood within the context of the Hirota model of displaced or phase-shifted polar nanoregions. We also report cold neutron measurements of the diffuse scattering in  $\text{PbMg}_{1/3}\text{Nb}_{2/3}\text{O}_5$  the small-q region near

the (110) Brillouin zone center between 100 K and the Burns temperature  $T_d$  ( $\sim 620 \text{ K}$ ). A strong quasielastic component of the diffuse scattering cross section is seen near 400 K. The reciprocal space geometry of the diffuse scattering cross section measured near (100) and (110) at 100 K changes dramatically at higher temperatures, which we believe reflects the underlying chemical short range order present above  $T_d$ .

### M3-C4 (14:30) Magnetic Excitations in Hexagonal Ferroelectric $\text{HoMnO}_3$

*O. P. Vajk, J. W. Lynn (NIST Center for Neutron Research), S.-W. Cheong (Department of Physics and Astronomy, Rutgers University, Piscataway, New Jersey 08854, USA), S.B. Kim (Rutgers University), C. Broholm (Department of Physics & Astronomy, Johns Hopkins University), M. Kenzelmann (NIST Center for Neutron Research)*

Materials with both magnetic and ferroelectric order are of great interest because of their potential applications as well as the novel physics that may result from the interplay of these two phenomena. Hexagonal  $\text{HoMnO}_3$  is a frustrated antiferromagnet with a complex magnetic phase diagram as well as strong ferroelectric order. Anomalies in the dielectric constant at magnetic phase transitions have shown a coupling of the ferroelectricity to the magnetic order. We have performed neutron scattering experiments on single-crystal  $\text{HoMnO}_3$ . Order parameter measurements are used to measure the multiple magnetic phase transitions, and inelastic measurements reveal a mostly two-dimensional excitation spectrum. Details of the magnetic field, electric field, and temperature dependence of the magnetic properties will be discussed.

### M3-C5 (14:45) Decoupling of lattice distortion and ferroelectric polarization in the relaxor system PMN-xPT

*Guangyong Xu (Physics Department, Brookhaven National Laboratory), D. Viehland, J. F. Li (Department of Materials Science and Engineering, Virginia Tech., Blacksburg, VA), C. Stock (Department of Physics, University of Toronto, Toronto, Ontario, Canada), P.M. Gehring (NIST Center for Neutron Research), Z. Zhong (National Synchrotron Light Source, Brookhaven National Laboratory, Upton, NY), G. Shirane (Physics Department, Brookhaven National Laboratory)*

We present neutron and x-ray scattering measurements on the structures of lead oxide perovskite relaxor system PMN-xPT ( $\text{Pb}(\text{MgNb})\text{O}_3\text{-xPbTiO}_3$ ), which has extraordinary piezoelectric properties. The current zero field phase diagrams of PMN-xPT, and its



close analog, PZN\_xPT, share many common features. The system is in a cubic phase for T above the Curie temperature  $T_c$ . When the temperature goes below  $T_c$ , it was long believed that a structural phase transition occurs to a rhombohedral phase for small x, and tetragonal phase for large x, separated by a narrow region of monoclinic phase.

Several recent studies have now uncovered evidence of a new phase located on the rhombohedral side of the phase diagram. High energy x-ray ( $\sim 67$  keV) diffraction work by Xu et al. on pure PZN single crystals show that the (111) Bragg peak does not split below  $T_c = 410$  K, and the inside of the crystal does not have any measurable (rhombohedral) lattice distortion, providing conclusive evidence of a new phase (X). While phase X has an undistorted unit cell shape the true symmetry of the phase is still unknown. Similar behavior has also been observed in PMN-xPT series. High q-resolution neutron scattering work by Gehring et al. and Xu et al. show that PMN-10 %PT and PMN-20 %PT also transforms into phase X instead of R below  $T_c$ . However, in PMN-27 %PT, the low temperature phase was found to be rhombohedral instead of X. These results indicate that the ground state for the inside of PMN-xPT is similar to that of PZN-xPT system, i.e., phase X for small x values, and with increasing x, rhombohedral distortions develop and the system changes into a true rhombohedral phase.

Another important finding during the x-ray diffraction work on pure PZN was the existence of an “outer-layer” with different structures than the inside of the crystal. Lower energy x-rays ( $\sim 10.2$  keV) were used to study the PZN single crystal, and a rhombohedral distortion was found to exist below  $T_c$  for the outer most 10 to 50  $\mu\text{m}$  of the crystal. This naturally explains the discrepancies between earlier x-ray powder diffraction and the recent neutron and high-energy x-ray scattering results. And the fact that x-ray studies of pure PMN have not observed a rhombohedral phase could be understood if PMN represents the limiting case of phase X with a very thin outer-layer.

Despite the absence of a rhombohedral distortion in phase X, ferroelectric polar order is still present in the system. Recently, neutron inelastic scattering measurements by Wakimoto et al. of the ferroelectric soft TO phonon in pure PMN revealed that the soft mode recovers at temperatures below  $T_c \sim 213$  K. Similar measurements on PZN were later performed by Stock et al., where  $T_c \sim 410$  K. The linear relationship between the soft TO phonon energy squared and T is a clear signature of an ordered ferroelectric

phase below  $T_c$ . Phase X is a very unusual phase where ferroelectric spontaneous polarization and an undistorted lattice coexist in a free-standing crystal.

An important question concerns the origin of phase X and its relationship with the polar nanoregions (PNR). We believe that the uniform phase shift of the PNR plays an essential role in stabilizing this phase (X), by creating an energy barrier thus preventing the PNR from melting into the surrounding ferroelectric phase. The balance between this energy barrier and the coupling between the polar nanoregions and the surrounding environment determines the stable phase of the system below  $T_c$ . With higher PT concentrations, the coupling becomes stronger and eventually phase X develops into the rhombohedral phase.

[1] G. Xu, Z. Zhong, Y. Bing, Z.-G. Ye, C. Stock, and G. Shirane, *Phys. Rev. B* 67, 104102 (2003).

[2] G. Xu, D. Viehland, J. F. Li, P. M. Gehring, and G. Shirane, *Phys. Rev. B* 68, 212410 (2003).

### M3-C6 (15:00) Structure of Nano-Polar Domains in Ferroelectric $\text{KTa}_{1-x}\text{Nb}_x\text{O}_3$

G. Yong (Lafayette College), R. Erwin (NIST Center for Neutron Research), O. Svitelskiy (Lehigh University), L. A. Boatner (Oak Ridge National Laboratory), B. Hennion (Laboratoire Léon Brillouin, C.E.A Saclay, 91191 Gif-sur-Yvette Cedex), J. Toulouse (Lehigh University), S. M. Shapiro (Brookhaven National Laboratory)

The temperature-dependent diffuse neutron scattering (DS) associated with the cubic-to-tetragonal (CT) transition in single crystals of ferroelectric  $\text{KTa}_{1-x}\text{Nb}_x\text{O}_3$  (KTN) has been characterized for  $x = 0.16$  and  $0.19$ . The features of the DS are similar to those found in relaxor-ferroelectric transitions. The DS is consistent with domain wall crossings in a direction perpendicular to the domain polarization. The DS intensity and measureable domain size are maximal near the temperature where macroscopic strains and relief of extinction appear. The measured DS does not overlap the inelastic scattering from soft optic phonons. An accommodation of the sublattice strain across domain walls is able to bring the observed and calculated DS structure factors into agreement.

### M3-C7 (15:15) Direct observation of the formation of polar nano region in $\text{Pb}(\text{Mg}_{1/3}\text{Nb}_{2/3})\text{O}_3$ using neutron pair distribution function

I.-K. Jeong, T. Darling, J.-K. Lee, T. Proffen, R. H. Heffner (Los Alamos National Laboratory), J. S. Park, K. S. Hong (Seoul National Univ.), W. Dmowski (University of Tennessee), T. Egami

(University of Tennessee; Oak Ridge National Laboratory)

We studied atomistic nature of Burns temperature and formation of polar nano region (PNR) in  $\text{Pb}(\text{Mg}_{1/3}\text{Nb}_{2/3})\text{O}_3$  using neutron pair distribution function (PDF) over wide temperature range between 15 K to 1000 K. Temperature dependence PDF shows that new structural peaks develop as the temperature decreases below the Burns temperature even though the average structure remains cubic. The intensities of these new peaks increase as the temperature decreases. We expect that these new peaks are due to the formation of PNR below the Burns temperature and our result show the first direct observation of the formation of PNR below Burns temperature.

### **M3-D, Dynamics in Chemical Systems, Chair: Dan Neumann (NIST), Room 1123 Blue**

#### **M3-D1 (13:30) Applications of vibrational spectroscopy by inelastic neutron scattering to problems in heterogeneous catalysis (Invited)**

*J. Eckert (LANSCE-12, Los Alamos National Laboratory, Los Alamos, NM 87545 and Materials Research Laboratory, University of California, Santa Barbara, CA 93106)*

Neutron scattering techniques offer some particularly powerful ways of accessing issues related to molecular binding and reactions at active sites in real catalysts. This is because the low absorption cross-sections of neutrons make it relatively easy to carry out *in situ* measurements in actual reactors or other realistic sample environments. Vibrational spectroscopy by means of inelastic neutron scattering (INS) is one such application of neutrons that may be used for the study of adsorbate dynamics and thereby to identify reaction intermediates and products. Experimentally, the contrast between adsorbate and framework vibrational spectra is achieved by using molecules with strongly scattering atoms (i.e., H) relative to those in the framework, whereby access to the entire vibrational spectrum of the sorbate is provided. INS spectra can also readily be computed from any theoretical approach that gives frequencies and atomic vibrational amplitudes because of the simplicity of the interaction of the neutron with the atomic nucleus. In our application of INS spectroscopy to problems in heterogeneous catalysis we use (1) a combined experimental and theoretical approach to the study of equilibrium sorption complexes, or (2) quench a reaction carried out in a reactor ex-situ, and examine the results by placing the cold reactor directly in the INS spectrometer. I will describe a number of such studies including the sorption of methylamines in zeolite rho, the decom-

position of methane on supported metal catalysts, H spillover effects for metal clusters in zeolites, and the epoxidation of propene in  $\text{H}_2$  and  $\text{O}_2$  over Au nanoparticles supported on titania. Several important findings have emerged from these studies including direct evidence for the active species formed in the propene epoxidation with  $\text{H}_2$  and  $\text{O}_2$ . This work was carried out in collaboration with the groups of D. W. Goodman (Texas A&M University), B. C. Gates (UC Davis) and LANL colleagues L. L. Daemen, M. Hartl, and N. J. Henson. It has benefited from the use of facilities at the Manuel Lujan Jr. Neutron Scattering Center, a National User Facility funded as such by the Office of Science, U. S. Department of Energy.

#### **M3-D2 (14:00) Recent Progress in the Measurement of Proton Momentum Distributions in Hydrogen Bonded Systems**

*G. F. Reiter (Physics Department, University of Houston), J. Mayers, T. Abdul-Redah (ISIS, Rutherford Appleton Laboratory), J.C. Li (Physics Department, University of Manchester), P. Platzman (Bell Labs-Lucent Technologies)*

Recent progress in Neutron Compton Scattering (Deep Inelastic Neutron Scattering) has made possible the detailed measurement of the momentum distribution of the proton in a variety of hydrogen bonded systems. The distribution is determined almost entirely by quantum localization effects, and hence the measurements provide a detailed picture of the localizing potential. Quantum effects such as tunneling are easily observed. We will provide an overview of the method and discuss the measurements in ice, room temperature water, supercritical water, water in confined geometries, and water with acid, base and salt impurities added. The supercritical water data exhibits a dramatic tunneling motion and provides additional evidence that water near a hydrophobic surface is in the vapor, not ice phase. The impurity measurements provide a direct observation of the localization of the acid proton and base hydroxyl groups. We will also discuss the ferroelectrics KDP, DKDP and the structural spin glass RDP-ADP, in which the tunneling motion of the hydrogen bonds that hold the crystal together are an essential feature of the observed structural phase transitions.

#### **M3-D3 (14:15) The "Bucket Brigade" Mechanism of Proton Diffusion in Superprotonic Conductors**

*T. Yildirim, D. A. Neumann, T. J. Udovic (NIST Center for Neutron Research)*

Proton diffusion plays a central role in many processes ranging from the regulation of biological functions to the production of electricity in fuel cells. The renewed emphasis on developing the next

generation of portable sources of power requires the development of light weight protonic conducting materials for use as electrolytic membranes. Furthermore, understanding the atomic-scale mechanism of proton diffusion in candidate materials is necessary to optimize their performance.

First-principles computational techniques combined with neutron scattering measurements provide detailed atomistic information about proton incorporation and dynamics in these materials. Here we briefly describe inelastic (INS) and quasielastic neutron scattering measurements (QNS) on superprotonic conductors of the general formula  $\text{MHXO}_4$  ( $M = \text{Rb, Cs, X = S, Se, etc}$ ) that reveal detailed information on the proton-conduction mechanism.

QNS measurements indicate that the hydrogen dynamics is dominated by two types of reorientational jumps of H-tetrahedra. Even though such dynamical orientational disorder brings hydrogen atoms from one molecule closer to the next one, it does not result in long-range proton conduction since the motions are localized on a single tetrahedron. However, when one combines these two motions with that of the dynamically disordered hydrogen bond inferred from INS, the mechanism of proton conduction can be surmised. Namely, the protons move between two neighboring tetrahedra via dynamically disordered hydrogen bonds. The tetrahedra then reorient, allowing the protons to move to a third tetrahedron, again via the dynamically disordered hydrogen bonds. Thus the tetrahedra play the role of a “bucket brigade” by accepting a proton from an adjacent tetrahedron then turning and handing it on to the tetrahedron on the other side. On the atomic scale, superprotonic conductivity occurs in the  $\text{MHXO}_4$  family compounds due to this efficient mechanism of transporting protons through the lattice.

#### **M3-D4 (14:30) Proton dynamics in short N-H—O hydrogen bonds**

*M. Hartl, L.L. Daemen (Los Alamos National Laboratory), J. Eckert (Los Alamos National Laboratory; Materials Research Laboratory, University of California, Santa Barbara), D. Hadzi, J. Stare (National Institute of Chemistry, Hajdrihova 19, SI-1000, Ljubljana, Slovenia)*

The role of proton dynamics in determining the physical properties and chemical reactivity of systems with very short hydrogen bonds continues to attract a great deal of theoretical and experimental efforts. In principle, infrared (IR) spectroscopy is useful to extract information on proton dynamics

(particularly the X-H stretch). In practice considerable discrepancies exist between observed frequencies and intensities and the results of *ab initio* calculations. Significant broadening in short hydrogen bonds further complicates the observation of other modes and the interpretation of the spectrum. The incoherent inelastic neutron scattering (IINS) vibrational spectrum is governed by entirely different (and less complex) neutron-nucleus interactions rather than photon-electron interactions. The IINS spectrum is easier to predict quantitatively from *ab initio* calculations and does not suffer from the problems mentioned above for IR spectroscopy. Despite these fundamental advantages, vibrational spectroscopy using inelastic neutron scattering remains underutilized in the study of hydrogen bonding.

Our study focused on acid-base complexes involving N-H—O hydrogen bonds. The weak Lewis bases pyridine and 3,5-dimethylpyridine (3,5-lutidine) were complexed with a number of weak carboxylic acids: benzoic acid, 2,4-dinitrobenzoic acid, and 3,5-dinitrobenzoic acid. By varying the substituents on the pyridine or benzoic ring, we were able to tune the strength of the hydrogen bonding interaction and alter the proton dynamics in the bond in a systematic fashion. For example, in the 3,5-dinitrobenzoic acid + 3,5-lutidine complex, the proton in this very strong hydrogen bond is fully disordered between O and N with two preferred H locations each with average occupancy of 0.5 [ $d(\text{N-H}1) = 0.82 \text{ \AA}$  and  $d(\text{N-H}2) = 1.65 \text{ \AA}$ ,  $d(\text{N-H}\dots\text{O}) = 2.56 \text{ \AA}$ ]. On the other hand in 2,4-dinitrobenzoic acid + pyridine, the hydrogen bond has the same length as in the preceding complex, but the proton is at a single location near N [ $d(\text{N-H}) = 1.05 \text{ \AA}$ ,  $d(\text{N-H}\dots\text{O}) = 2.56 \text{ \AA}$ ]. We used fully deuterated reagents to synthesize the complexes, then selectively deuterated and protonated the hydrogen bond. The difference between the spectrum of the protonated and deuterated materials facilitates mode assignments. All our data were collected on the Filter Difference Spectrometer at Los Alamos National Laboratory. We will present a systematic comparison between IR and IINS data, as well as a discussion of *ab initio* modeling results.

#### **M3-D5 (14:45) An inelastic neutron scattering and *ab initio* quasi-harmonic lattice dynamics study of simple alkali hydrides.**

*A. J. Ramirez-Cuesta (University of Reading), G. D. Barrera (University of Patagonia, Argentina)*

The alkali hydrides are of great interest not only as the possibly simplest series of solids but also because of their possible use in fuel cells. Although there are several works on the lattice dynamic of lithium



hydride this is not the case for the other alkali hydrides.

Though atomistic simulations have been widely used to calculate dynamic properties of solids we found that no simple interatomic potential provides a good description of the alkali hydrides.

However, presently available computer software and hardware allowed us to carry out several *ab initio* quasiharmonic lattice dynamics calculations for these solids over a wide range of temperatures and pressures. The results presented include dispersion curves, inelastic neutron scattering spectra and temperature dependence of lattice parameters and bulk moduli of all alkali hydrides (LiH, NaH, KH, RbH and CsH) and deuterides.

### **M3-D6 (15:00) Multi-phonon scattering and Ti-induced hydrogen dynamics in sodium alanate (Invited)**

*Jorge Iniguez (NIST Center for Neutron Research; Department of Materials Science and Engineering, University of Maryland)*

We use *ab initio* methods and neutron inelastic scattering (NIS) to study the structure, energetics, and dynamics of pure and Ti-doped sodium alanate ( $\text{NaAlH}_4$ ), focusing on the possibility of substitutional Ti doping. The NIS spectrum is found to exhibit surprisingly strong and sharp two-phonon features. The calculations reveal that substitutional Ti doping is energetically possible. Ti prefers to substitute for Na and is a powerful hydrogen attractor that facilitates multiple Al—H bond breaking. Our results hint at new ways of improving the hydrogen dynamics and storage capacity of the alanates.

Work done in collaboration with Taner Yildirim (NIST), T.J. Udovic (NIST), E.H. Majzoub (SNL), M. Sulic (U. Hawaii), C.M. Jensen (U. Hawaii).

### **M4-A, Cuprate Superconductors, Chair: Young Lee (MIT), Auditorium**

#### **M4-A1 (15:45) Recent Results on Cuprate Superconductors (Invited)**

*H. A. Mook (Oak Ridge National Laboratory), Pengcheng Dai (Department of Physics and Astronomy, University of Tennessee; Oak Ridge National Laboratory)*

Neutron scattering results on the cuprate superconductors will be discussed. The emphasis will be on the most recent results on both the hole and electron doped materials. Much of the talk will concentrate on the high-energy magnetic excitations in the YBCO class of materials that have been determined using the ISIS pulsed source. These have a large part of the

total spectral weight and are present above the superconducting transition. This makes them a good candidate for the glue that establishes the electron pairing and thus the superconductivity. The hole doping dependence of these excitations will be considered.

#### **M4-A2 (16:15) Quantum Magnetic Excitations from Stripes in Cuprate Superconductors**

*J. M. Tranquada (Brookhaven National Laboratory), H. Woo (Brookhaven National Laboratory; ISIS, Rutherford Appleton Laboratory), T. G. Perring (ISIS, Rutherford Appleton Laboratory), H. Goka (IMR, Tohoku Univ.), G. D. Gu, G. Xu (Brookhaven National Laboratory), M. Fujita, K. Yamada (IMR, Tohoku Univ.)*

The nature of the electronic correlations underlying high-temperature superconductivity in layered cuprates remains a topic of contention. The parent compounds are antiferromagnetic Mott insulators. Superconductivity is achieved by doping these materials with mobile holes, and it coexists with antiferromagnetic fluctuations. In one approach to the coexistence, the holes are believed to self-organize into stripes that alternate with regions of antiferromagnetic insulator. Such an unusual electronic state would necessitate a novel mechanism of superconductivity. Measurements of magnetic excitations in superconducting  $\text{YBa}_2\text{Cu}_3\text{O}_{6+x}$  appear to pose a problem for universal applicability of the stripe picture, as they are incompatible with the predictions for a stripe system based on semiclassical spin waves. To resolve this issue, we have performed neutron scattering measurements over a wide energy range on stripe-ordered  $\text{La}_{1.875}\text{Ba}_{0.125}\text{CuO}_4$  using the MAPS spectrometer at ISIS. We find, surprisingly, that the excitation spectrum is quite similar to that found in recent studies of  $\text{YBa}_2\text{Cu}_3\text{O}_{6+x}$ , and that the semiclassical predictions are not relevant. Instead, the measurements at higher energies can be understood in terms of the quantum excitations of a two-leg antiferromagnetic spin ladder, where the ladders are defined by the charge stripes. Thus, our results provide support for theories of superconductivity based on the existence of stripes.

JMT, HW, GDG, and GX are supported by the Office of Science, U.S. Department of Energy under Contract No. DE-AC02-98CH10886.

#### **M4-A3 (16:30) Field-Induced Square Vortex Lattices in High-Temperature Superconductors**

*J. Mesot, R. Gilardi (LNS, ETHZ & PSI, Switzerland), S. P. Brown, E. M. Forgan (Univ. Birmingham, UK), A. J. Drew, S. L. Lee (Univ. St-Andrews, UK), C. D.*

*Dewhurst, R. Cubitt (Institut Laue Langevin), T. Uefuji, K. Yamada (Tohoku University)*

The interest in the vortex matter of high- $T_c$  superconductors has been renewed by the recent observations, by means of small angle neutron scattering (SANS), of square vortex lattices (VL) at high magnetic fields in  $\text{La}_{2-x}\text{Sr}_x\text{CuO}_4$  [1] and  $\text{YBa}_2\text{Cu}_3\text{O}_7$  [2]. These observations are important since a square symmetry is indicative of the coupling of the VL to a source of anisotropy in the  $\text{CuO}_2$  planes, such as those provided by a d-wave superconducting gap [3], momentum dependent Fermi velocities [4], or the presence of stripes [5]. In order to discriminate between the above-mentioned theoretical models, SANS experiments as a function of doping and up to 10.5 Tesla have been performed. The outcome of the measurements will be presented

We will report here as well on the first SANS measurements of an ordered VL in the electron-doped cuprate superconductor  $\text{Nd}_{2-x}\text{Ce}_x\text{CuO}_4$  [6]. A square VL with the nearest neighbors oriented 45 degrees from the Cu-O bond directions is observed down to unusually low magnetic fields. Moreover, the vortex lattice intensity is found to decrease faster than expected with increasing magnetic field, possibly indicating a transition to a more disordered vortex glass phase.

Similarities and differences between electron- and hole-doped high-temperature superconductors will be discussed.

This work was supported by the Swiss National Science Foundation, the Engineering and Physical Sciences Research Council of the U.K. and the Ministry of Education and Science of Japan.

- [1] R. Gilardi et al., Phys. Rev. Lett. 88 (2002) 217003.
- [2] S.P. Brown et al., Phys. Rev. Lett. 92 (2004) 067004.
- [3] M. Ichioka et al., Phys. Rev. B, 59, 8902, (1999).
- [4] N. Nakai et al., Phys. Rev. Lett. 89 (2002) 237004.
- [5] Franz et al., Phys. Rev. Lett. 88 (2002) 257005.
- [6] R. Gilardi et al., to be submitted.

#### **M4-A4 (16:45) Novel Dynamic Scaling Regime in Hole-Doped Cuprates (Invited)**

*Ying Chen, Wei Bao (Los Alamos National Laboratory), J. E Lorenzo (Laboratoire de Cristallographie, CNRS, B.P. 166, 38042 Grenoble, France), Y. Qiu, S. Park (NIST Center for Neutron Research; University of Maryland, College Park), S.-H. Lee (NIST Center for Neutron Research), J. Sarrao (Los Alamos National Laboratory)*

Only 3 % hole doping by Li is sufficient to suppress

the long-range 3-dimensional antiferromagnetic order in  $\text{La}_2\text{CuO}_4$ , thus allowing experimental study of quantum spin dynamics of 2-dimensional (2D) spin liquid in a wide temperature range. The spin dynamics of such 2D quantum spin liquid was investigated with measurements of the dynamic magnetic structure factor  $S(\omega, \mathbf{q})$ , using cold neutron spectroscopy, for single crystalline  $\text{La}_2\text{Cu}_{1-x}\text{Li}_x\text{O}_4$  ( $x = 0.04, 0.06$  and  $0.1$ ). The  $S(\omega, \mathbf{q})$  peaks sharply at  $(\pi, \pi)$  for all these samples, suggesting that the  $(\pi, \pi)$  correlated dynamic spin clusters in Li-doped  $\text{La}_2\text{CuO}_4$  have developed to substantial size below 150 K. Furthermore,  $S(\omega, \mathbf{q})$  shows a crossover from the quantum critical (QC),  $\omega/T$  scaling, at high temperatures to a novel low temperature regime characterized by a constant energy scale upon cooling, which is observed first time experimentally. The observed crossover possibly corresponds to the theoretically expected crossover from the QC to the quantum-disordered regime of the 2D Heisenberg antiferromagnetic spin liquid. Possible role played by doped holes in modifying spin fluctuation spectrum will be discussed.

#### **M4-A5 (17:15) On the temperature dependence of the order parameter in YBCO**

*M. Yethiraj, D. K. Christen (Oak Ridge National Laboratory), D. McK. Paul, S. Crowe (University of Warwick), M. Arai (KEK - High Energy Accelerator Research Organization), L. Porcar (NIST Center for Neutron Research)*

An unusual feature of the FLL in  $\text{YBa}_2\text{Cu}_3\text{O}_7$  is the temperature (T) dependence of the Bragg intensity. Conventional theories predict very little variation in the intensity between 0 K and  $\sim T/3$ . Since the London penetration depth (of which the Bragg intensity is a measure) is an order parameter of the superconductivity, the unexpectedly rapid decrease in the intensity at low T seen in the first measurements at 0.8 Tesla were extremely interesting, particularly what it implied on the mechanism driving the transition in these materials. However, since disorder results in a decrease of the integrated Bragg intensity, detailed measurements are needed to gauge the effect of twin plane defects and lattice structural distortions on the Bragg intensity. Recent measurements of the temperature dependence of the intensity and vortex lattice structure at different fields in a clean but twinned sample of optimally doped YBCO will be discussed.

#### **M4-A6 (17:30) Field-induced magnetic correlation in high $T_c$ cuprates (Invited)**

*Kazuyoshi Yamada (Institute for Materials Research, Tohoku University)*

We present results of recent neutron scattering experiments on superconducting cuprates under magnetic field and discuss the interplay between magnetic order and high- $T_c$  superconductivity. In hole-doped  $\text{La}_{2-x}\text{Sr}_x\text{CuO}_4$  (LSCO), magnetic field applied perpendicular to the  $\text{CuO}_2$  planes of LSCO with  $x = 0.12$  and  $0.10$  and of  $\text{La}_2\text{CuO}_4$  with staged excess oxygen ions enhances the incommensurate elastic peak-intensity without changing both incommensurability and onset temperature of field-induced intensities. In these compounds, no static charge stripe order has ever been induced by magnetic field up to  $\sim 10$  Tesla. On the other hand, for  $\text{La}_{1.45}\text{Nd}_{0.4}\text{Sr}_{0.15}\text{CuO}_4$  with a static charge stripe order no remarkable field-effect has been observed for incommensurate peaks. Therefore, the field-induced enhancement of spin correlation is only observable in the superconducting samples accompanied by static/quasi-static spin-density-wave without static charge stripes. In the case of electron-doped superconductors, clear field-effects have been observed in the elastic magnetic peak centered at  $(\pi\pi)$ . In both  $\text{Nd}_{2-x}\text{Ce}_x\text{CuO}_4$  and  $\text{Pr}_{1-x}\text{La}_x\text{Ce}_x\text{CuO}_4$  (PLCCO) the field dependence of the induced component shows a peak at  $H = 5 \sim 6$  Tesla. For PLCCO magnetic field affects the onset temperature for the induced magnetic correlation. Similar to the hole-doped case, the field-induced intensity is observable only in the doping region where elastic magnetic peaks are observed in zero field. We compare these results with those observed by impurity-substitution.

Our recent neutron scattering experiments under magnetic field on LSCO and PLCCO have been done in collaboration with M. Fujita, M. Matsuda, S. Katano, T. Suzuki, C.H. Lee, J.M. Tranquada, C.P. Regnault, B. Khaykovich, S. Wakimoto and R.J. Birgeneau.

**M4-B, Neutron Properties and Interactions,  
Chair: Mohammed Arif (NIST), Room 2101/3/5  
Green**

**M4-B1 (15:45) Measurement of the parity-violating gamma-ray asymmetry in the neutron-proton capture (Invited)**

*F. W. Hersman (University of New Hampshire), for the NPDGamma Collaboration*

The NPDGamma experiment is currently being commissioned at the Los Alamos Neutron Science Center. The goal of the experiment is to measure the parity-violating gamma asymmetry  $A_\gamma$  in the reaction  $n + p \rightarrow d + \gamma$ . The asymmetry is predicted to be  $\sim 5 \times 10^{-8}$ , and its measurement will provide a theoretically clean measurement of the

weak pion-nucleon coupling, which is believed to be the longest range component of the hadronic weak interaction. The results of the winter 2004 commissioning run, including the performance of the polarized  $^3\text{He}$  spin filter and analyzer, will be presented. Production data collection with a proton target will begin in Fall 2004.

**M4-B2 (16:15) Search for the Radiative Decay Mode of the Neutron**

*B. M. Fisher, F. E. Wietfeldt (Tulane University), M. S. Dewey, T. R. Gentile, J. S. Nico, A. K. Thompson (National Institute of Standards and Technology), E. J. Beise, K. G. Kiriluk (University of Maryland, College Park)*

Beta-decay of the neutron into a proton, electron, and antineutrino is occasionally accompanied by the emission of a photon. Despite decades of detailed experimental studies of neutron beta-decay, this rare branch of a fundamental weak decay has never been measured. An experiment to study the radiative beta-decay of the neutron is currently being developed for the NG6 fundamental physics beam line at the NIST Center for Neutron Research. The experiment will make use of the existing apparatus for the NIST Penning-trap lifetime experiment, which can provide substantial background reduction by providing an electron-proton coincidence trigger. Tests and design of a detector for gamma rays in the 100 keV range are under development. The need for a large solid-angle gamma ray detector that can operate in a strong magnetic field and at low temperature has led us to consider scintillating crystals in conjunction with avalanche photodiodes. The apparatus has been installed at the NG6 beam line, and tests have begun. The status of the experiment will be discussed.

**M4-B3 (16:30) High-precision measurements of the n-p, n-d, and n- $^3\text{He}$  bound coherent scattering lengths**

*T. C. Black (University of North Carolina at Wilmington), P. R. Huffman (National Institute of Standards and Technology; North Carolina State University), M. Arif, D. L. Jacobson, S. A. Werner (National Institute of Standards and Technology), W. M. Snow (Indiana University; IUCF), K. Schoen (University of Missouri - Columbia)*

Recent measurements of the  $n$ - $d$  and  $n$ - $^3\text{He}$  bound coherent scattering lengths, conducted at the Neutron Interferometer and Optics Facility at NIST, are in significant disagreement with exact calculations of these observables using modern  $\text{NN} + 3\text{NF}$  potentials. The bound coherent  $n$ - $d$  scattering length was measured to be  $b_{nd} = (6.665 \pm 0.004)$  fm, which yields a new world average for this parameter of



$b_{nd} = (6.669 \pm 0.003)$  fm. In the  $n$ - $^3\text{He}$  system, the bound coherent scattering length was measured as  $b_{n-^3\text{He}} = (5.857 \pm 0.007)$  fm, which yields a new world average for this parameter of  $b_{n-^3\text{He}} = (5.854 \pm 0.007)$  fm. Combining these measurements with O. Zimmer's result for the bound incoherent scattering length of  $b_i = (-2.365 \pm 0.020)$  fm, one obtains the free singlet and triplet scattering lengths for the  $n$ - $^3\text{He}$  system;  $a_0 = (7.456 \pm 0.026)$  fm, and  $a_1 = (3.364 \pm 0.010)$  fm, respectively. Our measured value of the n-p bound coherent scattering length,  $b_{np} = (-3.7384 \pm 0.0020)$  fm is in agreement with the previous world average value of  $b_{np} = (-3.7410 \pm 0.0020)$  fm. The extreme precision of these new measurements renders them suitable for use in contemporary EFT calculations.

#### **M4-B4 (16:45) Search for New Physics from Neutron Beta-Decay**

*V. Gudkov (Department of Physics and Astronomy, University of South Carolina, Columbia, SC 29208)*

New Spallation Neutron Source at the Oak Ridge National Laboratory will provide unique opportunity to increase significantly the accuracy in measurements of parameters of neutron beta-decay. It will improve the precision of the value of axial-vector coupling constant, which is in high demand for neutrino physics, astrophysics, and other applications of the theory of weak interactions. Precise measurements of neutron decay will lead to the possibility to obtain the Cabibbo-Kobayashi-Maskawa matrix element in nuclear model independent way. The value of this matrix element dominates the unitarity condition of the Standard Model which is very sensitive to the possible manifestations of new physics. Measurements of angular correlations can clarify problems related to the possibility of existence of exotic interactions and violations of fundamental symmetries.

For precise determination of the fundamental constants and for an unambiguous search for new physics in neutron decay experiments, the careful analysis of all possible corrections to neutron decay process should be done. This talk presents analysis of these corrections: including radiative corrections calculated using both the standard approach [1] and the effective field theory [2]. The possibility to obtain parameters of neutron beta decay in model independent way is discussed (see, for example [3]). The given analysis can be used for the estimation of the sensitivity of neutron decay process to new physics.

[1] A. Sirlin, "General Properties of the Electromag-

netic Corrections to the Beta Decay of a Physical Nucleon", *Phys. Rev.* 164 (1967) 1767.  
 [2] S. Ando, H. W. Fearing, V. Gudkov, K. Kubodera, F. Myhrer, S. Nakamura and T. Sato, "Neutron beta decay in effective field theory", arXiv:nucl-th/0402100 (2004).  
 [3] V. Gudkov, "New generation of neutron decay experiments", *J. of Neutron Research* (2004) in press.

#### **M4-B5 (17:00) Review of fundamental physics with ultracold neutrons (Invited)**

*S. N. Dzhosyuk (Harvard University)*

Ultracold neutrons (UCN), typically with energies of order  $10^{-7}$  eV, allow for both long observation times and long interaction times with materials, thus making UCN a valuable tool for testing fundamental physics theories and symmetries. Several experiments using UCN aim to improve a precision of the measurement of the neutron lifetime and the neutron beta decay asymmetry coefficient "A." When combined, these parameters will help clarify present discrepancies in our understanding of the weak interaction. Another experiment, a measurement of the neutron electric dipole moment (EDM) using UCN in liquid helium, aims to improve the experimental limits by two orders of magnitude. This sensitivity will allow tests of models such as supersymmetry in the continuing quest to observe CP violation beyond the Standard Model, that is necessary to explain the cosmological baryon asymmetry. Several new UCN sources are being built in the U.S. and abroad. The higher densities of UCN that will soon be available will dramatically improve the precision of these measurements and open up the possibilities for additional condensed matter studies at low  $Q^2$ . A review of the current status of the above-mentioned experiments and new facilities for UCN production will be presented.

#### **M4-C, Confinement, Chair: Paul Sokol (Penn State), Room 1123 Blue**

##### **M4-C1 (15:45) Quasielastic neutron scattering investigation of the translational and rotational dynamics of supercooled water confined in nanoporous silica matrices**

*Sow-Hsin Chen, Li Liu, Antonio Faraone (Massachusetts Institute of Technology)*

Using incoherent quasielastic neutron scattering we investigated the dynamics of water confined in two nanoporous alumino-silicate matrices, from ambient temperature down to deeply supercooled states in a temperature range inaccessible in bulk water. We collected data using three instruments with widely



different resolutions, the Fermi chopper, the disk chopper, and the backscattering spectrometers, at the NIST Center for Neutron Research. The confining systems were lab synthesized nanoporous silica glasses MCM-41-S and MCM-48-S. The former matrix (25 Å pore diameter) has 1-D cylindrical tubes arranged in a hexagonal structure whereas the latter (22 Å pore diameter) has a 3-D bicontinuous morphology. Inside the pores of these matrices the freezing process of water is strongly suppressed, taking place at a temperature about 50 K less than in bulk water. Thus, with the combined use of different instruments, we were able to study an interesting temperature range, 200 K < T < 300 K. The data from all the three spectrometers were analyzed using a single consistent intermediate scattering function of water based on the relaxing cage models for the translational and rotational motions. An exponential slowing down of the translational and rotational relaxation times, as temperature is lowered, has been observed, indicating the existence of a kinetic glass transition temperature at about 220 K.

- [1] Liao, Ciya, F. Sciortino and S.H. Chen, "Model for Dynamics in Supercooled Water," Phys. Rev. E 60, 6776-6787 (1999).  
 [2] Liu, Li, Antonio Faraone and S.H. Chen, "A Model For the Rotational Contribution to Quasi-elastic Neutron Scattering Spectra From Supercooled Water," Phys. Rev. E. 65, 041506-8 (2002).  
 [3] Fraone, A., S.H. Chen, E. Fratini, P. Baglioni, L. Liu and C. Brown, "Rotational Dynamics of Hydration Water in Dicalcium Silicate by Quasi-Elastic Neutron Scattering," Phys. Rev. E. 65, 040501-4 (2002).  
 [4] Faraone, A., Li Liu, Chung-Yuan Mou, Pei-Chun Shih, John R.D. Copley, and Sow-Hsin Chen, "Translational and rotational dynamics of water in mesoporous silica materials: MCM-41-S and MCM-48-S," J. Chem. Phys. 119, 3963-3971 (2003).  
 [5] Faraone, A., Li Liu, and Sow-Hsin Chen, "Model for translation-rotation coupling of molecular motion in water," J. Chem. Phys. 119, 6302-6313 (2003).

#### **M4-C2 (16:00) Liquid-Gas Critical Phenomena Under Confinement: SANS Studies of CO<sub>2</sub> in Aerogel**

*Y. B. Melnichenko, G. D. Wignall (Condensed Matter Sciences Division, Oak Ridge National Laboratory), D. R. Cole (Chemical Sciences Division, Oak Ridge National Laboratory, Oak Ridge, TN 37831, USA), H. Frielinghaus (Forschungszentrum Jülich GmbH, Institut für Festkörperforschung, D-52425 Jülich, Germany)*

The effect of spatially fixed (quenched) impurities on phase transitions and critical phenomena remains a

challenging area for both theory and experiment. Small angle neutron scattering (SANS) is a well-established technique for investigating the behavior of confined binary liquid solutions, as it can probe the correlation length ( $\xi$ ) and susceptibility ( $\chi$ ) in pores on length scales  $\sim 1 - 100$  nm. We report results of the first SANS measurements of the critical behavior of a single-component fluid (CO<sub>2</sub>) in a highly porous aerogel and compare it with the critical behavior of the bulk fluid. We demonstrate that, although the scattering from blank aerogel exceeds that from CO<sub>2</sub> by two orders of magnitude, the temperature and pressure variation of thermodynamic properties of confined fluids can be extracted and explored. Pressure scans at temperatures, both far away and close to the liquid-gas critical temperature,  $T_c$  reveal the importance of the molecule-surface interactions, which become increasingly important in the critical region.  $\xi$  and  $\chi$  for the bulk fluid diverge as  $T \sim T_c$  and their variation is described by the Ising model exponents ( $\nu = 0.63$  and  $\gamma = 1.24$ , respectively). Furthermore, the scaling exponents of confined fluid are close to mean field predictions ( $\nu = 0.5$  and  $\gamma = 1.0$ ) and the absolute value of  $\xi$  does not exceed the pore size of aerogel ( $\sim 70$  Å) even at  $T \sim T_c$ . The results demonstrate that quenched disorder induced by aerogel works to depress density fluctuations in the critical region. Below  $T_c$ , the long-lived metastable domains are formed. Despite the negligible volume occupied by aerogel (< 4 %), the macroscopic phase separation of confined CO<sub>2</sub> into coexisting liquid and gaseous phases characteristic of the bulk fluid, is completely suppressed. Experimental data show that critical absorption is as important as the effect of confinement, even in highly porous systems.

#### **M4-C3 (16:15) Anomalously soft dynamics in nanotube-water: a revelation of nanoscale confinement (Invited)**

*A.I. Kolesnikov, C.-K. Loong, P. Thiyagarajan (Intense Pulsed Neutron Source, Argonne National Lab), J.-M. Zanotti (Intense Pulsed Neutron Source, Argonne National Lab; Laboratoire Léon Brillouin, C.E.A Saclay, 91191 Gif-sur-Yvette Cedex), C. Burnham (Department of Chemistry, University of Utah, Salt Lake City, Utah 84112), A.P. Moravsky, R.O. Loutfy (MER Corporation, 7960 South Kolb Road, Tucson, AZ 85706)*

Quasi-one-dimensional water encapsulated inside single-walled open-ended carbon nanotubes, here referred to as nanotube-water, was studied by neutron scattering (ND, INS and QENS) at different temperatures and pressures. This study reveals that nanotube-water is a new state of water manifested

by weak hydrogen bonds, extended intermolecular water-water and O-O distances, short O-H covalent bonds, very large amplitude of water molecules vibrations, and a continuous transition from solid to liquid state on heating. QENS study at high pressure also shows that at  $P = 0.14$  GPa the effect of very large amplitude of water molecules vibrations in SWNT is suppressed at low temperatures. MD simulations of nanotubes-water well describe the observed INS spectra and give a possible structure of water inside single-walled carbon nanotubes.

#### **M4-C4 (16:45) Molecular Rotation and Translation of Hydrogen Adsorbed on Planar Graphite and in Single-Wall Carbon Nanotubes**

*P.A. Georgiev, D.K. Ross, J. Fernandez-Garcia, I. Morrison (Institute for Materials Research, University of Salford, Salford, M5 4WT)*

We present neutron inelastic scattering spectra measured at 17 K on the TOSCA spectrometer, ISIS, UK, from different amounts of para-Hydrogen within the sub- and multilayer region physisorbed on Grafoil and high quality Single-Wall Carbon Nanotubes. Our results show that on the graphite surface and for concentrations of up to the densest monolayer the rotational motion of the adsorbed molecules is unperturbed. A downshift of 0.2 meV is attributed to the different Zero Point Energies (ZPE) of the Center-of-Mass (CoM) out of plane motion for the para- and ortho- molecular species, as well as, a small increase in the H-H bond length. On the contrary, a 1.5 meV splitting between the states within the  $J = 1$  manifold is observed at low surface coverage, where due to the twice higher binding energy as compared to flat graphite, the molecules are preferentially adsorbed on the groove sites of the nanotube bundles. At higher surface coverages the scattering is dominated by freely rotating molecules adsorbed at the external convex tube surface and in higher molecular layers. Our new and unique high-resolution data from a few concentrations in the multilayer region shows for first time that due to the vertical solid-like behavior of the second and possibly even the third molecular layers, the  $J = 0$  to  $J = 1$  rotational line of hydrogen adsorbed on Grafoil is also split. The higher molecular layers show no ZPE effect on the rotational line. The 0 - 1 rotational transition due to molecules adsorbed between the graphite surface and higher molecular layers is now split. It is anticipated that for these molecules the mixing between the different m-states of the  $J = 1$  level is now removed and a different rotational-translational coupling scheme operates.

The mean translational kinetic energies as functions

of the surface concentration are derived from the high-energy part of each spectrum.

#### **M4-C5 (17:00) Inelastic Neutron Scattering of H<sub>2</sub> Adsorbed on Activated Carbon**

*D.G. Narehood, P.C. Eklund, P.E. Sokol (Department of Physics and Materials Research Institute, Pennsylvania State University Park, Pennsylvania 16802)*

Inelastic neutron scattering provides a unique microscopic perspective of the state of molecules adsorbed on surfaces. We report inelastic neutron scattering studies of H<sub>2</sub> adsorbed on an activated carbon (AC). Deep inelastic neutron scattering (DINS) has been used to probe the single-particle momentum distribution of the adsorbed molecules. From these measurements the mean kinetic energy, which is directly affected by the extent of localization of the molecules, has been determined. In addition to the DINS measurements, the rotational spectrum of the adsorbed molecules was measured with incident neutrons with thermal energies. Peaks corresponding to transitions between the  $J = 0$  and  $J = 1$  rotational states are present in the collected scattering spectra. These spectra provide information on the ortho-to-para conversion of the adsorbed molecules through the time-dependent intensities of the peaks. DINS and rotational spectra have been collected for various surface coverages in order to study the importance of the affect of H<sub>2</sub>-H<sub>2</sub> interactions versus H<sub>2</sub>-AC interactions on the properties of the adsorbed molecules. This research was supported by the DOE under Grant No. DE-FG02-01ER45912.

#### **M4-C6 (17:15) Structure and dynamics of oligomer molecules within monolayer films on graphite**

*E.J. Kintzel, Jr., K.W. Herwig (Spallation Neutron Source, Oak Ridge National Laboratory), I. Peral (NIST Center for Neutron Research; Department of Materials Science and Engineering, University of Maryland)*

The structure and dynamics of monolayer films of the aromatic molecules o-terphenyl (o-3P), p-terphenyl (p-3P), p-quaterphenyl (p-4P), and p-sexiphenyl (p-6P) adsorbed onto the surface of graphite has been carried out using elastic and quasielastic neutron scattering. Structural results of the p-phenylene oligomer (p-nP) films indicate an orientation consistent with the long molecular axis parallel to the graphite surface. Initial dynamic results indicate a phase change within the p-nP films at approximately 300-325 K. At temperatures below 325 K, the scattering is consistent with reorientation of the phenyl rings around the long molecular axis. At temperatures above 300 K, the scattering is much

stronger and appears at lower momentum transfers, indicating some form of translational motion in combination with reorientation of the phenyl rings. Monolayer o-3P films exhibit molecular motions consistent with both reorientations of the phenyl rings as well as translations at temperatures as low as 190 K. There is no abrupt change in the character of the dynamics for the o-3P films.

#### **M4-D, Polymers and Colloids, Chair: Michael Kent (Sandia), Room 2100/2/4 Red**

##### **M4-D1 (15:45) Counterion undressing from flexible polyelectrolytes (Invited)**

*V. M. Prabhu, E.J. Amis (NIST Polymer Division),  
D. Bossev, N. Rosov (NIST Center for Neutron  
Research)*

At low ionic strength, organic counterions dress a flexible charged polymer as measured directly by small-angle neutron scattering (SANS) and neutron spin-echo (NSE) spectroscopy. This dressed state, quantified by the concentration dependence of the static correlation length, illustrates the polymer-counterion coupled nature on the nanometer length scale. The counterions, made visible by selective hydrogen and deuterium labeling, undress from the polymeric template by addition of sodium chloride. The addition of this electrolyte leads to two effects; increased Debye electrostatic screening and decoupled counterion-polymer correlations. Neutron spin echo spectroscopy measures a slowing-down of the effective diffusion coefficient of the labeled counterions at the length scale of 8 nm, the static correlation length, indicating the nanosecond counterion dynamics mimics the polymer. These experiments, performed with semidilute solutions of tetramethylammonium poly(styrene sulfonate) [(h-TMA + ) d-PSS], apply to relevant biopolymers including single and double stranded DNA and unfolded proteins, which undergo orchestrated dynamics of counterions and chain segments to fold, unfold and assemble.

##### **M4-D2 (16:15) The effect of chain architecture on the dynamics of copolymers in a homopolymer matrix**

*S. K. Kamath, M. Lay, R. Mehta, M. D. Dadmun  
(University of Tennessee, Knoxville)*

Copolymers can be used as interfacial modifiers in phase separated polymer blends and selective surface segregation. Important parameters in this process include the amount of copolymer that migrates to the surface and the rate of this process, both of which are altered by changing the copolymer microstructure. We have monitored the the diffusive

behavior of various copolymers of Styrene(S) and Methylmethacrylate (MMA) in a PMMA matrix using neutron reflectivity experiments. These results are compared to results from dynamic Monte Carlo simulations on a model blend containing copolymers of different architectures dispersed in a homopolymer matrix. In conjunction, these studies provide valuable insights into the effects of chain architecture on the structure and dynamics of copolymers in a homopolymer matrix.

##### **M4-D3 (16:30) SANS Microstructure and rheology of sterically stabilized colloidal dispersions with depletion attractions**

*L.N. Krishnamurthy, N.J. Wagner (Center for  
Molecular and Engineering Thermodynamics,  
Department of Chemical Engineering, University of  
Delaware, Newark, DE 19716)*

Colloidal particles are employed in a wide range of industries and products. A thorough understanding of dispersion rheology and stability is critical for successful formulation and processing of colloidal dispersions for practical applications. These properties are macroscopic manifestations of the microscopic interparticle interactions acting between the colloidal particles. The microscopic forces that can arise from polymer adsorption include bridging, steric, and depletion forces with a strongly coupled electrosteric force if the polymer is a polyelectrolyte. Rational design of stable dispersions requires the characterization of these interparticle interactions.

Rheological and small angle neutron scattering measurements are presented for a model dispersion of silica nanoparticles in a buffered, aqueous gelatin solution over a range of particle and gelatin concentrations. There is debate in the literature so to whether free polymer in an adsorbing polymer-colloid mixture can result in an attractive depletion interaction force. The adsorbed polymer layer and the resulting large excluded volume clearly dominate the rheology. However, comparison of SANS measurements with analysis of the rheology demonstrates the presence of weak attractions, which has a profound influence on the stability and rheology of these systems.

We model the attractive interactions within the classic Asakura-Yukawa framework for the depletion interactions. We propose a predictive semi-empirical model to describe the rheology of colloidal systems with attractive interactions. Excellent quantitative predictions of zero shear viscosity and SANS for a broad range of particle and polymer concentration validate our model.



#### M4-D4 (16:45) Highly Monodispersed Silica Nanoparticles: Controlled Formation and EDL Characterization by SANS

W. Wang (Oak Ridge National Laboratory), L. Porcar (NIST Center for Neutron Research), W. A. Hamilton (Oak Ridge National Laboratory), P. D. Butler (Oak Ridge National Laboratory; NIST Center for Neutron Research), L. Liang (Oak Ridge National Laboratory; Cardiff University, Cardiff CF24 0YF, UK), B. Gu (Oak Ridge National Laboratory)

Suspensions of monodispersed colloidal particles offer many scientific opportunities for new applications in emerging nanotechnologies, such as advanced coatings, photonic crystals and photonic band-gap materials. The goal of this project is to develop and apply small angle neutron scattering (SANS) to quantify the electric double layer (EDL) structure associated with silica nanoparticles in an aqueous solution containing organic electrolytes. The amount and the orientation of the ionic organic molecules present in the Stern layer, and the resulting thickness of the EDL all contribute to interaction energies during particle encounter.

In order to detect small changes in particle size due to sorption of the organic ions, a high monodispersity of colloidal particles is crucial. Although the preparation of silica nanoparticles has been extensively studied, synthesis of highly monodispersed silica colloids with sizes  $< 100$  nm remains a challenge. We optimized synthesis and purification procedures to produce monodispersed silica colloids in size range of 20-100 nm by hydrolysis of tetraethoxysilane. The particle sizes and polydispersity could be controlled by chemical reagent concentrations, reaction temperature, reaction time, or surfactant template media.

These monodispersed silica colloids were studied by SANS over a wide range of scattering vectors. These organic counterions, such as tetraalkylammonium and alkyltrimethylammonium ions, functionally serve as monovalent simple ions with a high volume density and therefore provide a model system to study ion adsorption and distribution on silica surfaces by SANS. The adsorption layer thicknesses of various organic cations at the silica nanoparticle-water interface were studied with contrast match technique. This deuteration accentuated different domains relative to others to provide the needed discrimination for specific domain structures such as particle core size, adsorbed monolayer or bilayer thicknesses, and solvent penetration in the organic layers. We fit the scattering spectra by PolyCoreShell Model to deduce the diameter, the size polydispersity, and the thickness of adsorbed organic layer on the spherical silica particles.

#### M4-D5 (17:00) Effect of Attractions on the Microstructure and Rheology of Dense Colloidal Suspensions and Gels

V. Gopalakrishnan, S. Ramakrishnan (Department of Chemical and Biomolecular Engineering), K. Schweizer (Department of Chemical and Biomolecular Engineering; Department of Materials Science and Engineering), C. Zukoski (Department of Chemical and Biomolecular Engineering)

Colloidal suspensions and gels are used in a number of technologically important applications – inks, paints and ceramics to name a few. Control of the microstructure of the suspension and the resulting flow properties is of utmost importance to achieving the desired properties in these applications.

Addition of non-adsorbing polymer to a colloidal suspension (particles of size  $R$ ) provides one with the ability to tune the microstructure and flow properties of the suspension with two independent variables – the molecular weight of the added polymer (radius of gyration  $R_g$ ) and concentration of the added polymer  $c_p$ . The non-adsorbing polymer induces attractions between the colloidal particles the range of which is controlled by  $R_g/R$  while the strength of attractions is controlled by  $c_p$ . For  $R_g/R$  values less than 0.1, the addition of increasing amounts of polymer causes the suspensions to gel thus drastically changing the flow properties at the gel point (divergent zero shear viscosity and appearance of a nonzero value of the elastic modulus).

In this work, we systematically characterize the microstructure (SANS and USAXS) and flow properties of the colloidal silica suspensions (suspended in decalin) with the addition of polystyrene. The size ratio  $R_g/R$  used in this work is 0.078 and 0.053. There are two regions which we focus on – (1) The equilibrium fluid : the polymer concentration is varied from dilute till the point where the suspensions gel and (2) The gel region: the polymer and colloid concentrations are varied over a wide range to give rise to substantial changes in flow properties. Our goal is to link the mechanical properties to microstructures through the appropriate models.

Here we report on decreases in the shear rate required to produce hydroclusters as the strength of attraction is increased. Hydroclusters are important in the high shear region where shear thickening is observed. With increasing strengths of attraction these clusters form at increasing smaller shear rates but shear thickening is lost. This is understood in terms of the shear rate dependencies of the hydrodynamic and thermodynamic contributions to the stress.

**MU - User Meetings and Reception (McHenry/  
Chesapeake Rooms; 19:00)**

**MP - Poster Session: Student Research Award  
(Main Concourse; 20:00) (Reception continues)**

**MP1: SANS Study of High Pressure Unfolding of  
Staphylococcal Nuclease**

A. Paliwal (Johns Hopkins University), D.P. Bossev  
(NIST Center for Neutron Research), ME Paulaitis  
(Johns Hopkins University)

Staphylococcal Nuclease (SN) is a 149 residues long, single domain globular protein whose folding characteristics conform to the two state model. Reversible folding of SN with pH, chemical denaturants and temperature as perturbing agents has been very well examined and characterized.<sup>1-2</sup> A series of equilibrium and kinetics studies of pressure induced unfolding of SN by Royer et al.<sup>3-4</sup> revealed that the folding reaction involves significant dehydration and collapse of the chain. The picture that emerges from these studies is that of a combination of increased solvation and decreased excluded volume in the unfolded state relative to the folded state. However, no direct efforts have been made towards quantifying this difference in the extent of hydration of the folded and the unfolded states from a large body of available experimental results. Recently, Hummer et al.<sup>5</sup> proposed that proteins stabilized by hydrophobic driving forces at ambient pressure are destabilized at elevated pressures due to water penetration into the hydrophobic core ("protein unfolding"). They argue that pressure-induced protein unfolding corresponds to the transfer of water into the protein interior, rather than to the transfer of nonpolar residues into water. This hypothesis, if correct, would resolve Kauzmann's paradox<sup>6</sup> for the pressure-induced denaturation of proteins, which results from the fact that the volume change of transfer of hydrocarbons into water is positive at high pressures.

In this study, we present a novel method recently developed<sup>7</sup> to extract the extent of hydration of SN as a function of pressure from our Small Angle Neutron Scattering (SANS) results at 25° C. The method, primarily makes use of the radius of gyration,  $R_g$  and the forward scattering intensity,  $I(0)$  values obtained directly from the scattering spectra. These hydration results are then discussed in context of the proposition put forward by Hummer et al. and the 'apparent' paradox first pointed out by Kauzmann.

*Reference:*

- [1] Shortle D. and Meeker A. K. (1986) *Proteins: struct., funct. and genet.* 1, 81.
- [2] Griko Y.; Privalov, P. L.; Sturtevant J.M and

Venyaminov, S. (1988) *Proc. Natl. Acad. Sci. U.S.A* 85, 3343.

[3] Vidugiris, G.J.A; Markley, J.L. and Royer, C. A (1995) *Biochemistry U.S* 34(15), 4909.

[4] Panick, G.; Vidugiris, G. J. A; Malessa, R; Rapp, G, Winter, R. and Royer, C. A (1999) *Biochemistry U.S* 38, 4157.

[5] Hummer, G.; Garde, S; Paulaitis, M. E. and Pratt, L. R. *Proc. Natl. Acad. Sci. U.S.A* (1998) 95, 1552.

[6] Kauzmann, W. *Nature* (1987) 325, 763.

[7] Lesemann, M.; Nathan, H.; DiNoia, T.; Kirby, K.; McHugh, M. A.; van Zantan J.H. and Paulaitis, M.E. *Ind. Eng. Chem. Res.* (2003) 42(25), 6425.

**MP2: Studying Protein Dimerization on Membranes  
by Small Angle Neutron Scattering**

K. Gupta (Dept. of Chemical and Biomolecular Eng.;  
Program in Computational Biology, Johns Hopkins  
Univeristy, Baltimore, MD), J. Pencer (Dept of  
Chemical and Biomolecular Engg., Johns Hopkins  
University, Baltimore, MD.; NIST Center for Neutron  
Research), D. Bossev, S. Krueger (NIST Center for  
Neutron Research), M. Paulaitis (Dept. of Chemical  
and Biomolecular Engg.; Program in Computational  
Biology, Johns Hopkins Univeristy, Baltimore, MD)

Clustering/oligomerization of membrane bound receptors is found to be important in cellular responses. It has been suggested that oligomerization is induced both by lipid membrane environment and by ligand binding. Though many studies have been focused on receptor clustering, the structural features of these oligomers are still lacking. We have developed a model system to study the role of membrane environment and ligand binding on the structural organization of membrane anchored proteins using small angle neutron scattering (SANS). Our model system consists of a mouse IgG Fab fragment covalently attached to unilamellar DMPC lipid vesicles on which dimerization/oligomerization is induced by anti-Fab antibody. Contrast matching of isotopically substituted phospholipids eliminates the contribution of the bilayer to the observed scattering, resulting in a scattering profile dependent on the structural organization of protein complexes on the bilayer. By comparing the scattering profiles from protein complexes in solution and on the bilayer, we have found that the complexes on the membrane have a smaller physical size and less flexibility than in the solution. Our results also suggest that anchoring proteins on a single component bilayer system does not increase their dimerization/oligomerization potential in the presence of a ligand. One implication of these results is that lipid domains (rafts) or other cellular components may be required in facilitating the oligomerization of membrane bound receptors.

**MP3: Influence of hydration on protein dynamics**

*J.H. Roh (University of Akron, Department of Polymer Science), G. Caliskan (Johns Hopkins University, Department of Biophysics), R. Gregory (Kent State University, Department of Chemistry), I. Peral, Z. Chowdhuri (NIST Center for Neutron Research), A.P. Sokolov (University of Akron, Department of Polymer Science)*

It is obvious that protein dynamics affects significantly their biological activity. Direct relationship between the protein dynamics and the enzymatic activity, however, remains unclear. One way to observe simultaneous changes in protein motions and their functions is to analyze dependence of these parameters on hydration level of a protein. We present analysis of internal motion of proteins at different hydration levels in nano- and picosecond time window. Quasielastic incoherent neutron scattering spectra have been measured in a broad energy range (from  $\sim 1 \mu\text{eV}$  up to  $\sim 10 \text{ meV}$ ) by combining data from backscattering and time of flight spectrometers. The data show nonlinear increase of quasielastic contribution with increase of hydration level. Three different regions are identified: (i) slight change with hydration up to  $0.20 \text{ g D}_2\text{O} / 1 \text{ g protein}$ ; (ii) strong change with hydration between  $0.20$  and  $0.55 \text{ g D}_2\text{O} / 1 \text{ g protein}$ ; (iii) asymptotic behavior with hydration above  $0.55 \text{ g D}_2\text{O} / 1 \text{ g protein}$ . The dynamic transition observed in the temperature dependence of mean square displacements (MSDs) around  $200 \text{ K}$  appears only at hydration levels higher than  $0.20 \text{ g D}_2\text{O} / 1 \text{ g protein}$ . We ascribe the observed variations to a change in the slow relaxation process. It is shown that the intensity of the slow process correlates to the enzyme activity. The results suggest that slow relaxation process might be the essential internal motion to trigger the onset of enzymatic activity in proteins.

**MP4: Neutron diffraction investigation of the structural deviations of components in cement clinker**

*V. K. Peterson (NIST Center for Neutron Research; University of Maryland, College Park)*

The deviations in structural models of tricalcium silicate phases in a Rietveld model of cement clinker after atomic position refinement using neutron powder diffraction data were investigated. Results for phase quantification before, and after, atomic position refinement are reported, and alterations to Bragg-R factors of phases are recorded. In this neutron study, relatively minor adjustments to some tricalcium silicate structural models resulted in decreased R-Bragg factors of those and other phases.

Tricalcium silicate is the major phase in cement clinker, and is crystallographically complex.

Tricalcium silicate exhibits polymorphism, and it is usual for several polymorphs to co-exist as a solid solution in cement clinker. At least seven polymorphs exist, and three have structural solutions that are commonly used in the Rietveld analysis of clinkers. Full-profile Rietveld methods have the ability to define the tricalcium silicate form. It is usual to include a polymorph of tricalcium silicate in each of the three crystal systems encountered when beginning a refinement and then exclude the crystal system(s) not found. Care must be taken so as not to enable one crystal system to alter itself to compensate for others not being modelled.

The crystallography of tricalcium silicate is further complicated as both triclinic and monoclinic forms of tricalcium silicate found in cement clinker are structurally modulated. The structural models used in the Rietveld analysis of cement clinker are averages or approximations only to these true, modulated structures. Additionally, only one triclinic and one monoclinic structural model exist to represent the three possible forms in each of these crystal systems.

Rietveld refinement is commonly used as a method of phase quantification of cement. Given that the structural models for tricalcium silicate may not be accurate or appropriate descriptions of the tricalcium silicate forms in cement clinker, the effect of refining these structures using data of real cement samples is of interest. Thus, any deviations of the "real" structures from the "model" structures can be investigated.

**MP5: Fundamental Tests of Ab Initio methods on Organic based Charge Transfer Crystals using Inelastic Neutron Scattering Spectroscopy**

*J.A. Ciezak (Syracuse University, Dept of Chemistry, 1-014 CST, Syracuse, NY 13244), C.M. Brown (Dept. Mechanical and Nuclear Engineering, University of Maryland/NIST, Gaithersburg, MD), B.S. Hudson (Syracuse University, Dept of Chemistry, 1-014 CST, Syracuse, NY 13244)*

Inelastic neutron scattering (INS) studies of solid-state charge transfer complexes will be presented in combination with ab initio calculations to provide insight into both the molecular properties and the crystalline environment. These crystals undergo electron transfer from a donor to acceptor upon excitation and have relatively unique bonding patterns and structural defects. The donor and acceptor molecules possess electrons that are able to move along the molecular stacks, making them



similar to one-dimensional conductors. In addition to their interesting electronic structure, obtaining an accurate DFT description of these complexes has presented considerable challenge in the past. Two charge transfer complexes, TCNQ:Anthracene and TCNE:Naphthalene, will be discussed, in addition to a relatively unique charge transfer complex, which also has hydrogen bonds, Quinhydrone. We will show that DFT calculations can provide an adequate description of isolated complexes of TCNQ:Anthracene and TCNE:Naphthalene. We will also show the potential use of the HCTH/120 functional in conjunction with full periodic boundary conditions to describe Quinhydrone.

#### **MP6: Orientation and Relaxation of Polymer-Clay Solutions**

*M. Malwitz (Louisiana State University), P. Butler (Oak Ridge National Laboratory), L. Porcar (National Institute of Standards and Technology), G. Schmidt (Louisiana State University)*

The influence of shear on viscoelastic poly(ethylene)oxide (PEO)-clay solutions (Montmorillonite, CNA) was investigated by means of rheology and small-angle neutron scattering (SANS). Steady state viscosity and SANS were used to measure the shear-induced orientation and relaxation of polymer and clay platelets. Anisotropic scattering patterns developed at much lower shear rates than in pure clay solutions. The scattering anisotropy saturated at low shear rates and the CNA clay platelets aligned by the flow, with the surface normal parallel to the gradient direction. Cessation of shear lead to partial and slow randomization of CNA platelets while extremely fast relaxation was observed for Laponite (LRD) platelets. This work on PEO-CNA network like solutions is compared to previously reported PEO-LRD networks and focuses on differences and similarities in shear orientation, relaxation, and on the polymer and the clay interactions.

#### **MP7: Structure Determination of Subcolloidal Zeolite Precursor Nanoparticles**

*J. M. Fedeyko, D. Vlachos, R. F. Lobo (Center for Catalytic Science and Technology, Department of Chemical Engineering, University of Delaware, Newark, DE 19713 USA)*

Upon mixing a solution of tetrapropylammonium hydroxide (TPAOH) and tetraethylorthosilicate (TEOS) at room temperature, a segregation of the solution into two metastable phases is observed. A continuous water-rich phase is formed containing most of the water and a small amount of  $\text{SiO}_2$  and TPAOH. At the same time, the silica is microsegregated into nanoparticles ( $\sim 4$  nm) that contain most of the

silica, a large fraction of the TPAOH and a small amount of water. It has been shown that the rate of growth of zeolites is controlled by the addition of these subcolloidal silica nanoparticles to the growing surface. However, many important aspects of these particles remain unresolved. For instance, the particle shape, particle size distribution, and fundamental properties such as the average composition, internal structure and charge are completely unknown. We have started a comprehensive investigation of this system in an attempt to resolve these issues and will use the information gathered to develop a zeolite growth model that describes the system as a function of intensive variables such as temperature, pressure and composition.

We have conducted contrast matching small-angle neutron scattering experiments in the dilute limit in combination with small-angle x-ray scattering and *in situ* NMR spectroscopy. Analysis of the SANS patterns of particles prepared in  $\text{D}_2\text{O}$  revealed that the particles are ellipsoidal shaped. Our study of the contrast matching and SAXS experiments indicates that the core of these particles is composed primarily of silica. *In situ*  $^{29}\text{Si}$  NMR gives information about the connectivity of the silica core. We find that about 78% of the silica groups are  $\text{Q}^3(\text{SiO}_3/2-\text{OH})$  and 22% of  $\text{Q}^2(\text{SiO}_2/2-(\text{OH})_2)$ . All this information is being used as input to a simulated annealing code that generates models of the nanoparticles with atomic detail. We will present a summary of our results and analysis.

#### **MP8: Electric field alignment of asymmetric diblock copolymer thin films**

*Ting Xu, Thomas P. Russell (Department of Polymer Science and Engineering, University of Massachusetts, Amherst)*

Electric fields alignment of asymmetric diblock copolymer thin films, polystyrene-block-poly(methyl methacrylate), was studied using small angle neutron scattering (SANS) and transmission electron microscopy (TEM). Starting from a poorly ordered state (as cast), surface fields and opposed electric fields biased the cylindrical microdomain orientation. With time upon annealing, the cylinders are locally disrupted to form ellipsoidal shape microdomains that connected into cylindrical microdomains in the applied field direction. Starting from an ordered state with cylinders parallel to the surface, the applied electric field enhanced fluctuations at the interfaces of the microdomains and disrupted cylindrical microdomains into spherical microdomains. This transition is similar to thermoreversible cylinder-to-sphere order-order transition. With time, the spheres deformed into ellipsoids and reconnected forming



cylindrical microdomains oriented at  $\sim 45^\circ$  with respect to the applied field. The tilted cylinders subsequently aligned along the applied field direction. This reorientation process is much slower than that from poorly ordered state.

#### MP9: Short Strong Hydrogen potential surfaces studied by INS

*Timothy Jenkins, Bruce Hudson, Damian Allis, Jenn Ciezak (Syracuse University, Syracuse, NY), Dale Braden (Schrödinger Inc., Portland, OR)*

Symmetric hydrogen bonds (e.g., O-H...O) have equivalent local minima for the H atom positions separated by a barrier at the position of equal O-H-O lengths. This barrier decreases in height as the O-O distances and apparently vanishes for sufficiently short distances. The short, strong hydrogen bonds that occur for small O-O distances are also known as "low barrier" hydrogen bonds. These systems were expected to display a failure of the harmonic dynamical treatment due to the anharmonic nature of the short, strong hydrogen bonds. We examined several co-crystals of varying O-O distances and both intermolecular and intramolecular hydrogen bonds by vibrational spectroscopy to provide a high-resolution basis calculation comparison. Neutron vibrational spectroscopy results are presented. Comparison calculations involving the short, strong hydrogen bond potential surfaces were also carried out using density functional methods. Potential surface models suggest that the surface is best fit by a quartic model resulting in agreement to the vibrational spectra. Vibrational spectrums were determined using FANS at NIST and TOSCA at ISIS, RAL.

#### MP10: Large Scale Structures in Polymer-Clay Solutions

*E. Loizou, M. Malwitz (Louisiana State University), P. Butler (Oak Ridge National Laboratory), L. Porcar, S. Lin-Gibson (National Institute of Standards and Technology), G Schmidt (Louisiana State University)*

The shear-orientation, structure and morphology of viscoelastic polymer-clay networks is investigated on several length scales by means of rheology, microscopy and small-angle neutron scattering (SANS, USANS).

#### MP11: A Method to Predict Small-angle Neutron Scattering Intensities of Nucleic Acids from High-resolution Structures

*J. Zhou (Department of Chemistry, UMBC, Baltimore, MD), S. Krueger (NIST Center for Neutron Research), S Gregurick (Department of Chemistry, UMBC, Baltimore, MD)*

Based on the original program, Xtal2SAS, which

calculates model SANS intensities of proteins from high-resolution structures, we propose a method to obtain model SANS intensities from nucleic acids. For a high-resolution structure of a nucleic acid, either from x-ray crystallography or structural prediction, we generate an ellipsoidal cylinder model for each nucleotide with calculated radii, length and volume from the coordinates file, e. g., a PDB file. Each ellipsoidal cylinder is filled with random points of the appropriate neutron scattering length density using a Monte Carlo method, and is superimposed on each nucleotide to represent the overall structure of the nucleic acid. The distance distribution function,  $P(r)$  is calculated by summing all possible pairs of points in the structure. Then, the scattering intensity  $I(Q)$  is then calculated through a Fourier transform of  $P(r)$ . We extend the original program, Xtal2SAS, for both proteins and nucleic acids, and we test our approach on a few examples of nucleic acids to check the effectiveness of this method.

#### MP12: Solvent Induced Stiffness in Poly(ethylene oxide)

*M.L. Alessi (University of Maryland, Department of Chemical Engineering), D.L. Ho (NIST Center for Neutron Research), S.C. Greer (University of Maryland, Department of Chemical Engineering; Department of Chemistry and Biochemistry)*

Poly(ethylene oxide) (PEO) is a simple polymer with repeating units [- C - C - O -] soluble in organic and aqueous solvents. In all solvents in which PEO has previously been studied, the PEO molecule forms a coil in solution. Small-angle neutron scattering of PEO in deuterated isobutyric acid shows a dramatic stiffening of the polymer chains, resembling a rod. Infrared spectroscopy and polarimetry measurements indicate that the rods are helical. PEO has been seen to form a helix in the solid phase and a local helical structure in aqueous solvents. A global helical conformation, however, has not been seen before in solution. The formation of nanoscale PEO rods may have applications in nanotechnology.

#### MP13: The effect of graft density and length on the surface segregation of graft copolymers in a homopolymer matrix.

*M. A. Lay (University of Tennessee, Knoxville), M. D. Dadmun (University of Tennessee, Knoxville)*

The effect of graft density and length on the surface segregation of graft copolymers in a homopolymer matrix.

Copolymers may be used to modify polymer interfaces in polymer blends. Copolymer architecture plays a substantive role in the ability of copolymers

to migrate to an interface. We have recently examined the diffusion of various graft copolymers in an effort to determine to what extent graft density and length affect surface segregation. Copolymers composed of a PS backbone and PMMA graft segments were prepared via ATRP. Interfacial broadening was studied as a function of annealing time, so that a diffusion coefficient could be determined. This insight into the architectural influence on surface segregation will help us better understand practical processes dependent upon diffusion such as adhesion, interface formation, and phase separation.

#### **MP14: Experimental Studies and Modeling of Clay/PolyDicyclopentadiene Resin and Carbon Nanofiber/Phenolic Resin Composites**

*Mitra Yoonessi, Hossein Toghiani (Dave C. Swalm School of Chemical Engineering, Mississippi State University), Charles Pittman, Jr. (Department of Chemistry, Mississippi State University)*

Hybrid organic-inorganic nanocomposites have received much attention by the researchers during the last five years due to their unexpected properties. A large number of different inorganic materials have been used to enhance matrix properties.

This work incorporated two types of nanophases, Montmorillonite clay and Carbon nanofibers (CNF) into polyDicyclopentadiene and phenolic resin matrices. Montmorillonite has a 2:1 structure consisting of an alumina octahedral layer sandwiched between two silica tetrahedral layers. The crystalline structure is continuous in the *a* and *b* directions, but stacked in the *c* direction. Carbon nanofibers are relatively inexpensive reinforcing agents composed of an inner filament made of highly graphitic carbon sheets packed as concentric cones which are aligned at a highly oblique angle along the fiber axis. The inner filament is covered with a turbostratic CVD carbon outer layer.

Clay nanocomposites were synthesized by stirring and sonication of organically modified clay into Dicyclopentadiene monomer, which caused expansion and further delamination of clay nanolayers (*In situ* polymerization). Highly delaminated composites were examined using x-ray diffraction, x-ray scattering and high resolution TEM. Composites with 0.5-1 weight percentage of clay showed improvements in Tg and flexural modulus. These composites were also studied using small angle neutron scattering (SANS) and ultra small angle neutron scattering (USANS). The slopes of scattering intensities,  $I(q)$ , versus wave vector,  $q$ , were in the range of  $-2.5$  to  $-2.7$ . The scattering intensities were fitted to the stacked disk

model. The resulting data were compared with HR-TEM analysis.

Carbon nanofibers (PR-19-HT) were dispersed within a resole phenolic resin, Hitco 134A to prepare CNF/phenolic nanocomposites. A solvent processing method was used to disperse 1-4 wt % CNF/phenolic resin composites. The viscoelastic properties of these composite were studied by DMTA. These showed improved glass transition temperatures with increases in CNF weight percent up to 4 wt %. The bending storage modulus below Tg was improved for all composites (1-4 wt %) relative to pure resin control samples. A major improvement in  $E'$  was observed at temperatures above the Tg, where the storage bending modulus stayed high up to  $\sim 300$  °C. Improvements in the CNF dispersion were studied by TEM. Better dispersions and surface wetting of the fibers were observed. TEM studies showed that fibers had diameters in the range of 50-100 nm and length in the range of 1-2 microns. Nanocomposites containing low weight percentages of CNF's (0.1-1 wt %) were further studied using SANS and USANS. When plotted on a logarithmic scale, the slope of the scattering intensities from particles as a function of wave vector,  $q$ , was in the range of  $-2.9$  to  $-3$  for the low  $q$  range. In the high  $q$  range,  $0.015$ - $0.07$  Å<sup>-1</sup>, the slopes were increased with increasing CNF concentrations.

#### **MP15: On the Structure of Liquid Hydrogen Fluoride**

*S. E. McLain (The University of Tennessee, Department of Chemistry; Intense Pulsed Neutron Source, Argonne National Lab), C. J. Benmore, J. E. Siewenie (Intense Pulsed Neutron Source, Argonne National Lab), J. F. C. Turner (The University of Tennessee, Department of Chemistry; Neutron Science Consortium)*

An experimental determination of the partial structure factors for liquid hydrogen fluoride has been in demand from theorists for more than two decades. However this is not a straightforward task, given the inherent difficulty of sample containment due to the chemically aggressive nature of the material. We present the first experimental determination of the partial structure factors  $S_{HH}(Q)$ ,  $S_{HF}(Q)$  and  $S_{FF}(Q)$  for liquid hydrogen fluoride at  $296 \pm 2$  K and  $1.2 \pm 0.2$  bar. This was accomplished by using a combination of isotopic substitution in neutron diffraction and high energy x-ray diffraction methods. Experiments were performed in custom built Alloy 400 cells. Despite the dearth of detailed experimental information, the structure of HF in the liquid state has been widely simulated using a variety of inter-atomic

potentials, as well as ab initio and quantum mechanical methods. The predictions range from the liquid being comprised of chains to clustering in the liquid state. Experimentally, the structure of the liquid is found to be composed of short, hydrogen-bound chains as evidenced by the hydrogen-fluorine partial correlation function. The results also show strong inter-chain interactions in the fluorine-fluorine partial radial distribution function. Reverse Monte Carlo modeling and coordination number analyses both indicate the existence of long winding chains with very little branching. The neutron diffraction data were collected on the Glass Liquids and Amorphous materials Diffractometer located at Intense Pulsed Neutron Source located and the high energy x-ray diffraction data were collect at the 11-IDC beam line on the BESSRC-CAT at the Advanced Photon Source, both located at Argonne National Laboratory.

**MP16: Application of Double Crystal Diffractometers for the Tomographic Reconstruction of Macroscopic Structures**

*M. Strobl, W. Treimer (University of Applied Sciences (TFH) Berlin; Hahn-Meitner-Institut Berlin), A. Hilger (Hahn-Meitner-Institut Berlin)*

Double crystal diffractometers (DCD) conventionally are applied for small angle scattering investigations in the ultra small angle range. In the case of neutrons (USANS) the  $q$ -range (app.  $10^{-4}$ - $10^{-1}$  nm $^{-1}$ ) overlaps and exceeds the range of small angle neutron scattering (SANS) experiments and enables the characterisation of structures with sizes up to some 10  $\mu$ m. It can be shown that such a high angular (momentum) resolution achieved by two perfect single crystals provides the possibility to investigate macroscopic structures in a range (in real space) between approximately 100  $\mu$ m up to several cm as well. Smallest beam deviations caused by refraction i.e., by phase gradients can be recorded. Combined with tomographic methods which means recording such data under several projection angles the macroscopic inner structure of test objects could be reconstructed with respect to different interactions within the sample. From the angular intensity distributions recorded in the DCD (stemming from defined beam paths) three sets of parameters could be deduced. The conventional parameter for tomographic imaging, the beam attenuation could be defined as well as a refraction and a USANS parameter. From each of them an independent reconstruction of the sample could be achieved containing redundant and/or complimentary (additional) (image) information about the sample. While the reconstruction from the beam attenuation parameter provides an image in terms of the attenuation coefficients, the refraction

parameter enables to reconstruct in terms of refractive index and the USANS parameter images areas of different scattering behaviour (different microscopic structure). The contrast behaviour is therefore not only dependent on the sample attenuation anymore as two more contrast methods could be introduced. Several examples will be given

**MP17: A Resonance Detector Technique Optimized for Inelastic Neutron Scattering Studies at the eV Energies in Condensed Matter**

*C. Andreani (Università degli Studi di Roma "Tor Vergata", Physics Department, Via della Ricerca Scientifica 1,00133 Italy; Istituto Nazionale per la Fisica della Materia), G. Gorini, E. Perelli-Cippo (Università degli Studi di Milano-Bicocca, Dipartimento di Fisica; Istituto Nazionale per la Fisica della Materia), A. Pietropaolo (Istituto Nazionale per la Fisica della Materia; Università degli Studi di Roma "Tor Vergata", Physics Department, Via della Ricerca Scientifica 1,00133 Italy), M. Tardocchi (Istituto Nazionale per la Fisica della Materia; Università degli Studi di Milano-Bicocca, Dipartimento di Fisica), E. M. Schooneveld (ISIS, Rutherford Appleton Laboratory), R. Senesi (Istituto Nazionale per la Fisica della Materia; Università degli Studi di Roma "Tor Vergata", Physics Department, Via della Ricerca Scientifica 1,00133 Italy), N. Rhodes (ISIS, Rutherford Appleton Laboratory)*

The talk will address a novel experimental neutron scattering technique (Resonance Detector Technique-RDT) suited for the study of high energy excitations in condensed matter. The technique is intended for neutron scattering experiments at very low angle scattering angle ( $1^\circ < 2\theta < 5^\circ$ ) on an inverse geometry instrument. It allows to perform High energy Inelastic Neutron Scattering (HINS) experiments in an extended (kinematical unlimited) energies transfer, i.e.,  $\omega < 300$  meV, coupled to low momentum transfer, i.e. in range  $3 \text{ \AA}^{-1} < q < 10 \text{ \AA}^{-1}$ . The RDT exploits a novel concepts for the detection of scattered neutrons at the eV energies, i.e., resonance radiative neutron capture for energy analysis. The detection system consists of scintillator detectors which are used to reveal the prompt  $\gamma$  radiation cascade emitted by an absorbing foil after resonance capture. The analyser foil is used as monochromator, to fix energy of neutron after scattering with the sample. The RDT principles will be revisited as compared to RFT (Resonance Foil Technique).

Systematic experimental work performed on VESUVIO in RDT configuration using NaI(Tl) and YAP scintillators as well as CZTe solid state detectors, will



be presented. The all set of detector devices were used coupled to a  $^{238}\text{U}$  analyser foils and experiments from a standard Pb samples and results compared to that measured in the standard RFS configuration.

Results from a series of HINS experiments, off ice and water, performed on the VESUVIO spectrometer operating at the ISIS pulsed neutron source, will be discussed. The instrument was specifically sets up in the Resonance Detector Spectrometer (RDS) configuration. These results well compared with previous best available results on the same system obtained through an Inelastic Neutron Scattering on a direct geometry instrument. In the case of ice the hydrogen projected density of states has been successfully derived. In water experimental results include the mean kinetic energy in water. As in previous example on ice, a satisfactory agreement is found with values of  $\langle E_k \rangle$  available from previous experiments.

Future development of this technique will be discussed, new areas of experimental research envisaged. These include energy excitations in condensed matter systems: dispersion relations of high energy excitations in metals, semiconductors and insulators, high lying molecular rotational-vibrational states, molecular electronic excitations and electronic level in solids.

#### **MP18: Search for Time-Reversal Violation in Neutron Beta Decay**

*H.P. Mumm (University of Washington), L.J. Broussard (Tulane University), T.E. Chupp, R.L. Cooper, K.P. Coulter (University of Michigan), M.S. Dewey (National Institute of Standards and Technology), S.J. Freedman, B.K. Fujikawa (University of California-Berkeley/LBNL), A. Garcia (University of Washington), S.R. Hwang (University of Michigan), G.L. Jones (Hamilton College), L.J. Lising (University of California-Berkeley/LBNL), J.S. Nico (National Institute of Standards and Technology), R.G.H. Robertson (University of Washington), A.K. Thompson (National Institute of Standards and Technology), C. Trull, F.E. Wietfeldt (Tulane University), J.F. Wilkerson (University of Washington)*

The emiT experiment tests time-reversal symmetry in the beta decay of polarized free neutrons by searching for the triple correlation  $D\sigma \cdot p_e \times p_p$ , where  $\sigma$  is the neutron spin and  $p_e$  and  $p_p$  are the decay product momenta for the electron and proton, respectively. A nonzero  $D$ -coefficient above the small effect from final state interactions would be a signal of direct time reversal symmetry (T) violation, independent of charge conjugation-parity (CP)

violation. Various extensions to the Standard Model, such as lepto-quarks and left-right symmetry, can give rise to a  $D$ -coefficient yet do not generate measurable electric dipole moments. Consequently, it is important to place the strongest possible limits in neutron decay. In December of 2003 the emiT collaboration completed a successful data run at NIST. In this run, more than  $3 \times 10^8$  neutron decays were measured, and a signal-to-background ratio of approximately 100:1 was obtained. Analysis of the data is underway, and the collaboration is optimistic that an improved limit on the  $D$ -coefficient will be achieved. Along with a discussion of theoretical motivation and the experimental technique, the status of the analysis and studies of systematic uncertainties will be presented. This work is supported by DOE, NSF, and NIST.

#### **MP19: Structure and dynamics of Inorganic nanoparticles templated by soft copolymer cubic structures**

*D.C. Pozzo, L.M. Walker (Department of Chemical Engineering, Center for Complex Fluids Engineering, Carnegie Mellon University, Pittsburgh PA)*

The design of nanometer scale inorganic-organic composites is one of the most exiting areas of material science and engineering. Particular attention is given to structured materials whose order arises at the molecular level but persists over macroscopic length scales. This is driven by the potential that these new materials have in the development of optics, electronics, catalysts, biotechnology devices and in manufacturing materials. Theoretical approaches demonstrate the phase richness of nanoparticles embedded in amphiphilic copolymer mesophases, but there is a lack of systematic experimental studies that characterize the influence of inorganic fillers on the 3D organized structures. We are utilizing water-soluble triblock copolymers (PEO-PPO-PEO) to provide thermoreversible micellar-cubic templates with typical dimensions of tens of nanometers. Using rheology and small-angle neutron scattering (SANS), we characterize the influence of the addition of inorganic nanoparticles (of similar dimensions to the block copolymer micelles) on the macroscopic sample properties and on the local structure. Using contrast matching techniques we demonstrate that the template approach is feasible as reasonable quantities of hydrophilic inorganic nanoparticles are incorporated into the block copolymer mesosphere without destroying the structure. It is also found that the cubic structure is transmitted to the silica particles and that the level of templating is dependent on a number of variables. We quantify the

results by studying the influence of relative concentration, relative dimensions and surface chemistry of the inorganic particles. Additionally, using dynamic light scattering (DLS) and contrast-matched neutron spin echo (NSE) experiments we individually study the complex motions of the various components that make up the composite materials. Furthermore the ability to alter these structures using a variety of external parameters including shear and temperature make these materials of considerable interest as processable templates for inorganic-organic nanocomposites.

**MP20: New structural model for Nafion® membranes and Study of proton dynamics**

*O. Diat (UMR 5819 SPrAM CEA Grenoble 17 Av des Martyrs, 38054 Grenoble cedex 9 France), L. Rubatat (UMR 5819 SPrAM CEA Grenoble 17 Av des Martyrs, 38054 Grenoble cedex 9 France; Department of Physics, Simon Fraser University, Burnaby, Canada)*

A global understanding of the ionomer Nafion® membrane structure, a benchmark system, from the Ångström up to the micrometer in relation with the transport properties, is essential for the optimisation of H<sub>2</sub>/O<sub>2</sub> fuel cell system.

We propose a new fibrillar structural model, based on polymeric chains aggregation in elongated objects, decorated with charges to explain i) the swelling process from the dry membrane to colloidal suspension, ii) the birefringence properties, iii) and the mechanical degradation in fuel cell operation. By using small angles scattering techniques (x-rays & neutrons) and microscopy (AFM & TEM), we have studied the polymer arrangement in bundles over a large range of scale and water content. Drawing experiments have permitted to confirm our model. The main characteristic of the material being to exhibit a hierarchical multi-scale structure, from nanometric aggregates to micronic domains of varying densities, the relaxation times associated to the proton dynamics in these systems are expected to range from the pico-second (local jump) to few tenths of seconds (macroscopic conductivity).

We have started a complete study of the proton dynamics with various complementary techniques, in order to couple these results to the knowledge that we have now on the structure. Quasi-elastic neutron scattering studies allowed to measure correlations at very short times (pico-second) and gradient field-pulsed NMR allows to measure macroscopic diffusion coefficients in the range of few milliseconds to few seconds. Intermediary region in between is directly accessible by the field cycling NMR relaxometry

technique. Our paper is more especially dedicated to the interest of “neutron” tools in using contrast variation method for SANS and QENS.

*A.L. Rollet et al., J. Phys. Chem B 106(12), (2002) 3033-3036.  
L.R. Rubatat et al., Macromolecules 35(10), (2002) 4050-4055.  
L. Rubatat et al. under submission to Macromolecules;  
P. van der Heijden et al. submitted to Macromolecules.*

**MP21: Highly Stable Phospholipid Unilamellar Vesicles from Spontaneous Vesiculation: A DLS and SANS Study**

*B. Yue, C-Y. Huang (Chemical Engineering Dept. NJIT), M-P. Nieh (National Research Council, Chalk River, Ontario, Canada), C. J. Glinka (National Institute of Standards and Technology), J. Katsaras (National Research Council, Chalk River, Ontario, Canada)*

Spontaneously formed unilamellar vesicles (ULVs) composed of short- and long-chain phospholipids, dihexanoyl (DHPC) and dimyristoyl phosphorylcholine (DMPC) mixtures doped with negatively charged dimyristoyl phosphorylglycerol (DMPG) were studied by small angle neutron scattering (SANS) and dynamic light scattering (DLS). Vesicle formation was found to follow a quick bicelle-to-vesicle transition mechanism. The SANS and DLS data showed that ULVs with narrow size distribution were highly stable at low lipid concentrations,  $C_{lp} < 0.50$  wt. %, and salt concentrations ( $C_s$ ). ULV size was found independent of both  $C_{lp}$  and  $C_s$ , when they were below 0.33 wt. % and 0.5 wt. % respectively. Surface charge is found to be an important factor for stabilizing ULVs with a constant size. This observation is not in total agreement with most previous experimental results and cannot be completely explained with previous theoretical predications based on equilibrium calculations for catanionic surfactant mixtures. The size of ULVs was almost constant over a wide temperature range below and above the phase transition temperature of DMPC, TM, for months, even after sonication.

**MP22: Suppression of Dewetting in Polystyrene Thin Films by Polymer Nanoparticles**

*H. Feng, R. M. Briber (Department of Materials Science and Engineering, University of Maryland), V. Y. Lee, R. D. Miller, Ho-Ch Kim (IBM Almaden Research Center, 650 Harry Road, San Jose CA 95120-6099)*

The influence of nanoparticles based on star polymers on the dewetting of spun-cast linear polysty-



rene (PS) films is investigated as a function of temperature. The star polymers have polystyrene-benzocyclobutene copolymer arms which can undergo intra-molecular crosslinking to form more compact nanoparticles. The addition of a small amount of nanoparticles (either the uncrosslinked star polymer or the intra-molecular crosslinked polymer) to the linear PS leads to inhibition of dewetting in thin (30 nm) films on silicon wafer substrates at 175°C. The different dewetting behavior between films containing the uncrosslinked star polymers or the crosslinked nanoparticles suggests that the system has the potential for tunable dewetting behavior, depending on the specifics of the star molecules. Neutron reflection (NR) measurements indicate there is an enrichment of nanoparticles at the polymer-silicon interface in as-cast PS films, and this segregation may be related to the suppression of dewetting in PS films by nanoparticles. Small angle neutron scattering data shows bulk PS are miscible with 5 wt % of nanoparticles over the temperature range of 23 °C to 175 °C, implying that the segregation is not due to the immiscibility of PS and nanoparticles.

#### **MP23: Effect of Molecular Architecture on the Pore Structure of Nanoporous**

##### **Poly(methylsilsequioxane) Thin Films**

*Z. Lin, R. M. Briber (Department of Materials Science and Engineering, University of Maryland), H. C. Kim, W. Volksen, R. D. Miller (IBM Almaden Research Center, 650 Harry Road, San Jose CA 95120-6099)*

Thin films of poly(methylsilsequioxane) (PMSSQ) containing nanoscopic pores are one of promising materials for ultra low dielectric constant interconnect material in next generation microchips. A viable route to nanoporous PMSSQ films is using the phase separation between matrix PMSSQ and organic polymers (porogen) with subsequent degradation of the porogen at high temperature. Previous studies show the pore size and morphology depend on the interaction between PMSSQ and porogen, molecular architecture and amount of porogen. In this study, we examine the effect of porogen molecular architecture on the phase behavior and final pore morphology of nanoporous PMSSQ using small angle neutron scattering (SANS), neutron reflectivity (NR) and transmission electron microscopy (TEM). A linear and a star shaped polymer were used as porogens. SANS experiments were performed as a function of temperature. TEM was used to confirm the pore morphologies. Depth profiles of pore distribution obtained by neutron NR will be also addressed.

#### **MP24: Characterization of Arborescent Graft Polystyrene Molecules by Small Angle Neutron Scattering**

*Kai-Chi Lai, Robert M. Briber (Department of Materials Science and Engineering, University of Maryland), Mario Gauthier (Department of Chemistry, Institute for Polymer Research, University of Waterloo, Waterloo, Ontario N2L 3G1, Canada), Seok-Il Yun (Condensed Matter Sciences Division, Oak Ridge National Laboratory)*

Arborescent graft polymers (AGP) are polymers resulting from successive cycles of random functionalization and subsequent end-grafting of anionic polymerized chains to form a highly branched polymer molecule. Small Angle Neutron Scattering (SANS) was used to characterize the size and shape of generation 3 and generation 4 polystyrene (PS) based arborescent graft polymers where the final generation of the polymer molecule was composed of deuterated PS. Contrast variation techniques were used to match the solvent to the either the PS core or the deuterated PS shell. A core-shell model was used to fit the SANS data with good success but the scattering length density of the core and shell were found to deviate from that of pure PS and deuterated PS respectively leading to the conclusion that there is some phase mixing between the final generation and the underlying polymer substrate molecule. This is consistent with the random functionalization of substrate prior to end-grafting the final generation.

#### **MP25: Water Mobility in Small Aerosol-OT Reverse Micelles**

*M. R. Harpham, N. E. Levinger, B. M. Ladanyi (Colorado State University), K. W. Herwig (Oak Ridge National Laboratory)*

Reverse micelles (RMs) are nanoscale droplets of polar solvent surrounded by a surfactant layer in nonpolar solvents. We have used quasielastic neutron scattering (QENS) to investigate the mobility of water molecules in small reverse micelles consisting of water/deuterated AOT/perdeuterated isooctane. Water/surfactant ratios of 1, 2.5, and 5 have been investigated using the QENS spectrometer at Argonne National Laboratory, IPNS division. This experimental data is reasonably well-fit by a jump-diffusion/isotropic rotation model, and gives diffusion constants that increase with  $w_0$  and rotational correlation times that decrease with  $w_0$ . Computer simulations of reverse micelles of these water/surfactant ratios have been performed and used to predict QENS spectra to further investigate the dynamics of the water and make comparisons to experimental data. A Fourier transform of the

simulation data convolved with the experimental instrument resolution function compares favorably to the experimental data. The simulations indicate that the dynamics of water is slower near the interface than at the core, and slower for small RMs than for large RM's. A mode coupling theory (MCT) analysis of the translational intermediate scattering function was performed. Results from this analysis indicate highly nonexponential behavior, and relaxation times that decrease as  $w_0$  increases.

#### **MP26: Nucleation of Phase Separation in Polymer Blends**

*T.J. Rappl (Department of Chemical Engineering, University of California, Berkeley), N.P. Balsara (Department of Chemical Engineering, University of California, Berkeley; Material Sciences Division, and Environmental Energies Technology, Lawrence Berkeley National Laboratory)*

The work presented is intended to supplement the material covered in the talk given by Nitash Balsara concerning nucleation of phase separation in polymer blends. In this work, neutron scattering was employed to investigate the nature of the structures formed during the onset of homogeneous nucleation, specifically, how the critical nucleus size varies with quench depth. Time-resolved small angle neutron scattering profiles were obtained from off-critical blends within the metastable regime of the phase diagram, revealing that the critical nucleus size decreases with increasing quench depth; this contradicts the theoretical prediction of Cahn and Hilliard that the critical nucleus size should diverge at the spinodal. Recent simulations (Chandler) of nucleation in the 3D Ising model are in agreement with our experimental data.

Additionally, within the metastable regime of a given blend we observed a line of demarcation below which phase separation could not be observed during experimental time scales via a direct quench. This line of demarcation corresponds well with the pseudospinodal, or limit of metastability, proposed by Z.-G. Wang. A series of double quench experiments were performed, wherein the system was studied consecutively at two separate locations within the metastable regime. A comprehensive comparison of the results obtained from direct quench and double quench experiments will be presented. Of note, this double quench method permitted the study of nucleation below the limit of metastability and also revealed the dissolution of small structures (created while aging below the limit of stability) upon the reduction of quench depth. This dissolution of small structures lends credibility to our notion of the critical

nucleus size as measured by time-resolved small angle neutron scattering.

#### **MP27: Size and shape of mixed micelles of non-ionic surfactants: puzzles and resolution**

*R. Zhang, P. Somasundaran (Columbia University), C. Glinka, B. Hammouda (NIST Center for Neutron Research), P. Cummins (Estee Lauder), Q. Zhou (Columbia University)*

Mixed surfactants are of considerable interest because of synergy in surface activity which depends on compatible molecular interactions. In this regard, in order to develop molecular structure-property relationships that control relevant colloidal phenomenon in mixed surfactant systems and to develop predictive theoretical models based on such relationships, it is necessary to acquire quantitative information on size and shape of micelles in these complex systems. Micellar shape has been correlated in this work with packing parameter for mixing and surfactant molecular structures in dilute solutions of binary nonionic polyethylene oxide nonyl phenol ethoxylated decyl ether (NP-10) / nonionic sugar-based n-dodecyl- $\beta$ -D-maltoside (DM) system using a multi-pronged approach. The packing results suggest that micelles undergo a sphere to cylinder transition with an increase in DM percentage. However, experimental results from SANS (small angle neutron scattering) along with those from analytical ultracentrifuge, cryo-TEM, FT-PGSE (pulsed gradient spin echo)-NMR contradict this prediction. By comparing the energy changes due to packing using molecular modeling, NP-10 is found to prefer to form close packed geometry in water. In order to account for these effects, we modify the packing parameter by taking molecular conformation and mixing into consideration.

#### **MP28: Rheo-SANS microstructure investigations of concentrated anisotropic particle dispersions near the shear thickening transition**

*R. G. Egres, N. J. Wagner (Department of Chemical Engineering, University of Delaware, Newark, DE 19716), L. Porcar, B. S. Greenwald (NIST Center for Neutron Research; University of Maryland, College Park)*

An experimental Rheo-SANS configuration with rheologically accurate quartz shear cell is described and validated using a rheometer in the NG7 SANS beamline at NIST. Rheo-SANS experiments were performed on concentrated dispersions of anisotropic particles exhibiting shear thickening behavior as a means of exploring microstructure evolution during shear flow. Concentrated dispersions of anisotropic particles exhibiting shear thickening behavior are

ubiquitous in industry, yet little has been done to investigate the microstructure of these dispersions during flow in order to obtain a mechanistic understanding of this observed rheological behavior. Our research involves rheological and microstructural investigations of stable polyethylene glycol based dispersions of acicular precipitated calcium carbonate (PCC) particles having three average particle aspect ratios. Rheological measurements performed on these dispersions demonstrate that increased particle aspect ratio results in extensive (discontinuous) shear thickening behavior at lower particle volume fractions. Small angle neutron scattering measurements have been used to determine particle geometry and microstructure as a function of concentration and aspect ratio. Rheo-SANS experiments show a significant degree of particle alignment with flow direction at low to moderate shear rates. Surprisingly, this alignment is maintained at the higher stresses associated with shear thickening. These observations invalidate earlier hypothesis suggesting that the shear thickening observed in anisotropic particle dispersions was the result of particle rotations out of flow alignment leading to particle jamming. Rather, the Rheo-SANS measurements support the hydrocluster mechanism of shear thickening known for spherical particle dispersions.

#### **MP29: De-Convoluting the Influences of Plastic Deformation and Heat on Residual Stresses during Friction Stir Welding of 6061-T6 Aluminum Plates**

*W. Woo (Material Science and Engineering Department, University of Tennessee, Knoxville, TN 37996, USA), H. Choo (Material Science and Engineering Department, University of Tennessee, Knoxville, TN 37996, USA; Metals and Ceramics Division, Oak Ridge National Laboratory), D. W. Brown (Materials Science and Technology Division, Los Alamos National Laboratory, Los Alamos, NM 87545, USA), Z. Feng (Metals and Ceramics Division, Oak Ridge National Laboratory), P. K Liaw (Material Science and Engineering Department, University of Tennessee, Knoxville, TN 37996, USA), S. A. David, C. R. Hubbard (Metals and Ceramics Division, Oak Ridge National Laboratory)*

Friction-stir welding (FSW) is a solid-state joining process that makes a strong metallurgical bonding through (1) a severe plastic deformation caused by rotation of a stirring pin and (2) frictional heat generated from pressing shoulder. However, the deformation and heat necessary for the joining are also the major sources of residual stresses in the welds, which are detrimental to the integrity of the joined component.

Three different weld specimens were prepared from

6061-T6 Aluminum plates: (Case 1) a plate processed only with pin, (Case 2) a plate processed only with the pressing shoulder, and (Case 3) a plate processed with both stirring pin and the pressing shoulder, i.e., a regular friction-stir weld. The longitudinal, transverse, and through-thickness strain components were measured across the weld line using neutron diffraction and converted to stresses. The comparison among the three cases shows distinctly different residual-stress profiles clearly revealing de-convoluted effects from the different welding parameters, i.e., deformation, heat, or the combination, for the first time. The relationships between the welding parameters and residual stresses will be discussed to provide a phenomenological understanding of the micro-mechanism of the residual stress formation during the FSW.

*Acknowledgements:* This work benefited from the use of the Los Alamos Neutron Science Center (LANSCE) at the Los Alamos National Laboratory. This facility is funded by the US Department of Energy under Contract W-7405-ENG-36. This work is supported by the NSF International Materials Institutes program under DMR-0231320.

#### **MP30: Effect of Internal Stress on Hydride Formation in a Hydrogen-Charged Zircoly-4**

*E. Garlea (Department of Materials Science and Engineering, The University of Tennessee, Knoxville, TN 37996, USA.), H. Choo (Department of Materials Science and Engineering, The University of Tennessee, Knoxville, TN 37996, USA.; Metals and Ceramics Division, Oak Ridge National Laboratory), D. W. Brown (Los Alamos National Laboratory), S. Park, L. L. Daemen (Los Alamos Neutron Science Center, Los Alamos National Laboratory), B. Yang, M. M. Morrison, R. A. Buchanan, P. K. Liaw (Department of Materials Science and Engineering, The University of Tennessee, Knoxville, TN 37996, USA.), C. R. Hubbard (Metals and Ceramics Division, Oak Ridge National Laboratory), H. F. Letzring (Pretreatment and Specialty Products, PPG Industries, Troy, MI 48083)*

Hydride formation is one of the main degradation sources of zirconium alloys in hydrogen-rich environments. When sufficient hydrogen is available in these alloys, zirconium-hydride precipitates can be formed. Cracking of the brittle hydrides near a crack tip can initiate crack growth between hydrides leading to premature failure of the material. Hydride formation is believed to be enhanced by the presence of residual or applied stresses. Therefore, the increase in stress field ahead of a crack tip may promote precipi-



tation of additional hydrides. In order to verify this, we investigated the effect of internal stresses on zirconium-hydride-precipitate formation in a zircaloy-4 alloy using neutron and x-ray diffraction.

First, spatially-resolved internal strain measurements were made on a fatigue pre-cracked compact-tension (CT) specimen using *in situ* neutron diffraction under applied loads of 667 and 4,444 newtons. The results provided a basic understanding of the strain profiles near the crack tip. Second, hydride formation was investigated using two different specimens: (1) a CT specimen with a fatigue pre-crack, hence with a built-in internal stress and (2) the same CT specimen but without the pre-crack. The two specimens were electrochemically charged with hydrogen under the same conditions x-ray diffraction results clearly showed that the pre-cracked specimen developed higher hydride fractions suggesting that the enhanced hydride formation was due to the presence of the internal stress. Finally, the profile of internal strains in the hydrogen-charged specimen was measured using neutron diffraction to provide an understanding of the effect of hydride on the strain profile near the crack tip in comparison to the strain data measured from a CT specimen before the hydrogenation.

*Acknowledgements:* This work benefited from the use of the Los Alamos Neutron Science Center (LANSCE) at the Los Alamos National Laboratory. This facility is funded by the US Department of Energy under Contract W-7405-ENG-36. The authors are grateful to the National Science Foundation International Materials Institutes Program (DMR-0231320), Integrative Graduate Education and Research Training Program (DGE-9987548), the NSF Combined Research and Curriculum Development Programs (EEC-9527527 and EEC-0203415), and Tennessee Advanced Material Laboratory Fellowship Program, managed by Drs. C. Huber, W Jennings, L. Goldberg, M. Poats, and Dr. W. Plummer, respectively.

### MP31: Residual Strain Distribution around Luders Bands

Y. Sun, B. Yang, T. A. Saleh, B. L. Benson, P. K. Liaw (Department of Materials Science and Engineering, The University of Tennessee, Knoxville, TN 37996, USA.), H. Choo (Department of Materials Science and Engineering, The University of Tennessee, Knoxville, TN 37996, USA.; Metals and Ceramics Division, Oak Ridge National Laboratory), M. R. Daymond (ISIS, Rutherford Appleton Laboratory), J. Y. Huang, R. C. Kuo (Institute of Nuclear Energy Research (INER), P. O. Box 3-14, 1000 Wenhua Road, Chiaan Village, Lungtan, Taiwan 325,

Republic of China), J. G. Huang (Taiwan Power Company, Taipei, Taiwan)

Lüders bands often indicate the onset of the plastic deformation at the vicinity of stress concentrations and inclusions, which may contribute to the crack initiations. Investigating the evolution process of Lüders bands will help understand the early stages of the mechanical damage behaviors. In the current research, Lüders bands have been developed on the plate samples of reactor pressure vessel (RPV) steel during fatigue tests. *In situ* thermography detection technique has been applied to control the amount of plastic deformation created by the Lüders bands. Two specimens with different amount of plastic deformation (with plastic strains of 1.25% and 1.83%) were prepared. Residual-strain distributions inside and outside the Lüders bands have been measured by neutron diffraction technique in various directions using ENGIN-X instrument at the ISIS Facility. Inside the Lüders bands, compression residual strain has been detected in the gauge-length direction, while tensile residual strain has been detected in the gauge-width direction. Outside the Lüders bands, the residual strains were close to zero. Based on the neutron results, theoretical models to provide better understanding of the Lüders-bands evolution processes have been attempted.

*Acknowledgement:* We would like to give thanks to (1) The National Science Foundation (NSF) International Materials Institutes (IMI) Program, Under DMR-0231320. (2) Combined Research-Curriculum Development (CRCD) Program, under EEC-9527527 and EEC-0203415. (3) The Integrative Graduate Education and Research Training (IGERT) Program, under DGE-9987548, with Dr. C. Huber, Ms. M. Poats, Dr. W. Jennings and Dr. L. Goldberg, as the contract monitors, respectively. (4) Mr. D. Fielden who machined the samples and grips for us.

### MP32: Development of Internal Strains During the Fatigue of Haynes 230 Nickel Based Superalloy

T. A. Saleh, M. L. Benson (Department of Materials Science and Engineering, The University of Tennessee, Knoxville, TN 37996, USA.), H. Choo (Department of Materials Science and Engineering, University of Tennessee, Knoxville, TN 37996, USA.; Metals and Ceramics Division, Oak Ridge National Laboratory), D. W. Brown (Los Alamos Neutron Science Center, Los Alamos National Laboratory), P.K. Liaw, R. A. Buchanan (Department of Materials Science and Engineering, University of Tennessee, Knoxville, TN 37996, USA.), D. L. Klarstrom (Haynes International, Inc., Kokomo, IN 46904, USA.), D.G. Park (Korea Atomic Energy Research

*Institute, Yuseong P.O. Box 105, Daejeon, 305-600, Korea)*

Haynes 230 is a solid solution strengthened, FCC, nickel based superalloy. This alloy is commonly used in flying and land-based turbines, and in other fatigue intensive applications. *In situ* neutron diffraction was used to investigate the behavior of internal strains in this alloy under both strain-controlled tension/compression, and stress-controlled tension/tension fatigue conditions. Experiments took place at the Spectrometer for Materials Research at Temperature and Stress (SMARTS) facility at the Los Alamos Neutron Science Center (LANSCE) and at the ENGIN-X spectrometer at ISIS. Residual strains were seen to develop and saturate during the first 100 fatigue cycles. Little, if any, strain relaxation was noted as 85 % of the fatigue life was reached. Characteristics of both *in situ* lattice strains and residual strains in various hkl directions during the fatigue deformation will be discussed in comparison to those observed during monotonic tensile testing.

Acknowledgements: The author acknowledges the financial support of the National Science Foundation, the Integrative Graduate Education and Research Training (IGERT) Program, under DGE-9987548, and the International Materials Institutes (IMI), under DMR-0231320, to the University of Tennessee, Knoxville, with Dr. W. Jennings, Dr. L. Goldberg, and Dr. C. Huber as contract monitors, respectively.

### **MP33: Strain and Texture Analysis of the Ferroelastic Behavior of $\text{Pb}(\text{Zr,Ti})\text{O}_3$**

*R. C. Rogan, E. Ustundag, S. M. Motahari (Department of Materials Science, California Institute of Technology, Pasadena, California 91125), M. R. Daymond (ISIS, Rutherford Appleton Laboratory)*

*In situ* uniaxial compression experiments were performed on various  $\text{Pb}(\text{Zr,Ti})\text{O}_3$  or PZT ceramics using neutron diffraction. PZTs near the edge of the morphotropic phase boundary as well as single-phase (tetragonal and rhombohedral) specimens were investigated. Analysis of the diffraction patterns allowed for observation of the onset and culmination of domain switching through modeling of the sample texture using the March-Dollase approach. This model also provided quantitative information about domain switching under applied stress. Elastic lattice strain data suggested a high degree of anisotropy and a complicated internal stress state. The effectiveness of electrical poling and mechanical depoling was also evaluated. The contrast between single and multiphase systems will be highlighted. Results will be compared to the predictions of a new self-consistent mechanics model of ferroelectric constitutive behavior.

### **MP34: Neutron Residual Stress Measurements of Aluminum Cold Spray Coating**

*L. Li (State University of New York, Stony Brook, NY 11794-2275), V. Luzin (National Institute of Standards and Technology; State University of New York, Stony Brook, NY 11794-2275), R. Neiser (Sandia National Laboratories, Albuquerque, NM 87123), H.-J. Prask (National Institute of Standards and Technology), S. Sampath (State University of New York, Stony Brook, NY 11794-2275)*

Cold spray technology is a novel method for producing dense, oxide free coatings with some other specific qualities that can not be easily achieved by the traditional thermal spray technique. Cold spraying process involves high particle velocities and impact momentum and less or no thermal input so that splat formation and coating deposition is very different from the “conventional” thermal spray process. Consequently residual stress formation is different for this process. It has been speculated that cold spraying produces significantly lower residual stresses than thermal spraying. This investigation was intended to elucidate this question and provide quantitative results on this subject.

In this study we investigated residual stress distribution in the aluminum-coating-on-aluminum-substrate sample by means of neutron diffraction. Neutron diffraction stress measurements were performed on the BT8 diffractometer at the NIST Center for Neutron Research (NCNR) with spatial resolution 0.5 mm through thickness using a gauge volume of  $0.5 \times 0.5 \times 7 \text{ mm}^3$ . The substrate thickness is approximately 3 mm and the coating thickness is about 2 mm, so that this spatial resolution is sufficient to obtain reliable through-thickness profiles of the in-plane stress distribution. Special care was taken for measurements of near-surface points. Since sample surface preparation before spraying involves sand (grit) blasting, which is known to produce residual stresses too, additional experiments on a substrate-only sample were done to determine the initial stress state of the substrate before spraying. Other methods of material characterization (electron microscopy, indentation, etc.) were employed to understand better the coating performance.

### **MP35: Quantum Critical Phase Diagram of a Quantum Magnet**

*M. B. Stone (Johns Hopkins University; Penn State University), C. Broholm (Johns Hopkins University; NIST Center for Neutron Research), D. H. Reich (Johns Hopkins University), I. Zaliznyak (Brookhaven National Laboratory), P. Vorderwisch (Hahn-Meitner-Institut Berlin), N. Harrison (National High Magnetic Field Laboratory (LANL))*



Piperazinum hexachlorodocuprate (PHCC) has been shown to be a quasi-two-dimensional Heisenberg antiferromagnet with a bilayer structure (M. B. Stone et al. PRB, **64**, 144405 (2001)). The bilayer structure and frustrated interactions leads to a cooperative singlet ground state at  $T = 0$  and  $H = 0$ . We present the field-temperature phase diagram of this unique quantum spin liquid as determined by neutron scattering and high field magnetic susceptibility measurements. Two field dependent quantum critical points were accessed:  $H_{c1} = 7.6$  T which is the field that closes the spin-gap and leads to three-dimensional long-range order for sufficiently low  $T$  and  $H_{c2} = 37$  T where the system transitions to a field induced ferromagnetic state. A gapless disordered phase with short-range spin correlations encloses the antiferromagnetically ordered phase in the field-temperature phase diagram. Close to the low field quantum critical point, a minimum in the phase boundary to long-range order indicates that weak interactions with lattice or nuclear spin degrees of freedom become important.

**MP36: NIST-DCS Neutron Measurements of Lattice Disorder in a dilute Ge-Si Crystal and in a Null-matrix  $^{62}\text{Ni}$ -Pt Alloy Crystal**

*J.A. Rodriguez, S.C. Moss (Physics Department, University of Houston), J.L. Robertson (Oak Ridge National Laboratory), J.R.D. Copley, D.A. Neumann (NIST Center for Neutron Research), J. Major, V. Bugaev, H. Reichert, H. Dosch (Max Planck Institute fuer Metallforschung, Stuttgart)*

Using the disk chopper spectrometer (DCS) at NIST in an elastic scattering mode, we have investigated two alloy crystals: 1) a dilute alloy of Ge in Si ( $\sim 10\%$ ) and 2) a null-matrix crystal of  $^{62}\text{Ni}_{0.52}\text{Pt}_{0.48}$ , so chosen ( $^{62}\text{Ni}$  has a negative scattering length) that all effects depending on the average lattice scattering (Bragg peaks and Huang diffuse scattering (HDS—due to displacement-displacement correlations) vanishes while the short-range order (SRO) and cross correlation between concentration and displacements, often called the size effect scattering (SE), are now given by the sum of the absolute values of the scattering lengths of the two components.

The Si-Ge crystal was initially studied in the  $(-110)$  plane in reciprocal space. After removing the can scattering and normalizing the data, the planar plot from this (previously determined) random alloy showed pronounced fans of diffuse scattering emanating strongly on the low angle side of the Bragg peaks. Selected asymmetric line scans confirmed our earlier SE and HDS scan (1) along  $\langle 110 \rangle$ , a sure sign that the size of Ge is larger than Si and its

displacement field extends to distant neighbors. This data is currently being analysed in Stuttgart by Prof. Bugaev and his students and additional scans in the (001) plane are underway.

The null-matrix data are truly extraordinary. There are only tiny specks of Bragg peaks (useful for alignment) and absolutely no HDS about the Bragg positions. The SRO and SE scattering are quite prominent and are being analysed in real space by Rodriguez and Robertson to extract both SRO and individual species-dependent displacements for each coordination shell, and in k-space by Prof. Bugaev and his colleagues.

The results as they come out will be discussed in the context of the electronic theory of alloy phase stability, determined from data above  $T_c$ , the first order phase transition temperature.

[1] D. LeBolloc'h et al., Phys. Rev. B **63**, 035204 (2001)

Research supported in Houston by the NSF on DMR-0099573

**MP37: Recent Neutron and X-ray Scattering Studies of the Electron-Doped Superconductor  $\text{Nd}_{2-x}\text{Ce}_x\text{CuO}_4$**

*P.K. Mang (Department of Applied Physics, Stanford University), M. Greven (Department of Applied Physics, Stanford University; Stanford Synchrotron Radiation Laboratory)*

We have performed a series of studies on the electron-doped high temperature superconductor  $\text{Nd}_{2-x}\text{Ce}_x\text{CuO}_4$ . Inelastic magnetic neutron scattering measurements of the evolution of the spin-spin correlation length with doping and temperature in non superconducting samples have revealed that magnetic correlations in the system are described at a quantitative level by the randomly diluted square-lattice quantum Heisenberg antiferromagnet (SLHAF) [1]. However the low temperature ordered moment evolves more rapidly than for the SLHAF, suggesting that quantum fluctuations manifest themselves differently for different observables. High energy resolution ( $\sim 6$  meV) inelastic x-ray scattering (IXS) has identified an anomalous softening of the highest energy ( $\sim 70$  meV) longitudinal optical phonon branch [2]. Similar features have been observed via neutron scattering in the hole-doped cuprate superconductors and a related “kink” structure was observed in the electronic dispersion by photoemission studies. These features have been interpreted as evidence for a strong electron-phonon coupling in the cuprate superconductors. We have established the existence of such a feature in NCCO, and determined that the feature is formed for concentrations  $x >$

0.04. Using x-ray diffraction we have established that the oxygen-reduction procedure commonly employed to induce superconductivity in NCCO results in the decomposition of a small fraction (0.1 % to 1 %) of the sample to a cubic phase of  $\text{Nd}_2\text{O}_3$  [3]. This secondary phase forms epitaxially with the copper-oxygen plane, but extends only a few lattice constants along the c-axis. A subset of structural diffraction peaks of the secondary phase overlap magnetic reflections associated with NCCO in reciprocal space, and at low temperatures the application of a magnetic field results in a dramatic polarization of the moment of the Neodymium atoms. These two effects have led others to mistakenly report the existence of a quantum phase transition from a superconducting to an antiferromagnetic phase.

[1] P.K. Mang et al., cond-mat/030793 (2003).

[2] M. d'Astuto et al., Phys. Rev. Lett. 88, 167002 (2002).

[3] P.K. Mang et al., Nature 426, 139 (2003).

#### **MP38: Nature of Jahn-Teller distortion in $\text{LaMnO}_3$ : order to disorder**

*X. Qiu, S. J. L. Billinge (Department of Physics and Astronomy, Michigan State University, E. Lansing, MI, 48824), Th. Proffen (Los Alamos Neutron Science Center, Los Alamos National Laboratory)*

One fully Jahn-Teller (JT) distorted  $\text{MnO}_6$  octahedron in the undoped  $\text{LaMnO}_3$  contains two long (2.16 Å), two medium (1.96 Å), and two short (1.92 Å) Mn-O bonds. The low temperature orthorhombic phase results from the long range cooperative ordering of the JT distorted orbitals (long and short Mn-O bonds alternating in *ab* plane). Excellent agreement between local and average structure studies confirms the static nature of the JT distortion. At high temperatures across the Jahn-Teller structural phase transition, average structure studies found that the  $\text{MnO}_6$  octahedron has six almost equidistant Mn-O bonds ( $\Delta d < 0.05$  Å), and the high temperature orthorhombic phase is pseudo cubic. However, evident from local structure studies, the  $\text{MnO}_6$  octahedra are *fully* JT distorted at all temperatures, suggesting they are oriented along all directions with equal probability at high temperatures. Here presented are experimental evidences from the combined local and average structure analysis using the atomic pair distribution function (PDF) technique. We further argue that the JT distorted orbitals are also dynamic, explaining the observed drastic drop of the resistivity across JT transition. The “local” ordering length of  $\text{MnO}_6$  will also be discussed.

#### **MP39: Field effect and quasi-2D rod magnetic structure on electron-doped superconductor**

*H. Kang (Department of Physics and Astronomy, University of Tennessee), P. Dai (Department of Physics and Astronomy, University of Tennessee; Condensed Matter Sciences Division, Oak Ridge National Laboratory), Y. Ando, Y. Kurita (Electrical Physics Department, Komae Research Laboratory, CRIEPI,)*

The interplay between the competing phases in high- $T_c$  superconductivity has been one of the important issues and intensive work has been done on this topic both experimentally and theoretically. Previous field-induced effects on hole-doped LSCO suggest that antiferromagnetism competes with superconductivity. We did a similar field-induced experiment on the electron-doped superconductor PLCCO ( $x = 0.12$ ) by applying a magnetic field along the c-direction to determine whether the antiferromagnetism is the competing order in high- $T_c$  cuprates regardless hole or electron-doping. We also show that the magnetic structure of superconducting sample is quasi-2 dimensional through the result from the 2 dimensional rod scan. Comparison of the temperature dependence of the antiferromagnetic peak (0.5,0.5,0) in the superconducting sample and non-superconducting sample shows that the quasi-2dimensional magnetic structure is related to superconductivity.

#### **MP40: Structural Phase Transitions in $\text{Cd}_2\text{Re}_2\text{O}_7$**

*J. He (University of Tennessee, Knoxville; Oak Ridge National Laboratory), B. Chakoumakos (Oak Ridge National Laboratory), D. Mandrus (University of Tennessee, Knoxville), M. Guttman, C. Wilson (CLRC Rutherford Appleton Laboratory, UK), J. Gardner (National Research Council, Chalk River, Ontario, Canada)*

The structural phase transitions at and below  $T^* \sim 200$  K in the pyrochlore oxide,  $\text{Cd}_2\text{Re}_2\text{O}_7$ , have been the subject of a number of studies, however, the exact nature of these structural distortions and symmetry changes has not been completely elucidated. Accompanying with the subtle structural changes are dramatic changes in the resistivity and magnetic susceptibility, and superconductivity is observed at  $T_c = 1.0$  K. On the other hand, the continuous cubic-to-tetragonal structural transition at  $T^*$ , the breaking of inversion symmetry and the sustained metallic behavior on both sides of  $T^*$  suggest this compound as the first example of “metallic ferroelectricity” proposed by P.W. Anderson in 1960s. We have collected single-crystal neutron diffraction data at the SXD instrument at ISIS, and powder diffraction data at C-2, NPMR, Chalk River

Laboratory, using isotopically enriched crystalline specimens. Data sets for several temperatures have been collected. We are testing a variety of lower symmetry structural models to determine the best description of the intermediate- and low-temperature range structural modifications before the onset of superconductivity.

**MP41: Mesoscopic magnetic and crystallographic phase separation in  $\text{La}_{1-x}\text{Ca}_x\text{MnO}_3$  ( $0 \leq x \leq 0.20$ )**

*H. Terashita, J.J. Neumeier (Department of Physics, Montana State University, Bozeman Montana 59717-3840), C.D. Ling (Institut Laue Langevin)*

We report on the magnetic and structural properties of hole-doped  $\text{La}_{1-x}\text{Ca}_x\text{MnO}_3$  ( $0 \leq x \leq 0.14$ ). Neutron powder diffraction and dc-magnetization measurements were carried out. We observed two distinct *Pnma* phases as well as ferromagnetic and antiferromagnetic low-temperature transitions for all samples. Details of the temperature and composition dependence of the phase fractions will be discussed in the context of the development of the local ferromagnetism, recently observed in this system [1]. Comparisons will be made with our results in the analogous electron-doped  $\text{Ca}_{1-x}\text{La}_x\text{MnO}_3$  ( $0 \leq x \leq 0.20$ ) [2].

- [1] M. Hennion, F. Moussa, G. Biotteau, J. Rodríguez-Carvajal, L. Pinsard, and A. Revcolevschi, *Phys. Rev. Lett.* 81, 1957 (1998); M. Hennion, F. Moussa, J. Rodríguez-Carvajal, L. Pinsard, and A. Revcolevschi, *Phys. Rev. B* 56, R497 (1997); M. Hennion, F. Moussa, G. Biotteau, J. Rodríguez-Carvajal, L. Pinsard, and A. Revcolevschi, *Phys. Rev. B* 61, 9513 (2000).  
 [2] C. D. Ling, E. Granado, J. J. Neumeier, J. W. Lynn, and D. N. Argyriou, *Phys. Rev. B* 68, 134439 (2003); E. Granado, C. D. Ling, J. J. Neumeier, J. W. Lynn, and D. N. Argyriou, *Phys. Rev. B* 68, 134440 (2003).

**MP42: The Solvation of Fulleride  $\text{C}_{60}^{5-}$  Anions in Potassium-Ammonia Solutions**

*C. A. Howard (Department of Physics & Astronomy University College London, UK; Rutherford Appleton Laboratory, UK), J. C. Wasse, N. T. Skipper, H. Thompson (Department of Physics & Astronomy University College London, UK)*

Investigation of fulleride  $\text{C}_{60}$  anions in solution is very important, for example, in the applications of fullerene purification and separation; the manipulation of fullerenes and their derivatives and for studying isolated fulleride anions.  $\text{C}_{60}$  can be sequentially reduced in metal ammonia solutions to form high concentrations solvated  $\text{C}_{60}^{n-}$  ( $n = 1-5$ ) anions [1].

This poster describes the results of new high resolution neutron diffraction studies of  $\text{C}_{60}\text{K}_5(\text{NH}_3)_{250}$  solutions taken on SANDALS at the ISIS facility.

Second order isotopic substitution of deuterium (D) for hydrogen (H), used together with Empirical Potential Structure Refinement (EPSR) provides us with a detailed picture of the structure in these liquids [2]. We find a highly developed solvent structure: the  $\text{C}_{60}^{5-}$  anion is strongly solvated by approximately 45 ammonia molecules, located around 7 Å from the centre of the fulleride with a second solvation shell present around this. These molecules direct one of their hydrogen atoms towards the centre of a fulleride ion. This strong solvation shells permit attainment of high concentrations of solvent isolated fulleride ions. As well as being interesting from the fundamental standpoint, our results demonstrate that wide angle neutron techniques can be used to investigate the order found around large ions in a polar solvent.

- [1] Fullagar, W. K. et al., *J. Chem. Soc., Chem. Comm.* 6, 525-527 (1993)  
 [2] Soper, *Mol. Phys.* 99, 1503-1516 (2001)

**MP43: Annealing-Dependent Phenomena in  $\text{Ga}_{1-x}\text{Mn}_x\text{As}$**

*B. J. Kirby (Department of Physics & Astronomy, University of Missouri), J. A. Borchers (NIST Center for Neutron Research), J. J. Rhyne (Los Alamos Neutron Science Center, Los Alamos National Laboratory; Department of Physics & Astronomy, University of Missouri), S. G. E. te Velthuis, A. Hoffmann (Materials Science Division, Argonne National Laboratory), K. V. O'Donovan (NIST Center for Neutron Research; Department of Materials Science and Engineering, University of Maryland), T. Wojowicz (Department of Physics, University of Notre Dame; Institute of Physics of the Polish Academy of Sciences), X. Liu, W. L. Lim, J. K. Furdyna (Department of Physics, University of Notre Dame)*

We have used polarized neutron reflectometry (PNR) to study the dilute ferromagnetic semiconductor  $\text{Ga}_{1-x}\text{Mn}_x\text{As}$ . There is great interest in the development of high Curie temperature ( $T_c$ ) ferromagnetic semiconductors for use in spintronics applications.  $\text{Ga}_{1-x}\text{Mn}_x\text{As}$  is a possible candidate for such applications, with  $T_c$  exceeding 150 K in some cases. The ferromagnetic behavior in this material originates from coupling between spin-5/2  $\text{Mn}^{2+}$  ions substituting for Ga. These substitutional Mn ions ( $\text{Mn}_{\text{Ga}}$ ) are acceptors, generating holes that mediate the ferromagnetic exchange. However,  $\text{Mn}_{\text{Ga}}$  are known to be partially compensated by Mn atoms that exist at interstitial sites in the lattice ( $\text{Mn}_i$ ).  $\text{Mn}_i$  align antiferromagnetically with  $\text{Mn}_{\text{Ga}}$ , and are double donors, fighting the ferromagnetic ordering. A very



interesting property of this material is that post-growth annealing greatly increases the magnetization and  $T_C$  in  $\text{Ga}_{1-x}\text{Mn}_x\text{As}$  thin films, as was first shown through conventional magnetometry.

PNR is a powerful experimental tool that can be used to establish magnetic and chemical depth profiles for thin films. We have used PNR to further examine the mechanisms through which annealing enhances the ferromagnetic ordering in  $\text{Ga}_{1-x}\text{Mn}_x\text{As}$ . This work has shown that annealing leads not only to an increased total magnetization, but also to a much more homogeneous depth distribution of magnetization. Additionally, these measurements have revealed that annealed films possess a non-magnetic surface layer with a composition different from the rest of the film. This result strongly corroborates the idea that annealing enhances the ferromagnetism by redistributing  $\text{Mn}_1$  to the surface of the film. Additional aspects of this work include studies of changes in the  $\text{Ga}_{1-x}\text{Mn}_x\text{As}$  magnetic and chemical depth profiles induced by varying Mn concentration, varying film thickness, and the addition of surface capping layers.

**MP44: Coherent Inelastic Neutron Scattering Study of Lattice Dynamics and Vibrational Entropy in Polycrystalline  $\text{Fe}_{71}\text{Ni}_{29}$  Undergoing a Low Temperature Martensitic Transformation**

*O. Delaire, M. G. Kresch, T. M. Kelley, B. T. Fultz  
(California Institute of Technology)*

Using the Pharos time-of-flight spectrometer at the Lujan center, we measured the neutron scattering function  $S(|Q|, E)$  for the alloy  $\text{Fe}_{71}\text{Ni}_{29}$  as function of temperature from 300K to 80K. We observed *in situ* the structural and dynamical effects of the fcc-bcc martensitic transformation taking place at low temperatures, with an emphasis on the entropy of the transformation. To gain insight into the phonon entropy of this martensitic transformation, we studied the lattice dynamics across the phase boundary. We tried to extract information about the interatomic force-constants from the Q- and E- dependence of the coherent scattering signal recorded with the pixelated Pharos detector array. The coherence in the data can be directly related to the polycrystalline averaged phonon dispersions for the two phases of the material. The inelastic scattering function  $S_{\text{inel}}(|Q|, E)$  for the high temperature phase was compared to a computer simulation based on the Born-von Karman model and inter-atomic force-constants determined previously. The good agreement between the experimental data and the simulation suggests new approaches for investigating the lattice dynamics of polycrystals. The vibrational entropies of the low- and high-temperature phases

were calculated from the phonon DOS curves. We found a significant entropy change upon transformation of  $-0.13 k_B$  per atom, typical of martensitic transformations.

**MP45: Inherited Tunneling in Supercritical Water.**

*D. Homouz, G.F. Reiter (Physics Department,  
University of Houston), P. Platzman (Bell Labs-  
Lucent Technologies)*

It has been observed in Neutron Compton Scattering measurements on supercritical water, that the momentum distribution of the proton appears to be consistent with the tunneling of the proton along the hydrogen bond over a distance of  $.3 \text{ \AA}$ . While there has been ample evidence of tunneling motion perpendicular to the bond observed by other means, this result was puzzling because of the stiffness of the bond, and the lack of any obvious geometrical interpretation. Using path integral Monte-Carlo methods, we show that tunneling motion perpendicular to the bond, when coupled to much stiffer harmonic motion along the bond, can show up in the momentum distribution as an apparent tunneling motion along the bond direction, with the apparent tunneling distance being characteristic of the transverse motion.

**MP46: High Resolution Neutron Scattering Experiments on Spin Excitations in  $\text{SrCu}_2(\text{BO}_3)_2$**

*S. Haravifard (Department of Physics and  
Astronomy, McMaster University, Hamilton, ON,  
Canada), B.D. Gaulin (Department of Physics and  
Astronomy, McMaster University, Hamilton, ON,  
Canada; Canadian Institute for Advanced Research,  
180 Dundas St. W., Toronto, Ontario, M5G 1Z8,  
Canada), S.H. Lee (National Institute of Standards  
and Technology), J.P. Castellan (Department of  
Physics and Astronomy, McMaster University,  
Hamilton, ON, Canada), A.J. Berlinsky (Department  
of Physics and Astronomy, McMaster University,  
Hamilton, ON, Canada; Canadian Institute for  
Advanced Research, 180 Dundas St. W., Toronto,  
Ontario, M5G 1Z8, Canada), H.A. Dabkowska  
(Department of Physics and Astronomy, McMaster  
University, Hamilton, ON, Canada), Y. Qiu (National  
Institute of Standards and Technology; Department  
of Materials Science and Engineering, University of  
Maryland), J.R.D. Copley (National Institute of  
Standards and Technology)*

We performed high resolution inelastic neutron scattering measurements on  $\text{SrCu}_2(^{11}\text{BO}_3)_2$  which has been proposed as a realization of the two dimensional Shastry-Sutherland system with an exact dimer ground state. Measurements were performed on the Disk Chopper Spectrometer (DCS) and the SPINS

triple axis spectrometer, located on cold neutron guides at the NIST Center for Neutron Research. Earlier inelastic neutron scattering measurements have identified three bands of excitations. We performed high  $Q$  resolution measurements using SPINS which show distinct  $Q$ -dependencies for the single and multiple triplet excitations, and that these excitations are largely dispersionless perpendicular to the basal (H,K,0) plane. Since the  $Q$ -dependence of the spin excitations show little L dependence, high energy resolution DCS measurements were integrated along L, which then could reveal the dispersion of the three single triplet excitations continuously across the (H,0) direction within its tetragonal basal plane. These correspond to  $S^z = +1, 0, -1$  transitions from the singlet ground state. We also measured the temperature dependence of both the single and double triplet excitations with SPINS, as well as that of the single triplet excitations with DCS. We observe identical temperature dependencies for the single and double triplet excitations and this temperature dependence to the inelastic scattering is well described as the complement of the dc susceptibility of  $\text{SrCu}_2(\text{BO}_3)_2$ .

#### MP47: Quantum Percolation in a Two-Dimensional Heisenberg Antiferromagnet

*O. P. Vajk (NIST Center for Neutron Research), P. K. Mang (Department of Applied Physics, Stanford University), M. Greven (Department of Applied Physics and Stanford Synchrotron Radiation Laboratory, Stanford, CA 94305), J. W. Lynn (NIST Center for Neutron Research)*

The study of quantum phase transitions in the presence of disorder is at the forefront of research in the field of strongly correlated electron systems, yet there have been relatively few experimental model systems. One important class of model systems for studying the effects of quenched disorder is magnetic materials with random site dilution. Percolation in classical high-spin magnetic systems has been studied extensively, and magnetic order persists in these materials up to the percolation threshold. The spin-1/2 square-lattice Heisenberg antiferromagnet (SLHAF) is of particular interest because of its connection to high-temperature superconductivity. Previous results for magnetic dilution in the spin-1/2 SLHAF have been confined to dilution levels well below the percolation threshold, leaving many questions about this complex quantum-impurity problem unanswered.

Single crystals of  $\text{La}_2\text{Cu}_{1-p}(\text{Zn,Mg})_p\text{O}_4$  at concentrations up to and beyond the site percolation threshold provide the first experimental realization of quantum

percolation in a spin-1/2 SLHAF. Complementary magnetometry, neutron scattering, and numerical experiments demonstrate that  $\text{La}_2\text{Cu}_{1-p}(\text{Zn,Mg})_p\text{O}_4$  is an excellent model material for studying this problem in the low-spin limit. Measurements of the ordered moment and spin correlations provide important quantitative information for tests of theories for this complex quantum-impurity problem. Quantum Monte Carlo results for the bilayer Heisenberg antiferromagnet allow the determination of the quantum-fluctuation versus geometric-disorder phase diagram, and indicate that the properties of  $\text{La}_2\text{Cu}_{1-p}(\text{Zn,Mg})_p\text{O}_4$  near the percolation threshold are controlled by the effective proximity to a new quantum critical point.

#### MP48: Magnetic structure of Cu(Mn)/Cu superlattices

*W. Donner, L.B. Carvalho (Department of Physics, University of Houston), J.L. Robertson (Reactor Division, Oak Ridge National Laboratory)*

Cu(Mn) alloys are the prototype for spin-glass behavior and at the same time exhibit spin-density waves of a limited (20 Å) correlation range. We are interested in short-range order in thin films in general and have chosen Cu(Mn) as a model system to study the effect of confinement on short-range order. In order to obtain a large enough number of scatterers for a neutron experiment we prepared superlattices of Cu(Mn) layers separated by Cu. The samples have been epitaxially grown by DC-magnetron sputtering onto Si(001) substrates with a Cu(001) buffer layer. They exhibit a mosaic of about 0.7 degrees and show very little structural disorder as evidenced by high-order structural satellite peaks in x-ray diffraction experiments.

We will present first results obtained at the High Flux Isotope Reactor in Oak Ridge (HB1A) on samples with varying Cu(20 at % Mn) and Cu thickness. Both strongly modulated magnetic short-range order and magnetic long-range order are present in the samples when the Cu(Mn) thickness is below 20 Å.

#### MP49: Quasi-elastic Neutron Scattering Study of the Diffusion of Methyl Iodide Confined in the GelTech-200

*Y.J. Glanville, P.E. Sokol (Pennsylvania State University, Dept. of Physics, University Park, PA, 16802), R.M. Dimeo (NIST Center for Neutron Research), C.M. Brown (NIST Center for Neutron Research; Department of Materials Science and Engineering, University of Maryland)*

The quasi-elastic scattering from methyl iodide confined in the pores of GelTech glass has been



measured on the Fermi Chopper Spectrometer at NIST. Methyl Iodide is a quantum rigid rotor with a bulk freezing temperature of 207 K. Measurements on cooling were carried out at an incident energy of 2.5 meV with an energy resolution of 90 meV, with  $Q$  values ranging from 0.68 to 2.45 Å<sup>-1</sup>, and temperatures ranging from 215 K to 150 K. The measured QENS spectra could be split into three distinct regions based on their  $Q$  dependence. The high temperature scattering, above 205 K, shows a distinct  $Q^2$  dependence indicating a liquid like jump diffusion. At 203 K there is a very dramatic change in the scattering and we observe a change from a quadratic to a linear  $Q$  dependence. We believe this is a transition from a liquid to a geometrically confined solid phase, which has a structure like that of a glass. This result is substantiated by x-ray scattering measurements performed by our group. At this sample temperature the x-ray spectra showed a Debye-Waller type dampening at high  $Q$  indicative of a solid. As the temperature was lowered further a transition occurred where the broadening was independent of  $Q$ .

We wish to acknowledge the support of this research by the funding of the Department of Energy through grant DE-FG02-01ER45912, and the Department of Commerce through their support of the NIST Center for Neutron Scattering.

#### **MP50: Role of solvent in protein preservation**

*G. H. Caliskan (The University of Akron, Polymer Science Department), M. T. Cicerone (NIST Polymer Division), M. Gangoda, R. B. Gregory (Kent State University, Department of Chemistry), A. Kisliuk (The University of Akron, Polymer Science Department), I. Peral (University of Maryland, College Park), J. H. Roh, A. P. Sokolov (The University of Akron, Polymer Science Department)*

Protein dynamics span over a broad time range from picoseconds, where vibrations take place, up to years, the target of pharmaceutical industry for biopreservation. Understanding the dynamics is vital in controlling the activity of biological macromolecules, and improving the designs for biopreservation formulations. High  $T_g$  sugars are usual choice for biopreservation at ambient temperatures. However, glycerol ( $T_g \sim 190$  K) is the most effective solvent for long-term (years) cryo-preservation. The reason for this difference in effectiveness of the solvents remains unclear.

We measured dynamics of hen egg white lysozyme in various solvent conditions, (glycerol, water, trehalose and dry state) in a broad temperature (150 K to 320 K) range. Time-of-Flight Spectrometer

at the National Institute of Standards and Technology Center for Neutron Research offered a broad range of energy from  $\sim 40$   $\mu$ eV up to  $\sim 65$  meV where the fast relaxation (local conformational fluctuations) and slow vibrations of proteins become accessible. Our results show that the fast relaxation depends strongly on the solvent. It is strongly suppressed in liquid glycerol compared to solid trehalose ( $T_g \sim 390$  K) at low temperatures. At high temperatures ( $> 270$  K), it becomes enhanced in glycerol and in water environments, as opposed to that in trehalose and in dry conditions. This observation quantitatively agrees with bioactivity measurements on Myoglobin in glycerol and trehalose at different temperatures. The results suggest that the viscosity of the solvent is not the only parameter affecting the protein dynamics. Fast picosecond relaxations should also be taken into consideration. We propose a mechanism that might explain extreme biopreservation efficiency of glycerol at low temperatures. Possible implications for development of better formulations are discussed.

#### **MP51: Cholera Toxin Assault on Lipid Monolayers Containing Ganglioside GM1 : a Neutron and X-Ray Scattering Study at the Air-Liquid Interface**

*C.E. Miller (Biophysics Graduate Group, University of California, Davis; Department of Chemical Engineering and Material Science, University of California, Davis), J. Majewski (Los Alamos Neutron Science Center, Los Alamos National Laboratory), K. Kjær, M. Weygand (Physics Department, Risø National Laboratory, Denmark), R. Faller (Department of Chemical Engineering and Material Science, University of California, Davis), T.L. Kuhl (Department of Chemical Engineering and Material Science, University of California, Davis; Biophysics Graduate Group, University of California, Davis)*

Many bacterial toxins bind to and gain entrance to target cells through specific interactions with membrane components. Using neutron/x-ray reflectivity and x-ray grazing incidence diffraction (GID), we have characterized the structure of mixed DPPE:GM1 lipid monolayers before and during the binding of cholera toxin (CTAB<sub>5</sub>) or its B subunit (CTB<sub>5</sub>). Structural parameters such as the density and thickness of the lipid layer, extension of the GM<sub>1</sub> oligosaccharide headgroup, and orientation and position of the protein upon binding are reported. The density of the lipid layer was found to decrease slightly upon protein binding. However, the alpha subunit of the whole toxin is clearly located below the B pentameric ring, away from the monolayer, and does not penetrate into the lipid layer prior to enzymatic cleavage. Using Monte Carlo simulations, the observed monolayer expansion was found to be consistent with

geometrical constraints imposed on DPPE by multivalent binding of GM<sub>1</sub> by the toxin. Our findings suggest that the mechanism of membrane translocation by the protein may be aided by alterations in lipid packing. Both CTAB<sub>5</sub> and CTB<sub>5</sub> were measured to have ~50 % coverage when bound to the lipid monolayer. X-ray GID experiments show that both the lipid monolayer and the cholera toxin layer are crystalline. The effects of x-ray beam damage have been assessed and the monolayer/toxin structure does not change with time after protein binding has saturated.

## Tuesday

### **T1-A, Chemical Applications of SANS, Chair: Charles Glinka (NIST), Room 2101/3/5 Green**

#### **T1-A1 (08:30) Probing the Structure of Nanoscale Aerosols (Invited)**

*Barbara Wyslouzil (Department of Chemical Engineering, Ohio State University), Gerald Wilemsk (University of Missouri – Rolla), Reinhard Strey (Universität zu Köln, Germany)*

Multicomponent nanometer sized droplets form readily in the supersonic expansion that occur, for example, in volcanic eruptions, jet exhausts and turbomachinery. From a fundamental point of view, particles with radii < 10 nm are important because they lie in the critical transition zone between large molecular clusters and bulk materials. The properties of the aerosol size distribution, i.e. the number density, the average particle size, and the polydispersity together determine the surface area of the aerosol. Differences between the surface and interior compositions, on the other hand affect the heterogeneous chemistry as well as the growth and evaporation kinetics. Unlike solid particles, that can be captured and subjected to further analysis, liquid droplets must be examined *in situ*.

Over the past 7 years, we have pioneered the use of small-angle neutron scattering (SANS) to study the properties of nanodroplet aerosols. With condensed phase volume fractions on the order of 10<sup>-6</sup>, aerosol-SANS experiments are technically challenging. The results from our experiments to date are, however, yielding important insights into particle formation processes and into the internal structure of the droplets themselves. This talk will focus on our efforts to use SANS to find direct evidence for and characterize surface enrichment in nanodroplets.

#### **T1-A2 (09:00) Neutron Scattering Study of Wax Crystal Modification by Crystallizable Polymers for Crude Oil Production**

*Robert K. Prud'homme, (Dept Chemical Engineering, Princeton University, Princeton, NJ 08544), H.S. Ashbaugh (Los Alamos National Laboratory, Los Alamos, NM 87545), A. Radulescu, D. Schwahn, D. Richter, L. J. Fetters (Institut für Festkörperforschung, Juelich, Germany)*

Self-assembly in organic phases is less well studied than self-assembly in aqueous phases in part because the driving forces for assembly are generally weaker in organic media. Crystallization, however, provides sufficient driving force in cases of wax precipitation

from oil phases. We present results on the self-assembly of co-polymers in organic solutions driven by crystallization. Polymers of both di-block and randomly distributed crystallizable domains were studied. The interesting phenomena occur when these polymers co-crystallize with wax phases upon cooling. Using neutron scattering and rheology we present a picture of the mechanism of co-assembly that leads to sterically stabilized wax crystals. The proper tuning of polymer architecture provides a means to control gel formation in crude oil production process.

#### **T1-A3 (09:15) Field and Shear Induced Orientational Order in Magnetic Nanoparticle Dispersions from SANS**

*Vemuru V. Krishnamurthy, B. He, M. Piao (MINT Center, The University of Alabama, Tuscaloosa, Alabama 35487-0209), L. Porcar (NIST Center for Neutron Research), D. E. Nikles, J. M. Wiest, G. J. Mankey (MINT Center, The University of Alabama, Tuscaloosa, Alabama 35487-0209)*

Acicular magnetic nanoparticles have technological applications. The suitability of nanoparticles for magnetic recording applications depends on the control of the orientational order in an external force field, such as a shear flow and a magnetic field. Using small angle neutron scattering, we have investigated the orientational order of polydisperse rod shaped iron nanoparticles in cyclohexane based magnetic dispersions in longitudinal shear flow and transverse magnetic field. The anisotropy of the scattering intensity observed in 3.2 vol. % and 3.9 vol. % iron nanoparticle dispersions in shear flow and/or magnetic field, shows that the particles start to orient either in a shear flow of  $100 \text{ s}^{-1}$  or in a magnetic field of 8 mT. In zero-applied-field, the orientational order is measured as a function of steady shear flow. In an applied field, both the degree of order and the tilt angle of the particles is measured as a function of steady shear flow. At zero shear rate, the anisotropy, i.e., the order parameter exhibits hysteresis as a function of applied magnetic field showing that the nanoparticles order in domains. The scattering from nanoparticles in the 3.9 vol. % dispersion exhibits second order anisotropy in an applied field greater than 5 mT.

#### **T1-A4 (09:30) On-line studies of electric fuel cell assemblies by neutron imaging methods**

*D. Kramer, G. Scherer (Paul Scherrer Institut, General Energy Department, Electrochemistry Laboratory, CH-5232 Villigen PSI, Switzerland), E. Lehmann (Paul Scherrer Institut, Research Department Condensed Matter Research with*

*Neutrons and Muons, CH-5232 Villigen PSI, Switzerland), J. Zhang (NISSAN Motor Co. Ltd., Powertrain and Environmental Research Laboratory, 1 Natsushima-cho, Yokosuka 237-8523, Japan), K.N. Clausen (Paul Scherrer Institut, Research Department Condensed Matter Research with Neutrons and Muons, CH-5232 Villigen PSI, Switzerland)*

Fuel cells are envisaged a key role for the development of the so-called hydrogen economy or for the future of individual transport systems in cities and other mobile applications. In Electric fuel cells hydrogen, natural gas or methanol in combination with oxygen is converted into electric power and non-poisonous reaction products (Water and  $\text{CO}_2$ ). The development of efficient, long lived, light, low cost fuel cells is therefore high on the agenda and many research groups world wide are studying both materials for use in fuel cells and their behavior during operation of the cell.

One of the reaction product for low temperature operation conditions within fuel cells is water, and since the humidity inside the so-called gas diffusion layer of the fuel cell, strongly influences the behavior and the performance of the whole assembly, it is of great interest to follow the production of water and how this water is transported out of the cell simultaneously with measurements of the local current density in an operating fuel cell.

Because of the high neutron attenuation coefficient for hydrogen in comparison to the structural materials of the fuel cell (carbon, aluminum etc.), the quantitative distribution of water can be studied by neutron imaging techniques.

The radiography beam line NEUTRA at the spallation neutron source SINQ has been used for such *in situ* studies of operating test fuel cells. The accumulation and distribution of water was studied both with a coarse time resolution with integration over about 10 s or very fast with up to 30 frames per second. In the first case, the image quality allowed for quantitative determination of the water distribution. In the later case, short term changes in the flow field could be detected.

The paper will describe in detail the experimental setup, the methodology to derive quantitative values for the water distribution from the neutron images and first results from a test cell. An outlook for further developments of the method will be given.

**T1-B, Thin Films and Membranes, Chair: Lee Magid (U. Tennessee), Room 2100/2/4 Red**

**T1-B1 (08:30) X-ray & Neutron Reflectivity Studies of Vectorially-Oriented 4-Helix Bundle Maquette Peptides (Invited)**

*J. K. Blasie, S. Ye, J. Strzalka (Department of Chemistry, University of Pennsylvania)*

Bundles of alpha-helices provide a scaffold for binding prosthetic groups at selected locations within the structure to mimic functions exhibited by biological proteins. For example, histidine residues can be strategically placed for the axial ligation of metalloporphyrin prosthetic groups involved in biological electron transfer reactions. The first designed artificial peptides, prepared by solid-phase chemical synthesis, used amphipathic di-helices which self-assembled in aqueous solution forming 4-helix bundles. These were called “maquettes” and they exhibited exceptional stabilities relative to their natural counterparts. Nevertheless, to realize any device applications based on their functionality, the peptides must be vectorially-oriented in an ensemble, e.g., at an interface. Incorporation of non-biological prosthetic groups further allows for the possibility of novel functionality and related device applications. Several examples will be provided concerning maquette design for vectorial orientation at soft interfaces. Both x-ray and neutron scattering techniques are key to ascertaining the detailed nature of these maquette structures and their vectorial orientation at soft interfaces. Each of these techniques has distinct advantages and disadvantages.

**T1-B2 (09:00) Detection by Small-Angle Neutron Scattering of Lateral Segregation or “Rafts” in Lipid – Cholesterol and Lipid – Ergosterol Mixtures in Large Unilamellar Vesicles**

*J. Pencer (Dept. of Chemical and Biomolecular Engineering, The Johns Hopkins University; NIST Center for Neutron Research), S. Krueger (NIST Center for Neutron Research), R. M. Epand (Biochemistry Department, McMaster University)*

Small-angle neutron scattering (SANS) measurements are used here to identify and characterize lateral heterogeneities or “rafts” in three component mixtures of lipids and cholesterol or ergosterol in 50 nm diameter unilamellar vesicles. By using deuterated lipid as the saturated lipid component in mixtures of lipids and cholesterol, and appropriate contrast conditions, we are able to enhance the contrast between heterogeneous membranes and the medium. This allows us to detect the onset of “raft” formation on cooling of homogeneously mixed membranes, and to measure the form factor of

heterogeneous membranes. We show evidence, for the first time using SANS, that nanoscopic domains form in unilamellar vesicles of a size several orders of magnitude smaller than similar vesicles used in fluorescence microscopy studies. It is found that, while “rafts” form in 1:1:1 mixtures of DOPC:DPPC:cholesterol and ergosterol, there is no such evidence for similar heterogeneities in 1:1:1 SOPC:DPPC:cholesterol. Furthermore, it is found that ergosterol has a greater ability to stabilize “rafts” than cholesterol.

**T1-B3 (09:15) Neutron Reflectometry Studies of Polymer Brushes in Confined Geometry**

*G. S. Smith (HFIR Center for Neutron Scattering, Oak Ridge National Laboratory, Oak Ridge, Tennessee 37831, USA.), T.L. Kuhl (Department of Chemical Engineering and Material Science, University of California, Davis), W.A. Hamilton (HFIR Center for Neutron Scattering, Oak Ridge National Laboratory, Oak Ridge, Tennessee 37831, USA.), N.A. Alcantar (Department of Chemical Engineering, University of South Florida, FL 33620, USA.), R.G. Toomey (Center for Ocean Technology, St.Petersburg, FL 33701, USA.), J. Majewski (Los Alamos Neutron Science Center, Los Alamos National Laboratory)*

Polymer molecules at solid or fluid interfaces have an enormous spectrum of applications in a wide variety of technologies as lubricants, adhesion modifiers, and protective surface coatings. Because polymer brushes have a great potential to be used in such applications, there is a need to determine their structure and efficiency in reduced spaces. Using neutron reflectivity and the newly developed Neutron Confinement Cell, we have directly quantified the density distribution of opposing polymer brushes in good solvent conditions under confinement. Our measurements show that the density profile in the overlap region between opposing polymer brushes flattens consistent with predictions from molecular dynamics simulations. In addition, a significant increase in density at the anchoring surfaces due to compression of the brush layers is observed. This compression or collapse of the brushes in restricted geometries strongly suggests that high-density brushes do not interpenetrate in good solvent conditions.

**T1-B4 (09:30) Analysis of Myoglobin Adsorption to Cu(II)-IDA and Ni(II)-IDA Functionalized Langmuir Monolayers by Grazing Incidence Neutron and X-ray Techniques**

*M. S. Kent, H. Yim, D. Y. Sasaki (Sandia National Laboratories, Albuquerque, NM 87123), S. Satija (National Institute of Standards and Technology), J.*



*Majewski (Argonne National Laboratory), T. Gog (Los Alamos National Laboratory)*

The adsorption of myoglobin to Langmuir monolayers of a metal-chelating lipid in crystalline phase was studied using neutron and x-ray reflectivity and grazing incidence x-ray diffraction (GIXD). In this system adsorption is due to the interaction between chelated  $\text{Cu}^{2+}$  and  $\text{Ni}^{2+}$  ions and the histidine moieties at the outer surface of the protein.  $\text{Cu}^{2+}$  is known to interact much more strongly with histidine than  $\text{Ni}^{2+}$ . Adsorption was examined by NR and XR under conditions of constant surface area with an initial pressure of 40 mN/m as well as under constant pressure at 40 mN/m. The adsorbed layer structure in the final state was examined for a variety of bulk concentrations on and below the adsorption plateau. In addition, since the adsorption process is rather slow for this system, the layer characteristics were obtained as a function of time during the adsorption process. Finally, corresponding GIXD experiments were performed under the same conditions to follow changes in the packing of the lipid tails upon protein adsorption. Significant differences in the evolution of the adsorbed protein layer are observed for chelated  $\text{Cu}^{2+}$  and  $\text{Ni}^{2+}$  ions that may indicate differing extents of protein denaturation in the two cases. In addition, the disruption of the lipid packing is found to occur for the constant pressure case (40 mN/m) but not for constant area (initial pressure - 40 mN/m).

### **T1-C, Magnetic Structures, Chair: Taner Yildirim (NIST), Room 1123 Blue**

#### **T1-C1 (08:30) Unusual Symmetry of the Kugel-Khomskii Hamiltonian for Orbitons (Invited)**

*A. B. Harris (University of Pennsylvania, Philadelphia PA 19104)*

The Kugel-Khomskii Hamiltonian,  $H_{\text{KK}}$ , has been used for about three decades to describe spin and orbital dynamics of cubic transition metal (TM) ions having a single electron in the three-fold degenerate  $t_{2g}$  crystal field levels ( $\alpha = X, Y, Z$ ). (An X orbital is a  $d_{yz}$  wavefunction,  $Y = d_{xz}$ , etc.) In this idealized model the electron hopping matrix element  $t(\alpha_i, \alpha_j)$  between nearest neighboring TM ions on a simple cubic lattice is nonzero only for  $\alpha_i = \alpha_j$  and only if  $\alpha_i = \alpha_j$  is not the same as the axis separating the two ions. KK showed that their model gives rise to a Heisenberg-like spin Hamiltonian with exchange integrals of order  $t^2/U$ , where  $U$  is the on-site Coulomb energy. Because electrons in, say, an X orbital cannot hop along the X axis, it is clear that the total number of electrons in X orbitals in any given plane perpendicular to the X axis is a good quantum number. We (ABH, T. Yildirim, A. Aharony, O. Entin-Wohlman, and I.

Korenblit) have shown in Phys. Rev. B69, 035107 (2004) that  $H_{\text{KK}}$  is invariant with respect to a global rotation of the spin of electrons in, say, X orbitals when summed over all ions in a single plane perpendicular to the X axis. We will give a qualitative discussion of this and other symmetries and show how they appear within numerical and mean field calculations.

The most striking consequence of these symmetries is that the spin correlations are two dimensional and long range spin order can not occur at any nonzero temperature. Since this result is in obvious disagreement with experimental results on systems such as lanthanum titanate, we conclude that the KK Hamiltonian can not be a 'minimum' model to describe such real systems. Stated differently, the KK Hamiltonian, unlike the Heisenberg Hamiltonian for conventional magnetic materials, does not give a zeroth order description of real materials.

Accordingly, it is essential, from the outset, to include the relevant perturbations that destroy these unusual symmetries, if one is to understand real materials. Alternatively, although it is probably impossible to find a real material with these exact symmetries, it may be possible to construct systems which are nearly ideal and whose anomalous properties would be a consequence of closely approximating the unusual symmetries described here.

#### **T1-C2 (09:00) Commensurate-Incommensurate Magnetic Phase Transition in Magnetoelectric Single Crystal $\text{LiNiPO}_4$**

*D. Vaknin, J. L. Zarestky (Ames Laboratory and Department of Physics and Astronomy, Iowa State University, Ames, Iowa 50011)*

Neutron scattering studies of single-crystal  $\text{LiNiPO}_4$  reveal a spontaneous first-order commensurate-incommensurate magnetic phase transition. Short- and long-range incommensurate phases are intermediate between the high temperature paramagnetic and the low temperature antiferromagnetic phases. The modulated structure has a predominant antiferromagnetic component, giving rise to satellite peaks in the vicinity of the fundamental antiferromagnetic Bragg reflection, and a ferromagnetic component giving rise to peaks at small momentum-transfers around the origin at  $(0, \pm Q, 0)$ . The wavelength of the modulated magnetic structure varies continuously with temperature. It is argued that the incommensurate short- and long-range phases are due to spin-dimensionality crossover from a continuous to the discrete Ising state. These observations explain the anomalous first-order transition seen in the



magnetoelectric effect of this system.

### **T1-C3 (09:15) Neutron Scattering Study of TbPtIn Intermetallic Compound**

*V. O. Garlea, J.L. Zarestky, E. Morosan, S.L. Bud'ko, P.C. Canfield, C. Stassis (Ames Laboratory and Department of Physics and Astronomy, Iowa State University, Ames, Iowa 50011)*

Neutron diffraction techniques have been used to study the magnetic properties of TbPtIn as a function of temperature and magnetic field. The measurements were performed on single crystals, using the HB1A triple-axis spectrometer at the High Flux Isotope Reactor (HFIR). This compound crystallizes in the hexagonal ZrNiAl-type structure and can be described as the alternate stacking of Tb-Pt and In-Pt layers perpendicular to the *c*-axis. The rare-earth sites form a triangular lattice; in the case of antiferromagnetic coupling between nearest neighbors, this topology induces a frustration of the magnetic interaction. In the absence of an externally applied magnetic field, the compound orders, below approximately 47 K, in an antiferromagnetic structure with propagation vector  $k = (\frac{1}{2}, 0, \frac{1}{2})$ . The magnetic moments were found to be along the [1-20] symmetry direction by measurements in the plane defined by the [101] and [1-20] directions. Measurements performed in the *a*-*c* plane, at 4.2 K, with a magnetic field applied along the [1-20] direction, reveal a transition from the zero field antiferromagnetic state to a state with a net ferromagnetic component, at approximately 2 T, followed by another transition to a state with a larger ferromagnetic component, at approximately 4 T. Field cooled and zero field cooled measurements were also performed with the magnetic field applied along the [-110] direction, perpendicular to the direction of the magnetic moments. Two transitions were observed: one at 2 T and the other at 5.5 T. Of particular interest is the fact that above the second transition, at 5.5 T, and up to 6.8 T, we did not observe any antiferromagnetic reflections or appreciable changes in the nuclear reflections. Models of the magnetic structure are used in the analysis of the experimental data.

### **T1-C4 (09:30) Spin Density Waves in Iron Aluminides**

*A. S. Arrott, D.R. Noakes (Virginia State University)*

The transition from ferromagnetism with increasing Al concentration in the iron-aluminides now appears to be a change from ferromagnetism to a complex spin density wave state. This discovery by neutron diffraction opens a new field of investigation that should have an impact comparable to that of the spin density waves in chromium over the past forty years.

If one views the magnetic structure of Cr considering only the atoms on the corners of the body centered cubic lattice, one finds a periodic modulation of the spin polarization over long distances. The same is true for the spin density wave in the iron aluminides. The difference between Cr and the iron aluminides is that the polarization of the center atoms of Cr is almost opposite to that of the corner atoms while for the iron aluminides the polarization of the center atoms is almost parallel to that of the corner atoms. The change from the spin density wave state in the iron aluminides to the ferromagnetic state can be viewed as an increase in the spatial period of the antiferromagnetic structure. This treats the wave vectors about the origin as being the most important ones. But if one takes the wave vectors that are close to the 110 reciprocal lattice vectors as controlling, then the transition is from an incommensurate spin density wave state to a commensurate spin density state where all the atoms are at the positive (or negative) peaks of wave. It is a trivial statement to say that every ferromagnet is such a spin density wave, but in the case of the iron aluminides there is a good reason to adopt that view. The transition from ferromagnetism then appears to be the swinging away of the spin density wave vector from matching the 110 reciprocal lattice vectors to reach the observed nearby incommensurate position. This suggests that wave vectors spanning the Fermi surface play an important role in the origin of ferromagnetism in this highly itinerant electron system.

### **T1-D, Neutron Sources, Chair: Roger Pynn (LANL), Auditorium**

#### **T1-D1 (08:30) Status of the Low Energy Neutron Source at Indiana University**

*D. V. Baxter, J. M. Cameron, V. P. Derenchuk, C. Lavelle, M. A. Lone, M. B. Leuschner, H. O. Meyer, H. Nann, T. Rinckel, W. M. Snow (Indiana University Cyclotron Facility, 2401 Milo Sampson Ln, Bloomington IN 47408)*

The National Science Foundation has recently approved funding for the LENS (Low Energy Neutron Source) facility at Indiana University and construction has begun. LENS represents a new paradigm for economically introducing neutron scattering into a university or industrial setting. Neutrons are produced in a long-pulse (1 ms) mode through (p,n) reactions on a water-cooled Be target and supplied to three instrument beam lines. We will describe how LENS will use neutrons to fulfill a three-fold mission in education, materials research, and developing novel instrumentation. Of particular interest are the

facility's ability to study cryogenic moderators at significantly lower temperatures than is possible at other facilities and the development of instruments that make use of the neutron spin to perform high-precision measurements of momentum transfer without significant collimation of the beam. The potential for these developments to expand significantly the range of problems amenable to exploration with neutron techniques will be discussed.

#### **T1-D2 (08:45) The Australian Replacement Research Reactor**

*R. A. Robinson, S. J. Kennedy (Bragg Institute, Australian Nuclear Science and Technology Organisation, Australia)*

The 20-MW Australian Replacement Research Reactor represents possibly the greatest single research infrastructure investment in Australia's history. Construction of the facility has commenced, following award of the construction contract in July 2000, and the construction licence in April 2002. First fuel will go into the reactor in November 2005, with the facility at full power in early 2006 and fully commissioned in July 2006. The project includes a large state-of-the-art liquid deuterium cold-neutron source and supermirror guides feeding a large modern guide hall, in which most of the instruments are placed. Alongside the guide hall, there is good provision of laboratory, office and space for support activities. While the facility has "space" for up to 18 instruments, the project has funding for an initial set of 8 instruments, which will be ready when the reactor is fully operational. Instrument performance will be competitive with the best research-reactor facilities anywhere. Staff to lead the design effort and man these instruments have been hired on the international market from leading overseas facilities, and from within Australia, and 7 out of 8 instruments have been specified and costed. At present the instrumentation project carries > 10 % contingency and 50 % of procurements have been placed. An extensive dialogue has taken place with the Australian user community and our international peers, via various means including a series of workshops over the last 2 years covering all 8 instruments, emerging areas of application like biology and the earth sciences, and computing infrastructure for the instruments.

In December 2002, ANSTO formed the Bragg Institute, with the intent of nurturing strong external partnerships, and covering all aspects of neutron and x-ray scattering, including research using synchrotron radiation.

#### **T1-D3 (09:00) The Fundamental Neutron Physics Beamline at the Spallation Neutron Source**

*G. L. Greene (University of Tennessee; Oak Ridge National Laboratory), T.V. Cianciolo (Oak Ridge National Laboratory), W.M. Snow (Indiana University), P. Huffman (National Institute of Standards and Technology; North Carolina State University), J. D. Bowman, M. Cooper (Los Alamos National Laboratory), J. Doyle (Harvard University)*

The Spallation Neutron Source (SNS), currently under construction at Oak Ridge National Laboratory with an anticipated start-up in early 2006, will provide the most intense pulsed beams of cold neutrons in the world. At a projected power of 1.4 MW, the time averaged fluxes and fluences of the SNS will approach those of high flux reactors. One of the flight paths on the cold, coupled moderator will be devoted to fundamental neutron physics. The fundamental neutron physics beamline is anticipated to include two beamlines; a broad band "cold" beam, and a monochromatic beam of 8.9 Å neutrons for ultra cold neutron experiments. The fundamental neutron physics beamline will be operated as a user facility with experiment selection based on a peer reviewed proposal process. An initial program of five experiments in neutron decay, hadronic weak interaction and time reversal symmetry violation have been proposed. A description of the proposed facility will be given and project status will be reviewed.

#### **T1-D4 (09:15) Experimental test of the cold coupled liquid H<sub>2</sub> moderator at LANSCE**

*M. Russina (Los Alamos Neutron Science Center, Los Alamos National Laboratory), F. Mezei (Los Alamos Neutron Science Center, Los Alamos National Laboratory; Hahn-Meitner-Institut Berlin), P. Lewis, T. Kozłowski (Los Alamos Neutron Science Center, Los Alamos National Laboratory), S. Penttilä (Los Alamos National Laboratory)*

We present the results of a performance test of the coupled cold liquid H<sub>2</sub> moderator installed at Manuel Lujan Jr. Neutron Scattering Center (Lujan Center) at LANSCE. This moderator is the first of its kind ever installed on a spallation source. To measure the moderator performance we have implemented a novel method based on two-dimensional time-of-flight (TOF) analysis to determine both the pulse shape and the absolute value of the flux. The key of the setup was a mechanical chopper with a small diaphragm placed close to half way between the moderator and a detector in the beam axis. The chopper run asynchronously to the source and neutron counts were stored in a two dimensional histogram  $I(t_o, t_{ch})$ , where  $t_o$  and  $t_{ch}$  are, respectively, the times elapsed since the last firing of the source

and the last chopper opening. The method functions with full efficiency without phasing the chopper to the source and it is in this sense a precursor example for the event recording data collection approach, which will enable us to fully eliminate the effects of the jitter of chopper phasing on pulsed source spectra.

Using this approach we determined the moderator time average- and the peak flux, the time structure of the pulse as a function of neutron wavelength as well as observed the influence of radiation on the performance of the supermirror neutron optics placed close to the source inside the bulk shield. In addition the temperature dependence of the moderator characteristics have been checked in the H<sub>2</sub> temperature range of 20 K to 25 K. For this purpose we used an improved experimental setup with higher resolution. The data show that the coupled moderator at LANSCE provides the highest cold neutron flux (both average and peak) at pulsed spallation sources in the world and that the peak intensity of the pulse exceeds the intensity of the ILL.

#### **T1-D5 (09:30) Technical Concepts for a Long-Wavelength Target Station for the Oak Ridge Spallation Neutron Source (Invited)**

*J. M. Carpenter (SNS, Oak Ridge National Laboratory, IPNS, Argonne National Laboratory)*

We describe technical concepts for a second target station for the Oak Ridge Spallation Neutron Source (SNS.) From the outset, the design for the SNS has included the capacity for a second target station, which we conceive to be one that emphasizes provisions for long-wavelength applications. A group centered at Argonne has worked out and evaluated the design of a Long-Wavelength Target Station (LWTS) with a suite of possible instruments and supporting scientific cases. The LWTS will use the same proton delivery system as the High-Power Target Station (HPTS) now nearing completion, sharing a fraction of the available beam power in short, 10-Hz pulses and, for purposes of concept evaluation, 333 kW of beam power, and complementing the capabilities of the HPTS. The concept incorporates a number of new features, emphasizing cold neutron production and utilization, especially extensive use of neutron guides. The instrument suite, compiled mainly for reference purposes, will enable measurements that extend the range accessible at HPTS.

#### **TP - Poster Session II (Main Concourse; 10:30)**

##### **TP1: Influence of Cholesterol and Temperature on the Thickness of SOPC and DOPC Unilamellar Vesicles measured by Small-Angle Neutron Scattering**

*J. Pencer (Department of Chemical and Biomolecular Engineering, The Johns Hopkins University; NIST Center for Neutron Research)*

Cholesterol-rich lateral domains or “rafts” are believed to serve a number of crucial roles in biological function. The formation of such domains in model systems has been shown to depend on the miscibility of lipids and cholesterol, and, in particular, on the degree of lipid chain unsaturation. There is evidence that the miscibility of cholesterol with different lipids is correlated with its influence on membrane bilayer properties such as fluidity, acyl-chain order parameters, and membrane thickness. Thus, measurements of cholesterol’s influence on lipid bilayer thickness should provide information regarding lipid – cholesterol interactions and miscibility.

In this study, small-angle neutron scattering (SANS) is used to characterize the influence of cholesterol on the thickness of large unilamellar vesicles (LUVs) composed of either stearyloleoylphosphatidylcholine (SOPC) or dioleoylphosphatidylcholine (DOPC). It is found that the presence of ~ 40 % cholesterol in SOPC LUVs results in an apparent increase of membrane thickness of approximately 4.5 Å, while ~ 40 % cholesterol in DOPC LUVs results in an apparent thickness decrease of 1.5 Å. The thickness of SOPC and DOPC LUVs with and without cholesterol was also studied as a function of temperature. It was found that membrane thickness decreased linearly with increasing temperature for all membrane compositions examined. Our results suggest that there are significant differences in cholesterol’s interactions with SOPC and DOPC over physiologically relevant temperatures (from 25 °C to 55 °C). We comment on the implications of our results for the relative efficacy of SOPC and DOPC as non-raft components in raft-forming lipid mixtures.

##### **TP2: Structural Comparison of Two EUO-type Zeolites Investigated by Neutron Diffraction**

*I. Peral (Department of Materials Science and Engineering, University of Maryland; NIST Center for Neutron Research), C. Y. Jones (NIST Center for Neutron Research), S. P. Varkey (Department of Chemical Engineering, Northwestern University, Evanston, IL 60208), R. F. Lobo (Center for Catalytic Science and Technology, University of Delaware, Newark, DE 19716)*



Souvereinjs et al. [1] found different molecular selectivity properties in two EUO-types zeolites that are crystallized in presence of two organic templates: hexamethonium (HM) and dibenzylammonium ions (DBDMA). They suggested that this dissimilarity in the molecular shape selectivity is originated from a different distribution of the active sites over the side pockets and the main channels of the EUO zeolites. We have studied the structure of both zeolites by neutron diffraction to investigate their thesis. The structural comparison of the two EUO-type zeolites agrees with the model proposed by Souvereinjs et al. [1].

[1] W. Souvereinjs, L. Rombouts, J.A. Martens and P.A. Jacobs, *Microporous Materials*, 4 (1995) 123.

**TP4: Neutron diffraction of  $ZrBe_2D_{1.5}$ ,  $ZrBe_2H_x$  and inelastic scattering studies of hydride phases in  $ZrBe_2H_{0.6}$**

*Z. Chowdhuri (NIST Center for Neutron Research; University of Maryland, College Park), R.L. Cappelletti, T.J. Udovic, Q. Huang (NIST Center for Neutron Research)*

$ZrBe_2$  has the  $P6/mmm$  structure (also found in  $MgB_2$ ) consisting of triangular nets of Zr separated by honeycomb nets of Be. The hydrides  $ZrBe_2H_x$  display a phase having the same structure in which H diffuses among the honeycomb interstitial sites in the triangular Zr planes. Phases with ordering of the H atoms on a sublattice of the honeycomb appear below an ordering temperature that depends on  $x$ . The results of neutron quasielastic scattering measurements made at widely different resolutions on two spectrometers (DCS: FWHM 64  $\mu$ eV, and HFBS: FWHM 1  $\mu$ eV) are reported on a powder sample of the  $ZrBe_2H_{0.6}$ . The data for all momentum transfers (0.3  $\text{\AA}^{-1}$  to 1.7  $\text{\AA}^{-1}$ ) at each temperature are analyzed in terms of a one-parameter model for independent particle hopping on a honeycomb lattice for the quasielastic portion and an additional elastic term. Monte Carlo calculations verify the validity of the independent particle approximation at this concentration. This work utilizes facilities supported in part by the National Science Foundation under Agreement No. DMR-0086210.

**TP5: Hydration-kinetics and Water Content of Cement: Quasi-Elastic Neutron Spectroscopy Studies**

*N. M. Nemes (NIST Center for Neutron Research; Department of Materials Science and Engineering, University of Maryland), J. C. McLaughlin, D. A. Neumann (NIST Center for Neutron Research), R. A. Livingston (Office of Infrastructure R&D, Federal Highway Administration, McLean, VA 22101)*

Portland cement is a complex non-homogeneous material, with many different constituent phases and structure over a wide range of length scales. The hydration of Portland cement is a complex process involving several simultaneous chemical reactions. All of these reactions involve water, and as hydration proceeds, more of the water that is initially mixed with the cement powder becomes chemically bound into reaction product phases. Quasi-elastic neutron scattering (QENS) allows for the study of the state of water in hydrating cement paste *in situ* over time and over a wide range of temperatures. QENS provides a direct measure of the conversion of free water to structurally/chemically bound water and to water constrained in the pores of the cement paste.

We studied the hydration kinetics of synthetic cement paste with varying alite/belite (dicalcium silicate or  $C_2S$  and tricalcium silicate or  $C_3S$ ) and varying water/cement ratios. The time-dependent free, constrained and bound water results are analyzed in terms of the Avrami-model for the nucleation and growth regime and in terms of a diffusion-limited growth model for the later period. The results reveal the complex nature of the chemistry governing the hydration of cement as the dependence of the model parameters on the  $C_2S/C_3S$  ratio is highly non-linear.

The role of the water/cement ratio (w/c) on the hydration kinetics has been investigated using QENS. For a range of w/c from 0.3 to 1, the bound-water index was extracted from the neutron scattering data, and fitted to hydration kinetics model developed in previous QENS studies. The w/c ratio had no significant effect on the model parameters for the diffusion limited period, but it did affect the nucleation and growth stage.

We also studied the water content of mature samples by drying to varying degrees in saturated salt solutions. The results indicate that the free and constrained water contents are lost at a similar rate.

**TP6: Neutron scattering studies of hydrogen dynamics in  $Pr_2Fe_{17}H_x$**

*E. Mamontov (University of Maryland, College Park; NIST Center for Neutron Research), T.J. Udovic (NIST Center for Neutron Research), O. Isnard (Institut Laue Langevin), J. J. Rush (NIST Center for Neutron Research)*

Hydrogen has a profound influence upon the structural and magnetic properties of the fundamentally interesting  $R_2Fe_{17}$  rare-earth compounds. Typical of such compounds,  $Pr_2Fe_{17}$  crystallizes in the  $Th_2Zn_{17}$  rhombohedral ( $R\bar{3}m$ ) structure. Hydrogen can insert into  $Pr_2Fe_{17}$  to form the hydrides  $Pr_2Fe_{17}H_x$ . Neutron



diffraction results indicate that the first three hydrogen atoms fully occupy the interstitial 9e octahedral (o) sites, whereas the last two hydrogen atoms occupy one-third of the available interstitial 18g tetrahedral (t) sites [1]. Because the t-site hydrogen is believed to occupy only two diametrically opposed sites at the corners of a hexagon composed of six 18g sites [2], it is expected that the t-site hydrogen atoms in  $\text{Pr}_2\text{Fe}_{17}\text{H}_4$  and  $\text{Pr}_2\text{Fe}_{17}\text{H}_5$  would readily jump between the available 18g sites. Our quasielastic neutron scattering measurements confirm the presence of localized hydrogen motion in  $\text{Pr}_2\text{Fe}_{17}\text{H}_3$  and  $\text{Pr}_2\text{Fe}_{17}\text{H}_5$ . The time between jumps is on the order of 100 ps at 200 K and decreases as temperature is increased. Neutron vibrational spectra of  $\text{Pr}_2\text{Fe}_{17}\text{H}_x$  ( $x = 3, 5$ ) and  $\text{Pr}_2\text{Fe}_{17}\text{D}_x$  ( $x = 2, 3, 4, 5$ ) are found to be consistent with the hydrogen locations determined by diffraction. For example, for  $\text{Pr}_2\text{Fe}_{17}\text{H}_3$ , two peaks centered at  $\sim 105$  meV and 85 meV correspond to the normal modes of the octahedral hydrogens in the ab plane and along the c axis, respectively. For  $\text{Pr}_2\text{Fe}_{17}\text{H}_5$ , the c-axis mode for the o-site hydrogen softens considerably, in part due to the large lattice expansion along the c direction caused by the extra hydrogen occupying some of the t sites. In addition to the slightly softened ab-planar modes of the o-site hydrogen, there is extra scattering intensity at 110 meV and above due to the relatively higher-energy normal modes of the t-site hydrogen.

[1] O. Isnard, S. Miraglia, J. L. Soubeyroux, D. Fruchart, and A. Stergiou, *J. Less-Common Met.* 162, 273 (1990).

[2] O. Isnard, S. Miraglia, J. L. Soubeyroux, and P. L'Heritier, *J. Magn. Mater.* 137, 151 (1994).

**TP7: Electronic, Magnetic and Structural Properties of SrAMnMO<sub>6</sub> Double Perovskites (A = Sr, La; M = Mo, Ru)**

*P. M. Woodward, J. Goldberger, P. N. Santhosh (Department of Chemistry, Ohio State University), P. Karen (Department of Chemistry, University of Oslo), A. R. Moodenbaugh (Department of Materials and Chemical Science, Brookhaven National Laboratory)*

The electronic, magnetic and structural properties of  $\text{Sr}_2\text{MnMoO}_6$ ,  $\text{SrLaMnMoO}_6$ ,  $\text{Sr}_2\text{MnRuO}_6$  and  $\text{SrLaMnRuO}_6$  have been investigated. Powder diffraction measurements show that both  $\text{Sr}_2\text{MnMoO}_6$  and  $\text{SrLaMnMoO}_6$  adopt long-range, rock salt ordering of the transition metal ions, while transition electron microscopy reveals short-range cation order in  $\text{Sr}_2\text{MnRuO}_6$  and  $\text{SrLaMnRuO}_6$ . All indicators suggest that  $\text{Sr}_2\text{MnMoO}_6$  and  $\text{SrLaMnMoO}_6$  are Mott-insulators. They exhibit relatively low conductivities

( $1 \times 10^{-2} \Omega^{-1}\text{-cm}^{-1}$  at 290 K), Curie-Weiss magnetic behavior, and well defined transition-metal valence and spin states:  $\text{Sr}_2\text{Mn}^{2+}\text{Mo}^{6+}\text{O}_6$  adopts a G-type antiferromagnetic structure ( $T_N \sim 10$  K), whereas  $\text{SrLaMn}^{2+}\text{Mo}^{5+}\text{O}_6$  is a spin glass ( $T_G \sim 85$  K). The ruthenates are more conductive by roughly four orders of magnitude at room temperature.  $\text{Sr}_2\text{MnRuO}_6$  has a room temperature conductivity of  $1 \times 10^2 \Omega^{-1}\text{-cm}^{-1}$ , with a temperature dependence characteristic of Mott variable-range hopping behavior. It orders antiferromagnetically (C-type) near 180 K, and exhibits a cooperative Jahn-Teller distortion (orbital ordering). The room-temperature electrical conductivity of  $\text{SrLaMnRuO}_6$  is similar to that of  $\text{Sr}_2\text{MnRuO}_6$  ( $4 \times 10^1 \Omega^{-1}\text{-cm}^{-1}$ ) and bond distances suggest that both compounds contain  $\text{Mn}^{3+}$ . However, the substitution of  $\text{La}^{3+}$  for  $\text{Sr}^{2+}$  leads to a disappearance of the cooperative Jahn-Teller distortion, a change in the conductivity mechanism (diffusion-assisted small-polaron hopping), and stabilizes a ferromagnetic ground state ( $T_C \sim 220$  K).

**TP8: Investigation of the State of Water in Hydrating Layered and Amorphous Sodium Disilicate (Alkali-Silica Reactants) by Quasi-elastic Neutron Scattering.**

*J.W. Phair, R.A. Livingston (Office of Infrastructure Research and Development, Federal Highway Administration, McLean, VA), C.M. Brown (NIST Center for Neutron Research; Department of Materials Science and Engineering, University of Maryland), A.J. Benesi (Department of Chemistry, The Pennsylvania State University, University Park, PA)*

The structure and state of water within hydrating layered and amorphous sodium-disilicate were monitored for the first time using quasi-elastic neutron scattering (QENS) and x-ray diffraction (XRD). The QENS kinetic data collected for the first 12 hours of the reaction, were fitted to a model consisting of a Lorentzian and a Gaussian function each convoluted with the energy resolution of the instrument. This allows the QENS signal from water to be associated with two states that include bound and free water, as confirmed by thermogravimetric analyses and 2H NMR. In situ QENS data were collected for a set of sodium disilicate and silica mixtures at a series of discrete temperatures between 20 and 40 °C. The bound water was successfully modelled with Langmuir adsorption kinetics to explain the formation of a layered silicate structure within kanemite. Langmuir adsorption kinetics were also used to model the reaction using amorphous starting material suggesting the presence of layered structure in the reaction product. The presence of the

layered structure in amorphous material was confirmed by XRD analyses. The consequences this has for alkali-silica reaction (ASR) gel reaction and its swelling mechanism are discussed. Based on these results, a standard test for ASR reactivity of aggregates could be developed using natrosilite as standard reagent, and the kinetic parameters as a scale of reactivity.

#### **TP9: Quantitative Texture Analysis of Highly Absorbing Materials from Neutron TOF Data**

*H. Volz, S. Vogel, J. Roberts, D. Williams, A. Lawson, L. Daemen, T. Medina, M. Geelan (Los Alamos National Laboratory)*

The orientation distribution functions (ODF) of rolled foils of dysprosium and erbium metals were determined from neutron time-of-flight (TOF) data using full pattern Rietveld analysis with GSAS. The ODF were fit with spherical harmonics. Both Dy and Er have a hexagonal close-packed (hcp) crystal structure, and are strong absorbers for neutrons with thermal absorption cross-sections of 994 barns for Dy and 159 barns for Er at  $\lambda = 1.8 \text{ \AA}$ . Various stacks of foils of each material, along with combinations of absorbing and less-absorbing foils, were measured on the neutron powder diffractometer HIPPO at LANSCE. The focus of this work is on the comparison of absorption corrections implemented in the GSAS Rietveld code, and the impact of strong absorption on data analysis. We compare our resulting pole figures from the ODF with those in the literature, and find good agreement.

#### **TP10: Octahedral Tilting Distortions in 2:1 B-site Ordered Perovskites**

*Michael Lufaso (Ceramics Division, MSEL, National Institute of Standards and Technology)*

Perovskite materials that exhibit a 2:1 ordered cation arrangement and also undergo an octahedral tilting distortion exhibit interesting changes in the temperature dependence of the dielectric properties, when compared to the untilted 2:1 ordered perovskites (e.g.,  $\text{Ba}_3\text{ZnTa}_2\text{O}_9$ ). The onset of octahedral tilting in the 2:1 B-site cation ordered perovskites is well-known to influence the physical properties; however the crystal structures have not been reported. Polycrystalline samples of  $\text{Sr}_3\text{MM}'_2\text{O}_9$  ( $M = \text{Mg, Ni}$ ;  $M' = \text{Nb, Ta}$ ) were synthesized and neutron powder diffraction data were collected, at the High-Intensity Powder Diffractometer at the Los Alamos Neutron Science Center, as a function of temperature. The structural parameters, obtained from a neutron time-of-flight data analysis via Rietveld refinement, are compared.

#### **TP11: Neutron Diffraction Study of Magnetic, Structural, and Charge Ordering in $\text{La}_{1-x}\text{Ca}_x\text{MnO}_3$ and $\text{La}_{0.52}\text{Ca}_{0.48}\text{MnO}_3$**

*E. Rodriguez, T. Proffen, A. Llobet, J.J. Rhyne (Los Alamos Neutron Science Center, Los Alamos National Laboratory)*

Mixed valence manganites show an enormously rich range of magnetic, structural, and transport properties with varying stoichiometric composition and temperature. Neutron powder diffraction studies were done on the perovskite manganite  $\text{La}_{1-x}\text{Ca}_x\text{MnO}_3$  series for compositions  $x = 0.48$  and  $x = 0.52$ . The interplay between the magnetic, charge, and structural ordering forms a complex system due to an admixture of  $\text{Mn}^{4+}$  and  $\text{Mn}^{3+}$  ions in these compositions. These two compositions alone exhibit interesting physical properties such as coexisting ferromagnetic and anti-ferromagnetic phases at the same temperature. Studies have shown the  $x = 0.5$  composition to be the metal-insulator transition (MIT) interface for this manganite series. Therefore, phase separation at lower temperatures and the magnetic transition temperatures are important characteristics examined in this analysis. The neutron powder measurements were done on two spallation-source diffractometers located at the Manuel Lujan Jr. Neutron Scattering Center at Los Alamos National Laboratory. In addition to crystallographic and magnetic structure analysis, a pair-distribution function (PDF) study was done as well. A PDF analysis provides short-range order information of manganites such as the distortion of its perovskite structure due to the Jahn-Teller effect. This study hopes to understand the magnetic, structural, and transport properties of these manganites for compositions close to and on opposite sides of the MIT boundary.

#### **TP12: Neutron Diffraction Investigation of Shape-Memory Alloys during Mechanical Loading at Cryogenic Temperatures**

*S. Shmalo, T. Woodruff, C.R. Rathod (AMPAC/MMAE, University of Central Florida), V. Livescu, M.A.M. Bourke (Los Alamos National Laboratory), W. Notardonato (NASA Kennedy Space Center), R. Vaidyanathan (AMPAC/MMAE, University of Central Florida)*

The shape-memory effect refers to a phenomenon wherein a material on being heated, "remembers" and returns to a preset shape due to a phase transformation. In the process of returning to the preset shape, the phase transformation can work against large forces, resulting in their use as actuators. While shape-memory alloys have been commercially used at cryogenic temperatures in single-use applications

(e.g., couplings), their use at cryogenic temperatures in cyclic, switch-type applications has been limited by a lack of understanding of the underlying deformation mechanisms (i.e., phase transformation and twinning) at cryogenic temperatures. Such an understanding could extend the range of use of shape-memory alloys to, among others, spaceport related technologies such as latch and/or release mechanisms, thermal switches for cryogenic liquefaction and storage systems, fluid-line repair, valves, seals and self-healing gaskets.

At Los Alamos National Laboratory, in situ diffraction measurements at stress and elevated temperature have been routinely used to provide quantitative, phase specific information on the evolution of strains, texture and phase volume fractions. However, a capability for simultaneous loading and neutron diffraction spectra acquisition at cryogenic temperatures was unavailable. In order to investigate deformation in shape-memory alloys at cryogenic temperatures, the design of a low temperature loading capability for in situ neutron diffraction measurements has been analyzed and implemented on the Spectrometer for Materials Research at Temperature and Stress (SMARTS). An aluminum vacuum chamber with liquid nitrogen circulating to cool platens in contact with compression specimens was used. Preliminary results are reported here of quantitative, in situ measurements of evolving internal strains, texture, phase and twin volume fractions in the rhombohedral and monoclinic phases of shape-memory NiTiFe at cryogenic temperatures. This work is supported by grants from NASA and NSF (CAREER DMR-0239512).

#### TP13: Understanding Octahedral Tilting Distortions in $A_2M^{3+}M^{5+}O_6$ Perovskites ( $M^{5+} = \text{Ta, Nb, Sb}$ )

*P. W. Barnes (The Ohio State University; Argonne National Laboratory), P. M. Woodward (The Ohio State University), P. Karen (University of Oslo, Norway), M. W. Lufaso (The Ohio State University; National Institute of Standards and Technology)*

The perovskite structure with 1:1 *M*-site cation ordering (i.e., double or complex perovskites;  $A_2MM'X_6$ ) is a well-known and extensively studied structure type in solid-state chemistry. The ideal double perovskite has cubic symmetry, but many are distorted from the ideal structure. Structural distortions seen in complex perovskites are caused by electronic factors (e.g., Jahn-Teller ions), random or partial *M*-cation ordering, and most commonly, octahedral tilting. Tilting of the octahedra within the perovskite structure leads to lowering of its symmetry. A major factor that influences the degree of octahedral tilting in a given compound is the nature

of the cuboctahedral *A*-cation. Perovskites with  $\text{Ba}^{2+}$  as the *A*-site cation typically exhibit cubic symmetry and those with  $\text{Ca}^{2+}$  have orthorhombic or monoclinic symmetry. Changes (or lack of) in space group symmetry for  $A = \text{Ba}^{2+}$  and  $\text{Ca}^{2+}$  are often easily seen in the x-ray powder diffraction data (XRPD) of their respective compounds. Yet, compounds with  $A = \text{Sr}^{2+}$  are prone to subtle octahedral tilting distortions that are not readily seen in XRPD, so many are mistakenly assigned to the incorrect space group. In this study, twelve pseudo-symmetric double perovskites with  $A = \text{Sr}^{2+}$  ( $M^{3+} = \text{Sc, Cr, Mn, Fe, Co, Ga, Y}$ ;  $M^{5+} = \text{Nb, Ta, Sb}$ ),  $\text{Ba}_2\text{YNbO}_6$ , and  $\text{Ca}_2\text{CrTaO}_6$  were examined by Rietveld refinement of XRPD and neutron powder diffraction data (NPD) in order to appropriately discern their respective crystallographic symmetry. The approach taken for determining appropriate possible space groups for these compositions, the extent of *M*-site cation ordering, the degree of octahedral tilting, and a comparison of the driving forces behind these two distortions in compounds containing transition metal vs. main group metal cations will be discussed.

#### TP14: Neutron and Thermodynamic Investigation of Alkane Adsorption on MgO(100) Surfaces

*R. E. Cook, S. Chanaa, M. J. Farinelli, P. N. Yaron (The University of Tennessee - Department of Chemistry), T. Arnold (Oak Ridge National Laboratory - Chemical Sciences Division), L. L. Daemen (Los Alamos Neutron Science Center, Los Alamos National Laboratory), T. Ramirez-Cuesta (ISIS, Rutherford Appleton Laboratory), S. Clarke (University of Cambridge - Department of Chemistry), J. Z. Larese (The University of Tennessee - Department of Chemistry; Oak Ridge National Laboratory - Chemical Sciences Division)*

The adsorption properties of the first four members of the normal alkanes (methane, ethane, propane, butane) and films on the MgO (100) surface were investigated using neutron scattering and volumetric isotherm techniques. A series of high-resolution, adsorption isotherm measurements were performed using an automated adsorption apparatus. These data were used to determine both the two-dimensional isothermal compressibility and the isosteric heat of adsorption and to identify regions where phase transitions might occur. In all cases we find evidence for the presence of at least three layering transitions. We present our results to date of our investigations of the monolayer and multilayer solid phases using neutron diffraction and inelastic neutron spectroscopy (rotational and vibrational). Some preliminary indications of the nature of the dynamical properties of these solid phases will be presented by making



comparisons of the neutron spectra with calculations of the molecular-vibrational modes. We will compare our results to other related experimental investigations where appropriate.

#### **TP15: Studies on long range and short range ordering in Y-doped $\text{La}_2\text{Zr}_2\text{O}_7$**

*E.A. Payzant, S.A. Speakman, R.D. Carneim, T.R. Armstrong (Oak Ridge National Laboratory, Oak Ridge, TN), T.E. Proffen (Los Alamos National Laboratory, Los Alamos, NM)*

Selected compositions in the  $\text{La}_2\text{Zr}_2\text{O}_7$ - $\text{LaYO}_3$  system have been produced using glycine-nitrate process, as potential candidate materials for gas separation membranes. Refinement of x-ray diffraction data from such materials cannot resolve the oxygen site positions and occupancies to sufficient precision because of the presence of high-Z scatterers such as La, Y, and Zr, yet this is precisely the information that is critical to explain the ion mobility. Neutron scattering data was acquired using the high-resolution total scattering neutron powder diffractometer NPDF at LANSCE. A combination of structural (i.e., Reitveld) and pair distribution (i.e., PDF) analyses of the diffraction data provide important insight into the property-structure relationships in these materials. Research sponsored by the Laboratory Directed Research and Development Program of Oak Ridge National Laboratory (ORNL), managed by UT-Battelle, LLC for the U. S. Department of Energy under Contract No. DE-AC05-00OR22725. This work has benefited from the use of the Los Alamos Neutron Science Center at the Los Alamos National Laboratory. This facility is funded by the US Department of Energy under Contract W-7405-ENG-36.

#### **TP16: Inelastic Neutron Scattering Spectra of Simple Porphyrins**

*N. Verdal, B. S. Hudson (Department of Chemistry, Syracuse University, Syracuse, NY), P. Kozlowski (Department of Chemistry, University of Louisville, Louisville, KY)*

Porphine is the simplest of all porphyrins, a group of molecules pervasive in biological systems and thus in itself an interesting molecule. The biologically active porphyrin, typically an iron porphyrin, or heme group, is often involved in an oxidation/reduction reaction and thus small movements are important to biological function. In addition, it is used as a probe in resonance Raman studies in which the vibrational spectrum of the resonant group is used to probe changes in the protein environment associated with conformational changes. A more complete understanding of the porphine vibrations will place these probe applications on a more firm basis.

Inelastic neutron scattering (INS) spectra have been collected for both porphine and zinc porphine using the ISIS TOSCA spectrometer. These spectra have been compared with the results of both *ab initio* and the semi-empirical scaled quantum mechanical method calculations. The scaled quantum mechanical method uses a force field calculated by density functional theory using the B3LYP functional and the 6-31G\* basis set. These calculations have been previously compared with IR and Raman spectra with good agreement [see J. Phys. Chem. 1996, 100, 7007-7013]. The advantage of INS is that it is not subject to optical selection rules and allows a more complete comparison with the frequency and intensity output from *ab initio* and semi-empirical calculations. Good agreement between the INS spectra and the scaled quantum mechanical results are observed.

#### **TP17: Neutron Diffraction Studies on the Superionic-conducting Composite $(\text{AgI})_{0.6}(\text{NaPO}_3)_{0.4}$**

*E. Kartini (R & D Center for Materials Science and Technology, National Nuclear Energy Agency, Tangerang 15314, Indonesia), M.F. Collins (Department of Physics and Astronomy, McMaster University, Hamilton, ON, Canada), A. Purwanto (R & D Center for Materials Science and Technology, National Nuclear Energy Agency, Tangerang 15314, Indonesia; Neutron Science Laboratory, KEK, Tsukuba, Japan), T. Kamiyama (Neutron Science Laboratory, KEK, Tsukuba, Japan), K. Itoh (Kyoto University Research Reactor Institute, Kumatori-cho, Japan), T. Sakuma (Department of Physics, Ibaraki University, Mito, Japan)*

Superionic conductors are of considerable interest from both application and fundamental point of view. An ionic conductivity of at least  $10^{-3}$  S/cm is needed for use in solid electrolytes, batteries, fuel cells and sensors. We have successfully made a new superionic composite  $(\text{AgI})_{0.6}(\text{NaPO}_3)_{0.4}$  by melt quenching. This material exhibits a high ionic conductivity of about  $2 \times 10^{-3}$  S/cm at ambient temperature, whereas the conductivity of crystalline AgI and  $\text{NaPO}_3$  glass are orders of magnitude lower.  $(\text{AgI})_{0.6}(\text{NaPO}_3)_{0.4}$  is a composite material containing both crystalline and glass phases. To understand the ionic conduction mechanism two neutrons experiments have been performed. Firstly to investigate the crystalline phase measurements have been made by the high-resolution powder diffractometer VEGA, and secondly, the structure factor of the glass phase has been measured by the time of flight High Intensity Total Scattering instrument (HIT-II). Both measurements were performed at the Neutron Science Laboratory (KENS), KEK, Japan.



### TP18: Vibrational Spectroscopy with the NIST Filter-Analyzer Neutron Spectrometer (FANS)

*J.B. Leao, T.J. Udovic (NIST Center for Neutron Research), C.M. Brown (NIST Center for Neutron Research; Department of Materials Science and Engineering, University of Maryland), D.A. Neumann (NIST Center for Neutron Research)*

Neutron vibrational spectroscopy (NVS) is an invaluable technique for investigating solid-state vibrational dynamics. In particular, the typical range of energies accessible with reactor- and pulse-source-based neutrons spans the region of important lattice and molecular vibrations. Moreover, the unique nature of the neutron-nucleus interaction permits the observation of all vibrational modes in an NVS experiment, not just those that satisfy appropriate symmetry-based selection rules as in photon spectroscopies. NVS is particularly useful for characterizing hydrogenous materials since the incoherent scattering cross section for hydrogen is much larger than for virtually all the other elements. Over the past couple of years, neutron vibrational spectra have been collected for a broad array of both hydrogenous and nonhydrogenous systems utilizing the significantly improved Filter-Analyzer Neutron Spectrometer (FANS) at the NIST Center for Neutron Research. Here we exemplify the impact that FANS can have as a unique spectroscopic probe of materials within the fields of physics, chemistry, and biology.

### TP19: Progress Toward Thermal Neutron Laue Diffraction at the NCNR

*B. H. Toby, C. Y. Jones, A. Santoro, P. C. Brand, T. Prince (NIST Center for Neutron Research), T. D. Pike (Department of Physics & Astronomy, Johns Hopkins University; NIST Center for Neutron Research), D. L. Jacobson (Physics Laboratory, National Institute for Standards & Technology, Gaithersburg, MD 20899-8461)*

A test station is being developed to explore small molecule single-crystal neutron diffraction using a thermal neutron beam ( $\lambda \sim 0.9 \text{ \AA}$  to  $2.5 \text{ \AA}$ ) from the CNBS thermal column. Detection for this simple and compact prototype will be performed by activating dysprosium foils, and replicas of the resulting activation patterns will be recorded on image plates. In concert, novel algorithms are being developed for data analysis from these Laue diffractograms. The goal of this project is to make maximal use of the full thermal spectrum and correspondingly reduce the crystal size needed for data collection.

### TP20: Neutron Guides and Scientific Neutron Equipment at CILAS/GMI

*P. Gautier-Picard (CILAS, 8 avenue buffon, BP 6319,*

*45063 Orléans, FRANCE)*

CILAS company is the world's leading supplier of complete neutron guides systems. The neutron optics with multilayer coatings produced by CILAS have become an international standard for neutron beam transportation in the modern research institutes. During the last 30 years, CILAS designed, produced and installed more than 5000 meters of guides in many European, American and Asian countries. To reinforce its leadership and presence in neutron research, CILAS acquired the company Grenoble Modular Instruments (GMI), a leading company in high precision mechanics, engineering and manufacturing of spectrometers and scientific equipment for neutron and synchrotron research. In this article, the differences between the different kind of neutron guides using Borkron, borofloat, and float glasses will be presented. They indeed show different behavior under neutron flux as well in coating quality.

### TP21: ZrH as a moderator for pulsed spallation neutron sources

*B. J. Micklich, J. M. Carpenter (Argonne National Laboratory)*

Several types of neutron scattering instruments, including spectrometers such as HRMECS at IPNS and perhaps TOF-USANS, could profitably use a source of neutrons prolific in the few hundred meV range. A moderator of  $\text{ZrH}_2$ , which has energy levels at  $\hbar\omega$  where  $\hbar\omega = 0.137 \text{ eV}$ , could provide such a neutron energy spectrum when operated at elevated temperature.  $\text{ZrH}_2$  has seen application as a moderator for nuclear reactors, either alone or in the form of  $\text{ZrH-U}$  fuel elements of a TRIGA reactor, because of its unusual temperature-dependent thermalization properties and its high hydrogen density.  $\text{ZrH}_2$  (0.07066 atoms/bn-cm) has a higher hydrogen atom density than water (0.0662 atoms/bn-cm). Metal alloy phase diagrams for the  $\text{Zr} + \text{H}$  system indicate that the material is stable (defined here as a hydrogen pressure less than or equal to about 1 atm) for  $\text{ZrH}_{1.9}$  at 800 K or  $\text{ZrH}_{1.6}$  at 1200 K. This pressure could be supported by a vacuum-insulated stainless steel container.

We calculated neutron spectral intensities and neutron emission time distributions for a  $\text{ZrH}_2$  moderator in the H moderator position at IPNS using the radiation transport code MCNPX and  $\text{ZrH}_2$  neutron scattering kernels available for temperatures between 300 K and 1200 K. The moderator was decoupled and poisoned with  $9.7 \cdot 10^{20} \text{ at/cm}^2$  gadolinium at the midplane. No attempt was made to optimize the moderator thickness or the location of the poison plate. Our results show that the spectral

intensity over the energy range 0.1 eV to 1 eV increases as the temperature of the moderator increases. Increases up to a factor of three over the installed solid methane moderator are seen in this energy range. These additional neutrons show up in neutron time distributions that have both higher peak intensities and a broader distribution in time.

#### **TP22: Origin and removal of spurious background peaks in vibrational spectra measured by filter-analyzer neutron spectrometers**

*T.J. Udovic, D.A. Neumann, J.B. Leao (NIST Center for Neutron Research), C.M. Brown (NIST Center for Neutron Research; Department of Materials Science and Engineering, University of Maryland)*

Inelastic neutron scattering is an invaluable technique for measuring the vibrational spectra of materials. One of the standard methods for analyzing the energies of neutrons scattered by vibrational modes involves the use of polycrystalline beryllium filters. We demonstrate that the spurious background features between 50 meV and 85 meV accompanying vibrational spectra measured with filter-analyzer neutron spectrometers are due to phonon excitations of the beryllium filter. These features are significantly reduced by an auxiliary polycrystalline bismuth filter placed in front of the main filter. Such a bismuth filter can result in only a minor attenuation in sample scattering intensity concomitant with a reduction in the thermal- and fast-neutron background from the sample.

#### **TP23: A multi-rotor T0 chopper for HYSPEC**

*V.J. Ghosh, I. A. Zaliznyak, S.M. Shapiro, L. Passell (Brookhaven National Laboratory)*

One of the design goals for HYSPEC has been to achieve the highest possible signal-to-background ratio. For neutron spectrometers in general, when the sample environment is in the direct line of sight of the neutron source the performance of the T0 chopper becomes crucial to achieving low beam-related backgrounds and, therefore, high instrument performance. The traditional design of these T0 choppers involves a single rotor, 30 to 40 cm thick, phased so that it blocks the beam at the time of arrival of the prompt gamma-rays and the highest-energy neutrons. As the power of the source increases, so does the radiation load on the T0 choppers. Consequently, the requirements for the amount and type of material of which these choppers are made become more and more demanding. In addition, for optimum efficiency these massive rotors should rotate at rates of 60-120 Hz. The design of these choppers often becomes a delicate balance between neutronic performance and mechanical

safety. We propose the use of a multi-rotor setup for HYSPEC so that we do not have to compromise either neutronic efficiency or mechanical performance. We have studied a setup consisting of two counter-rotating rotor pairs, where each rotor is a 10 cm thick disk, made of tungsten, inconel or stainless steel. These counter-rotating pairs act as velocity selectors, the doubling of the effective rotation rate allows us to reduce the beam-related background. In addition this setup allows us to use a lot of heavy material for stopping the fast neutrons without compromising mechanical safety. The performance of the HYSPEC multi-rotor T0 chopper setup was studied using ray-tracing (MCSTAS) and neutron transport (MCNP-X) codes. These results will be presented and compared with the results for a traditional T0 chopper.

#### **TP24: Optimization of a Gd-CsI neutron converter for a GEM based neutron detector**

*R. Berliner (Instrumentation Associates Inc.; University of Michigan Department of Nuclear and Radiological Sciences)*

In a prototype SNS neutron detector, a CsI screen, covering a layer of metallic Gd, produces low energy secondary electrons (SE) that are then amplified and localized by a Gaseous Electron Multiplier<sup>1</sup> (GEM) followed by a dual charge-division X-Y pickup anode. The efficiency of the detector is critically dependent on the thickness of the Gd and CsI layers that make up the active portion of the neutron converter. The geometry of the neutron converter for the neutron GEM has been optimized by Monte-Carlo calculations of primary electron production in the Gd and SE production in the CsI layers. Benchmark calculations with a modified version of Penelope,<sup>2</sup> a standard Monte-Carlo electron transport code, were used to reproduce the results of earlier detailed model analysis of SE production.<sup>3</sup> These calculations were then extended to analyze realistic GEM neutron detector geometries. The results of these calculations and comparison to experimental results with the GEM neutron detector will be presented.

Supported by the DOE SBIR program under grant DE-FG02-03ER83685.

[1] F. Sauli, GEM, a new concept in electron amplification in gas detectors, *Nuc. Inst. And Meth.* A386 (1997) 531-534.

[2] J. Sempau, J.M. Fernandez-Varea, E. Acosta and F. Salvat: Experimental benchmarks of the Monte Carlo code PENELOPE. *Nuclear Instruments and Methods B* 207 (2003) 107-123.

[3] A. Akkerman, A. Gibrekhterman, A. Breskin and R. Chechik, *J. Appl. Phys.* 72 (11) (1992) 5429-5436.

#### **TP25: The NCNR MBE Facility for *In Situ* Neutron Scattering**

*J. A. Dura (NIST Center for Neutron Research)*

A molecular beam epitaxy, MBE, facility has been built to enable *in situ* neutron scattering measurements during growth of epitaxial layers. While retaining the full capabilities of a research MBE chamber, this facility has been optimized for polarized neutron reflectometry measurements. Optimization includes a compact, light weight, portable design, a neutron window, controllable magnetic field, large sample area with exceptional growth uniformity, and sample temperatures continuously controllable from 38 K to 1300 K. A load lock chamber allows for sample insertion, storage of up to 4 samples, and docking with other facilities. The design and performance of this chamber are described here.

#### **TP26: Modifying High Temperature Furnaces to Extend Operating Capabilities**

*J.S. Fieramosca (Argonne National Laboratory)*

Sometimes it is possible to modify existing sample environment equipment beyond its originally designed operating parameters, such as extending its temperature range, sample containment, etc., to accommodate newer and more demanding scientific studies. The Intense Pulsed Neutron Source (IPNS) has modified one of its high temperature furnaces, a vanadium foil vacuum furnace, to satisfy the requirements of recently proposed user experiments. The vanadium foil vacuum furnace is a resistive-heating element type furnace able to heat samples to 1000 °C. It consists of two heat shields, a heating element, a separate sample vacuum housing, and sample container, all cylindrically concentric and constructed of vanadium. The original sample housing maintains a separate high vacuum around the sample and allows sample changes during the experiment without breaking vacuum to the furnace element. A recently proposed experiment required a modification to the furnace to accommodate a controlled atmosphere about the sample. The furnace modification consisted of substituting for the sample housing and container an open-ended fused silica tube with an imbedded silica frit for supporting a powder sample in the beam. The use of fused silica was dictated by the corrosiveness of the gas used in the experiment. A controlled atmosphere flows through the fused silica tube and over the sample at temperature. Gas composition and flow rates are controlled using EPICS interfaced automated mass flow controllers.

#### **TP27: Fast Exchange Refrigerator for Neutron Science (FERNS)**

*J.E. Rix (Containerless Research, Inc.), L.J.*

*Santodonato (Spallation Neutron Source, Oak Ridge National Laboratory), J.K.R. Weber (Containerless Research, Inc.)*

Modern neutron science can exploit new techniques that locate samples in a neutron beam while controlling experimental variables such as temperature, pressure, and magnetic field. The Fast Exchange Refrigerator for Neutron Science (FERNS) instrument is being developed to enable efficient use of beamline resources, achieve a high throughput of samples, and meet needs expressed by the user community for an capability that combines: (i) reliable cryogenic temperature control, (ii) remote automated sample exchange and storage, (iii) rapid thermal response, and (iv) ease-of-use with various sample experimental configurations. The FERNS instrument is designed to exploit the fast measurement capabilities of high flux beamlines by integrating automated sample handling and cryogenic temperature control via a computerized operating and sample management system. We present results of testing of a prototype FERNS device using a cryogenic system, results of cooling and sample exchange testing, describe software control capabilities, and outline plans for a beamline instrument that can be programmed to process multiple samples.

Supported by DOE Phase I SBIR contract number DE-FG02-03ER83633.

#### **TP28: Variations on a Theme: The Closed-Cycle Refrigerator in Neutron Scattering**

*B. Clow, E. Fitzgerald, D. Dender (NIST Center for Neutron Research)*

The closed-cycle refrigerator is ubiquitous at neutron scattering facilities due to its reliability, ease-of-operation, and useful temperature range. Being common, though, does not mean being boring. This basic platform is shown in a variety of interesting arrangements that show the versatility of this equipment and the science that is made possible by its use.

#### **TP29: Development of neutron reflectometer at HANARO**

*J.S. Lee, C.H. Lee, B.S. Seong, C.M. Shim, G.P. Hong, B.H. Choi, Y.H. Choi, S.J. Cho, E.J. Shin, Y.J. Kim (Korea Atomic Energy Research Institute, Yuseong P.O. Box 105, Daejeon, 305-600, Korea)*

The neutron reflectometer was developed on ST3 horizontal beam port in HANARO, 30 MW research reactor. According to the characteristics of neutron source, constant wavelength methods using 0.245



nm with PG monochromator,  $\beta = 0.4^\circ$ , and vertical sample geometry were taken. The dimension of the instrument is 5.4 m for neutron source-monochromator, 3.0 m for monochromator-sample and 1.6 m for sample-detector. The distance between two slits to define width of incident beam to sample position is 2.4 m. In order to reduce the contamination of neutron reflection pattern due to the second order reflection of PG monochromator, PG filter with  $\beta = 3.5^\circ$  was taken. By the gold wire activation method, neutron flux at monochromator and sample position was measured to  $4.5 \times 10^9$ ,  $4.4 \times 10^6$  n/cm<sup>2</sup>/sec. After the installation of the instrument, the characteristics of transmitted neutron beam through the slits were evaluated with neutron camera. And also, by measuring neutron reflectivity curve for the typical samples like glass and Si, instrument capacity such as minimum reflectivity,  $Q$  range and instrumental resolution was evaluated. A vacuum furnace and polarizing accessories will be developed to enhance the instrument performance.

#### **TP30: New Thermal Triple Axis Spectrometers at the NCNR**

*M. Murbach, C. Wrenn, C. Brocker (NIST Center for Neutron Research; Department of Materials Science and Engineering, University of Maryland), P. Brand, J. W. Lynn (NIST Center for Neutron Research)*

As part of the modernization of the thermal neutron spectrometers, and new state-of-the-art thermal neutron instrument is now being installed at the BT-7 thermal beam port. There is a choice of filters and collimations in the reactor beam that bring neutrons onto a choice of  $20 \times 20$  cm<sup>2</sup> double focusing monochromators. The sample stage incorporates an independent magnet axis in addition to the usual motorized sample orientation and rotation angles. The analyzer and detector system will be housed in a single unit on air pads. The analyzer will also provide horizontal focusing capability, or it can use a flat crystal array coupled with a position-sensitive detector to allow the simultaneous collection of data over a range of ( $Q, E$ ), or it can use a choice of different conventional collimators, all remotely and under computer control. The analyzer/detector system is designed to be self-contained so that it can be easily interchanged with a different style of analyzer as new systems are developed. Guide fields are incorporated throughout the instrument to enable polarized beam operation. A similar spectrometer is being developed for the BT-9 beam port.

#### **TP31: Concept and performance of the TOF strain scanner POLDI with multiple frame overlap**

*U. Stuhr, W. Wagner (Paul Scherrer Institut, 5232*

*Villigen-PSI, Switzerland)*

POLDI is a new neutron diffraction instrument at the Swiss continuous spallation neutron source SINQ at PSI, primarily dedicated to residual stress investigations. The instrument has realized a novel type of time-of-flight (TOF) diffractometer allowing multiple frame overlap. Besides for the benefit of higher intensity (as compared to a conventional single-pulse mode), this concept allows an independent tuning of intensity and resolution, an immense advantage for a flexible adjustment to dedicated experiments. The concept makes use of the mutual dependence of the neutron's arrival time at the detector and the related scattering angle to assign the neutrons to the originating pulse at the chopper. The principle concept of the instrument, some special components, and the performance in terms of intensity, resolution and flexibility for strain mapping and structure analysis will be presented.

#### **TP32: A new polarized Neutron Reflectometer at Dhruva Reactor**

*Surendra Singh, Saibal Basu (Solid State Physics Division, Bhabha Atomic Research Centre, Mumbai -85 INDIA)*

A new Polarized Neutron Reflectometer has been installed at Guide Tube Laboratory of Dhruva Reactor, BARC, India. Unlike the conventional  $q-2q$  instrument, this instrument uses a linear Position Sensitive Detector and a high precision rotational sample table. This arrangement, immensely, helps collecting data in off specular mode. In this paper we present the specification of instrument and few examples of specular reflectivity data as well as off specular reflectivity data of thin films and multilayers, measured by this instrument, both for polarized and unpolarized mode. The reflectivity data are analyzed using a genetic algorithm based  $x^2$  minimization program developed by us.

#### **TP33: New High-Flux SANS Instrumentation at Oak Ridge National Laboratory**

*G.W. Lynn, M.V. Buchanan, P.D. Butler, W.T. Heller, D.A.A. Myles, V.S. Urban, G.D. Wignall (Oak Ridge National Laboratory)*

A number of upgrades are in progress at the High Flux Isotope Reactor (HFIR), including the installation of a supercritical hydrogen moderator ( $T \sim 20$  K) that will be one of the "brightest" cold sources currently available. It will feed four cold neutron guides (CG1-4), each with new instrumentation. CG2 and CG3 are reserved for two new small-angle neutron scattering (SANS) instruments. A 40 m SANS instrument (SANS1), funded by the Department of Energy (DOE) Office of Basic Energy Sciences and



the University of Tennessee, Knoxville is designed for CG2. The 35 m small-angle neutron scattering facility (Bio-SANS on CG3) is optimized for the study of biological systems and is the cornerstone of the Center for Structural Molecular Biology (CSMB), funded by the DOE Office of Biological and Environmental Research. The facilities will be housed in a recently completed Guide Hall, along with a suite of other instruments, including a reflectometer and a cold triple-axis spectrometer. Both SANS facilities will have variable wavelength and large area ( $1\text{ m}^2$ ) high count-rate detectors ( $> 10^5$  Hz) that can translate 45 cm off axis to increase the dynamic Q-range ( $< 0.001 \text{ \AA}^{-1}$  to  $1.0 \text{ \AA}^{-1}$  overall). As the HFIR is one of only two reactors with a core flux greater than  $10^{15}$  neutrons/sec/cm<sup>2</sup>, the beam intensities (up to  $10^7$ /sec/cm<sup>2</sup>) will be comparable to the best facilities worldwide. This will improve both the quantity and quality of data that we can collect from synthetic and biological macromolecules, allowing us to increase throughput, to use smaller sample volumes and to perform kinetic (time-resolved) experiments.

#### **TP34: POWGEN3: A High Resolution Third Generation Powder Diffractometer**

*J.P. Hodges (Spallation Neutron Source, Oak Ridge National Laboratory)*

POWGEN3 is a fundamental departure from previous designs for a powder diffractometer at a spallation neutron source. POWGEN3 may be considered the world's first third-generation time-of-flight powder diffractometer. For the first time, a high-resolution powder diffractometer is able to take advantage of a high source repetition rate. Combined with a supermirror neutron guide system, POWGEN3 is a very efficient instrument. The high count rates thus achieved together with high-resolution characteristics present a big leap forward in performance over previous diffractometer designs. POWGEN3 will thus provide unprecedented opportunities for new science in the study of crystalline materials.

#### **TP35: Monte Carlo Beam Line Simulation for Neutron Interferometry at NIST**

*K.P. Schoen (University of Missouri - Columbia),  
S.A. Werner (University of Missouri - Columbia;  
National Institute of Standards and Technology)*

The uncertainty in neutron interferometry measurements is typically limited only by the intensity and not system resolution. There are several ways to increase the intensity of neutrons at the interferometer, including varying monochromator crystal size, allowing monochromator crystals to be vertically focusing, and installing supermirror guides along the flight path leading to the interferometer. A Monte

Carlo beam line simulation was performed for each of these configurations for the NIST Neutron Interferometer and Optics Facility and compared to the neutron intensity for the current configuration in use. The results for each simulation configuration are presented; the configuration yielding the largest increase in neutron intensity provided a gain of a factor of 5 over the current experimental setup.

#### **TP36: Some Effects of Multiple Scattering Encountered in SANS**

*J. G. Barker (NIST Center for Neutron Research)*

General methodologies for calculating multiple scattering effects are presented. Several specific examples of multiple scattering corrections found in small angle neutron scattering (SANS) are presented. The cases presented here were chosen to provide particular insights into the more routine problems encountered in handling multiple scattering, but as yet have not been sufficiently espoused in the considerable literature on this subject. For scattering occurring at sufficiently small angles, the semi-analytical technique of Schelten & Schmatz [*J. Appl. Cryst.* (1980), **13**, 385-390] was used. Monte Carlo simulations were also used, and were found to be a more robust method of calculating many problems. Power series corrective expressions have been determined for the forward cross-section  $I_m(0)$ , and the radius of gyration  $R_g$ , used to characterize the central part of the scattering curve for five different scattering functions: Gaussian shaped scattering, the scattering from spheres, the DAB model, the Sabine function ( $p = 3/2$ ) and Lorentzian scattering. Other cases presented are scattering from narrow Gaussian peaks, and corrections to power-law scattering at large  $q$ . Effect of multiple scattering upon the forward cross-section of isotropically scattering samples, such as from water and vanadium, are also presented.

#### **TP37: Dynamically Polarized Hydrogen Target as a Broadband, Wavelength Independent Neutron Spin Polarizer**

*J.K. Zhao (Spallation Neutron Source, Oak Ridge National Laboratory), V. Garamus, R. Willumeit (GKSS Research Center, Geesthacht, Germany.)*

The feasibility of using dynamically polarized hydrogens as wavelength independent neutron spin polarizers was investigated. A modified setup of the Dynamics Nuclear Polarization station at the GKSS research center was used with the standard GKSS solvent sample as the target. The 2.8mm thick sample consisted of 43.4 % water. The rest is mostly glycerol with a small amount of EHVA-Cr(v) complex providing the needed paramagnetic centers. Non polarized neutrons ( $8.5 \text{ \AA}$ ) first pass through the

polarized target. The polarization of the transmitted neutrons was then analyzed with a supermirror analyzer. At the highest hydrogen polarization of 68.6 % that was achieved during the experiment, the polarization of the transmitted neutrons was measured at 51.8 %. All the measured polarizations agree nicely with theoretical calculations for the used sample. Further experiments will test the feasibility of using methane samples as the target, which theoretically would allow us to achieve neutron polarizations of over 95 % with transmissions greater than 30 %.

### **TP38: A semiconductor based transmission monitor for the SAND instrument at IPNS**

*P. Thiyagarajan (Intense Pulsed Neutron Source, Argonne National Lab), Patrick M. De Lurgio (CIS-EL, Argonne National Laboratory, 9700 South Cass Avenue, Argonne, IL 60439), Raymond T. Klann, Charles Fink (NE, Argonne National Laboratory, 9700 South Cass Avenue, Argonne, IL 60439), Douglas S. McGregor (Kansas State University, 151 Rathbone Hall, Manhattan, KS 66506), Istvan Naday (CIS-EL, Argonne National Laboratory, 9700 South Cass Avenue, Argonne, IL 60439), Denis Wozniak, Ed Lang (Intense Pulsed Neutron Source, Argonne National Lab)*

A semiconductor based neutron detector was developed for the time-of-flight Small Angle Neutron Diffractometer (SAND) instrument at the Intense Pulsed Neutron Source, Argonne National Laboratory for the simultaneous measurement of transmitted neutron beam intensity and the scattering data. SAND uses neutrons from a pulsed spallation source moderated by a coupled solid methane moderator that produces useful neutrons in the wavelength range of 0.5 to 14 angstroms that are sorted by time-of-flight into 68 constant  $\delta T/T = 0.05$  channels. In addition to allowing effective use of valuable beam time this detector offers higher precision data in the experiments involving complicated sample environment and samples. The detector is constructed using a 0.5 micron thick coating of boron-10 on a gallium-arsenide semiconductor wafer and is mounted directly within a cylindrical (2.2 cm dia. and 4.4 cm long) enriched boron-10-carbide beam stop in the SAND instrument. Since this detector is buried inside the beam stop it does not cause any additional parasitic background. The boron-10 coating on the GaAs detector enables the detection of the cold neutron spectrum with reasonable efficiency. This detector can be readily adapted for the SANS instruments at the steady-state sources as well. This paper describes the details of the detector fabrication, the beam stop monitor design, gamma rejection, radia-

tion resistance and overall performance based on the experience during several run cycles at the IPNS.

This work benefited from IPNS, ANL funded by U.S. DOE-BES under contract W-31-109-ENG-38 to U of Chicago and SNS, ORNL funded by DOE-BES under contract DE-AC05-00OR22725 to UT-Battelle, LLC.

### **TP39: ENGIN-X; from crystals to crankshafts**

*Mark R Daymond (ISIS Facility, Rutherford Appleton Laboratory, Chilton, Didcot, OX11 0QX, UK) and Lyndon Edwards (Dept. of Materials Engineering, The Open University, Milton Keynes, MK7 6AA, UK)*

ENGIN-X, the recently constructed diffractometer at ISIS which was optimised for diffraction engineering measurements of stress, has just finished its first complete year of running. Along with an order of magnitude improvement in performance over the previous instrument, major hardware and software improvements have been implemented that considerably simplify the process of planning and executing an experiment for the average user.

These include easy changing all three dimensions of the gauge volume, CMM based laser scanning of objects prior to experimentation, computer controlled positioning and planning of experiments and automated data analysis.

The performance improvements achieved with ENGIN-X and the way that these innovations have simplified the way that experiments are carried out will be illustrated through a series of examples covering fundamental science explorations and the solution of real industrial problems.

### **TP40: VISION: A Neutron Vibrational Spectrometer for SNS**

*J.Z. Larese (Chemistry Dept., Univ. of Tennessee; Oak Ridge National Laboratory), L.L. Daemen, P.A. Seeger (Los Alamos Neutron Science Center, Los Alamos National Laboratory), B.S. Hudson (Chemistry Dept., Syracuse Univ.), J. Eckert (Los Alamos Neutron Science Center, Los Alamos National Laboratory)*

There is a need in the United States for a state-of-the-art neutron scattering instrument for vibrational spectroscopy to investigate the structure and dynamics of condensed matter systems by the simultaneous use of elastic diffraction and moderate resolution (1-2%  $\Delta E/E$ ) inelastic scattering over a broad energy transfer range. The use of neutron vibrational spectroscopy (NVS) is growing at a significant rate in Europe thanks to the second-generation instrument TOSCA at ISIS, the spallation neutron source at the

Rutherford-Appleton Laboratory in England.

We will outline our proposal to design a next generation, time of flight (TOF) spectrometer named, VISION, which is not an acronym, to investigate a vast array of molecular dynamics and structure.

Under optimal conditions this instrument will

- have a throughput two orders of magnitude greater than TOSCA –currently the best instrument in the field;
- cover an energy transfer range of 0-500 meV (0-4000  $\text{cm}^{-1}$ );
- have a 1-2% energy resolution while simultaneously enabling diffraction studies for structural characterization;
- offer a wide range of sample environments (low temperature, high-pressure, flow cell, thermal analysis, etc).

Our approach will incorporate neutron techniques developed during the decade since TFXA and TOSCA were first designed and built. This includes improved supermirror technology, parametrically matched crystal analyzer-helium gas detectors, efficient electronics for high rate data acquisition, high-performance data analysis algorithms, novel moderator concepts, and well-developed Monte Carlo software for neutron optics and instrument design and optimization. This new design combined with the flux available at SNS will enable time-resolved vibrational measurements for the first time at a neutron source.

Proposals to form an Instrument Design Team (IDT) and a subsequent proposal describing the scientific background for VISION have been presented to the Spallation Neutron Source (SNS) Experimental Facilities Advisory Committee (EFAC) and have been positively received. (EFAC has enthusiastically endorsed the science case presented by the IDT and a beamline position for installation and construction of VISION has been identified by SNS.)

#### **TP41: Simple functional forms for total cross sections from neutron-nucleus collisions.**

*P. K. Deb (Department of Physics, The Ohio State University, Columbus, OH 43210, USA), K. Amos (School of Physics, The University of Melbourne, Victoria 3010, Australia)*

Total cross sections have been predicted for neutrons scattering from nuclei ranging in mass from 6 to 238 and for projectile energies from 10 MeV to 800 MeV. So also have been the mass variations of those cross sections at selected energies when they have been calculated using coordinate space optical potentials formed by full folding effective two-nucleon (NN)

interactions with one body density matrix elements (OBDME) of the nuclear ground states. Good comparisons with data result when effective NN interactions defined by medium modification of free NN  $t$  matrices are used. There is a simple three parameter functional form that produces the partial wave total cross section values determined from those optical potential calculations. Adjusting the theoretical defined parameter values has enabled us to fit the actual measured data values from the scattering involving 9 nuclei spanning the mass range from  ${}^6\text{Li}$  to  ${}^{238}\text{U}$  and for neutron energies from 10 MeV to 600 MeV. The parameter values vary smoothly with mass and energy. Total cross sections are well reproduced by using simple functional form.

#### **TP42: Measurement of the Neutron Lifetime Using a Proton Trap**

*F. E. Wletfeldt (Tulane University), M. S. Dewey, D. M. Gilliam, J. S. Nico (National Institute of Standards and Technology), X. Fei, W. M. Snow (Indiana University), G. L. Greene (University of Tennessee/Ornl), J. Pauwels, R. Eykens, A. Lamberty, J. Van Gestel (IRMM, Belgium)*

We describe a recent measurement of the neutron lifetime by the absolute counting of in-beam neutrons and their decay protons. Protons were confined in a quasi-Penning trap and counted with a silicon detector. The neutron beam fluence was measured by capture in a thin  ${}^6\text{LiF}$  foil detector with known absolute efficiency. The combination of these simultaneous measurements gives the neutron lifetime:  $\tau_n = 886.8 \pm 1.2$  [stat]  $\pm 3.2$  [sys] s. The systematic uncertainty is dominated by uncertainties in the mass of the  ${}^6\text{LiF}$  deposit and the  ${}^6\text{Li}(n,t)$  cross section. This is the most precise measurement of the neutron lifetime to date using an in-beam method.

#### **TP43: Some Principal Problems in Physics and Neutron Low Energy Physics**

*Yu. A. Alexandrov (Senior Scientist of FLNP, JINR, Dubna)*

Physics is a single whole, therefore the answers to some principal questions should be sought for not only in high-energy physics, but also in other divisions of physics, e.g., in low energy neutron physics. Especially since the accuracy of experiments in neutron physics is frequently much higher.

In this report the questions connected with the internal structure of particles (e.g., of neutron) are discussed.

The first question deals with the charge neutron radius connected with the value of neutron-electron scattering length determined at low neutron energies.



At present, the obtained accuracy allows us to speak not only about the value of the charge neutron radius, but also on the division of it into Dirac and Foldy terms. The sign of the Dirac term is connected directly with the fundamental Yukawa theory explaining the origin of nuclear forces.

The second question also concerns the subject of the structure of the neutron, namely its deformation. The notion of deformation (polarizability) of the nucleon in electromagnetic field was introduced in mid 50s. In the report the reasons are given in favor of the opinion that the neutron polarizability was observed for the first time in neutron experiments already in 1957, i.e. earlier than the proton polarizability was detected (1960).

Finally, the third question deals with the search for a magnetic charge of the neutron. The beautiful experiment (Finkelstein, Shull, Zeilinger, 1986) testifying with high accuracy the absence of a magnetic charge of the neutron is discussed. The existence of an isolated magnetic charge in the nature would explain the quantization of electric and magnetic charges (Dirac, 1931).

#### **TP44: Consequences of the interaction between dynamical diffraction and the Sagnac effect in LLL perfect single crystal interferometers**

*K.C. Littrell (Intense Pulsed Neutron Source, Argonne National Lab)*

The LLL perfect single crystal interferometer is an exciting tool for exploring a variety of topics of fundamental importance in understanding quantum mechanics and for precision measurement of neutron scattering lengths. One of the limiting factors in many neutron interferometry experiments is the overall size of the interferometer. Hence, ever-larger interferometers would seem to be preferable. However, according to the theory of dynamical diffraction, neutrons that nearly but not exactly satisfy the Bragg condition take different trajectories through the crystal, splitting into two current branches at blade of the interferometer; thus there are sixteen mutually interfering wavefunctions that contribute to the measurement of an interferogram. This complexity gives rise to shifts in the measured phase difference and a loss of contrast of the interferogram in the presence of potentials which are dependent on the spatial differences between the trajectories of the neutron through the interferometer. This effect has already been experimentally verified for the gravitational potential; here we discuss the similar effects of dynamical diffraction on the phase shift due to the Sagnac effect and their

consequences on the observable contrast in large-scale interferometers.

#### **TP45: Pressure/Temperature Induced Phase Behavior of Triblock Copolymer PEO133PPO50PEO133 in Electrolyte Solutions.**

*Lixin Fan\*, L. Guo, P. Thiyagarajan (Intense Pulsed Neutron Source, Argonne National Lab)*

The pressure/temperature dependent phase behavior of 5wt. % triblock copolymer PEO133PPO50PEO133 (F108) in aqueous solutions containing different  $[\text{Na}_2\text{CO}_3]$  has been studied by small-angle neutron scattering. These studies show that pressure, temperature and sodium carbonate have strong effects on the micellization and phase transition of F108 in these solutions. At 40 °C, F108 in 0.3M  $\text{Na}_2\text{CO}_3$  solution forms spherical interacting micelles. As the pressure increases from 1bar to 1kbar, the micelle association number and the radii of the core, corona and hard sphere decrease. Further increase of pressure leads to a transition from spherical micelles to rod-like micelles. The radius of the rod-like micelles does not change significantly with increasing pressure up to 2kbar, while the length monotonically increases with pressure. The structures formed in this region of the phase map are thermodynamically reversible. At 55 °C spherical and rodlike micelles coexist in a pressure range of 1 bar to 1 kbar. At 1.7 kbar the radius of rod-like micelles jumps to higher value reflecting the association of rodlike micelles. At 2 kbar we observed a lamellar phase. In 0.5M  $\text{Na}_2\text{CO}_3$  solution phase transitions from spherical interacting micelles to rod-like micelles and then to an ordered phase can be observed with increasing pressure even at room temperature. Interestingly, at higher pressures the order in the system decreases with increasing pressure leading to a solution of unimers.

This work benefited from the use of Intense Pulsed Neutron Source at Argonne National Laboratory, which is funded by the Office of BES, US DOE.

\*current address: Advanced Photon Source, Argonne National Laboratory, 9700 South Cass Ave, Argonne, IL 60439, USA

#### **TP46: Characterization of Cryptophycin- and Dolastatin-Induced Tubulin Rings**

*H. Boukari (National Institutes of Health, Bethesda, Maryland, USA), S. Krueger (National Institute of Standards and Technology), R. Nossal, D. L. Sackett (National Institutes of Health, Bethesda, Maryland, USA)*

We have applied small-angle neutron scattering (SANS) and dynamic light scattering (DLS) to probe



interactions of the protein,  $\alpha\beta$ -tubulin, with either cryptophycin 1 or dolastatin 10, two small peptides extracted from marine products. These two peptides inhibit the polymerization of tubulin into microtubules and, instead, induce the formation of tubulin rings of about 24 and 44 nm diameter, respectively [1]. Under the studied conditions, the SANS and DLS measurements on cryptophycin-tubulin samples indicate a narrow structural dispersity with a predominant structure made of 8 tubulin dimers assembled into non-interacting rings. In contrast, dolastatin-tubulin samples show additional aggregation of the primary rings, composed mostly of 14 dimers, resulting in large structures that settle to the bottom of their container under the effect of gravity. Further modeling of the SANS profiles indicate, remarkably, that the dolastatin-tubulin aggregates are ordered structures, most likely columns of rings [2]. These rings can be used as potential models for investigating the behavior of closed ring polymers, which may intrinsically differ from open-ended linear biological polymers such as microtubules and actin filaments.

[1] H. Boukari, R. Nossal, D. L. Sackett, *Biochemistry* **42**, 1292 (2003).

[2] H. Boukari, V. Chernomordik, S. Krueger, R. Nossal, and D. L. Sackett, *Physica B* (in press).

#### TP47: Reflectometry Studies of Multi-Layered Non-Linear Optical Films

*E. Watkins, J. Majewski, J. Robinson, H. Wang, P. Chiarelli, J. Casson, F. Trouw (Los Alamos National Laboratory)*

Neutron and x-ray reflectivity measurements were used to characterize the structure of non-linear optical (NLO) films containing S-azo-C18 molecules. Langmuir-Blodgett (LB) multilayers were prepared by the sequential transfer of S-azo-C18 and stearic acid molecules on octadecyltrichlorosilane (OTS) coated quartz and silicon substrates. To provide good contrast for neutron measurements, the stearic acid molecules were deuterated. One and two bilayer samples were prepared for both possible layer orderings. Neutron measurements were performed on the SPEAR reflectometer at the Los Alamos Neutron Science Center (LANSCE) and complementary x-ray reflectivity measurements were used to pin down certain aspects of the molecular architecture.

For the single bilayer samples, the Kiessig fringe spacing observed ( $dQ \sim 0.07 \text{ \AA}^{-1}$ ) corresponds to a length scale of approximately 90 Å and matches the predicted thickness of the bilayer. Competing length scales make it difficult to identify the complementary

fringe spacing for the two-bilayer samples. Box model fitting of the data sets show the following: (1) well packed layers of OTS are present, (2) the density of the stearic acid layers are low indicating either patchy layers or intermixing of molecules with adjacent layers, (3) the thickness of the layer corresponding to the S-azo molecules is greater than predicted, and (4) intermixing and disorder is apparent within a single bilayer and the degree of disorder increases with additional layers. Despite second harmonic generation (SHG) measurements that indicate a linear increase in the SHG signal with increasing bilayer number, reflectivity measurements show that the films are disordered on the molecular scale.

#### TP48: Low Dimensional Magnetism in the Molecular Magnet $\text{Cu}(\text{pz})_2(\text{ClO}_4)_2$

*F.M. Woodward (NIST Center for Neutron Research), C.P. Landee (Clark University Physics Department, Worcester MA, 01610), M.M. Turnbull (Clark University Chemistry Department, Worcester MA, 01610)*

$\text{Cu}(\text{pz})_2(\text{ClO}_4)_2$  belongs to a family of compounds composed of magnetic  $\text{Cu}^{2+}$  ions linked by pyrazine molecular units forming Cu-pz layered materials. Magnetic susceptibility, isothermal magnetization, electron spin resonance, and neutron scattering data indicate that the molecular magnet,  $\text{Cu}(\text{pz})_2(\text{ClO}_4)_2$ , exhibits a low dimensional antiferromagnetic character, conforming to the two dimensional Heisenberg antiferromagnetic model, with a moderate exchange strength ( $J = -18 \text{ K}$ ). The results of an investigation of  $\text{Cu}(\text{pz})_2(\text{ClO}_4)_2$  via neutron diffraction shows characteristics similar to other two dimensional systems. Analysis of neutron diffraction data result in a model of the spins in the 3D order state.

#### TP49: Structural Comparison of Supercooled Water and Intermediate Density Amorphous Ices

*J. Urquidi (Dept. of Physics, New Mexico State University; Los Alamos Neutron Science Center, Los Alamos National Laboratory), C. J. Benmore (Intense Pulsed Neutron Source, Argonne National Lab), P. A. Egelstaff (Dept. of Physics, University of Guelph), M. Guthrie (Intense Pulsed Neutron Source, Argonne National Lab), S. E. McLain (Dept. of Chemistry, University of Tennessee), C. A. Tulk (Spallation Neutron Source, Oak Ridge National Laboratory), D. D. Klug (National Research Council, Chalk River, Ontario, Canada), J. F. C. Turner (Dept. of Chemistry, University of Tennessee)*

Presented here are new neutron diffraction data on ultrapure bulk supercooled heavy water measured down to 262 K. The data are analyzed in terms of the

trends observed in the first sharp diffraction peak (FSDP) parameters. The neutron FSDP position, height and width are compared to literature data for supercooled water, water under pressure and to the same parameters obtained for recently discovered intermediate density amorphous ices. It is found that the FSDP parameters in supercooled water and the amorphous ices generally exhibit a similar behavior, suggesting a new structural regime may occur in deeply supercooled water at about  $Q_0 \sim 1.83 \text{ \AA}^{-1}$  ( $T \sim 251 \text{ K}$ ) associated with increased intermediate range ordering. It is argued that this structural regime may be linked to a similar trend in the density, which appears when the density is plotted as a function of FSDP position. A detailed comparison of the neutron and x-ray structure factors for supercooled water and intermediate density amorphous ices having the same FSDP positions is also made. The diffraction data show that although the overall general structures are qualitatively very similar, the amorphous ice correlations are considerably sharper and extend to much higher radial distances.

#### TP50: Inelastic Neutron Scattering Studies of the Single Molecule Magnet $\{\text{Fe}_{30}\text{Mo}_{72}\}$

*V. O. Garlea (Ames Laboratory and Department of Physics and Astronomy, Iowa State University, Ames, Iowa 50011), S. E. Nagler (Oak Ridge National Laboratory), J. L. Zarestky, C. Stassis, D. Vaknin, P. Kögerler (Ames Laboratory and Department of Physics and Astronomy, Iowa State University, Ames, Iowa 50011), D. F. McMorrow (Risø National Laboratory, DK-4000, Roskilde, Denmark; Department of Physics & Astronomy University College London, UK), C. Niedermayer (Laboratory for Neutron Scattering, Paul Scherrer Institute & ETH Zurich, CH-5232 Villigen, Switzerland), Y. Qiu (NIST Center for Neutron Research, Gaithersburg, Maryland, 20899 & Department of Materials Science and Engineering, University of Maryland, College Park, Maryland, 20742)*

Materials consisting of magnetic molecules are ideal prototypes for the study of fundamental problems of magnetism at the nanoscale level. The Keplerate material  $\{\text{Fe}_{30}\text{Mo}_{72}\}$  is a singlet ground state single molecule magnet system with isolated clusters of 30  $s = 5/2$  ions on the vertices of an isododecahedron. We report cold-neutron inelastic scattering measurements on  $\{\text{Fe}_{30}\text{Mo}_{72}\}$  carried out using the triple axis spectrometer RITA-II at PSI and the Disc Chopper Spectrometer at NIST Center for Neutron Research. Results for temperatures  $T < 200 \text{ mK}$  reveal a magnetic excitation at an energy transfer near  $0.65 \text{ meV}$ . The peak broadens and shifts dra-

matically in the presence of an applied magnetic field. The results are discussed in the context of the effective rotational band model of Luban and co-workers [1].

[1] J. Schnack, M. Luban, and R. Modler, *Europhys. Lett.* 56, 863 (2001).

#### TP51: Neutron Diffraction Studies of the $\text{Tb}_5(\text{Si}_x\text{Ge}_{1-x})_4$ Magnetoelastic Compounds

*J. L. Zarestky, V. O. Garlea (Ames Laboratory and Department of Physics and Astronomy, Iowa State University, Ames, Iowa 50011), C. Y. Jones (National Institute of Standards and Technology), D. L. Schlagel, T. A. Lograsso, A. O. Pecharsky (Materials and Engineering Physics Program, Ames Laboratory, Ames, Iowa, 50011), V. K. Pecharsky, K. A. Gschneidner Jr. (Materials and Engineering Physics Program, Ames Laboratory, Ames, Iowa, 50011; Dept. of Materials Science and Engineering, Iowa State University, Ames, Iowa, 50011), C. Stassis (Ames Laboratory and Department of Physics and Astronomy, Iowa State University, Ames, Iowa 50011)*

The  $\text{R}_5(\text{Si}_x\text{Ge}_{1-x})_4$  [1] pseudobinary alloys exhibit a number of diverse and unique properties associated with both their naturally layered crystal structures and the combined magnetic-crystallographic transformations at low temperatures. In particular, this family of compounds is attractive for its potential applications as a magnetic refrigerant and/or magnetostrictive and magnetoresistive transducers. Progress in understanding the properties of these compounds has been hindered by the difficulty of growing single crystals. Recently a single crystal of  $\text{Tb}_5\text{Si}_{2.2}\text{Ge}_{1.8}$  was grown at the Ames Laboratory and this motivated us to initiate a neutron diffraction study of this compound as a function of temperature. The single crystal measurements were performed using the HB1A triple axis spectrometer at the High Flux Isotope Reactor (HFIR). The measurements performed in the  $a$ - $c$  and  $a$ - $b$  planes indicate the occurrence, at approximately  $115 \text{ K}$ , of a phase transition from monoclinic/paramagnetic to an orthorhombic/ferromagnetic structure. Below  $50 \text{ K}$ , a change in the intensities of selected reflections has been observed. In addition to the single crystal study, neutron powder diffraction measurements were also performed using the BT-1 powder diffractometer at the NIST Center for Neutron Research (NCNR). Models of the magnetic structure are used to interpret the experimental results.

[1] V.K.Pecharsky, K.A.Gschneidner Jr., *Phys. Rev. Lett.* 78 (1997) 4494

### TP52: Crystal structure and magnetic properties of $(\text{Zr,Mn})\text{Co}_{\delta+2}$ compounds.

*E. Sherstobitova, A.P. Vokhmyanin (Institute of Metal Physics Ural Branch or RAS.)*

The binary Laves-phase compounds  $\text{ZrCo}_2$  and  $\text{ZrMn}_2$  are Pauli paramagnetic. The spontaneous magnetization was observed in nonstoichiometric  $\text{ZrCo}_{2+x}$ - $(\text{Zr}_{1-y}\text{Co}_y)\text{Co}_2$  compounds with  $x > 0.8$  and the  $T_c$  of them reached up to 160 K. Curie temperature ( $T_c$ ) of the ternary  $\text{Zr}_{1-x}\text{Mn}_x\text{Co}_{\delta+2}$  compounds is about 600 K and the magnetization is 100 emu/g at room temperature. It is of interest to look into the reasons of an occurrence of magnetism in that compounds. For that using the x-ray and neutron powder diffraction we studied the crystal and magnetic structure of  $\text{Zr}_{1-x}\text{Mn}_x\text{Co}_2$  and  $\text{Zr}_{1-x}\text{Mn}_x\text{Co}_{2.45}$  system compounds. Assuming a substitution of Zr-atoms by Mn-atoms, one can consider former system as stoichiometric, and the latter as nonstoichiometric. We found that  $\text{Zr}_{0.8}\text{Mn}_{0.2}\text{Co}_2$  compound crystallized in the  $\text{MgCu}_2$  type cubic structure, (Fd $\bar{3}m$  space group). The Zr- and Mn-atoms randomly occupy the 8(a) position and Co atoms occupy 16(d)-one. On the x-ray diagram of  $\text{Zr}_{0.64}\text{Mn}_{0.36}\text{Co}_2$  compound the peaks can be well described in assumption that space group is Fd $\bar{3}m$  too. However, neutron diagram includes additional peaks (for example, (002)), it can be described in assumption of  $\text{AuBe}_5$  type structure (space group F-43m). In case of  $\text{Zr}_{0.64}\text{Mn}_{0.36}\text{Co}_{2.45}$  compound additional peaks appear on both neutron and x-ray diagrams and they are well described in according to  $\text{AuBe}_5$  type. For this nonstoichiometric compound Zr- and Mn-atoms distributions are similar as in stoichiometric  $\text{Zr}_{0.64}\text{Mn}_{0.36}\text{Co}_2$  compound, and the Co atoms occupy 16(e) position fully and 4(a) and 4(c) partly. All the compounds are ferromagnetic. An appearance of the ferromagnetism in  $\text{Zr}_{1-x}\text{Mn}_x\text{Co}_{\delta+2}$  alloys can be considered, within the scope of a model of the itinerant electrons, which was before suggested for an explanation of a magnetic behavior of the  $\text{ZrCo}_{2+x}$  alloys.

### TP53: Bose condensation of magnons in anisotropic Haldane spin chains

*A. Zheludev (Condensed Matter Sciences Division, Oak Ridge National Laboratory), C. L. Broholm (Department of Physics & Astronomy, Johns Hopkins University; NIST Center for Neutron Research), S. M. Shapiro (Physics Department, Brookhaven National Laboratory), Z. Honda (Faculty of Engineering, Saitama University, Urawa, Saitama 338-8570, Japan), K. Katsumata (The RIKEN Harima Institute, Mikazuki, Sayo, Hyogo 679-5148, Japan), B. Grenier, L.-P. Regnault (DRFMC/SPSMS/MDN, CEA-Grenoble, 17 rue des Martyrs, 38054 Grenoble*

*Cedex, France)*

Inelastic neutron scattering experiments on the Haldane-gap quantum antiferromagnet NDMAP are performed at mK temperatures in magnetic fields of almost twice the critical field  $H_c$ . Geometries in which the field is applied perpendicular [1,2] or parallel [3] to the axis of magnetic anisotropy are both explored. The observed closing of the Haldane gap at  $H_c$  [1] leads to a *Bose condensation of magnons* and the appearance of long-range antiferromagnetic order [4]. This ordered (spin-solid) high-field phase is not to be confused with a conventional antiferromagnet. In the latter model the spectrum consists of two spin wave branches that correspond to spin precessions around the direction of ordered staggered magnetization. In contrast, in NDMAP at  $H > H_c$  we clearly observe *three* distinct branches of long-lived massive (gapped) excitations [2,3]. These “breather” states can not be understood in the framework of quasiclassical theories. However, more sophisticated quantum models can account for the observed behavior quite well. The main conclusion is that at even  $H > H_c$  quantum fluctuations are crucial, and a magnetized anisotropic Haldane spin chain is a *quantum spin solid*.

- [1] A. Zheludev, Y. Chen, Z. Honda, C. Broholm and K. Katsumata, Phys. Rev. Lett. 88, 077206 (2002).
- [2] A. Zheludev, Z. Honda, C. L. Broholm, K. Katsumata, S. M. Shapiro, A. Kolezhuk, S. Park and Y. Qiu, Phys. Rev. B 68, 134438 (2003).
- [3] A. Zheludev, S. M. Shapiro, Z. Honda, K. Katsumata, B. Grenier, E. Ressouche, L.-P. Regnault, Y. Chen, P. Vorderwisch, H.-J. Mikeska, and A. K. Kolezhuk, Phys. Rev. B, Phys. Rev. B 69, 054414 (2004).
- [4] Y. Chen, Z. Honda, A. Zheludev, C. Broholm, K. Katsumata and S. M. Shapiro, Phys. Rev. Lett. 86, 1618 (2001).

### TP54: Spin singlet formation in $\text{MgTi}_2\text{O}_4$ : evidence of a helical dimerization pattern

*M. Schmidt (ISIS, Rutherford Appleton Laboratory; Department of Physics and Astronomy, Michigan State University, E. Lansing, MI, 48824), W. Ratcliff II (Department of Physics and Astronomy, Rutgers University, Piscataway, New Jersey 08854, USA), P. G. Radaelli (ISIS, Rutherford Appleton Laboratory; Department of Physics and Astronomy, University College London, London, WC1E 6BT, United Kingdom), K. Refson (ISIS, Rutherford Appleton Laboratory), N. M. Harrison (Department of Chemistry, Imperial College London, London, SW7 2AY, United Kingdom; CCLRC, Daresbury Laboratory, Warrington, WA4 4AD, United*



Kingdom), S.W. Cheong (Department of Physics and Astronomy, Rutgers University, Piscataway, New Jersey 08854, USA)

The transition metal spinel  $\text{MgTi}_2\text{O}_4$  was studied using a combination of neutron and x-ray powder diffraction, electrical resistivity and magnetic susceptibility measurements.  $\text{MgTi}_2\text{O}_4$  undergoes a metal-insulator transition on cooling below  $T(\text{M-I}) = 260\text{K}$  and a step-like reduction of the magnetic susceptibility below  $T(\text{M-I})$ . The temperature dependence of transport properties suggests an onset of a magnetic singlet state. Using high-resolution synchrotron and neutron powder diffraction, we have solved the low-temperature crystal structure of the oxide.  $\text{MgTi}_2\text{O}_4$  has tetragonal crystal structure below 260K (S.G: P41 21 2,  $a = 6.02201(1)\text{\AA}$ ,  $c = 8.48482(2)\text{\AA}$  at 200K) which is found to contain dimers with short Ti-Ti distances (the locations of the spin singlets). The shortest Ti-Ti bonds alternate with longest bonds to form helices running along the tetragonal  $c$  axis. Additional band structure calculations based on hybrid exchange density functional theory show that, at low temperatures,  $\text{MgTi}_2\text{O}_4$  is an orbitally ordered band insulator.

#### **TP55: Magnetic-field induced transition to static long-range magnetic order in underdoped LSCO**

*B. Khaykovich (Massachusetts Institute of Technology), S. Wakimoto (University of Toronto), K. Yamada (Tohoku University), R. J. Birgeneau (University of Toronto), Y. S. Lee, M. A. Kastner (Massachusetts Institute of Technology), P. Vorderwisch, P. Smeibidl (Hahn-Meitner-Institut Berlin)*

High-temperature cuprate superconductors often have dynamic and sometimes static magnetic order, which coexist with superconductivity. Underdoped  $\text{La}_{2-x}\text{Sr}_x\text{CuO}_4$  has static magnetic order when  $x < 0.14$ . At higher doping, the static magnetic order is destroyed and a spin-gap opens when it is optimally- or slightly over-doped. We present recent neutron scattering results, which show that applied magnetic field induces static magnetic order in  $\text{La}_{2-x}\text{Sr}_x\text{CuO}_4$ .

#### **TP56: Spin fluctuations in superconducting $\text{YBa}_2\text{Cu}_3\text{O}_{6.35}$ near the transition to antiferromagnetism**

*C. Stock (Physics Department, University of Toronto, Toronto, Ontario, Canada), W. J. L. Buyers (National Research Council, Chalk River, Ontario, Canada), R. Liang, D. Peets, D. Bonn, W.N. Hardy (Physics Department, University of British Columbia, Vancouver, B. C., Canada), R. J. Birgeneau (Physics Department, University of Toronto, Toronto, Ontario, Canada)*

The discovery of superconductivity in the cuprates has resulted in a vast amount of interest in the spin fluctuations of these nearly two-dimensional materials. Despite the extensive research that has occurred, there is no generally accepted theory of the pairing mechanism in these materials. Due to the strong interplay between antiferromagnetism and superconductivity, spin fluctuations are drastically altered by doping of the parent insulator and are strongly correlated with superconductivity. Understanding the spin fluctuations in the cuprates is an important step to understanding superconductivity.

Despite the vast amount of attention that the bilayer  $\text{YBa}_2\text{Cu}_3\text{O}_{6+x}$  superconductor system has received, little work has been done in investigating the spin fluctuations near the boundary of antiferromagnetism and superconductivity. We present neutron elastic and inelastic scattering results, utilizing both polarized and unpolarized beams, on the  $\text{YBCO}_{6.35}$  superconductor ( $T_c = 18\text{K}$ ). In contrast to the Ortho-II  $\text{YBCO}_{6.5}$  system ( $T_c = 59\text{K}$ ), we find that the spectral weight of  $\text{YBCO}_{6.35}$  has been shifted to very low-energies resulting in a broad over-damped peak at around 2 meV. In comparison to higher oxygen concentrations, we speculate that this mode may be interpreted as a resonance peak. We also observe a broad central peak indicative of slowly fluctuating copper spins with correlation lengths of about 20  $\text{\AA}$  in the  $\text{CuO}_2$  plane and about 15  $\text{\AA}$  along the  $c$ -axis. By comparing data taken with  $E_f = 5\text{meV}$  and  $E_f = 14.5\text{meV}$ , we suggest that the properties observed in  $\text{YBCO}_{6.35}$  are analogous to the spin-glass phase observed in the LSCO system. This suggests that the spin-glass phase may be a common characteristic of cuprate systems near the transition from antiferromagnetism to superconductivity.

#### **TP57: A Quantum Multicritical point in $\text{CeCu}_{6-x}\text{Au}_x$**

*R. A. Robinson (Bragg Institute, Australian Nuclear Science and Technology Organisation, Australia), D. Goossens (Bragg Institute, Australian Nuclear Science and Technology Organisation, Australia; Research School of Chemistry, Australian National University, Canberra, ACT 0200, AUSTRALIA), M. S. Torikachvili (Department of Physics, San Diego State University, San Diego, CA 92182, USA), K. Kakurai (Advanced Science Research Center, JAERI, Tokai-mura, Ibaraki-ken 319-1195, JAPAN)*

$\text{CeCu}_{6-x}\text{Au}_x$  is a well-known heavy-fermion system in which the ground state is antiferromagnetically ordered for  $x > 0.1$  and temperatures below 1K. Non-Fermi-liquid behaviour occurs around this critical concentration. The parent compound,  $\text{CeCu}_6$ , exhibits a structural phase transition near 230K, where it



changes from the Pnma orthorhombic room-temperature structure to the P21/c monoclinic structure. The monoclinicity increases as temperature falls, with  $\beta$  reaching  $91.44^\circ$  at 10K. In the work presented here, powder neutron diffraction is used to explore the monoclinicity at 10K as a function of composition for  $0.0 < x < 0.08$ , just short of the critical concentration. Extrapolation of the square of the monoclinic strain,  $(abc\cos(\beta))^2$ , suggests that the distortion vanishes by  $x = 0.14$ . A reanalysis of single-crystal diffraction data on the magnetically ordered side of the phase diagram indicates that long-range magnetic order disappears at the same critical concentration. At a minimum, the structural distortion and antiferromagnetism seem to be competing with each other, and this raises the intriguing possibility that lattice degrees of freedom are important in the non-Fermi-liquid regime.

**TP58: Ferromagnetic quantum critical fluctuations in  $Zr_{1-x}Nb_xZn_2$  ( $x = 0.05$ )**

*D. Sokolov, M. C. Aronson (The University of Michigan, Ann Arbor), J.W. Lynn, B. Hammouda (NIST Center for Neutron Research), Z. Fisk (Florida State University)*

$ZrZn_2$  is a weak itinerant ferromagnet with the Curie temperature  $T_c = 18$  K. Magnetization measurements showed that doping with Nb acts like a chemical pressure suppressing both  $T_c$  and the spontaneous moment to zero at 5% of Nb. We have studied the development of long range critical fluctuations above  $T_c$  in both compositions, and below  $T_c$  in  $ZrZn_2$  using the NG3 SANS instrument at the NIST Center for Neutron Research.

In undoped  $ZrZn_2$  above  $T_c$ , a suppression of scattering for  $0.002 < q < 0.008 \text{ \AA}^{-1}$  was observed, suggesting the development of extremely long wavelength correlations with lowered temperature. Surprisingly, the magnetic scattering is still temperature dependent at the smallest wave vectors at temperatures as large as 100 K. It was also observed that the small angle scattering increases below  $T_c$  in undoped  $ZrZn_2$ , implying the development of a new scattering mechanism involving ferromagnetic domains. For the quantum critical composition  $Zr_{1-x}Nb_xZn_2$  ( $x = 0.05$ ), magnetic scattering develops suddenly below 1 K. The scattering is enhanced at small ( $q < 0.004 \text{ \AA}^{-1}$ ) wave vectors and suppressed at intermediate ( $q > 0.006 \text{ \AA}^{-1}$ ) wave vectors indicating transfer of intensity from intermediate ( $q > 0.006 \text{ \AA}^{-1}$ ) to small ( $q < 0.004 \text{ \AA}^{-1}$ ) wave vectors at lower temperatures, consistent with incipient ferromagnetic correlations, albeit with relatively shorter ranges than those found in undoped  $ZrZn_2$ .

The work at the University of Michigan was carried out under NSF-DMR-9977300 grant.

**TP59: Polarized Neutron Studies of  $Pd_{40}Ni_{22.5}Fe_{17.5}P_{20}$  Spin Glass**

*D.H. Yu, E.P. Gilbert (Bragg Institute, Australian Nuclear Science and Technology Organisation, Australia), R. Woodward (School of Physics, University of Western Australia, Perth, 6009, Australia), R.A. Robinson (Bragg Institute, Australian Nuclear Science and Technology Organisation, Australia)*

Magnetic metallic glasses have enormous technological importance in, for example, magnetic recording, magnetic refrigeration and the construction of electrical transformers and motors. Traditionally these amorphous materials were prepared by melt spinning ( $106 \text{ K s}^{-1}$ ) to form ribbons. Bulk magnetic metallic glasses based on the quaternary alloy Pd-Ni-Fe-P exhibit interesting phase behaviour depending on temperature and applied magnetic field. For the alloy of  $Pd_{40}Ni_{22.5}Fe_{17.5}P_{20}$ , paramagnetic, superparamagnetic, ferromagnetic and spin glass regions are all evidenced [1]. It is proposed that the complex phase transitions in these kinds of materials may be due to the materials not being truly amorphous. The possible large-scale chemical inhomogeneities within the alloy may lead to clustering of magnetic ions. On cooling, frustration due to competing interactions between clusters may result in the observed spin glass-like behaviour. We will present preliminary studies, employing neutron depolarization and small-angle neutron scattering, on the alloy of  $Pd_{40}Ni_{22.5}Fe_{17.5}P_{20}$  as a function of temperature (RT to 5K) and applied magnetic field (0 to 5T).

[1] Shen T. D., Schwarz R. B. and Thompson J. D., J. Appl. Phys. 85, 4110-4119, 1999.

**TP60: Magnetic structure and magnetization density in the layered  $Tb(Dy)BaCo_2O_{5.5}$**

*S.N. Barilo (Institute of Solid State & Semiconductor Physics, BAS, Minsk 220072, Belarus), V.P. Plakhty, Yu. P. Chernenkov (Petersburg Nuclear Physics Institute RAS - Gatchina, 188300 St. Petersburg, Russia), A. Goukassov (Laboratoire Léon Brillouin, C.E.A Saclay, 91191 Gif-sur-Yvette Cedex), S. Streule, A. Podlesnyak (Laboratory for Neutron Scattering, Paul Scherrer Institute & ETH Zurich, CH-5232 Villigen, Switzerland), S.V. Shiryayev, G.L. Bychkov (Institute of Solid State & Semiconductor Physics, BAS, Minsk 220072, Belarus), A. Furrer (Laboratory for Neutron Scattering, Paul Scherrer Institute & ETH Zurich, CH-5232 Villigen, Switzerland)*

The cobaltites  $\text{LnBaCo}_2\text{O}_{5.5}$  ( $\text{Ln} = \text{Y, Pr-Ho}$ ) present spin-state, MI and field-induced transitions, as well as charge and orbital ordering phenomena. This family of layered cobaltites displays alternating BaO and  $\text{LnO}_{0.5}$  layers along the  $c$ -axis and alternating oxygen octahedral and pyramidal planes along the  $b$ -axis. In spite of the extensive studies, neither magnetic structure nor spin state in two different  $\text{Co}^{3+}$  sites are definitely established. Precisely oxygenated powder sample of  $\text{TbBaCo}_2\text{O}_{5.5}$  and as large as 50 mm<sup>3</sup> flux grown single crystals of  $\text{Tb}_{0.9}\text{Dy}_{0.1}\text{BaCo}_2\text{O}_{5.45}$  have been used for neutron diffraction studies in the temperature range of 7-300 K using the powder diffractometer DMC of SINQ, Villigen and 5C2, 6T2 diffractometers of LLB, Saclay. The results obtained are rather different of everything, which has been published before. The following 3 phases of  $\text{TbBaCo}_2\text{O}_{5.5}$  have been offered: 1) A very narrow by temperature ferrimagnetic phase in the range around 260 K (the unit cell doubled along short axis because of the spin state ordering in octahedra). The structure presents a simple ferrimagnetic with all moments are along  $a$ -axis in the octahedra and a simple AFM in pyramids. 2) At  $T = 230$  K an AFM phase does appear. Magnetic cell is a previous one doubled along  $c$ -axis due to antiferromagnetic ordering with the wave vector  $k = (0, 0, 1/2)$ . There is an antitranlation to the upper part of the unit cell. 3) Finally at  $T \sim 170$  K a transition to another AFM takes place. Now the unit cell is doubled along the  $c$ -axis because of the spin value ordering in pyramids. This low temperature AFM phase of a single crystal  $\text{Tb}_{0.9}\text{Dy}_{0.1}\text{BaCo}_2\text{O}_{5.45}$  have been studied by elastic neutron scattering in the  $kl$ -plane to show peaks indexed as  $(0, 0, -1/2)$  are purely magnetic and can be attributed to appearance below 200 K an AFM phase, consisting of ferromagnetic, AFM and nonmagnetic chains. We have also reconstructed the spin density distribution in a  $\text{Tb}_{0.9}\text{Dy}_{0.1}\text{BaCo}_2\text{O}_{5.45}$  single crystal. Statistically significant flipping ratios for 46 reflections have been measured in the field of 7 T. Refinement have been made to reveal the spin density difference between octahedral and pyramidal sites. These results should be considered as preliminary to show the spin density distribution over the different sites can be obtained for this twinned crystal.

#### TP61: Low energy nuclear spin excitations in $\text{NdGaO}_3$

*T. Chatterji, B. Frick (Institut Laue Langevin)*

We have investigated the low energy excitations in  $\text{NdGaO}_3$  in the  $\mu\text{eV}$  range by a back scattering neutron spectrometer. The energy scans on a  $\text{NdGaO}_3$  single crystal revealed inelastic peaks at  $E = 1.650 \mu\text{eV}$  at  $T = 50$  mK on both energy gain and

energy loss sides. The inelastic peaks move gradually towards lower energy with increasing temperature and finally merge with the elastic peak at the electronic magnetic ordering temperature  $T_N = 975$  mK. We interpret the inelastic signal observed in  $\text{NdGaO}_3$  to be due to the excitations of the Nd nuclear spins  $I = 7/2$  of the  $^{143}\text{Nd}$  and  $^{145}\text{Nd}$  isotopes. In a first approximation one can consider these inelastic peaks to arise due to the transitions between the hyperfine-field-split nuclear levels. This is the single-nucleus effect. However the nuclear spins are coupled through Suhl-Nakamura interaction [1,2]. So one expects nuclear spin wave excitations (cooperative lattice effect) discussed by de Gennes et al. [3]. The nuclear spin waves should show dispersions at small momentum transfers. Word et al. [4] have discussed the possibility of measuring nuclear spin waves by inelastic neutron scattering. They have calculated the differential scattering cross section and polarization of neutrons scattered by nuclear spin systems described by Suhl-Nakamura Hamiltonian in the formalism of van Hove correlation function. In our experiment, however, we failed to detect so far the expected dispersion of the nuclear spin waves. This is perhaps due to the insufficient  $Q$  resolution of the back-scattering spectrometer. The dispersion of the nuclear spin waves can probably be measured by a neutron spin echo (NSE) spectrometer using a PG-analyzer at a strong spallation neutron source.

[1] H. Suhl, Phys. Rev. 109, 606 (1958)

[2] T. Nakamura, Progr. Theoret. Phys. (Kyoto) 20, 542 (1958)

[3] P.G. de Gennes et al., Phys. Rev. 129, 1105 (1963)

[4] R. Word, A. Heidemann and D. Richter, Z. Phys. B 28, 23 (1977)

#### TP62: Transport and magnetic properties of the perovskites $\text{Bi}_{1-x}\text{Ca}_x\text{Mn}_{0.95}\text{Cr}_{0.05}\text{O}_3$ with $x = 0.4, 0.5$

*C. C. Yang, F. C. Tsao, P. J. Hwang, W.-H. Li (Department of Physics, National Central University, Chung-Li, 32054 Taiwan), J. W. Lynn (NIST Center for Neutron Research), J. R. Sun (State Key Laboratory of Magnetism, Institute of Physics and Center for Condensed Matter Physics, Chinese Academy of Sciences, Beijing 100080, China)*

Polycrystalline samples of  $\text{Bi}_{1-x}\text{Ca}_x\text{Mn}_{0.95}\text{Cr}_{0.05}\text{O}_3$  with  $x = 0.4$  and  $0.5$  were prepared by conventional ceramic route. Crystalline structures of the compounds were investigated by using the high-resolution neutron diffraction patterns and the Rietveld method. At room temperature, they crystallized into an orthorhombic Pbnm phase. Jahn-Teller distortion was found at around 280 K for the  $x = 0.4$  sample. AC susceptibility reveals a charge ordered state in both

samples, which occur at 280 and 285 K for the  $x = 0.4$  and  $0.5$  samples, respectively. An applied magnetic field of strength 9 T can melt the charge ordered state. The transport behavior of both samples may be described by using the variable-range hopping mechanism. The magnetic structures for both compounds were studied by neutron magnetic diffraction measurements. The spins of both compounds become ordered below 90 K. Spin clusters were realized in both compounds, and phase separation was clearly revealed in the  $x = 0.4$  compound. Detailed magnetic structures will be discussed.

### TP63: Magnetic Order and Spin Dynamics in Triangular Magnets

*Y. Li, Z. M. Hasan (Princeton University), S. Park, J. W. Lynn (NIST Center for Neutron Research), W. Ratcliff, S. Cheong (Rutgers University)*

We have recently studied two classes of triangular spin systems—Seignette magnets and Thiospinels. Our studies of  $\text{Ba}_3\text{CoSb}_2\text{O}_9$ ,  $\text{Ba}_3\text{NiSb}_2\text{O}_9$  Seignette (2-D xy Heisenberg) magnets suggest that these systems exhibit 3-D long-range order at low temperatures without coupling to the lattice and exhibit conventional spin dynamics. On the other hand, 3-D topologically frustrated magnets such as thiospinels take more complex paths to ordering. For example,  $\text{ZnCr}_2\text{S}_4$  first enters a helical long-range ordered phase before coupling to the lattice but only at lower temperatures achieves a 3-D commensurate order and exhibits a local resonance similar to the oxide counterpart. This complex magnetism in this system is a direct consequence of competing interactions under geometrical constraints.

### TP64: Magnetic and Structural Studies of the Spinel $\text{GeNi}_2\text{O}_4$ and $\text{GeCo}_2\text{O}_4$

*M.K. Crawford, R.L. Harlow, R. Flippen (DuPont CR&D, Wilmington, DE), R.W. Stevens, B.F. Woodfield, J. Boerio-Goates (Brigham Young University, Provo, UT), P.L. Lee, Y. Zhang (Advanced Photon Source, Argonne National Laboratory, Argonne, IL), J. Hormadaly (Ben Gurion University, Beer Sheeva, Israel), R.A. Fisher (Lawrence Berkeley National Laboratory), Q. Huang, J. W. Lynn, Y. Qiu, J.R.D. Copley (NIST Center for Neutron Research)*

Transition metal oxide spinels that have magnetic ions located only on the B-sublattice exhibit interesting phenomena, including Néel ordering accompanied by structural phase transitions. Neutron powder diffraction measurements show that  $\text{GeNi}_2\text{O}_4$  (spin-1) and  $\text{GeCo}_2\text{O}_4$  (spin-3/2) become antiferromagnetic at  $T_N = 12$  K and 21 K, respectively. However,  $\text{GeNi}_2\text{O}_4$  remains cubic, while  $\text{GeCo}_2\text{O}_4$  becomes tetragonal,

below  $T_N$ . Thus the behavior of  $\text{GeCo}_2\text{O}_4$  is similar to that of  $\text{ZnCr}_2\text{O}_4$  (spin-3/2), although the  $\text{Co}^{2+}$  ion has unquenched orbital angular momentum and the  $\text{Cr}^{3+}$  ion does not. The Néel transition in  $\text{GeNi}_2\text{O}_4$  occurs in two discrete steps, while the other materials have single Néel transitions. Neutron inelastic scattering measurements demonstrate that both  $\text{GeNi}_2\text{O}_4$  and  $\text{GeCo}_2\text{O}_4$  have energy gaps in their Néel states, consistent with the results of heat capacity measurements. The Néel transition and magnetic structure of  $\text{GeCo}_2\text{O}_4$  are very sensitive to an applied magnetic field, whereas the Néel transitions in  $\text{GeNi}_2\text{O}_4$  are only weakly affected by a field. In this presentation we will describe the results of magnetic and structural studies of these materials, and discuss their different behaviors.

### TP65: Neutron Scattering studies of $\text{Yb}_{14}\text{MnSb}_{11}$

*S. E. Nagler, M. Yethiraj, H. A. Mook, D. G. Mandrus, B. C. Sales (Oak Ridge National Laboratory)*

The tetragonal ( $a = b = 16.6$  Å,  $c = 21.95$  Å) material  $\text{Yb}_{14}\text{MnSb}_{11}$  is a ferromagnetic semiconductor where the only magnetic ion is Mn present at the level 3.8 atomic percent. With a magnetic transition near 50 K,  $\text{Yb}_{14}\text{MnSb}_{11}$  is a promising compound for investigating the physics of carrier mediated ferromagnetism in dilute magnetic semiconductors without the possible complications of clustering or impurity phases. We report here on some preliminary results of our neutron scattering investigations of magnetism in single crystals of  $\text{Yb}_{14}\text{MnSb}_{11}$ .

### TP66: Quasielastic scattering in the magnetic spinel $\text{Co}_2\text{RuO}_4$

*G. E. Granroth, D. Abernathy (Spallation Neutron Source, Oak Ridge National Laboratory; Condensed Matter Sciences Division, Oak Ridge National Laboratory), S. E. Nagler (Condensed Matter Sciences Division, Oak Ridge National Laboratory), D. Mandrus (Condensed Matter Sciences Division, Oak Ridge National Laboratory; Department of Physics and Astronomy, University of Tennessee), V. Keppens (Department of Physics, University of Mississippi, Oxford, MS 38677), J. R. D. Copley (NIST Center for Neutron Research)*

Bulk magnetization measurements of the spinel  $\text{Co}_2\text{RuO}_4$  have revealed a “spin glass like” ground state [1]. To further elucidate the properties of this ground state, temperature (T) dependent quasielastic neutron scattering studies have been performed using the DCS instrument at NIST. For T greater than the spin glass transition temperature ( $T_g \sim 15$  K), the quasielastic peak can be fit by a Lorentzian of width  $181 \pm 9$   $\mu\text{eV}$  convoluted with the instrumental resolution. Furthermore the Q dependence of the



scattering is broad and oscillatory consistent with short range ordered states involving nearest and next nearest neighbor sites [2]. For  $T < T_g$ , approximately 1/3 of this scattering is moved to the elastic position at a  $Q$  corresponding to the (200) position of the spinel lattice. The other 2/3 of the scattering remains in a Lorentzian component of width  $130 \pm 10 \mu\text{eV}$ . This behavior is consistent with a reduction of short time scale dynamics observed in a spin glass.

[1] D. Mandrus, V. Keppens, and B. C. Chakoumakos, *Mat. Res. Bull.*, **34**, 1013 (1999).

[2] G. E. Granroth et al. to be published.

#### TP67: Magnetic Excitation Spectrum in

##### $\text{Ca}_{2-x}\text{Sr}_x\text{RuO}_4$

*M.D. Lumsden (Condensed Matter Sciences Division, Oak Ridge National Laboratory), S. Wilson (Department of Physics and Astronomy, University of Tennessee), S.E. Nagler (Condensed Matter Sciences Division, Oak Ridge National Laboratory), P. Dai (Department of Physics and Astronomy, University of Tennessee; Condensed Matter Sciences Division, Oak Ridge National Laboratory), R. Jin (Condensed Matter Sciences Division, Oak Ridge National Laboratory), D. Mandrus (Condensed Matter Sciences Division, Oak Ridge National Laboratory; Department of Physics and Astronomy, University of Tennessee)*

We have studied the concentration dependence on the magnetic excitation spectrum in single crystal samples of  $\text{Ca}_{2-x}\text{Sr}_x\text{RuO}_4$  for  $2 > x > 0.4$ . For large  $x$ , the spectrum is similar to that observed in pure  $\text{Sr}_2\text{RuO}_4$  with incommensurate excitations strongly peaked in  $Q$  at  $(+/-0.3, +/-0.3, q_z)$  consistent with Fermi-surface nesting wavevectors. As the concentration approaches the quantum critical point at  $x = 0.5$ , the spectrum evolves into a multippeak structure in  $Q$  centered around the 2d ferromagnetic zone center. The spectrum observed near the quantum critical concentration is qualitatively quite similar to that observed in  $\text{Sr}_3\text{Ru}_2\text{O}_7$  which is also in the vicinity of a quantum critical point.

#### TP68: Electronic transport and magnetic properties of the natural spin valve $\text{Mn}_{0.25}\text{NbS}_2$

*C.J. Metting, S.E. Lofland (Dept. of Physics and Astronomy, Rowan University, Glassboro, NJ), K.V. Ramanujachary (Dept. of Chemistry and Biochemistry, Rowan University, Glassboro, NJ), J.D. Hettinger (Dept. of Physics and Astronomy, Rowan University, Glassboro, NJ), J.W. Lynn (NIST Center for Neutron Research, Gaithersburg, MD)*

We have completed magnetotransport, magnetiza-

tion, and neutron diffraction studies on polycrystalline and single crystal samples of  $\text{Mn}_{1/4}\text{NbS}_2$ . These metallic intercalated compounds, which alternate between four  $\text{NbS}_2$  layers and one layer of Mn, show ferromagnetic order below 100 K which is accompanied by sizeable ( $> 15\%$ ) magnetoresistance in polycrystalline material. However, the magnetoresistance along the  $a$  axis, parallel to the ferromagnetic Mn layers, is very small in the single crystals. Thus it appears that the large magnetoresistance in the polycrystalline material is a result of transport along the  $c$  axis, through the Mn layers which act as natural spin valves between the conducting  $\text{NbS}_2$  layers.

#### TP69: DAVE—Software facilitating science at the NCNR

*R.M. Dimeo (NIST Center for Neutron Research), R.T. Azuah, L.R. Kneller, Y. Qiu (NIST Center for Neutron Research; University of Maryland, College Park)*

The DAVE software package is a free suite of tools for reducing, visualizing, and analyzing data collected on the inelastic neutron spectrometers at the NIST Center for Neutron Research. The design goal for the software is to provide easy-to-use, powerful tools that facilitate data interpretation. This poster presentation will demonstrate the existing capabilities of the software package and highlight new features such as triple-axis data reduction, neutron spin-echo data reduction, improved data visualization, and model fitting applications.

This work is based upon activities supported by the National Science Foundation under Agreement No. DMR-0086210.

#### TP70: Upgrading Data Analysis Software for the Glass, Liquid and Amorphous materials Diffractometer at IPNS using ISAW

*J.Z. Tao, C.J. Benmore, T.G. Worlton (Intense Pulsed Neutron Source, Argonne National Lab), D. Mikkelsen, R.L. Mikkelsen (University of Wisconsin-Stout), A. Chatterjee, J.P. Hammonds (Intense Pulsed Neutron Source, Argonne National Lab)*

We are porting, upgrading and designing new analysis software for the GLAD instrument as part of time-of-flight neutron scattering data visualization and analysis package ISAW. GLAD has continuous angular coverage from  $2\theta = 3^\circ$  to  $117^\circ$  using 235  $^3\text{He}$  linear position sensitive detectors. Data is currently processed using the ATLAS data analysis suite produced at ISIS combined with the IPNS Glass Analysis Package, which operates on an aging VAX/VMS system. The software upgrade has lifted the detector



grouping restriction imposed by the limited VAX/VMS computing power, and brought the analysis routines in line with more sophisticated software development methods and tools. The first stage of the project consists of instrument dependent raw data corrections: dead-time, delayed neutron, detector efficiency and conversion of time-of flight to  $Q$ . The second stage involves data normalization with respect to a vanadium standard and application of attenuation and multiple-scattering corrections. The new detector-by-detector analysis uses the full  $Q$  range available, is not subject to averaging effects, and results in a smoother neutron time-of-flight differential cross section function. The detector grouping flexibility in ISAW will extend the instruments capability to lower  $Q$ -values, which will augment the study of intermediate range order in glasses, supercritical fluids and layering in clays for example. It will also enable us to investigate the feasibility of the anomalous neutron diffraction technique on a pulsed source.

#### **TP71: Sharing neutron data and software**

*T. G. Worlton (Intense Pulsed Neutron Source, Argonne National Lab), D.J. Mikkelson, R. L. Mikkelson, C. Bouzek (University of Wisconsin-Stout), A. Chatterjee, J. P. Hammonds (Intense Pulsed Neutron Source, Argonne National Lab)*

Neutrons are becoming more important to scientists in the United States each year and many scientists now use more than one neutron scattering facility. Collection of data usually takes a short time, but analysis of the data can be quite lengthy. Productivity of scientists will be greatly improved by providing software which can automate data reduction and allow them to visualize and analyze data from different facilities. The NeXus specification for storage and interchange of neutron scattering data makes it possible to write software which is useable at different facilities with very little modification. The ISAW package developed at Argonne can be used to read, visualize, and analyze data from different facilities which write data in the NeXus format. ISAW is an open source package which includes capabilities for users to write their own scripts and operators to customize their data reduction and analysis. We will demonstrate how a user can write operators and scripts to automate processing of data using examples from the ISAW distribution. Both built-in and user-written operators will automatically appear in ISAW menus and can be used in ISAW scripts without recompiling ISAW. Documentation from user-written operators will also appear automatically in the interactive help menus.

#### **TP72: New Instrument Control Software at the NCNR**

*N.C. Maliszewskyj (NIST Center for Neutron Research), M Doucet (University of Maryland, College Park), S. Pheiffer*

The construction and installation of a state of the art thermal triple axis at the NCNR presents us with the opportunity to similarly craft new software that addresses the needs of our local staff and outside users. An autonomous instrument control server will mediate interactions of users with hardware, manage data acquisition, and sequence commands for batch execution. Client programs incorporating experiment planning tools will be used to compose scans, issue instantaneous commands to be executed by the server, and provide the first layer of live status information. A tiered permission scheme will permit certain types of remote operation in this client-server system.

This software is designed with portability in mind. A hardware abstraction layer ("middleware") encapsulates the most platform dependent portions of the code while the remainder of the instrument control server is essentially a platform independent python script. We will present an architectural overview of this suite and an update of the current state of the project.

#### **TP73: Data Reduction Software for Chopper Spectrometers**

*T. M. Kelley, B. T. Fultz, M. M. McKerns, M. G. Aivazis (California Institute of Technology)*

The raw data of an inelastic chopper spectrometer are time histograms of neutron counts in each detector pixel; reducing these histograms to energy and momentum coordinates requires substantial computation. With higher pixel counts and shorter data collection times, upcoming SNS instruments such as ARCS will need highly efficient reduction codes. We are designing an object-oriented system in which compiled and optimized C++ components are bound at run time by the Python interpreter. This results in software that has the flexibility of an interpreted language and the performance of a compiled language. Where possible, we have pursued separation between data structures and algorithms analogous to the C++ Standard Template Library. The object-oriented nature of the system insulates components that carry out data transformation from those that describe instrument properties; this makes a number of the components independent of instrument, and they may be reusable for other spectrometers.

#### **TP74: Detectors for Neutron Science—How to find a Neutron?**

*L. Crow, C. Hoffmann (SNS, Oak Ridge National Laboratory), G. Smith (Brookhaven National Laboratory), R. Copper (SNS, Oak Ridge National Laboratory)*

Condensed matter physics, chemistry, metallurgy, geo-, and bio-sciences have benefited greatly from using neutrons to probe structure, magnetism, and dynamics of materials. In many of these studies, however, presently available neutron detector systems lack the performance to fully exploit future neutron flux. With the approaching completion of SNS in 2006 we are challenged to use this window of opportunity to build a research effort of sustained development of gas and scintillation detectors, and for investigation of new scintillator materials, semiconductor detectors, new types of gas detectors, and low efficiency neutron monitors. Neutron detector research has made advances in the past few years – this has happened quietly, but nevertheless has enabled the establishment of new scientific research in traditional and new fields.

#### **T2-A, Proteins: Structure and Hydration, Chair: Dean Myles (ORNL), Room 2100/2/4 Red**

##### **T2-A1 (13:30) The PCS Neutron Protein Crystallography Facility at Los Alamos (Invited)**

*P. Langan, B.P. Schoenborn (Los Alamos National Laboratory)*

The PCS (Protein Crystallography Station) at Los Alamos Neutron Science Center, is a high performance neutron protein crystallography beam line funded by the Office of Biological and Environmental Research of the U.S. Department of Energy. Beam-time is free to expert and non-expert users and is allocated twice a year through a call for proposals and a peer review process.

Although most protein structures are determined using x-rays, the position of hydrogen atoms and the coordination, sometimes even the position of water molecules, cannot be directly determined at resolutions typical for most protein crystals. Hydrogen atoms are the primary motive force in most enzymatic processes. Neutron diffraction is a powerful technique for locating hydrogen atoms even at resolutions of 2 Å to 2.5 Å and can therefore provide unique information about enzyme mechanism, protein hydrogen and hydrogen bonding.

For an experiment on the PCS, protein crystals have to be  $\sim 1 \text{ mm}^3$  in volume. Crystals of perdeuterated protein can be significantly smaller. Users of the PCS have access to neutron beam-time, perdeuteration

facilities and also support for data reduction and structure analysis. The beam-line exploits the pulsed nature of spallation neutrons and a large electronic detector in order collect wavelength resolved Laue patterns using all available neutrons in the wavelength range 1 Å to 5 Å. This talk shall be used to describe the facility, some groundbreaking results from our second year of operation, and provides information about obtaining beam-time. Future technological developments that will greatly improve the performance of the PCS facility will also be discussed, as well as prospects for neutron protein crystallography at the SNS.

For more information about the PCS and experimental requirements, contact Paul Langan (505) 665 8125, [langan\\_paul@lanl.gov](mailto:langan_paul@lanl.gov) or Benno P. Schoenborn (505) 665 2033, [schoenborn@lanl.gov](mailto:schoenborn@lanl.gov). The PCS is funded by the Office of Science and the Office of Biological and Environmental Research of the U.S. Department of Energy.

##### **T2-A2 (14:00) SANS Molecular Modeling of Biological Macromolecules from Low Resolution to High Resolution Techniques**

*S. K. Gregurick, J. Zhou (Department of Chemistry and Biochemistry, UMBC, 1000 Hilltop Circle, Baltimore MD, 21250), F. Schwartz (Center for Advanced Biotechnology, National Institute of Standards and Technology, 9600 Gudelsky Dr., Rockville MD, 20850), S. Krueger (NIST Center for Neutron Research)*

Within the past decade, small angle scattering measurements (SANS and SAXS) have played an important role in molecular biology, including the studies of protein-DNA interactions, protein-protein interactions, domain interactions within a given protein and the study of nucleic acid structures (DNA, RNA and peptide nucleic acids, or PNA). In order to model a three-dimensional macromolecular structure from an experimental scattering profile ( $I(Q)$  vs.  $Q$ ), we have developed a series of modeling and simulation programs. Our talk will highlight our recent work on developing molecular models of proteins and nucleic acid structures, based on small angle neutron scattering data in solution. We shall discuss both the methodology and applicability of our low resolution Monte Carlo technique, LORES, and our newly developed high resolution technique, Xtal2SAS. We will illustrate the ability of both methods to model SANS intensities of biological structures in solution. In particular, we will focus on the melting of a heterogeneous PNA/DNA construct, the dynamics of a 10-mer double stranded DNA construct and the protein CRP, in solution. Our methods will be com-

pared to other modeling software, when applicable. Our results will illustrate both the power and limitations of our current approach to develop a comprehensive software package for modeling of nucleic acid and protein structures in solution.

### **T2-A3 (14:15) The role of “anchoring” molecules and residual water on the stability of biomolecules**

*A. M. Pivovar, S. Takata, J.E. Curtis (NIST Center for Neutron Research)*

In order to slow the deactivation of a biologically active material, biomaterials are commonly stored within glass networks formed by small molecules with extensive hydrogen bonding interactions (e.g., saccharides or polyols). The glass network is believed to reduce the rate of deactivation by suppressing the dynamic mobility of biomolecular residues through thermodynamically favorable interactions between the glass and the surface of the native biomolecule. The “rigidity” imparted on the biomolecule by the glass matrix is dependent upon both the inherent rigidity of the glass and the strength of the interactions “anchoring” the biomolecule to the glass. To ascertain the role of the anchoring interactions on biopreservation, we have measured the ensemble temperature dependent mean square displacement dynamics of lysozyme-glucose composites using the High Flux Backscattering Spectrometer at the NIST Center for Neutron Research. Selective isotopic substitution of deuterium for hydrogen permits exclusive measurement of the dynamics of the biomolecular component in the mixture and evaluation of the total scattering from a fully hydrogenated sample allows us to ascertain the dynamics of the sugar. As expected, our results indicate that the dynamics of the biomolecule are suppressed through interactions with the anchoring sugar when compared with a pure lysozyme powder. However, the results also indicate that the dynamics of the anchored glucose molecules is less than what is observed in a pure glucose glass. We believe these results imply a strong dependence between the residual water present in the mixtures and biostability enhancement. The details of this conclusion and its ramifications on biopreservation formula design will be discussed.

### **T2-A4 (14:30) Hydration Dynamics near a Model Protein Surface**

*D. Russo (Department of Bioengineering, University of California, Berkeley), G. Hura (Graduate Group in Biophysics, University of California, Berkeley), T. Head-Gordon (Department of Bioengineering, University of California, Berkeley; Graduate Group in Biophysics, University of California, Berkeley)*

The evolution of water dynamics from dilute to very high concentration solutions of a prototypical hydrophobic amino acid with its polar backbone, N-acetyl-leucine-methylamide (NALMA), is studied by quasi-elastic neutron scattering (QENS) and molecular dynamics (MD) simulation for both the completely deuterated and completely hydrogenated leucine monomer. The NALMA-water system and the QENS data together provide a unique study for characterizing the dynamics of different hydration layers near a prototypical hydrophobic sidechain and the backbone to which it is attached. We observe several unexpected features in the dynamics of these biological solutions under ambient conditions. The translational and rotational water dynamics at the highest solute concentrations, are found to be highly suppressed as characterized by long residential time and slow diffusion coefficients. The analysis of the more dilute concentration solutions models the first hydration shell with the 2.0 M spectra. We find that for outer layer hydration dynamics that the translational diffusion dynamics is still suppressed, although the rotational relaxation time and residential time are converged to bulk-water values. Molecular dynamics analysis of the first hydration shell water dynamics shows spatially heterogeneous water dynamics, with fast water motions near the hydrophobic side chain, and much slower water motions near the hydrophilic backbone. We discuss the hydration dynamics results of this model protein system in the context of protein function and protein-protein recognition

### **T2-B, Materials Chemistry, Chair: John Larese (U. Tennessee), Room 1123 Blue**

#### **T2-B1 (13:30) States of Water in Hydrating Portland Cement**

*R. A. Livingston (Federal Highway Administration), D. A. Neumann, A. Allen, N. Nemes (National Institute of Standards and Technology)*

The essential reaction in the hardening of Portland cement occurs between tricalcium silicate and water. The kinetics of this reaction are complex with up to five different stages, but have been characterized using neutron scattering methods. These reveal at least three states of water that are called: free, confined and chemically bound. These can be related to the conventional cement chemistry classifications of non-evaporable water, gel pore water and capillary pore water. Following these states individually as a function of temperature, particle-size distribution and water/cement ratio provides insights into the rate controlling mechanism of each stage. These can also be related to macroscopic property development in the concrete such time of initial and final set. It has



been proposed that water also exists in a glassy or solid state in the hydrated cement, but this does not seem possible from thermodynamic considerations.

### **T2-B2 (13:45) Combined USANS/SANS Contrast Matching to Distinguish Calcium Hydroxide and Calcium-Silicate-Hydrate Gel Contributions to Hydrating Cement Microstructures**

*A. J. Allen (Ceramics Division, MSEL, National Institute of Standards and Technology), J.J. Thomas, J.J. Chen (Department of Civil Engineering, Northwestern University, Evanston, IL), J.G. Barker (NIST Center for Neutron Research)*

Characterization and modeling of the microstructure of hydrating cement using both SANS and SAXS has long been pursued by groups from around the world. The durability and mechanical properties of concrete are intimately connected to the development of calcium-silicate-hydrate (CSH) gel within the hydrating cement component. SAS techniques are particularly useful because the CSH is amorphous, rendering diffraction ineffective, and is altered by sample preparation for electron microscopy. Also, the CSH gel structure (which exhibits fractal properties) extends over length scales appropriate for SAS. Quantifying CSH structure is complicated by the presence of water (H) in various states ranging from OH groups to trapped liquid in nanopores. A further complication for conventional SANS and SAXS, and even for USAXS, is the presence of calcium hydroxide (CH) crystals in intimate mixture with C-S-H, which makes it necessary to determine the fine CH structure at all length scales so that CSH can be unambiguously characterized. Recently, combined USANS and regular SANS measurements performed on contrast matched cement paste specimens have allowed the CH morphology to be revealed and surveyed over the full range of required sizes. All the H in CSH exchanges readily with deuterium oxide (D) in contrast variation studies, while CH is crystalline and does not take part in H/D exchange. Hydrated samples were studied by USANS and SANS in H/D mixes of 100 % H, 32 % D (CH contrast match), and 80 % D (effective CSH/D contrast match). Corresponding samples were also studied after the CH phase was removed by leaching. Comparing leached and unleached sample data for the various H/D mixes has allowed the CH and CSH components to be distinguished to an unprecedented degree, and has highlighted previously unobserved structures in the USANS range. A fully quantitative microstructure analysis of CSH over its whole scale range has thus been obtained for the first time.

### **T2-B3 (14:00) Changes in Ettringite Crystalline Structure Associated with Thermal Dehydration**

*M. R. Hartman, R. Berliner (University of Michigan, Ann Arbor, MI 48109)*

Neutron powder diffraction studies have been performed on deuterated ettringite,  $\text{Ca}_6[\text{Al}(\text{OD})_6]_2(\text{SO}_4)_3(\sim 26\text{D}_2\text{O})$ , synthesized in the laboratory by precipitation from solutions of  $\text{Ca}(\text{OD})_2$  and  $\text{Al}_2(\text{SO}_4)_3$  in  $\text{D}_2\text{O}$ . Structural studies were performed at 10K using Rietveld refinement on fully hydrated material as well as samples that had been thermally treated to 6 %, 15 %, 21 %, and 27 % weight loss. Changes in the lattice parameters were observed with the c-axis exhibiting a linear contraction from 21.34948(18) Å in the fully hydrated state to 21.2662(17) Å for the specimen with 27 % weight loss. Conversely, the a-axis was observed to exhibit a linear expansion from a value of 11.16474(7) Å in the fully hydrated state to 11.1849(10) Å in the specimen with 27 % weight loss. The occupations of the hydroxyl and water sites were refined on the dehydrated samples to determine the order in which these sites are depopulated during the dehydration process. In contrast to prior investigations employing thermogravimetric analysis and  $^{27}\text{Al}$  NMR, which proposed an orderly depopulation of specific crystalline sites, the present study showed that the water and hydroxyl sites are simultaneously depopulated in the dehydration process. Additionally, an *in situ* thermal dehydration of ettringite was performed at 50 °C by passing dry nitrogen through a column of ettringite. The ettringite sample dehydrated *in situ* was dehydrated to a weight loss of 26.1 %. Comparison of the *in situ* dehydration data showed good agreement with the structural data of the statically dehydrated material.

### **T2-B4 (14:15) Probing the Mechanism of Metal-Halide Network Formation and Crystal Growth (Invited)**

*J. D. Martin (Department of Chemistry, North Carolina State University)*

The ability to design the structure of a material, and to control the influence of that structure on the material's properties is fundamentally important to the development of advanced materials. Crystal engineering has successfully articulated structural principles for the construction diverse materials. However, little is understood regarding the mechanism(s) by which networks are templated and crystals grow. Using a series of low temperature melting network liquids  $\text{ZnCl}_2$ ,  $\text{CuAlCl}_4$  and  $\text{CuGaCl}_4$  as well as the templated sodalite-type network  $[\text{HNMe}_3]\text{CuZn}_5\text{Cl}_{12}$  we are able to articulate fundamental mechanistic aspects of network formation



and crystallization reactions. Because several of these materials readily form glasses we are able to investigate cold crystallization (from the glass) and hot crystallization (from the melt) allowing us to study crystallization under nucleation- and growth-controlled conditions, respectively. Data from amorphous and crystalline neutron scattering, inelastic neutron scattering, time-resolved synchrotron diffraction, and DSC measurements will be discussed.

### **T2-B5 (14:45) Neutron Diffraction Studies on Metal Pseudohalide between 300 K and 50 K**

*D. J. Williams, L. Daemen, S. Vogel (Los Alamos Neutron Science Center, Los Alamos National Laboratory)*

The structural investigation of metal pseudohalide compounds (e.g., cyanides, cyanates, etc.) has been the object of numerous studies over more than a century. Several unresolved problems remain. Those have been addressed inconclusively with x-ray scattering and a variety of other techniques providing indirect structural information. One such outstanding structural question in binary pseudohalide compounds is whether only carbon or only nitrogen atoms in the polyhedron coordination sphere surround the metal cation. This structural question regarding the coordination sphere of the metal cation in cyanide and cyanate compounds is still debated among chemists.

The use of powder and single crystal x-ray diffraction techniques has been limited because the scattering contrast between neighboring elements, carbon, nitrogen, and oxygen, is weak. The possibility of disorder further complicates the matter. Fourier-Transform Infrared Spectroscopy (FT-IR) has been used to shed light on the nature of the metal to C or N bonding. However most of the information that is obtained is  $n(\text{C-N})$ ,  $n(\text{C-O})$  stretches, and broad  $n(\text{M-(C, N, O)})$  stretches at low wave numbers. (When the latter can be observed at all, it usually does not reveal any information about the metal cation preferred bonding orientation to the cyanide ligand.) Other spectroscopic techniques like Raman and NMR have had equally limited success. Because of the difference in neutron scattering length among C, N, and O, powder neutron diffraction should prove useful in resolving controversial structural issues in binary pseudo-halides. Similarly, incoherent inelastic neutron scattering is an attractive, alternative to conventional spectroscopies to provide chemical bonding information on the metal to pseudo-halide ligand. With LANSCE's newly commissioned powder diffractometer HIPPO (High Pressure Preferred Orientation powder diffractometer) and FDS (Filter

Difference Spectroscopy) a complete structural investigation of AgCN and AuCN was performed at 300 K, 200 K, 150 K, 100 K, and 50 K. The results confirm that cyanide ligands in these simple binary compounds are disordered throughout the crystal structure. The ordering/disordering of cyanate ligands has also been investigated (e.g., NaOCN, KO-CN, AgOCN...) using neutron scattering to determine whether the metal cation (e.g., Na, K...) is completely surrounded by the nitrogen or the oxygen end of a cyanate ion (e.g., OCN-M-NCO, NCO-M-NCO, NCO-M-OCN, etc...). These results will be discussed in detail.

### **T2-B6 (15:00) Single Crystal Analyses of the Structure and Bonding in Transition-Metal Sigma Complexes**

*A. J. Schultz, T. F. Koetzle, J. A. Cowan, M. E. Miller, X. Wang (Intense Pulsed Neutron Source, Argonne National Lab)*

In this presentation we will discuss a series of structures of B-H and Si-H sigma complexes that were recently obtained based on data from the IPNS Single Crystal Diffractometer (SCD). Transition-metal sigma complexes are coordination compounds in which two electrons in an X-H sigma bond form a dative bond with a transition metal. This three-center, two-electron bond can be further stabilized by pi-backbonding from the metal to the X-H sigma\* antibonding orbital. Transition metal sigma complexes are typically reactive intermediates that precede oxidative addition of substrates having an X-H bond. Sigma complexes are, therefore, identified as intermediates in catalytic hydrogenation ( $X = \text{H}$ ), activation and functionalization of hydrocarbons ( $X = \text{C}$ ), hydrosilylation ( $X = \text{Si}$ ), and hydroboration ( $X = \text{B}$ ) reactions. Characterizing the structure and bonding of the intermediate species is important to our understanding of these reactions and to improving catalytic processes. Single crystal neutron diffraction has played a critical role in characterizing the structure and bonding of sigma complexes, for which the positional and thermal parameters of the hydrogen atom in close proximity to a metal atom are clearly of utmost importance.

This research was supported by the U.S. DOE, Office of Basic Energy Sciences, under contract W-31-109-ENG-38.

T2-C, Instrumentation, Chair: Kenneth Herwig (ORNL), Auditorium

### **T2-C1 (13:30) Spin-analyzed diffuse scattering measurements of magnetic thin films with a $^3\text{He}$ analyzer and a position-sensitive detector**

*W. C. Chen (National Institute of Standards and Technology; Indiana University), K.V. O'Donovan (NIST Center for Neutron Research; University of Maryland, College Park), J.A. Borchers, C.F. Majkrzak, T.R. Gentile (National Institute of Standards and Technology)*

Polarized  $^3\text{He}$  gas, produced by optical pumping, can be used to polarize or analyze neutron beams because of the strong spin dependence of the neutron absorption cross section for  $^3\text{He}$ .  $^3\text{He}$  spin filters have been identified as important polarizing elements in the development of polarized neutron scattering instruments for the upcoming spallation neutron source (SNS) because they are broadband and suitable for divergent scattered beams. Here we report efficient polarization analysis of diffusely reflected neutrons in a reflectometry geometry using a hyperpolarized  $^3\text{He}$  spin filter in conjunction with a position-sensitive detector (PSD). We obtained spin-analyzed two-dimensional  $Q_x$ - $Q_z$  reciprocal space maps for a patterned array of Co antidots in the saturated and the demagnetized states. We compared data obtained from a  $^3\text{He}$  analyzer and a PSD with those obtained from a conventional supermirror analyzer, and they are in good agreement. The preliminary results for the upcoming experiment with a  $^3\text{He}$  analyzer and a PSD using a patterned dot sample and/or a rare-earth alloy exchange spring will also be reported. For these experiments,  $^3\text{He}$  gas is polarized by the spin-exchange optical pumping (SEOP) method and stored in a uniform magnetic field provided by a shielded solenoid. We address two important issues for achieving the better performance of the  $^3\text{He}$  spin-analysis device: high  $^3\text{He}$  polarization and long relaxation time of the cell. Using a spectrally narrowed diode laser array we have recently achieved  $^3\text{He}$  polarizations of 74 % to 79 % in  $^3\text{He}$  cells ranging from 260  $\text{cm}^3$  to 500  $\text{cm}^3$  in volume.

### **T2-C2 (13:45) Convergent Beam Neutron Crystallography**

*W. M. Gibson, R. Youngman (X-Ray Optical Systems, Inc., 15 Tech Valley Drive, East Greenbush, NY 12061), A. J. Schultz, J. W. Richardson, J. M. Carpenter, M. E. Miller, E. R. Maxey (Intense Pulsed Neutron Source, Argonne National Lab), D. F. R. Mildner, H. H. Chen-Mayer (National Institute of Standards and Technology)*

Two monolithic polycapillary optics of different focal length and beam convergence are used to investigate the use of focusing lenses for the neutron convergent

beam method for time-of-flight crystallography with a broad wavelength band. The lens of short focal length (15.5 mm) with a beam convergence of  $16.8 \pm 1.0$  degrees has a focal width of about 120 microns. For a single crystal sample of this diameter on a pulsed neutron source, this lens gives an integrated intensity gain of  $\sim 50$  for a (020) Bragg peak in  $\text{MnF}_2$  with 3.2 Å neutrons and a measured peak width (FWHM) of 4.5 degrees. Further measurements on a powder diffractometer show that the expected diffracted beam intensities have gains as much as 500 for powder samples of this diameter. The degradation of resolution is minimized in the back scattering geometry. The intensity gains for the powder diffraction peaks increase with wavelength and closely follow the expected transmission of the optic as a function of wavelength.

Work at XOS was supported by the US DOE, BES-MS, contract nos. OF-01385 and DE-FG02-02-ER83575. Work at Argonne National Laboratory was supported by the US DOE, BES-MS, under contract no. W-31-109-ENG-38. We also thank the NIST Center for Neutron Research.

### **T2-C3 (14:00) Neutron optical elements from HMI Berlin**

*Th. Krist, F. Mezei (Hahn-Meitner-Institut Berlin)*

In the last several years solid-state and other neutron optical devices have been developed at BENSC, especially polarizers and collimators. We show results of a solid state polarizing bender which polarizes neutron beams of arbitrary width and with wavelengths above 2.4 Å to flipping ratios above 40 (polarization above 95 %). The mean transmission amounts to  $61 \pm 4$  % at 4.7 Å. Solid-state collimators with absorbing and also with reflecting walls were first built in our group and results will be shown, e.g., of a collimator with a FWHM of 8' and a transmission above 70 %. A solid-state radial bender for the polarization analysis of neutrons over a wide angular range was built and tested at BENSC. A total angular interval of 3.8 deg could be analyzed. A solid-state radial collimator channel was built and tested. The angular range of the transmitted intensity could be doubled. Our first experiment on a solid-state neutron lens will be presented which shows a clear focusing of neutrons. Results for a solid-state bender used in transmission together with a solid-state collimator are shown.

Finally the design of a two dimensional polarization analyzer for an angular range of 5° in both directions and first results are presented.

### T2-C4 (14:15) 2D-Multi-Wire Position-Sensitive Gaseous Neutron Detectors with Relative Resolutions higher than 0.5%

R. Kampmann (Institute for Materials Research, GKSS Research Centre, 21502 Geesthacht, Germany); DENEX Detectors for Neutrons and X-rays GmbH, Moldenweg 9a, 21335 Lueneburg, Germany), M. Marmotti (DENEX Detectors for Neutrons and x-rays GmbH, Moldenweg 9a, 21335 Lueneburg, Germany), R. Georgii (ZWE FRM-II / Physik-Department E21, Technical University Munich, 85748 Garching, Germany), M. Haese-Seiller, V. Kudryashov (Institute for Materials Research, GKSS Research Centre, 21502 Geesthacht, Germany)

Two delay-line based 2D-multi-wire position-sensitive gaseous detectors (MW-PSGD) with very high relative resolution ( $R_r$ ) defined as the position resolution in percentage of the detector dimension have recently been developed for the instruments REFSANS and MIRA at the new German high flux reactor FRM-II. The REFSANS detector has an active area of  $A_a = (500 \text{ mm})^2$ , a wire pitch of 2 mm and  $R_r = 0.4 \%$ , the MIRA detector is smaller ( $A_a = (200 \text{ mm})^2$ ) and has a wire pitch of 1 mm resulting in  $R_r = 0.5 \%$ . These  $R_r$ -values demonstrate a substantial progress in the technology of 2D-MW-PSGD's because hitherto the actual limit of resolution for such detectors has been  $R_r = 0.8 \%$ . The design, the spatial resolution and the discrimination of gamma-radiation of the detectors are presented. Finally, the count rate capability of these modern delay-line based detectors is discussed for the case that they are linked to modern multi-hit TDC based data acquisition systems.

### T2-C5 (14:30) Neutron Diffraction from Levitated Liquids — a Technique for Measurements on Liquids under Extreme Conditions

J.K.R. Weber, J.E. Rix, K.J. Hiera, J.A. Tangeman (Containerless Research, Inc.), C.J. Benmore, J.E. Siewenie (Intense Pulsed Neutron Source, Argonne National Lab)

Combining neutron diffraction and containerless techniques enables the structure of solids and liquids to be probed at extreme temperatures and under highly non-equilibrium conditions. Results complement data obtained by x-ray techniques and permit a more detailed understanding of the relaxation of liquid structures. This paper will describe the implementation of experiments on molten aluminates and zirconium oxide under containerless conditions at high temperature. Data were obtained at the Glass Liquids and Amorphous Diffractometer at IPNS using aerodynamic levitation and  $\text{CO}_2$  laser beam heating of 3 mm to 3.5 mm diameter samples. Levitation was

performed in argon gas and using pure vanadium nozzles. Structure factors were measured for liquids with the compositions  $\text{CaAl}_2\text{O}_4$ ,  $\text{Ca}_{67}\text{Al}_{66}\text{O}_{166}$ ,  $\text{Sr}_{67}\text{Al}_{66}\text{O}_{166}$ ,  $\text{Y}_3\text{Al}_5\text{O}_{12}$  and  $\text{ZrO}_2$  at temperatures up to 3350 K. Results will be compared to data for glasses with the same chemical compositions. Plans for development of a system for SNS research will be summarized.

Supported by DOE under contract numbers DE-FG02-01ER86121 (CRI) and W 31 109 ENG 38 (IPNS).

### T2-C6 (14:45) A New *In Situ* Vapor Sorption Apparatus for SANS Measurements

Man-Ho Kim (NIST Center for Neutron Research; Department of Materials Science and Engineering, University of Maryland), Charles J. Glinka (NIST Center for Neutron Research)

An apparatus for quantitative *in situ* vapor phase sorption, based on a prototype developed by NIST's Polymers Division [1], has been constructed for SANS measurements. The apparatus facilitates determining pore size distributions of microporous materials, enhancing scattering contrast in structural studies of semi-crystalline polymers, and the adsorption and desorption of solvent mixtures in porous media for rapid contrast variation with a single sample. The apparatus consists of a temperature-controlled titanium sample cell with demountable quartz windows and variable path length of 1 mm to 5 mm. The cell has ports for evacuating or admitting vapor to the sample space while monitoring and controlling absolute pressure. The apparatus can also be used to continuously flow a carrier gas through the sample. Mass flow controllers in the system allow the carrier gas to mix specific molar ratios of saturated vapor from two temperature-controlled solvent reservoirs to provide continuous control of the H/D ratio in the vapor reaching the sample. Examples of vapor condensation in microporous silica and the selective absorption of deuterated vapor in semi-crystalline polyethylene will be shown to demonstrate the performance of the apparatus.

[1] Ronald C. Hedden, Hae-Jeong Lee, and Barry J. Bauer, *Langmuir*, 2004, 20, 416-422

### T2-C7 (15:00) Novel time-of-flight diffractometer for very high resolution and extreme sample environment.

J. Peters, D. Clemens, K. Lieutenant (Hahn-Meitner-Institut Berlin), F. Mezei (Hahn-Meitner-Institut Berlin; Los Alamos Neutron Science Center, Los Alamos National Laboratory)

The Extreme Environment Diffractometer (EXED) powder diffractometer is under construction at the



Hahn-Meitner-Institut (HMI) in Berlin. It is based on the time-of-flight (TOF) principle, which offers a number of advantages on a continuous source compared with the usual crystal monochromator instruments: a) It can provide higher resolutions, matching those achieved by now on synchrotron radiation sources; b) It makes small d spacing readily accessible; c) It is more efficient in terms of neutron intensity for conventionally high resolution neutron diffraction work and d) it facilitates the use of extreme sample environment equipment by providing a full coverage of the relevant Q domain at very limited angular access in scattering angles, for instance due to the magnet geometry. EXED will be installed on an innovative multispectral neutron guide, delivering both the thermal and the cold neutron spectrum to the sample at about 80 m from the neutron source. This will assure an exceptionally broad incoming wavelength band of 0.7 Å to 20 Å, i.e. d spacing from 0.35 Å to 10 Å, or a momentum transfer Q domain 0.63 Å<sup>-1</sup> to 17.9 Å<sup>-1</sup> can be studied in the high resolution backscattering configuration at scattering angles 155° to 178°. The symmetric forward scattering range of 2° to 25° will make accessible Q values 0.01 Å<sup>-1</sup> to 3.9 Å<sup>-1</sup>. With 54 m flight-path between the chopper and the sample, the highest resolution will be achieved using a 36000 RPM curved Fermi chopper for 6 μs FWHM pulse length and the resolution will be adjustable according to the needs of the experiment by extending the pulse length up to 4000 μs with the help of alternate choppers (lower resolution straight Fermi chopper and a disc chopper pair with variable slit width). The highest resolution in backscattering geometry will achieve  $\delta d \sim 3.5 \times 10^{-4}$  Å, i.e.,  $\delta d/d = 2.4 \times 10^{-4}$  for common d spacing in the 2 Å range. The wavelength range to be explored will be defined by the phases and angular velocities of the choppers and can be scanned continuously.

The instrument is to be equipped with an immobile steady state magnet (25 T, later envisaged 40 T) of tapered solenoidal shape, which form allows us to achieve higher fields than the conventional split pair design. Low temperature and high pressure sample environments will also be available at high magnetic fields. Four position sensitive gas detectors with a space coverage of 50 x 80 cm<sup>2</sup> each and a resolution of 1 cm x 1 cm will be arranged around the sample, to provide fairly full coverage of the forward and backward scattering angle domains left accessible by the form of the magnet. EXED can be further extended for small angle and inelastic scattering work in high magnetic fields.

## **T2-C8 (15:15) Capabilities for Texture Measurements of the New Neutron Diffractometer HIPPO**

*S. C. Vogel (Los Alamos National Laboratory), C. Hartig (Technical University Hamburg-Harburg, 21071 Hamburg, Germany), L. Lutterotti (University of Trento, Italy; UC Berkeley, Berkeley, CA94720-4767), C.T. Necker (Los Alamos National Laboratory), R.B. Von Dreele (Los Alamos National Laboratory; Argonne National Laboratory), H.R. Wenk (UC Berkeley, Berkeley, CA94720-4767), D.J. Williams (Los Alamos National Laboratory)*

In this presentation we describe the capabilities for texture measurements of the new neutron time-of-flight diffractometer HIPPO (High Pressure Preferred Orientation) at the Los Alamos Neutron Science Center (LANSCE). The orientation distribution function (ODF) is extracted from multiple neutron time-of-flight histograms using the full-pattern analysis first described by Rietveld. Both, the well-established description of the ODF using spherical harmonics functions and the WIMV method, more recently introduced for the analysis of time-of-flight data, are available to routinely derive the ODF from HIPPO data. At ambient conditions, total count time of less than 30 minutes is ample to collect sufficient data for texture analysis in most cases. The large sample throughput for texture measurements at ambient conditions possible with HIPPO requires a robust and reliable, semi-automated data analysis. HIPPO's unique capabilities to measure large quantities of ambient condition samples and to measure texture at temperature and uniaxial stress are described. Examples for all types of texture measurements are given. We will also critically compare the ODF obtained from neutron time-of-flight data with the ODF obtained from x-ray diffraction or electron back-scatter diffraction for selected cases.

## **T2-D, Heavy Fermion Systems, Chair: Raymond Osborn (ANL), Room 2101/3/5 Green**

### **T2-D1 (13:30) Recent progress on heavy fermion f-electron systems (Invited)**

*M. B. Maple (Dept. of Physics and Inst. for Pure and Applied Physical Sciences; University of California, San Diego)*

Heavy fermion compounds are metallic compounds containing a sublattice of rare earth (R) or actinide (A) ions, which have electronic specific heat  $C_e$  coefficients  $\gamma = C_e/T$  with enormous values as large as several J/mol K<sup>2</sup>, corresponding to quasiparticle masses of several hundred times the free electron mass. For most heavy fermion compounds, which are based on Ce, Yb, or U, the nonmagnetic heavy Fermi liquid ground state is believed to be associated



with the Kondo effect arising from an antiferromagnetic exchange interaction between conduction electron spins and magnetic moments of the R or A ions with partially-filled f-electron shells (Kondo lattice). The nonmagnetic heavy Fermi liquid ground state is unstable with respect to the formation of other novel strongly correlated electron states, including unusual magnetically ordered states, unconventional (non s-wave) superconductivity with an energy gap that has line or point nodes on the Fermi surface, which sometimes coexists with magnetic order, and non-Fermi liquid (NFL) behavior in the normal state physical properties in the vicinity of a quantum critical point (QCP). NFL behavior and/or superconductivity have been observed under pressure in both antiferromagnetic (e.g., CeIn<sub>3</sub>, CePd<sub>2</sub>Si<sub>2</sub>) and ferromagnetic (e.g., UGe<sub>2</sub>) heavy fermion compounds in the vicinity of the critical pressure where the magnetic ordering temperature is suppressed to 0 K (magnetic QCP). This suggests that magnetic dipole moment fluctuations are responsible for the NFL behavior and mediate the pairing of superconducting electrons in at least some of these materials. Heavy fermion behavior has been observed in several Pr compounds with nonmagnetic Pr<sup>3+</sup> ionic ground states in the crystalline electric field that appears to be due to the interaction between the charges of the conduction electrons and Pr<sup>3+</sup> electric quadrupole moments. One of these heavy fermion Pr compounds, PrOs<sub>4</sub>Sb<sub>12</sub>, was found to exhibit unconventional superconductivity. In this compound, the superconducting state appears to consist of several distinct superconducting phases and to break time reversal symmetry, suggesting that the superconductivity may involve triplet spin pairing of electrons. The basic properties of heavy fermion systems with emphasis on recent developments are reviewed in this talk. This research was supported by the U. S. Department of Energy under Grant No. DE-FG02-04ER46105 and the National Science Foundation under Grant No. DMR-0335173.

**T2-D2 (14:00) Coexistence of superconductivity and magnetism in heavy fermion family of compounds: CeMIn<sub>5</sub>**

*A. Llobet (Los Alamos Neutron Science Center, Los Alamos National Laboratory), A.D. Christianson (Los Alamos National Laboratory; Colorado State University), J.S. Gardner (NIST Center for Neutron Research), W. Bao, N.O. Moreno, P.G. Pagliuso, J.L. Sarrao (Los Alamos National Laboratory), J.W. Lynn (NIST Center for Neutron Research; Center for Superconductivity Research, University of Maryland, College Park, MD 20742), J.M. Mignot (Laboratoire Léon Brillouin, C.E.A Saclay, 91191 Gif-*

*sur-Yvette Cedex), K. Prokes (Hahn-Meitner-Institut Berlin)*

We report the first evidence of the correlation between long-range magnetic order and the development of a superconducting ground state in the Ce-based heavy fermion family of compounds CeRh<sub>1-x</sub>M<sub>x</sub>In<sub>5</sub> (M = Ir, Co). Our neutron diffraction study describes the evolution of the magnetic structure with Ir or Co doping. Upon doping, the ground state is driven from an AFM helical structure ( $k_1 = (1/2, 1/2, 0.297)$ ) in CeRhIn<sub>5</sub> to a more complex magnetic structure characterized by commensurate and incommensurate components. Remarkably, the presence of the commensurate propagation vector seems strongly correlated with the development of superconductivity in this alloy series. Further, the magnetic structure is unaffected by the development of the superconducting state and a large Ce staggered magnetic moment coexists with superconductivity at low temperatures. Hydrostatic pressures as well as the application of magnetic fields have been also used to destroy or induce the superconducting state, and neutron diffraction studies reveal the interplay between magnetism and superconductivity in this series of heavy fermion compounds. This study lends credibility to the idea that the formation of the unconventional superconducting state may be favored by specific types of magnetic fluctuations. It also provides more evidence of the possible duality of the 4f electrons in these Ce-based compounds.

**T2-D3 (14:15) Crystalline Electric Field Effects in CeMIn<sub>5</sub>: Superconductivity and the Influence of Kondo Spin Fluctuations**

*A. D. Christianson (University of California at Irvine), E. D. Bauer (Los Alamos National Laboratory), J. M. Lawrence (University of California at Irvine), P. S. Riseborough (Temple University, Philadelphia, Pennsylvania 19122), N. O. Moreno, P. G. Pagliuso, J. L. Sarrao, J. D. Thompson, M. P. Hehlen, F. R. Trouw (Los Alamos National Laboratory), E. A. Goremychkin (Argonne National Laboratory), R. J. McQueeney (LANL and Iowa State University, Ames, Iowa 50011)*

We have measured the crystalline electric field excitations (CEF) of the CeMIn<sub>5</sub> (M = Co, Rh, Ir) series of heavy fermion superconductors by means of inelastic neutron scattering (INS). Fits to a CEF model reproduce the INS spectra and the high temperature magnetic susceptibility. The CEF parameters, energy level splittings, and wavefunctions are tabulated for each member of the CeMIn<sub>5</sub> series and compared to each other as well as to the results of previous measurements. Our results indicate that the CEF level splitting in all three materials is similar, and can be

thought of as being derived from the cubic parent compound  $\text{CeIn}_3$  in which an excited state quartet at  $\sim 12$  meV is split into two doublets by the lower symmetry of the tetragonal environment of the  $\text{CeMIn}_5$  materials. In each case, the CEF excitations are observed as broad lines in the INS spectrum. We attribute this broadening to Kondo hybridization of the localized f moments with the conduction electrons. The evolution of the superconducting transition temperatures in the different members of  $\text{CeMIn}_5$  can then be understood as a direct consequence of the strength of this hybridization. Due to the importance of Kondo spin fluctuations in these materials, we also present calculations within the non-crossing approximation to the Anderson impurity model including the effect of CEF level splitting for the INS spectra and the magnetic susceptibility.

#### T2-D4 (14:30) Crystal fields in $\text{UO}_2$ - revisited

*H. Nakotte, R. Rajaram (Physics Department, New Mexico State University, Las Cruces NM 88003), R. McQueeney (Los Alamos Neutron Science Center, Los Alamos National Laboratory), S. Kern (Physics Department, Colorado State University, Fort Collins CO 80524), G.H. Lander (Institute for Transuranium Compounds, D-76125 Karlsruhe, Germany)*

Uranium Dioxide ( $\text{UO}_2$ ) is an important nuclear fuel material. We performed high-resolution inelastic neutron scattering using PHAROS at the Los Alamos spallation source LANSCE in order to re-investigate the crystal field splitting in  $\text{UO}_2$ , determined with the knowledge of the dipole-allowed transitions. We obtained the crystal field parameters and the 5f electron eigen functions for  $\text{UO}_2$ . The fourth- and sixth-degree crystal field parameters were found to be  $V_4 = -116.24$  and  $V_6 = 25.78$ , in good agreement with previously published results by Amoretti et al. [1]. On the other hand, these previous studies did reveal four crystal-field excitations in the 150 meV to 180 meV range, only three of which can be explained by the crystal-field model. Our experiments on a different  $\text{UO}_2$  sample show that the previously observed peak at about 180 meV is a spurious one, thus it is not intrinsic to  $\text{UO}_2$ .

[1] G. Amoretti et al., Phys. Rev. B 15 (1989) 1856

#### T2-D5 (14:45) Unusual phonon softening in delta-phase plutonium (Invited)

*R. J. McQueeney (Iowa State University/Ames Laboratory), A. C. Lawson, A. Migliori (Los Alamos National Laboratory), T. M. Kelley, B. Fultz (California Institute of Technology), J. C. Lashley (Los Alamos National Laboratory)*

The phonon density-of-states and adiabatic sound

velocities were measured on fcc-stabilized  $^{242}\text{Pu}_{0.95}\text{Al}_{0.05}$ . The phonon frequencies and sound velocities decrease considerably (soften) with increasing temperature despite negligible thermal expansion. The frequency softening of the transverse branch along the (111) direction is anomalously large ( $\sim 30\%$ ) and is very sensitive to alloy composition. The large magnitude of the phonon softening is not observed in any other fcc metals and may arise from an unusual temperature dependence of the electronic structure in this narrow 5f-band metal.

#### T3-A, Charge, Orbital, and Spin Ordering in Oxides, Chair: Michael Crawford (Dupont), Auditorium

##### T3-A1 (15:45) Charge, orbital and spin ordering in $\text{RBaFe}_2\text{O}_{5+x}$ perovskites (Invited)

*P. M. Woodward (Department of Chemistry, Ohio State University), P. Karen (Department of Chemistry, University of Oslo)*

Transition-metal oxides adopting the perovskite structure (or closely related structure types) are well known for their interesting electronic properties (i.e. High  $T_c$  superconductivity, colossal magnetoresistance, charge disproportionation, etc.). The oxygen-deficient double perovskites  $\text{RBaFe}_2\text{O}_{5+x}$  ( $R = \text{Nd, Sm, Tb, Ho, Y}$ ) are among the more interesting classes of perovskite related compounds. When  $x = 0$  these compounds contain square-pyramidal iron with an average valence of  $+2.5$ . By changing temperature all three Robin-Day classes of iron mixed-valence can be observed. In the high temperature paramagnetic state all iron atoms are equivalent. Upon cooling antiferromagnetism sets in, followed by a two-step charge-localization process. The localization of the conduction electrons triggers phenomena such as charge and orbital ordering, reorientation of the antiferromagnetic structure and in some cases induced magnetism of the rare-earth sublattice. Variable temperature high-resolution synchrotron x-ray and neutron powder diffraction measurements, neutron thermodiffraction, transport and magnetic susceptibility measurements are used to characterize the behavior of this interesting family of compounds.

##### T3-A2 (16:15) Charge Ordering, Long and Short Range Magnetic Ordering in the $\text{Mn}^{3+}/\text{Mn}^{4+}$ Oxide, $\text{Pb}_3\text{Mn}_7\text{O}_{15}$ .

*J.E. Greedan, J. Barbier, J.F. Britten, N. Penin, H. Ghazi (BIMR and Chemistry Dept., McMaster University, Hamilton CANADA), C.R. Wiebe (Department of Physics and Astronomy, McMaster University, Hamilton, ON, Canada), H. Dabkowska*

(BIMR, McMaster University, Hamilton, CANADA),  
I.P. Swainson (National Research Council, Chalk  
River, Ontario, Canada)

Manganate  $Mn^{3+}/Mn^{4+}$  oxides have been of intense interest in recent years. In particular the perovskite based materials,  $A_{1-x}Ln_xO_3$  ( $A$  = divalent alkaline earth,  $Ln$  = trivalent lanthanide) exhibit charge ordering, a variety of magnetic phenomena, metal insulator transitions and of course, CMR. As well, the spinel  $LiMn_2Mn_4O_4$  shows partial charge ordering, complex long range and short range ordering and is of interest as a battery cathode.  $Pb_3Mn_7O_{15}$  is an under-investigated manganate with approximately equal concentrations of  $Mn^{3+}$  and  $Mn^{4+}$  and is structurally related to spinel in that the Mn-O octahedra are linked by edge-sharing. The compound forms in an orthorhombic structure (Cmcm) with pronounced hexagonal pseudo-symmetry. Neutron powder diffraction was instrumental in confirming the Cmcm structure at room temperature and that the charge ordering is only partial. The Mn sublattice is based on layers of edge-sharing triangles and is thus prone to geometric frustration. This is reflected in the magnetic susceptibility that shows an extended region of short range order from above 350 K to 72 K followed by magnetic transitions at 72 K and 55 K. The magnetic structure between 72 K and 55 K is described by  $\mathbf{k} = (000)$  while a larger cell,  $\mathbf{k} = (1/2 1/2 0)$ , sets in below 55 K. Neutron diffuse scattering is clearly seen in the form of a broad Lorentzian background centered at  $Q = 1.36 \text{ \AA}^{-1}$  which is observed over the range from  $\sim 60$  K (below the first magnetic transition) to at least 180 K. The correlation length derived from the Lorentzian peak width is  $\sim 4.6 \text{ \AA}$  which is three Mn neighbor distances, slightly longer than found for  $LiMn_2O_4$ .

### T3-A3 (16:30) Magnetic Field Induced Metal-Insulator Transition in $Pr_{1-x}(Ca_{1-y}Sr_y)_xMnO_3$ ( $x = 0.45, y = 0.15$ )

F. Ye, J. A. Fernandez-Baca (Condensed Matter Sciences Division, Oak Ridge National Laboratory), P. Dai (Condensed Matter Sciences Division, Oak Ridge National Laboratory; Department of Physics and Astronomy, University of Tennessee), Y. Tomioka (Correlated Electron Research Center, National Institute of Advanced Industrial Science and Technology), Y. Tokura (Department of Applied Physics, University of Tokyo)

Recently, the electronic phase diagram of  $Pr_{1-x}(Ca_{1-y}Sr_y)_xMnO_3$  ( $x = 0.45$ ) has been studied in the vicinity of the metal-insulator transition boundary. By controlling the  $e_g$  electron bandwidth  $W$ , the ground state can be tuned to change from a charged-ordered (CO) and orbitally-ordered (OO) state

( $y \leq 0.2$ ) to a ferromagnetic metallic state ( $y > 0.25$ ). This system has been reported to exhibit bicritical features near  $y = 0.25$ . We have used elastic and inelastic neutron scattering to study the magnetic correlations and spin dynamics of the sample near the insulator-metal boundary. The insulating CO/OO ground state of  $y = 0.15$  can be melted by the application of external field. The evolution of the CO/OO when a magnetic field is applied will be discussed in the context of the competing interactions that may be responsible for the CMR effect.

This work was supported by the U.S. DOE under Contract No. DE-AC05-00OR22725 with UT-Batelle, LLC; and by NSF grant DMR-0139882.

### T3-A4 (16:45) Spin dynamics of CMR manganites

T. Chatterji (Institut Laue Langevin), N. Shannon (Max Planck Institute for PKS, Dresden, Germany), L.P. Regnault (CEA, Grenoble, France)

We have investigated the spin dynamics of the hole-doped infinite-layer and bilayer manganites,  $La_{0.7}Ba_{0.3}MnO_3$  and  $La_{1.2}Sr_{1.8}Mn_2O_7$ , showing colossal magnetoresistive properties close to the ferromagnetic transition temperatures, by inelastic neutron scattering. The infinite-layer manganite  $La_{0.7}Ba_{0.3}MnO_3$  is a three-dimensional high- $T_c$  ferromagnet with  $T_c = 350$  K whereas the bilayer manganite  $La_{1.2}Sr_{1.8}Mn_2O_7$  is a quasi-two-dimensional low- $T_c$  ferromagnet with  $T_c = 120$  K. The spin dynamics of these ferromagnets at low temperature, show important deviations from that expected for a localized Heisenberg ferromagnet. The spin wave stiffness and bandwidth scaled to  $k_B T_c$  show that these ferromagnets are closer to the itinerant ferromagnets. The experimentally determined spin wave dispersions in both these ferromagnets at low temperatures show zone-boundary softening. Also the spin waves are heavily damped especially close to the zone boundary. We developed a spin wave theory of these ferromagnets on the basis of minimal double exchange model. This model reproduces qualitatively both the softening and damping of the spin waves. According to this model retarded interaction between spin waves mediated by the charge susceptibility of the itinerant electrons generates interaction between non-nearest-neighbor spins, and so modifies the spin wave dispersion. Also the spin waves can decay into lower energy states by giving up energy to electron-hole pairs and so become damped. However, this model falls short to reproduce quantitatively the experimental results. We have measured the temperature dependence of the spin waves in these ferromagnets. The temperature dependence of the spin waves of the hole-doped ferromagnets shows



deviations from that expected from the localized Heisenberg model. These deviations can be explained qualitatively from the minimal double exchange model. The spin excitations in these ferromagnets are found to persist above the ordering temperatures.

### **T3-A5 (17:00) Structure and Magnetism in Sr-Doped Rare Earth Cobaltates**

*M. James (Bragg Institute, Australian Nuclear Science and Technology Organisation, Australia), D. J. Goossens, R. L. Withers (Research School of Chemistry, Australian National University, Canberra, ACT 0200, AUSTRALIA)*

Substantial interest has recently been generated by rare earth cobaltate compounds as cathode materials for solid oxide fuel cells. We have synthesized a wide range of single-phase perovskite-based rare earth cobaltates ( $Ln_{1-x}Sr_xCoO_{3-d}$ ) ( $Ln = La^{3+}, Pr^{3+}, Nd^{3+}, Sm^{3+}, Gd^{3+}, Dy^{3+}, Y^{3+}, Ho^{3+}, Er^{3+}, Tm^{3+}$  and  $Yb^{3+}$ ;  $0.60 < x < 1.00$ ). For the first time we have mapped the perovskite phase boundaries for these materials (synthesized under 1 atmosphere of oxygen). A combination of electron and x-ray diffraction of these compounds reveals three different classes of tetragonal superstructures. A phase boundary exists between compounds containing large and small rare earths (between  $Nd^{3+}$  and  $Sm^{3+}$ ) and also at the highest Sr-doping levels ( $x > 0.90$ ). Powder neutron diffraction has been used in conjunction with the other diffraction techniques to reveal cation and oxygen vacancy ordering within these materials.

These phases show mixed valence ( $3 + 4 +$ ) cobalt oxidation states that increases with Sr content; exceeding 50 % Co(IV) for the compositions  $Ln_{0.05}Sr_{0.95}CoO_{3-d}$ . A range of magnetic behaviors has been observed using susceptibility techniques and in a number of instances we have observed ordered ferromagnetism at elevated temperatures ( $\sim 300$  K). In these cases, the magnetic structures of these materials were further characterized by powder neutron diffraction.

### **T3-A6 (17:15) Spin and lattice correlations in $La_{1-x}Sr_xCoO_3$ cobaltites**

*S. Rosenkranz, P.J. Chupas, R. Osborn, J.F. Mitchell (Argonne National Laboratory), J.W. Lynn (NIST Center for Neutron Research), D. Louca (Virginia University)*

The cobaltites  $La_{1-x}Sr_xCoO_3$  show intriguing spin, lattice, and orbital properties similar to the ones observed in colossal magnetoresistive manganites. The  $x = 0$  parent compound is a non-magnetic insulator at low temperatures, but shows evidence of spin-state transitions of the cobalt ions above 100 K

from low-spin to intermediate and/or high-spin configurations. Upon doping, these systems show spin glass-like behavior with a sharp transition to ferromagnetic order at  $x \sim 0.2$ . There is a concomitant metal-insulator transition, which appears analogous to similar transitions in the phase diagram of CMR manganites. We have recently succeeded in growing large ( $\sim 5$  g), high-quality, single crystals of these compounds, which are suitable for studying in detail the spin, lattice, and orbital correlations, and their possible connection to transport properties. Our neutron and synchrotron x-ray scattering investigations of  $x = 0.2$  doped system reveal a relatively large gap in the spin-wave excitation spectrum below, and the existence of structural distortions above  $T_c$ .

This work is supported by US DOE BES-DMS W-31-109-ENG-38 and the NSF.

### **T3-B, Polymer Dynamics, Chair: Jyotsana Lal (ANL), Room 2100/2/4 Red**

#### **T3-B1 (15:45) The Influence of Environment on Polymer Mobility: Quasielastic Neutron Scattering on PEO/PMMA Blends (Invited)**

*J. K. Maranas, V. Garcia-Sakai, C. Chen (Pennsylvania State University), Z. Chowdhuri, I. Peral, N. Rosov (National Institute of Standards and Technology)*

The focus of this presentation is the use of quasielastic neutron scattering to assess mobility in polymers. Background on the dynamic behavior of polymers on time-scales assessable by neutron instruments will be covered. We are interested in the changes in this mobility when the environment of the polymer is changed in some way. One might imagine doing so by introducing nanoparticles, placing a neat polymer in a mixture, or incorporating the polymer as a di- or tri-block copolymer – materials with nanoscale ordered regions. One of these manipulations, changes that occur when the polymer is placed in a mixture, will be illustrated with measurements made over the last year on backscattering, time-of-flight and neutron spin echo spectrometers on a blend of poly(methyl-methacrylate) [PMMA] and poly(ethylene oxide) [PEO]. These two constituent polymers have dynamic behavior separated by many orders of magnitude, a behavior that we find persists in the mixture using incoherent scattering with selective deuteration to isolate the dynamic responses of each component in turn. One challenge faced with this system is the extremely stretched nature of the relaxations – the decay is very slow and thus not much is observed within the typical time windows of neutron spectrometers. Another chal-



lenge is to separate each components motion in coherent measurements where labeling is less helpful. We will discuss the potential for using chemically realistic simulations to assist in meeting these challenges.

### **T3-B2 (16:15) Dynamics in Thin Polymer Films**

*C. L. Soles, J. F. Douglas, W.-L. Wu (NIST Polymer Division)*

Incoherent neutron scattering is presented as a powerful tool for interpreting changes in the molecular dynamics as a function of film thickness for a range of polymers. Motions on a time scale of approximately a nanosecond and faster are quantified in terms of a mean-square atomic displacement (MSD) from the Debye-Waller factor. We find that thin film confinement generally leads to a reduction of the MSD in comparison to the bulk material, this effect becoming especially pronounced when the film thickness approaches the unperturbed dimensions of the macromolecule. Generally we always observe a suppression (never an enhancement) of the MSD at temperatures  $T$  above the bulk calorimetric glass transition temperature,  $T_g$ . Below  $T_g$ , the reduction in the magnitude of the MSD depends upon the polymer and the length scales being probed. Polymers with extensive segmental or local mobility in the glass are particularly susceptible to reductions of the MSD with confinement, especially at the  $Q$  vectors probing longer length scales, while materials lacking these sub- $T_g$  motions are relatively less sensitive. We also demonstrate that a reduced MSD correlates with a reduced mobility at long time and spatial scales, as measured by diffusion in the thin polymer films. Finally, we find that this reduced thin film mobility is not reliably predicted by thermodynamics assessments of an apparent  $T_g$ , as measured by discontinuities or kinks in the  $T$  dependence of the thermal expansion, specific volume, index of refraction, specific heat, etc. This is illustrated through series polycarbonate films simultaneously characterized with specular x-ray reflectivity and beam positron annihilation lifetime spectroscopy. In total, these measurements illustrate that the MSD is a powerful and predictive tool for understanding dynamic changes in thin polymer films.

### **T3-B3 (16:30) Applying Neutron Scattering to Polymer Coating Research**

*L. Sung (Building and Fire Research Laboratory, National Institute of Standards and Technology, Gaithersburg, MD 20899), D. L. Ho (NIST Center for Neutron Research), X. Gu, S. Scierka (Building and Fire Research Laboratory, National Institute of Standards and Technology, Gaithersburg, MD*

*20899), J. Barker (NIST Center for Neutron Research)*

Nanostructure and heterogeneity of coating materials are the key parameters to affect the physical and mechanical properties of coatings and their service life. It is curial to understand the relationship between the nanostructure, heterogeneity and the durability of coating materials for surface life prediction. Complementary to the conventional microscopic characterization tools often used in coating industry, small angle neutron scattering (SANS) technique provides bulk spatial information in a large sample area without extensive manual labor, and is proven to be useful for assessing the state of structure and dispersion of polymer coating materials. This outcome may help to bring a new solution to a long-standing pigment dispersion measurement problem in the coating industry. In this presentation, SANS studies on (1) the effect of pigment concentration on spatial distribution (dispersion) of pigmentary or nanoparticles in acrylic coatings and (2) the effect of nanostructure on UV degradation of fluoropolymer based coatings will be reported and compared to microscopy results.

### **T3-B4 (16:45) Intramolecular Diffusive Motion in Alkane Monolayers Studied by High-Resolution Quasielastic Neutron Scattering and Molecular Dynamics Simulations**

*H. Taub (Department of Physics and Astronomy and University of Missouri Research Reactor, University of Missouri-Columbia, Columbia, Missouri 65211), F.Y. Hansen (Department of Chemistry, Technical University of Denmark, IK 207 DTU, DK-2800 Lyngby, Denmark), L. Criswell (Department of Physics and Astronomy and University of Missouri Research Reactor, University of Missouri-Columbia, Columbia, Missouri 65211), D. Fuhrmann (Department of Physics and Astronomy and University of Missouri Research Reactor, University of Missouri-Columbia, Columbia, Missouri 65211; Infineon Technologies, Memory Products, Balanstr. 73, D-81541 Munich, Germany), K.W. Herwig (Spallation Neutron Source, Oak Ridge National Laboratory), A. Diama, H. Mo (Department of Physics and Astronomy and University of Missouri Research Reactor, University of Missouri-Columbia, Columbia, Missouri 65211), R.M. Dimeo, D.A. Neumann (NIST Center for Neutron Research), U.G. Volkman (Facultad de Física, Pontificia Universidad Católica de Chile, Santiago 22, Chile)*

Monolayers of intermediate-length alkane molecules such as tetracosane ( $n\text{-C}_{24}\text{H}_{50}$  or C24) serve as prototypes for studying the interfacial dynamics of more complex polymers, including bilayer lipid

membranes. Molecular dynamics simulations of a C24 monolayer adsorbed on a graphite basal-plane surface show that there are diffusive motions associated with the creation and annihilation of *gauche* defects occurring on a time scale in the range 0.1 ns to 4 ns. We present evidence that these relatively slow motions are observable by high-energy-resolution quasielastic neutron scattering (QNS) thus demonstrating QNS as a technique, complementary to nuclear magnetic resonance, for studying conformational dynamics on a nanosecond time scale in molecular monolayers.<sup>1,2</sup>

[1] F.Y. Hansen et al., Phys. Rev. Lett. **92**, 046103 (2004).

[2] This work was supported by the NSF under Grant Nos. DMR-9802476 and DMR-0109057, by the Chilean government under FONDECYT Grant No. 1010548, and by the U.S. Department of Energy through grant DE-FG02-01ER45912. The neutron scattering facilities in this work are supported in part by the National Science Foundation under Agreement No. DMR-0086210.

### **T3-B5 (17:00) Neutron Spin Echo Study of the Local Dynamics in a Polymer Micellar Solution**

*Hasan Yardimci (Department of Physics & Astronomy, Johns Hopkins University), Brian Chung, James Harden (Department of Chemical Engineering, Johns Hopkins University), Robert Leheny (Department of Physics & Astronomy, Johns Hopkins University)*

We investigate the local dynamics of aqueous solutions of the triblock copolymer polyethylene oxide – polypropylene oxide – polyethylene oxide (Pluronic F108) by neutron spin echo (NSE). In solution the pluronic self-associates into spherical micelles composed of cores of polypropylene oxide (PPO) with corona of solvated polyethylene oxide (PEO). Depending on concentration and temperature, which affect the conformation of the corona chains and hence influence the interactions between micelles, the micelles order in either a liquid or crystal state. In particular, as the PEO becomes less hydrophilic with increasing temperature, collapse of the corona drives a melting transition on heating. Our small angle neutron scattering measurements on Pluronic F108 solution demonstrate the changes in the structure on heating from room temperature associated with the formation of micelles and their ordering into a crystal followed by melting of the crystal upon further heating.

The micellar dynamics as probed in NSE show a clear systematic dependence on concentration and

temperature as the phase boundaries between polymer solution, micelle crystal and micelle liquid are traversed. However, these local dynamics are surprisingly insensitive to phase behavior and macroscopic rheology. For example, the relaxation time of a 21 % micellar solution changes only by a factor of approximately four across the melting transition near 80 °C. Analysis of the wave-vector dependence across the transition over the range of  $0.02 < Q < 0.12 \text{ \AA}^{-1}$  indicates the specific local micellar motions probed by NSE.

T3-C, Mechanical Behavior and Residual Stress, Chair: Camden Hubbard (ORNL), Room 1123 Blue

### **T3-C1 (15:45) Neutron Diffraction Studies of Micromechanics of Material Deformation (Invited)**

*E. Ustundag (Department of Materials Science, California Institute of Technology, Pasadena, California 91125)*

Neutron powder diffraction offers unique opportunities to study material deformation *in situ* under a variety of conditions. In addition to phase information, one can also collect data on texture and lattice strain as a function of stress, temperature and sample environment. The diffraction data are then complemented with micromechanics modeling for full interpretation and to obtain the *in situ* constitutive behavior of the material. The latter is very difficult to deduce from *ex situ* tests and is crucial for predicting the long term performance in service.

The recent construction of dedicated engineering diffractometers such as SMARTS at the Los Alamos Neutron Science Center has elevated the engineering neutron diffraction field to a new level of sophistication. It is now possible to perform tests at stresses exceeding 3 GPa, temperatures above 1500 °C and in numerous controlled environments. These capabilities allow the *in situ* investigation of most practical materials. This presentation will describe recent work on bulk metallic glass composites, structural ceramics and metal matrix composites. It will also offer insight into exciting future developments.

### **T3-C2 (16:15) Implications of Different Strengthening Mechanisms on Intergranular Strains in Various Aluminum Alloys**

*T. A. Saleh, J. W. Jeon (Department of Materials Science and Engineering, The University of Tennessee, Knoxville, TN 37996, USA.), J. Pang, C. R. Hubbard (Metals and Ceramics Division, Oak Ridge National Laboratory), D. W. Brown (Los Alamos Neutron Science Center, Los Alamos National Laboratory), H. Choo (Department of Materials Science and Engineering, The University*

of Tennessee, Knoxville, TN 37996, USA.; Metals and Ceramics Division, Oak Ridge National Laboratory), P. K. Liaw (Department of Materials Science and Engineering, The University of Tennessee, Knoxville, TN 37996, USA.), M. A. M. Bourke (Los Alamos Neutron Science Center, Los Alamos National Laboratory)

The presence of intergranular strains in deformed polycrystalline samples due to inhomogeneous deformation is widely recognized. However, the effects of different types of strengthening mechanisms in alloys on the generation of intergranular strains have not been studied systematically. In this experiment, lattice strains were measured for different (hkl) reflections in a series of Al alloys under uniaxial tensile load up to 7 % plastic strain. Precipitation-strengthened Al-2024, Al-7075-T6, Al-6061, and solid-solution strengthened Al-5083 alloys were studied. Both Al-2024 and Al-7075-T6 showed similar lattice strain responses. Reflection (200) shows the largest response with residual strains, upon unloading from 150 MPa, of  $-1000 \mu\epsilon$  and  $+850 \mu\epsilon$  parallel and transverse to the tensile axis for Al-2024. The corresponding strain values for Al-7075-T6 were  $-700 \mu\epsilon$  and  $+720 \mu\epsilon$  respectively. The behavior of the solid-solution strengthened Al-5083 differs from the precipitation-strengthened alloys with the largest residual strain found in reflection (311), not the (200), with a compressive strain of  $-1000 \mu\epsilon$  along the tensile axis. Lattice strains for the other reflections in Al-5083 are within  $\pm 300 \mu\epsilon$  for both the longitudinal and transverse directions compared to the other alloys. The differences between the Al-5083 sample and the other alloys will be discussed in context of the effect of strengthening mechanism as well as texture.

This work benefited from the use of the Los Alamos Neutron Science Center (LANSCE) at the Los Alamos National Laboratory. This facility is funded by the US Department of Energy under Contract W-7405-ENG-36. This research was also sponsored by the Assistant Secretary for Energy Efficiency and Renewable Energy, Office of FreedomCAR and Vehicle Technologies, as part of the High Temperature Materials Laboratory User Program, Oak Ridge National Laboratory, managed by UT-Battelle, LLC, for the U.S. Department of Energy under contract number DE-AC05-00OR22725.

Additionally, this work is supported by the NSF International Materials Institutes (IMI) Program under Contract DMR-0231320, with Dr. Carmen Huber as the program director.

### **T3-C3 (16:30) Residual Stresses in Deep Drawn Cups as Standard Specimens for Springback Characterization**

*T. Gnaeupel-Herold (NIST Center for Neutron Research; Department of Materials Science and Engineering, University of Maryland), T. J. Foecke (NIST Metallurgy Division), H. J. Prask (NIST Center for Neutron Research)*

Springback is the elastic shape change of a sheet metal part after forming upon removal of the die. It is created by residual stresses which, in turn, originate from plastic strains that are inhomogeneous both within the sheet plane and through thickness. One focus of current efforts for a more accurate prediction of springback are the measurement and modeling of residual stresses in deep drawn cups which are considered as promising candidates to become standard specimens for springback characterization. From neutron and synchrotron strain measurements the residual stresses were found to vary non-linearly in all three directions. The most pronounced changes were found in the through-thickness direction with similar general features regardless of material or sheet thickness.

### **T3-C4 (16:45) Using inter- and intra-granular strains as a guide to understand fatigue behaviors of polycrystalline engineering materials**

*X.-L. Wang (Spallation Neutron Source, Oak Ridge National Laboratory; Metals and Ceramics Division, Oak Ridge National Laboratory), A. D. Stoica, Y. D. Wang (Spallation Neutron Source, Oak Ridge National Laboratory), D. J. Horton (Spallation Neutron Source, Oak Ridge National Laboratory; Department of Materials Science and Engineering, The University of Tennessee, Knoxville, TN 37996, USA.), H. Tian, P. K. Liaw (Department of Materials Science and Engineering, The University of Tennessee, Knoxville, TN 37996, USA.), E. Maxey, J. W. Richardson (Intense Pulsed Neutron Source, Argonne National Lab)*

Time-of-flight neutron diffraction technique provides reliable data on inter- and intra-granular grain-orientation-dependent strains generated during the plastic deformation of polycrystalline materials [1-2]. A study of 316 stainless steel samples at different stages of fatigue life provides experimental evidence of the effect of cyclic loading on grain-level micromechanics [3]. The experimental data show that residual inter-granular strains develop after each half loading cycle as a result of the elastic anisotropy, which induce a highly heterogeneous loading redistribution at the grain level. In the early stage of fatigue life the grain-orientation-dependent inter-granular strains oscillate between two extremes states corre-



sponding to the ends of a tensile or compressive half loading cycle showing almost identical symmetry but a sign reversal [4]. In the late stage, the inter-granular strains vanish for tests ending in tension, but are surprisingly stable for tests ending in compression. The different behaviors in tension and compression are related to the crack initiation and could be linked to a crack closure mechanism. Separately, the diffraction line broadening analysis allows probing the intra-granular strains and evaluating the stored energy, which is a fingerprint of the material hardening process and can be directly related to the successive stages of deformation. As the intra-granular strains are mainly induced by immobile dislocations, the diffraction response to the lattice distortion is highly anisotropic and can be used to identify the average dislocation character and distribution. In the case of 316 stainless steel, neutron diffraction data have shown that the immobile dislocations generated by cyclic loading are mainly edge, rather than screw, type. This finding was corroborated by recent transmission electron microscopy studies.

This research was supported by Division of Materials Sciences and Engineering, Office of Basic Energy Sciences, U.S. Department of Energy under Contract DE-AC05-00OR22725 with UT-Battelle, LLC.

- [1] X.-L. Wang, Y. D. Wang, and J. W. Richardson, *J. Appl. Cryst.*, **35**, 533-537 (2002)
- [2] Y. D. Wang, X.-L. Wang, A. D. Stoica, J. W. Richardson, and R. Lin Peng, *J. Appl. Cryst.* **36**, 14-22 (2003).
- [3] Y.D. Wang, H. Tian, A. D. Stoica, X.-L. Wang, P. K. Liaw, and J.W. Richardson, *Nature Materials*, **2**, 103-106 (2003).
- [4] X.-L. Wang, et al., *Mat. Sci. Eng.* (in press)

### **T3-C5 (17:00) Small-Angle Neutron Scattering: a Pioneering Tool to Comprehend Processing-Structure-Property Relationships in Thermal Barrier Coatings**

*A. Kulkarni (Dept. of Matls Sci and Eng, Univ. at Stony Brook, Stony Brook, NY 11794-2275)*

Thermal barrier coatings (TBCs) are extensively applied on hot sections in gas turbine engines to provide protection against thermo-mechanical and hot corrosion environments. Critical properties of the TBCs are governed by the nature and architecture of the void microstructures, an enhanced understanding of which will lead to improvements in coating performance during service. These ceramic TBCs are presently deposited using plasma spray and electron beam physical vapor deposition (EB-PVD) processes, each producing distinctive microstructures. A

multidisciplinary approach involving advanced neutron scattering and x-ray imaging techniques has been undertaken, in this joint NIST-SUNY Stony Brook program, to establish the salient processing-structure-property relationships in TBCs. Microstructure information on porosity, void orientation distribution, mean opening dimensions and internal surface areas is obtained and important connections are established with the measured deposit properties, such as thermal conductivity and elastic modulus. In particular, SANS has succeeded in a) establishing rational process-induced porosity-property correlations and b) quantifying the sintering kinetics and phase stability of TBCs during the high-temperature conditions encountered in service. The microstructural parameters determined by SANS studies have been assembled into a finite element model that shows promise for providing a truly predictive capability for determining coating properties and performance. SANS is increasingly recognized as a successful research tool in advanced TBC development.

### **T3-C6 (17:15) Quantitative Texture Analysis of Experimentally Deformed Fine-grained D<sub>2</sub>O ice by Neutron Diffraction**

*S.M. McDaniel (Los Alamos National Laboratory; University of Washington), K.A. Bennett (Office Of Basic Energy Sciences/DOE), W.B. Durham (Lawrence Livermore National Laboratory), E.D. Waddington (University of Washington), V. Luzin (NIST Center for Neutron Research)*

Quantitative textures measurements of fine-grain D<sub>2</sub>O ice experimentally deformed polycrystalline D<sub>2</sub>O ice cylinders were performed by neutron diffraction on BT-8 at the NIST Neutron Research Reactor. The aim was to determine the primary mechanism of ice deformation, grain-size sensitive (GSS) creep or dislocation creep. Textures in three samples (2 samples approximately 1 inch diameter X 1 inch long, 1 sample a 8mm sphere, grain size 10-100 microns) of deuterated hexagonal ice were measured by neutron diffraction using 4 principal diffraction peaks (100), (002), (101) and (102), with  $\lambda = 1.878 \text{ \AA}$ , and a He-3 displax closed-cycle cryostat in conjunction with a four-circle goniometer. Experimental pole figures were collected using the so-called hexagonal grid with angular resolution of less than 5 degrees. The Orientation Distribution Functions for each sample were calculated using POPLA and BEARTEX texture packages.

Comparison of experimental pole figures to recalculated figures show good experimental accuracy. Samples were deformed at T = 222 K, 224 K, and 226



K, and to 30 %, 22.5 % and 30 % strain, respectively. All samples show typical fiber texture common to hexagonal ice, with (001) parallel to the sample axes, and the axes of compression. Texture analyses reveal a similar pole distribution in all samples, with twice as many (001) poles parallel to the compression axis than to the perpendicular axis. Under the deformation conditions, grain-size sensitive (GSS) creep was expected to dominate, resulting in no texture development. However, the neutron data results indicate significant texture and grain growth, suggesting that deformation may be dominated by dislocation creep over GSS and temperature conditions, even at very low temperatures, for fine-grained ice.

**TB: Banquet at College Park Aviation Museum (19:00) (Buses depart Inn starting at 18:30)**

**W1-A, Neutron Sources (Plenary), Chair: Michael Rowe (NIST), Auditorium**

**W1-A1 (08:30) An Overview of North American Neutron Sources (Plenary)**

*R. M. Briber (Neutron Scattering Society of America; Department of Materials Science and Engineering, University of Maryland)*

An overview of recent developments at North American neutron sources will be presented. New instruments, both in the development stage and recently brought on-line will be discussed. In addition, source upgrades and procedures for submitting beam time proposals will be covered.

**W1-A2 (09:00) Neutron Scattering Worldwide: Contrasting Perspectives (Plenary)**

*J. Mesot (Laboratory for Neutron Scattering, Paul Scherrer Institute & ETH Zurich, CH-5232 Villigen, Switzerland)*

After decades of incremental steps, the neutron scattering landscape has started to change and will do so even more rapidly in the coming years.

While third generation sources are being realized in the US (SNS) and Japan (J-PARC), a 20 MW Research Replacement Reactor is under construction in Australia. With the recent decision to put the ESS project on hold, the future of neutron scattering in Europe appears, at first sight, less bright. The severe consequences of this decision for the European neutron scattering community will, however, be attenuated by both the start of the FRM-II reactor in Munich (Germany) and various developments at existing sources. This includes, among others, the realization of a second target at ISIS (United Kingdom), an upgrade of instrumentation at the Institute Laue-Langevin (Grenoble-France), the construction of a second guide hall at Hahn-Meitner-Institute (Berlin-Germany), or an upgrade of the continuous spallation source SINQ (Villigen-Switzerland).

A survey of the above-mentioned projects, together with a summary of the planned developments at running sources worldwide will be presented.

**W1-A3 (09:30) The Spallation Neutron Source: Overview (Plenary)**

*T. E. Mason (Oak Ridge National Laboratory)*

The Spallation Neutron Source will use an accelerator to produce the most intense beams of pulsed neutrons in the world when it is complete in 2006. The

project is being built by a collaboration of six U.S. Department of Energy laboratories. It will serve a diverse community of users with interests in condensed matter physics, chemistry, engineering materials, biology, and beyond. The construction phase of the SNS is over 75 % complete and, together with initiatives such as the Center for Nanophase Materials Science, will offer the neutron scattering community unprecedented new capabilities.

### **WP - Poster Session III (Main Concourse; 10:30)**

#### **WP3: Using Deuterated Actin to Reveal the Conformation of Ca<sup>2+</sup>-Activated Intact Gelsolin Bound to Monomeric and Filamentous Actin by Small Angle Neutron Scattering.**

*Ashish, J.K. Krueger (UNC Charlotte Chemistry Department)*

This work attempts to elucidate the conformational changes of Ca<sup>2+</sup>-activated gelsolin when it binds to actin through the use of small angle neutron scattering contrast variation experiments using specifically deuterated actin. In the presence of Ca<sup>2+</sup>, gelsolin binds to monomeric G-actin in a 1:2 molar ratio, effectively catalyzing the nucleation step in actin polymerization. In an apparently contradictory role Ca<sup>2+</sup>-gelsolin also participates in severing the filamentous F-actin and capping the resultant fragments. Gelsolin is comprised of six structurally similar domains, G1 through G6. In the Ca<sup>2+</sup>-free inactive state, these domains of intact gelsolin are packed in a manner where none of the actin-binding sites are accessible. Activation by Ca<sup>2+</sup> causes large conformational changes altering the relative positions and orientations of the six domains, which exposes several actin-binding surfaces. We have small-angle x-ray scattering data that follows the conformational changes within gelsolin as a result of binding Ca<sup>2+</sup> and although new x-ray crystallographic data has been obtained on the N- and C-terminal halves of gelsolin +/- an actin monomer, there is no direct structural information on intact Ca<sup>2+</sup>-activated gelsolin or intact Ca<sup>2+</sup>-activated gelsolin bound to either two monomers of G-actin or to filamentous F-actin. For our neutron scattering studies on the gelsolin-actin complexes, deuterated actin was obtained from the slime mold *Dictyostelium discoideum*, which was fed deuterated *Escherichia coli*. The actin was purified by ion-exchange and gel filtration chromatography. NMR and mass spectroscopy on non-deuterated and deuterated actin was used to determine the level of actin deuteration. Using small-angle x-ray scattering, we will first

optimize the experimental conditions to obtain structural data of Ca<sup>2+</sup>-activated gelsolin bound to two actin monomers. Small-angle neutron scattering experiments are planned in which we will vary solvent's deuterium composition and use the resultant data to extract out the basic scattering function for the actin-bound Ca<sup>2+</sup>-gelsolin. Comparison of the molecular shapes obtained from the neutron scattering data with those obtained from x-ray studies, will provide insight into the mechanism by which Ca<sup>2+</sup>-gelsolin interacts with, and regulates actin polymerization.

#### **WP4: Phase-sensitive Neutron Reflectometry Studies of a Biomineralization Peptide**

*S. Krueger (NIST Center for Neutron Research), U.A. Perez-Salas (Dept. of Physiology & Biophysics, Univ. of Calif. Irvine, Med. Sci. I, D-346, Irvine, CA 92697-4560; NIST Center for Neutron Research), D.J. McGillivray (Department of Biophysics, Johns Hopkins Univ., 3400 N. Charles St., Baltimore, MD 21218-2685; NIST Center for Neutron Research), C. F. Majkrzak, N.F. Berk (NIST Center for Neutron Research), W.J. Shaw (Battelle Labs, PO Box 999, MS K2-57, Richland, WA 99352)*

A phase-sensitive neutron reflectometry (NR) method was used to study the surface orientation of the biomineralization peptide, LRAP. Naturally occurring biominerals possess an impressive array of strength, order and nanostructure, resulting directly from protein controlled-nucleation and templated mineral growth. The secondary and tertiary structures of biomineralization proteins are often implicated in these processes. However, very few techniques exist which can quantitatively characterize secondary structure of surface immobilized proteins. Phase-sensitive NR methods provide an essentially exact determination of the neutron scattering length density (SLD) profile perpendicular to the plane of the surface, limited only by sample integrity and the quality of the data.

LRAP is a 59-amino acid residue variant of the biomineralization protein, amelogenin, a protein that is found to control tooth enamel development. Peptides for the NR measurements were prepared with 7 amino acids near the C-terminus of the LRAP labeled with deuterium in order to increase their neutron SLD with respect to the non-labeled residues. The peptide was bound to an 11 Å-thick C<sub>11</sub>-ethylene oxide layer with a COO- group presented at the surface. The entire system was supported on planar, gold-coated substrates and measured in a humidity chamber filled with Argon gas saturated with D<sub>2</sub>O at ~92% humidity. The phase-sensitive NR method

used to determine the orientation of the LRAP peptide on this surface will be described and the resultant compositional depth profiles, derived from the SLD profiles, will be presented.

**WP5: SANS Reveals that Protein Kinase A RI $\alpha$  Dimer Undergoes a Large Conformational Change upon Binding C Subunits**

*W. T. Heller (Condensed Matter Sciences Division, Oak Ridge National Laboratory), D. Vigil, S. Brown (Department of Chemistry and Biochemistry and Howard Hughes Medical Institute, University of California, San Diego, La Jolla, CA 92037), D. K. Blumenthal (Departments of Pharmacology and Toxicology and Biochemistry, University of Utah, Salt Lake City, UT 84112), S. S. Taylor (Department of Chemistry and Biochemistry and Howard Hughes Medical Institute, University of California, San Diego, La Jolla, CA 92037), J. Trehella (Bioscience Division Los Alamos National Laboratory)*

Small-angle neutron scattering with contrast variation was used to study the type I $\alpha$  isoform of the cAMP-dependent protein kinase A (PKA) holoenzyme in solution. PKA consists of two catalytic (C) subunits bound to a regulatory (R) subunit dimer. Information on the shapes and dispositions of the C subunits and R subunit homodimer within a holoenzyme reconstituted with deuterated R subunits was derived from the data. The study demonstrates for the first time that a large-scale conformational change occurs within the R subunit homodimer upon binding the C subunits. The results infer that inhibition of C subunit activity is a multi-step process involving local conformational changes both in the cAMP-binding domains and the linker region of the R subunit that impact the global structure of the R subunit dimer. The scattering data also show that, despite extensive sequence homology between the isoforms, the type I $\alpha$  holoenzyme adopts a significantly more compact conformation than the type II $\alpha$  isoform. A model of the type I $\alpha$  holoenzyme was constructed to fit the SANS data using available structures of the component subunits and domains. In this model, the type I $\alpha$  holoenzyme forms a flattened V shape with the R subunit dimerization domain at the point of the V and the R subunit cAMP-binding domains and the C subunits at the ends.

**WP6: Dynamics in Lecithin/Cholesterol Membranes by Deuterium Labeling**

*D. Worcester (Biology Division, University of Missouri, Columbia, MO 65211), J. Torbet (School of Medicine, University of Pennsylvania, Philadelphia, PA 19104), H. Kaiser (Research Reactor, University of Missouri, Columbia, MO 65211), E. Oldfield, C.*

*Lea (Chemical & Life Sciences, 600 S. Matthews Ave., Urbana, IL 61801)*

Dynamic properties of lecithin/cholesterol membranes were measured by deuterium labeling and neutron diffraction from multi-layers. Deuterium was introduced at specific molecular sites to provide a localized label for difference analysis. One hydrocarbon chain of dimyristoyl-phosphatidylcholine was labeled at seven different methylene groups and at the terminal methyl group. The methyl groups of the lecithin choline were labeled and cholesterol was labeled with five deuterium near the hydroxyl group. B-values of the Debye-Waller factors were obtained by fitting difference structure factors in reciprocal space. Diffraction patterns with at least eight orders of Bragg diffraction were obtained for hydration ranging from 58% to nearly 100% relative humidity. Positions of the label were readily determined with uncertainty less than 1% of the repeat unit. The B-values were more difficult to determine and uncertainties were about 10%. The results show clear differences in the B-values of the different molecular groups. The cholesterol label had the smallest B-value, as expected for the rigid steroid ring. The hydrocarbon chain of dimyristoyl-phosphatidylcholine is well-ordered, with similar B-values along the chain. The results indicate that molecular packing is an important aspect of the preferential interaction of cholesterol with saturated lipids.

**WP7: A SANS Contrast Variation Study to Elucidate Structural Requirements for the Initial Recognition Step between Myosin Light Chain Kinase and Its Activatory Protein, Calmodulin**

*J.K. Krueger, N. Modi (University North Carolina Charlotte), W.T. Heller (Oak Ridge National Laboratory), D.J. Black, A. Persechini (University of Missouri Kansas City), J.T. Stull (University of Texas Southwestern Medical Center at Dallas), C.-S. Tung, J. Trehella (Los Alamos National Laboratory)*

A wide variety of Ca<sup>2+</sup>-dependent processes in the cell are regulated by the ubiquitous protein calmodulin via interactions with and subsequent activation of a diverse array of target proteins including a number of kinases, (proteins responsible for phosphorylation of other proteins). The Ca<sup>2+</sup> - calmodulin (CaM)-dependent activation of myosin light chain kinase (MLCK) has served as a model for CaM-kinase interactions. We have collected small-angle neutron scattering data at several contrasts (0%, 15%, 30%, 70% and 80% D<sub>2</sub>O) on MLCK complexed with 60%-deuterated mutant CaM (delNCam). This mutant CaM missing an N-terminal leader sequence [residues #1-8 (A1DQLTEEQ8)] binds MLCK with high affinity but fails to activate

catalysis. The small-angle scattering data reveal that deINCaM occupies a position near the catalytic cleft in its complex with the kinase, whereas the native protein translocates to a position near the C-terminal end of the catalytic core. Interestingly, the SANS data show that the CaM is in the collapsed state, suggesting that the deINCaM has bound to the autoinhibitory sequence of MLCK, rather than simply docking onto the surface of the MLCK in the extended state. A molecular model built from our SANS data will be used to provide the molecular boundaries for the individual protein components within the complex for which high-resolution crystal structures are known. The result will be a model of what is the initial recognition step in the CaM/MLCK interaction providing a detailed atomic description of the binding events between CaM and MLCK prior to the kinase activation step.

#### **WP8: Compaction of a Bacterial Group I Ribozyme by cations studied by SANS and SAXS**

*U.A. Perez-Salas (National Institute of Standards and Technology; University of California at Irvine), G.H. Caliskan (National Institute of Standards and Technology; Johns Hopkins University), P. Rangan (Johns Hopkins University; New York University), S. Krueger (National Institute of Standards and Technology), R.M. Briber, D. Thirumalai (University of Maryland, College Park), S.A. Woodson (Johns Hopkins University)*

Counterions are critical to the self-assembly of RNA tertiary structure because they neutralize the large electrostatic forces which oppose the folding process. Changes in the size and shape of the *Azoarcus* group I ribozyme as a function of  $Mg^{2+}$  and  $Na^+$  concentration were followed by small angle neutron scattering (SANS) experiments performed at the NIST Center for Neutron research. In low salt buffer, the RNA was expanded, with an average radius of gyration (Rg) of  $53 \pm 1 \text{ \AA}$ . A highly cooperative transition to a compact form (Rg)  $31.5 \pm 0.5 \text{ \AA}$  was observed between 1.6 and 1.7 mM  $MgCl_2$ . The collapse transition, which is unusually sharp in  $Mg^{2+}$ , has the characteristics of a first-order phase transition. Partial digestion with ribonuclease T1 under identical conditions showed that this transition correlated with the assembly of double helices in the ribozyme core. Fivefold higher  $Mg^{2+}$  concentrations were required for self-splicing, indicating that compaction occurs before native tertiary interactions are fully stabilized. No further decrease in Rg was observed between 1.7 and 20 mM  $MgCl_2$ , indicating that the intermediates have the same dimensions as the native ribozyme, within the uncertainty of the data ( $\pm 1 \text{ \AA}$ ). A more gradual transition to a final Rg of approximately

$33.5 \text{ \AA}$  was observed between 0.45 and 2 M NaCl. This confirms the expectation that monovalent ions not only are less efficient in charge neutralization but also contract the RNA less efficiently than multivalent ions.

Complementary small angle x-ray scattering experiments were recently performed at the Advanced Photon Source at Argonne National Laboratory on the Basic Energy Sciences Synchrotron Radiation Center (BESSRC) beamline and on the Biophysics Collaborative Access Team (Bio-CAT). These preliminary experiments, which followed the size of the *Azoarcus* group I ribozyme as a function of the concentration of  $Na^+$ ,  $Mg^{2+}$ ,  $Ca^{2+}$  and  $Co^{3+}$  cations, show that the efficiency of charge neutralization increases with the increasing valence of the condensing cation. As observed in the SANS experiment, the collapse the ribozyme into a compact state does not coincide with self splicing activity yet the dimensions of the ribozyme in the compact state show no further decrease in Rg even after native conditions are reached. The compact intermediates in  $Na^+$ ,  $Ca^{2+}$  and  $Co^{3+}$ , at their corresponding transition concentrations, show similar dimensions and only a couple of  $\text{\AA}$  larger than the compact state in  $Mg^{2+}$ . It is also observed that the transition to a collapsed state in  $Mg^{2+}$  and  $Ca^{2+}$  occurs at different cation concentrations, indicative of a cation size effect. In contrast with  $Na^+$ , a ten-fold increase in  $Ca^{2+}$  beyond the collapse transition concentration shows the ribozyme compacting further to a dimension equivalent to the compact state in  $Mg^{2+}$ . Although it is predicted that the Rg of the ribozyme is inversely proportional to the square of the cation valence, no further compactation of the ribozyme in  $Co^{3+}$  could be observed because it precipitated out of solution before this could occur.

#### **WP9: The Center for Structural Molecular Biology at Oak Ridge National Laboratory**

*V.S. Urban (Chemical Sciences Division, Oak Ridge National Laboratory), W.T. Heller, G.W. Lynn (Chemical Sciences Division, Oak Ridge National Laboratory; Condensed Matter Sciences Division, Oak Ridge National Laboratory), P.D. Butler, G.D. Wignall (Condensed Matter Sciences Division, Oak Ridge National Laboratory), M.V. Buchanan, D.A.A. Myles (Chemical Sciences Division, Oak Ridge National Laboratory)*

A Center for Structural Molecular Biology (CSMB), which is funded by the Department of Energy's (DOE) Office of Biological and Environmental Research (OBER), has been established at Oak Ridge National Laboratory (ORNL). The CSMB will integrate



the existing strengths in the neutron sciences at ORNL with new capabilities being developed in computational biology and stable isotope labeling of proteins and make them available to a broad user community. The cornerstone of the CSMB is a small-angle neutron scattering instrument (Bio-SANS) that is currently under construction at the High Flux Isotope Reactor (HFIR) at ORNL. Bio-SANS will have a neutron flux and performance that is unprecedented in the US and that will provide the user community with world-leading capabilities in the field. The development of new computational methods for the analysis of biological scattering data and of facilities for the selective H/D labeling of complex macromolecular assemblies will provide the tools necessary to fully exploit these advantages in the application of SANS to complex problems in biology. Bio-SANS will be a critical resource for the US structural biology community and the CSMB will provide a wide range of scientific and educational opportunities for scientists and students working in the field.

Research sponsored by the Office of Biological and Environmental Research, U.S. Department of Energy, under contract No. DE-AC05-00OR22725 with Oak Ridge National Laboratory, managed and operated by UT-Battelle, LLC.

#### **WP10: Oxidation of propane in zeolite Y studied by *in situ* inelastic neutron scattering**

*M. Hartl, L.L. Daemen (Los Alamos Neutron Science Center, Los Alamos National Laboratory), J. Eckert (Los Alamos Neutron Science Center, Los Alamos National Laboratory; Materials Research Laboratory, University of California, Santa Barbara), B. Mojet, J. Xu (Department of Chemistry, University of Twente)*

Short alkanes, such as propane, are present in natural gas and in volatile petroleum fractions. These molecules can be converted by oxidation into an important feedstock for the production of synthetic materials (plastics) and fine chemicals. Zeolites containing alkaline or alkaline earth cations have been shown to be promising materials (F. Blatter, H. Sun, S. Vasenkov, H. Frei, Catal. Today, 41 (1998) 297) for the oxidation of these small hydrocarbons by low-temperature catalysis in the presence of small oxidant molecules such as O<sub>2</sub>. At the present time, however, the interaction between these zeolites and the oxidized reactants has not been studied extensively. Frei and collaborators discussed a possible alkane-oxygen charge transfer state stabilized by the electrostatic field of the cations in the zeolite, but this has not been established.

The electrostatic field inside the pore structure of zeolite Y and the available space for the reactants on the inner surface of the catalyst can be varied by using different cations (Na<sup>+</sup> and Ca<sup>2+</sup>) in zeolite Y with similar ionic radii but different positive charge. Vibrational spectroscopy by incoherent inelastic neutron scattering (IINS), as well as variety of other *in situ* techniques, have resulted in an improved understanding of the activation of the reactant molecules and the desorption of the oxidation products. Information on the adsorption sites, surface bonding, and local chemical environment can be inferred from the IINS spectra of the adsorbed molecules. Vibrational spectra of the zeolites NaY, CaY and NaCaY were recorded after their calcination in vacuum, after the adsorption of propane and oxygen inside the zeolite, and after the oxidation of propane by oxygen. Our results combined with IR spectroscopic studies provide useful insights into the sorbate-zeolite host interaction as well as the mechanism of the oxidation reaction, which should lead to the design and development of new catalysts for the selective oxidation of hydrocarbons.

#### **WP11: Neutron and Thermodynamic investigations of H<sub>2</sub> on MgO Surfaces**

*T. Arnold (Oak Ridge National Laboratory), L. Frazier (University of Tennessee), A. Ramirez-Cuesta (ISIS, Rutherford Appleton Laboratory), R. Hinde (University of Tennessee), J. Z. Larese (Oak Ridge National Laboratory; University of Tennessee)*

We will discuss recent thermodynamic and neutron scattering measurements that probe the growth of molecular hydrogen films on MgO (100) surfaces. Our thermodynamic investigations indicate that at temperatures in the neighborhood of 10K, 6 or 7 layering transitions are easily observable. Using inelastic neutron techniques we have identified a feature in the spectrum that we believe can be associated with the ortho-para rotational transition in the neighborhood of 11 meV (88 cm<sup>-1</sup>). This feature is significantly lower than the equivalent transition in bulk H<sub>2</sub> which appears at 14.7 meV. The position and shape of this feature has been recorded as a function of temperature. Distinct shifts in the peak position and symmetry are recorded between one and three layers. In the vicinity of three layers a sharp feature near the bulk transition appears and continues to grow in intensity with additional increases in the hydrogen film thickness. Comparison of these results with simple calculations and structural data will be made. Relationship of these data to others recorded when H<sub>2</sub> is adsorbed other metal oxide materials will be discussed.

**WP12: The pillared perovskites  $\text{La}_5\text{Os}_3\text{MO}_{16}$  ( $\text{M} = \text{Mn}, \text{Co}$ ) Synthesis, crystal structure and magnetism**

*Lisheng Chi (National Research Council, Chalk River, Ontario, Canada; Department of Chemistry & Brockhouse Institute for Materials Research, McMaster University, Hamilton, Ontario L8S 4M1, Canada), Ian Swainson (National Research Council, Chalk River, Ontario, Canada), John E. Greedan (Department of Chemistry & Brockhouse Institute for Materials Research, McMaster University, Hamilton, Ontario L8S 4M1, Canada)*

Two new Os-containing compounds  $\text{La}_5\text{Os}_3\text{MnO}_{16}$ ,  $\text{La}_5\text{Os}_3\text{CoO}_{16}$  with pillared perovskite type structures have been synthesized by solid state reactions. Rietveld profile refinement revealed that both compounds crystallize in space group C-1 with cell parameters  $a = 7.9648(9) \text{ \AA}$ ,  $7.9360(7) \text{ \AA}$ ;  $b = 8.062(1) \text{ \AA}$ ,  $8.0481(7) \text{ \AA}$ ;  $c = 10.156(2) \text{ \AA}$ ,  $10.0788(8) \text{ \AA}$ ;  $\alpha = 90.25(1)^\circ$ ,  $90.300(4)^\circ$ ;  $\beta = 95.5(1)^\circ$ ,  $95.340(4)^\circ$ ;  $\gamma = 89.95(2)^\circ$ ,  $89.914(6)^\circ$  for  $\text{La}_5\text{Os}_3\text{MnO}_{16}$  and  $\text{La}_5\text{Os}_3\text{CoO}_{16}$ , respectively. The structure consists of corner-sharing, site-ordered octahedral layers of composition  $\text{Os}^{5+}\text{M}^{2+}\text{O}_6$ , pillared by diamagnetic  $\text{Os}_2\text{O}_{10}$  triply-bonded dimers and separated by  $> 10 \text{ \AA}$ . SQUID measurements in the paramagnetic regime show nearly spin only effective moments for  $\text{Os}^{5+}$  ( $S = 3/2$ ) and the  $\text{M}^{2+}$  ions.  $\text{La}_5\text{Os}_3\text{MnO}_{16}$  has two magnetic transitions at 178 K and 78 K, corresponding to long range ordering and spin reorientation, respectively. Isothermal magnetization data are characteristic of meta-magnetic behavior.  $\text{La}_5\text{Os}_3\text{CoO}_{16}$  has a single magnetic transition at 36 K. The magnetic structure of  $\text{La}_5\text{Os}_3\text{MnO}_{16}$  consists of ferrimagnetically coupled  $\text{Os}^{5+}$  and  $\text{Mn}^{2+}$  moments within the layers which then couple antiferromagnetically between layers. The ordered moments are  $3.7(2) \mu_B$  for Mn and  $1.9(2) \mu_B$  for Os and are parallel to the c-axis.

**WP13: Evaluating Organoclays for Nanocomposites by Small-Angle Scattering and Microscopy**

*D.L. Ho (University of Maryland, College Park; NIST Center for Neutron Research), C.J. Glinka (National Institute of Standards and Technology), R.M. Briber (University of Maryland, College Park)*

Understanding the structure of organophilic clays and the interaction between clay platelets dispersed in organic solvents is important to characterizing nanocomposites formed by organophilic clays and polymers. In order to understand and optimize potential processing conditions, organically modified montmorillonite clays were dispersed in a number of organic solvents covering a range of solubility parameters and characterized using small-angle

neutron scattering and wide-angle x-ray scattering techniques. The organic modifier was dimethyl dihydrogenated tallow ammonium. Both as-received (unextracted) and purified (extracted) organically modified clays were studied. The scattering profiles and dispersion behavior in organic solvents of the dry powder of unextracted and of extracted dimethyl dihydrogenated tallow montmorillonite are significantly different confirming that the organic modifiers are present in excess in the unextracted material as reported by the industrial provider. The scattering data show that both unextracted and extracted organically modified clay platelets were fully exfoliated in chloroform while the platelets retain their lamellar structure and swell to a similar extent in benzene, toluene and p-xylene, but the extracted material has a stronger tendency to gel. The scattering profiles indicate that the swollen tactoids of extracted material are thinner, and therefore more numerous, which may account for the bulk suspension behavior. The extracted clay dispersion exhibited a concentration dependence to the scattering for all the organic solvents studied except chloroform while the unextracted clay dispersion did not. Neither the extracted nor the unextracted dispersions exhibited any temperature dependence to the scattering. The thickness of unmodified montmorillonite platelets was found to be  $9.9 \text{ \AA}$  while that of organically modified montmorillonite platelets was determined to be  $24.3 \text{ \AA}$  using wide angle x-ray scattering. The lateral size of organically modified montmorillonite platelets was observed to be in the range of 0.4 micron to 1.0 micron using atomic force microscopy.

**WP14: Small angle neutron scattering from single-wall carbon nanotube suspensions: evidence for isolated rigid rods and rod networks**

*W. Zhou (MSE Dept., U. Penn.), M. F. Islam (Dept. of Physics & Astronomy, U. Penn.), H. Wang (MSE Dept., Michigan Tech), D. L. Ho (NIST Center for Neutron Research), A. G. Yodh (Dept. of Physics & Astronomy, U. Penn.), K. I. Winey, J. E. Fischer (MSE Dept., U. Penn.)*

We report small angle neutron scattering (SANS) from dilute suspensions of purified individual single wall carbon nanotubes (SWNTs) in  $\text{D}_2\text{O}$  with added sodium dodecylbenzene sulfonate (NaDDBS) ionic surfactant. The scattered intensity scales as  $Q^{-1}$  for scattered wave vector,  $Q$ , in the range  $0.005 < Q < 0.02 \text{ \AA}^{-1}$ . The  $Q^{-1}$  behavior is characteristic of isolated rigid rods. A crossover of the scattered intensity power law dependence from  $Q^{-1}$  to  $Q^{-2}$  is observed at  $\sim 0.004 \text{ \AA}^{-1}$ , suggesting the SWNTs form a loose network at 0.1 wt % with a mesh size of

~ 160 nm. SANS profiles from several other dispersions of SWNTs do not exhibit isolated rigid rod behavior; evidently the SWNTs in these systems are not isolated and form aggregates.

### **WP15: Study of Oxygen Dissolution in a2-Ti<sub>3</sub>Al: Combining the Analysis of Pair Distribution Functions from Total Scattering with First Principles Calculations**

*I. Peral (NIST Center for Neutron Research; Department of Materials Science and Engineering, University of Maryland), E. Copland (Case Western Reserve University and Materials Division, NASA Glenn Research Center, Cleveland, OH 44135 USA), X. Qiu (Department of Physics and Astronomy, Michigan State University, E. Lansing, MI, 48824), S. Short (Materials Science Division, Argonne National Laboratory), C. Y. Jones (NIST Center for Neutron Research)*

The most promising of the g-TiAl-based intermetallic alloys for application as high-temperature structural components are g-TiAl + a2-Ti<sub>3</sub>Al mixtures based on the composition Ti-48 atom % Al. Oxygen interstitials stabilize a2-Ti<sub>3</sub>Al relative to g-TiAl, thus in a2-Ti<sub>3</sub>Al + g-TiAl mixtures a2-Ti<sub>3</sub>Al behaves as an oxygen scavenger. However, limited data are available on the dissolution of O in a2-Ti<sub>3</sub>Al.

Recently, high-resolution constant wavelength neutron powder diffraction data were used to refine the crystal structures of several a2-Ti<sub>3</sub>Al alloys with varying O content [1]. This study confirmed that O resides in octahedral sites surrounded by six Ti atoms, as proposed by Menand et al. [2]. From this work, it was possible to obtain the average structure, that is, the atomic composition in the unit cell and the atomic positions of the atoms. However, there is no complete information about the local environment of the atoms. A more thorough investigation of the effect of oxygen interstitials on the structure and stability of a2-Ti<sub>3</sub>Al is required to understand the dramatic difference in O affinity and the behavior of the duplex alloys.

We have measured the total scattering from two specimens of a2-Ti<sub>3</sub>Al alloys with O weight percentages of 0.025 % and 7.7 %, to determine from the Pair Distribution Function (PDF) the various correlation lengths for O, Ti, and Al. The comparison of the experimental PDF to the calculated PDFs of a number of local structure models shows that the average structure can describe most of the features of the experimental PDFs and that the PDF is sensitive to the different possible local environments of the atoms. The sampling of the different local structure

models is a work still in progress as well as the model refinement to the experimental PDFs. We use Density Functional Theory to probe the energy of models that describe different local structures.

From our preliminary modeling and model refinement, it is observed that the agreement experiment-model is better for local structural models where the atoms that present positional disorder in the system (the aluminum atoms that can be distributed over the titanium sites and the oxygen atoms) are distributed randomly, rather than for models where the aluminum atoms cluster around the oxygen atoms.

- [1] Jones C. Y., Luecke W. E. and Copland E. (submitted to Intermetallics)
- [2] Menand A., Huguet A., Nerac-Partaix A., Acta Mater. 1996, 44(12), 4729-4737.

### **WP16: Structure of a Liquid Crystalline Polymer In an Amorphous Polymer Matrix**

*R. Metha, M. D. Dadmun (Department of Chemistry, University of Tennessee, Knoxville, TN 37923)*

Molecular composites, composed of uniformly dispersed rigid-rod liquid crystalline polymer (LCP) molecules in a flexible amorphous polymer matrix, have remained hitherto elusive due to a scarcity of miscible systems containing a LCP and an amorphous polymer. The production of such a blend with a large miscibility window, which is experimentally accessible, has become possible by modifying the architecture of the flexible polymer, so as to induce favorable enthalpic interactions between the flexible polymer and LCP. Specifically, liquid crystalline polyurethanes (LCPU) are found to be miscible with a copolymer of styrene and vinyl phenol. Here miscibility is promoted by realizing intermolecular hydrogen bonding between the carbonyl groups of the urethane linkages with the hydroxyl groups present in the styrenic matrix.

Availability of a truly miscible molecular composite presents a unique opportunity of studying the confirmation of polymer chains containing rigid-rods that are uniformly dispersed in a flexible coil matrix. A system consisting of the LCPU and the deuterated styrenic copolymer containing 10 % vinyl phenol is examined by Small Angle Neutron Scattering at the National Center for Neutron Research at the National Institute of Standard and Technology, and the Institute of Solid State Research (IFF) at Jülich. The radius of gyration of the LCPU is determined by fitting the low angle portion of the scattering curve to the traditional Guinier and Zimm methods. The conformation of LCPU molecules is also determined by analysis of the scattering curve using a wormlike



model and Kratky Porod analysis.

Support towards this work by NSF DMR-0241214, The Joint Institute of Neutron Sciences at the University of Tennessee, NCNR (NIST), and IFF (FZ-Jülich) is gratefully acknowledged.

#### **WP17: Influence of Plastic Deformation on the Stress-Induced Transformation in Superelastic NiTi**

*C.R. Rathod (AMPAC/MMAE, University of Central Florida), B. Clausen, M.A.M. Bourke (Los Alamos National Laboratory), R. Vaidyanathan (AMPAC/MMAE, University of Central Florida)*

The superelastic effect in NiTi occurs due to a reversible stress-induced phase transformation from a cubic B2 austenite phase to a monoclinic B19' martensite phase. There is usually a hysteresis associated with the forward and reverse transformations which translates to a hysteresis in the stress-strain curve during loading and unloading. This hysteresis is reduced in cold-worked NiTi and the macroscopic stress-strain response is more linear, a phenomenon called linear superelasticity. Here we report on *in situ* neutron diffraction measurements during loading and unloading in plastically deformed (up to 11 %) NiTi. The experiments relate the macroscopic stress-strain behavior (from an extensometer) with the texture, phase volume fraction and strain evolution (from neutron diffraction spectra) in linear superelastic NiTi. The roles of starting texture and cyclic loading following plastic deformation are also investigated. This work is supported by NSF (CAREER DMR-0239512).

#### **WP18: Structure of potentially superconducting silver fluorites**

*S. Mclain (University of Tennessee; Argonne National Laboratory), J. Turner (University of Tennessee), T. Proffen (Los Alamos National Laboratory), M. Dolgos (University of Tennessee)*

High temperature superconducting cuprates have been investigated extensively in recent years. Spin-1/2 ions that possess similar or identical structural chemistry to the Cu(II) ions in the high T<sub>c</sub> cuprates are rare. One such ion is Ag(II), which, being unstable in an oxide lattice context is stable in various fluoride phases, that are structurally analogous to the 214 Ag<sub>2</sub>CuO<sub>4</sub>. Here we present the results of neutron scattering studies on the fluoride-based 214 analog Cs<sub>2</sub>AgF<sub>4</sub>, which displays the strongly correlated spin interactions expected of a S = 1/2 ion in a structure similar to that of K<sub>2</sub>CuF<sub>4</sub>.

Understanding of these materials obviously requires a detailed understanding of the atomic structure. It has become more and more apparent that structure

analysis based on Bragg intensities alone gives an incomplete picture, completely ignoring disorder or the local structure of these materials. One approach to extract local structural information from the total scattering pattern, i.e. Bragg and diffuse scattering, is the Pair Distribution Function (PDF) method. Much progress has been made understanding the local structure of cuprates using the PDF [1].

Variable temperature neutron diffraction studies on NPDF at LANSCE over a Q range of 50 Å<sup>-1</sup> have allowed both Bragg analysis of the long range order and pair distribution function (PDF) analysis of the local structure of this material. The structure and the temperature behavior of the structure will be presented and parallels drawn with similar PDF studies on structurally related cuprate and manganite materials.

[1] E. S. Bozin, S. J. L. Billinge, H. Takagi and G. H. Kwei, Neutron diffraction evidence of microscopic charge inhomogeneities in the CuO<sub>2</sub> plane of superconducting La<sub>2-x</sub>Sr<sub>x</sub>Cu<sub>4</sub> (0 ≤ x ≤ 0.30), Phys. Rev. Lett. 84, 5856 (2000).

#### **WP19: Neutron investigations of selected heteropolyacids**

*C. M. Brown (Department of Materials Science and Engineering, University of Maryland; NIST Center for Neutron Research), R. Burns (Chemistry, School of Environmental and Life Sciences, The University of Newcastle, Australia), E. Gilbert, J. Schulz (Bragg Institute, Australian Nuclear Science and Technology Organisation, Australia)*

Heteropolyacids and their hydrates have been cited as the fastest proton conductors known, possible electrolytes for solid acid batteries, composites for polymer membrane fuel cells and industrial catalysts. Examples of the latter include the oxidation of methacrolein, and the oxidative dehydrogenation of isobutyric acid, both of which yield methacrylic acid. The product, when reacted with methanol, gives methyl methacrylate, which in turn is polymerized to form poly(methyl methacrylate) or PMMA. However, despite their commercial use, their structure and catalytic function at a molecular level remains unclear. Consequently, we have initiated investigations into the structure and vibrational spectroscopy from a series of catalysts of the type Cs<sub>3-n</sub>H<sub>n</sub>[PMo<sub>12</sub>O<sub>40</sub>] where n is varied from 0 to 3, with a goal to resolving these fundamental issues.

#### **WP20: Dynamics of water in zeolites — a QENS study of the effects of charge, confinement, and hydration level**

*W. A. Kamitakahara (NIST Center for Neutron*



Research), N. Wada (Toyo University, Saitama, 350-8585 Japan)

We have made a series of quasielastic neutron scattering (QENS) measurements on water molecules confined to the pores of zeolite materials, comparing the effects of several factors that influence their motion. The most important factor determining the speed of translational diffusion arises from the charges on the aluminosilicate framework and counterbalancing cations. Using the high flux back-scattering spectrometer (HFBS) at NIST, we observe that the QENS broadening is roughly an order of magnitude larger at 300 K in a high-silica, nearly neutral, zeolite (Si/Al ratio  $r = 180$ ) than in a highly charged zeolite (NaX,  $r = 1.25$ ), while spectra for zeolites with  $r = 14.5$  and  $r = 2.75$  show intermediate broadening. All of these materials are Na-zeolites with the same basic structure, i.e., faujasite, so that the charge effect can be isolated. The degree of hydration also influences the motions significantly. As the water content is varied from a mass fraction of 0.1 to 0.3 in several of the zeolites, we observe a roughly proportional amount of QENS broadening. Reducing the hydration level not only slows the water motions, it also increases the temperature width over which the motions freeze out. The effects of substituting a  $2^+$  cation (Ca) for  $Na^+$  are also under investigation. In fixed-window scans ( $E = 0$ ,  $T$  varied), water in the nearly neutral zeolite shows structure and large hysteresis in the freezing transition, unlike the transitions in the more highly charged zeolites, which show smaller hysteresis and smooth transitions. This work employed facilities supported in part by the National Science Foundation under agreement No. DMR-0086210.

#### **WP21: Protein Solvent Coupling in Native and Glass Environments**

J. E. Curtis, D. A. Neumann (NIST Center for Neutron Research), D. J. Tobias (Chemistry Department, University of California, Irvine 92697)

Recent experimental and computational studies have conclusively shown that water is essential in the activation of dynamical motions required for biologically relevant protein function. We have found that the microscopic origins of this affect in native environments are directly related to the temperature dependence of the diffusion of water from the protein surface. We are extending our studies of protein dynamics through the use of molecular dynamics simulations of the protein RNase A in both native and non-native glassy environments. We have found that binary glass mixtures can reduce protein dynamics at high temperature. Detailed analysis of the microscopic origins of this effect will be presented.

#### **WP22: Structure of polymer-nanocomposites – A SANS and USAXS study**

R. A. Narayanan, P. Thiyagarajan (Intense Pulsed Neutron Source, Argonne National Lab), B.J. Ash, S.S. Sternstein, A.J. Zhu, L. Schadler (Materials Science and Engineering Department, Rensselaer Polytechnic Institute, Troy, NY- 12180)

Alumina/ polymethylmethacrylate (PMMA) nanocomposites synthesized by an *in situ* free-radical polymerization in the presence of 38 nm alumina nanoparticles exhibit unusual brittle-to-ductile transition with a large increase in the strain-to-failure. In order to understand the molecular mechanisms responsible for the reinforcement of polymeric materials by nano-sized inorganic fillers, we have undertaken small-angle neutron (SANS) and ultra small angle x-ray scattering (USAXS) measurements on alumina-PMMA and silica-PVAc nanocomposites, in combination with studies on their mechanical behavior. SANS studies of alumina-PMMA composites show a large degree of aggregation and agglomeration of alumina that depends on the size of the nanoparticles. Moreover, composites containing 5 and 10 wt. % deuterated PMMA indicate that addition of nanoparticles does not seem to affect the  $R_g$  of the polymer (PMMA). These results have to be investigated further by contrast matching the scattering from the alumina using appropriate mixture of deuterated and normal PMMA. USAXS data on silica-PVAc nanocomposites a large degree of aggregation of silica is observed. The particles show an average aggregation of about 250 Å which is significantly reduced in the case of surface treated fillers. Evidence suggests that the surface fractal dimension, which is a measure of surface roughness, is directly related to reinforcement characteristics of the composite.

This work benefited from a grant from Office of Naval Research to LS at RPI, and IPNS and APS facilities funded by DOE under contract no. W-31-109-ENG-38 to the University of Chicago. UNICAT facility is supported by the DOE, the State of Illinois-IBHE-HECA, NSF, NIST (U.S. DOC) and UOP LLC.

#### **WP23: The crystalline enol of 1,3-cyclohexanedione and its complex with benzene: vibrational spectra, simulation of structure and dynamics and evidence for cooperative hydrogen bonding**

B. S. Hudson, D. G. Allis, Y. Lan (Department of Chemistry, Syracuse University, Syracuse, NY), D. A. Braden (Schrödinger Inc., Portland, OR), C. T. Middleton, T. Jenkins (Department of Chemistry, Syracuse University, Syracuse, NY), R. Withnall (School of Chemical and Life Sciences, University of

Greenwich, Chatham Maritime Campus, Chatham, Kent ME4 4TB, UK.), S. Baronov (Syracuse University/NSF REU Participant, Summer 2000. Current address: Department of Chemistry, Moscow State University, Moscow, Russia.), C. M. Brown (Department of Materials Science and Engineering, University of Maryland, College Park, MD 20742-2115 and NIST Center for Neutron Research, National Institute of Standards and Technology, Gaithersburg, MD 20899-8562)

The inelastic incoherent neutron scattering spectra of 1,3-cyclohexanedione (CHD) in its crystalline enol form and its cyclamer complexes with benzene and benzene-d<sub>6</sub> are compared with each other, with IR and Raman spectra and with the results of calculations using density functional theory (DFT). We have also determined the INS spectra of a variety of methyl and deuterium substituted derivatives of CHD. Deuterium isotopic substitution can be used to confirm spectra assignments. The crystal packing of the CHD enol is a linear hydrogen-bonded chain with conjugated donor and acceptor groups analogous to that found in peptide hydrogen bonding. Methyl substitution can have very large effects on the crystal packing of CHD. The benzene complex is a closed hexameric hydrogen-bonded cycle. A DFT treatment is applied to the full hexamer of the benzene:CHD complex. The CHD chain is treated as a series of finite linear clusters by DFT, while the infinite one-dimensional chain and the three-dimensional crystal are treated by periodic DFT. Comparison is made with both the observed crystal structures and the vibrational spectra. The very good to excellent agreement of the computed vibrational spectra with experiment demonstrates that the models and computational treatments used are reliable. The theoretical treatment of linear chain clusters exhibits a continuous change with increasing chain length, converging to values near the observed crystal structure. Emphasis is placed on the cooperative nature of hydrogen bonding in CHD as revealed by these systematic trends. The calculations show that the energy of a linear chain of hydrogen bonded CHD molecules becomes increasingly stable and increasingly more dipolar as that chain length increases. This is consistent with the hypothesis that the cooperative hydrogen bonding of CHD is due to polarization of the structure. The significance of this effect with regard to the analogous case of peptide hydrogen bonding and its relevance to the stability of the globular form of proteins will be discussed. The ability of DFT methods to treat hydrogen bonding in solids appears to be roughly as accurate as the crystal structure determinations.

#### **WP24: NCNR High Pressure Sample Environment**

J.B. Leao, D.C. Dender (NIST Center for Neutron Research)

The NIST Center for Neutron Research currently provides a variety of pressure apparatus ranging from 20 MPa to as high as 400 MPa that are specially designed for neutron spectroscopy. Most of the pressure equipment can be mounted in a variety of instruments throughout NCNR's facility allowing for experimental flexibility and maximizing beam time use. The available NIST Center for Neutron Research pressure equipment, as well as a few experimental results that explore its diversified use in neutron spectroscopy, is presented here.

#### **WP25: Application of high frequency ultrasound for the simultaneous upgrade intensity and resolution of the double crystal and Bonse - Hart diffractometers**

E. Iolin, L. Rusevich (Institute of Physical Energetic, 21 Aizkraukles, LV-1006 Riga, Latvia), M. Strobl, W. Treimer (Hahn-Meitner-Institut Berlin; University of Applied Sciences (TFH) Berlin), P. Mikula (Nuclear Physics Institute, 25068 Rez near Prague, Czech Republic)

It is known that neutron Double Crystal (DCD) and Bonse-Hart (BHD) diffractometers are used for the ultra small angle scattering research. However, this technique is flux limited. It is also known that h.f. ultrasound leads to the increasing of the diffracted beam intensity at the perfect s.c. Unfortunately this increasing is accompanied by a loss of the momentum resolution. Some time ago it was argued (E.Iolin, Zh.Tekhn.Fiz.Pis'ma 15, 52, 1989) that it should be possible to improve simultaneously resolution and intensity for the case of DCD. It could be achieved by the excitation of the h.f ultrasound with the same frequency in monochromator AND analyser. Such a perspective is especially interesting for the case of BHD. Ultrasonic satellites exist as additional zones of the almost total reflections for the case of symmetrical Bragg scattering. Reflectivity between phonon satellites is suppressed due to the multiply reflections inside BHD. Each satellite is narrow, but they are numerous. The whole effective diffracted neutron beam phase space volume is increased that's led to the upgrade of the diffractometer parameters. Here we report the first results of corresponding experiments. We excited longitudinal and transversal (LAW, TAW) acoustic waves with frequency 70.27 MHz in Si(111) plate and analysed the reflected beam by means of similar Si plate (DCD regime) or by triple-bounces BH analyser, respectively. The neutrons wavelength was 0.523 nm. Using the triple bounce BH analyser we observed a *strong* improvement of

phonon satellites contrast with moderate,  $\sim 20\%$ , loss of the main peak intensity. This was due to the suppression of the wings of the Darwin curve. In this case BH analyser “allows” to observe up to  $\pm 3$  ultrasonic phonon satellites.

We studied DCD with simultaneously ultrasonically excited monochromator (LAW) AND analyzer (TAW). We observed  $\sim 25\%$  narrowing of the main peak, its intensity increasing up to  $70\%$  and simultaneously the ultrasonic phonon satellites contrast is *strongly* improved in this “double-sound” case. These results were observed for the first time. It seems that our approach can be also applied for the improvement of the neutron imaging for the case of the refraction contrast.

#### **WP26: ToF-Neutron Reflectometer REFSANS at FRM-II Munich / Germany: Design and Potential for Investigations on Surfaces and Interfaces**

*R. Kampmann, M. Haese-Seiller, V. Kudryashov (Institut für Werkstofforschung, GKSS-Forschungszentrum Geesthacht GmbH, D-21502 Geesthacht, Germany), A. Okorokov, B. Toperverg (Petersburg Nuclear Physics Institute, Gatchina, 188350, Russian Federation), A. Schreyer (Institut für Werkstofforschung, GKSS-Forschungszentrum Geesthacht GmbH, D-21502 Geesthacht, Germany), E. Sackmann (Physik-Department E22, Technical University Munich, 85748 Garching, Germany)*

The reflectometer REFSANS is being built at the high flux reactor FRM-II in Munich. Novel time-of-flight (TOF) design and neutron optics allow for equal resolution adjustment of both the wavelength and the incidence angle to measure the specular reflectivity at maximum beam intensity over an extremely large range of momentum transfer of  $\sim 0.02 \text{ nm}^{-1} < q < 20.0 \text{ nm}^{-1}$ . The resolution in momentum transfer can be set in the wide range of  $0.25\% < \Delta q/q < 15\%$  (FWHM). At low  $q$ -resolution, beam intensities are expected to be sufficiently high to measure minimum reflectivities of  $R \sim 10^{-10}$ . REFSANS also provides new perspectives for characterizing lateral surface structures by means of small-angle scattering at grazing incidence (GI-SANS). Such experiments can be performed with the highest beam flux at a low wavelength resolution of  $\Delta\lambda/\lambda \sim 10\%$  and with novel scattering geometries, in particular the option to focus 13 point-collimated or slit height-smeared beams in the detector plane. Polarized neutrons can be used optionally for all mentioned scattering geometries and  $^3\text{He}$ -based polarization analysis will be made available in 2005. REFSANS is being put into operation this year and will be open for national as well as international users.

#### **WP27: The Upgraded General Purpose Powder Diffractometer at IPNS-ANL**

*J. W. Richardson, E. R. Maxey, Y. Li, A. Huq (IPNS Division, Argonne National Laboratory)*

The General Purpose Powder Diffractometer (GPPD) at IPNS has been upgraded according to a new concept for neutron powder diffractometer design that combines in an optimal way the strengths of reactor-based angle-dispersive and pulsed-source time-of-flight instrument designs. The key to this performance is to combine a continuous detector bank, extending over a large solid angle from back scattering to forward scattering, with time focusing techniques that allow all scattered neutrons to be combined into a single histogram. Without changing any instrument hardware, performance can be software/electronically optimized with respect to resolution, count rate, and d-spacing range to match the experiment being performed. A  $\sim 20$  times data rate increase is achieved in high intensity mode, where detectors covering a  $75^\circ$  2-theta range are time-focused and summed. Changing chopper phasing allows the optimum resolution to be moved to d-spacings up to  $6\text{-}8 \text{ \AA}$  for the study of larger unit cells, mixed phases, or subtle distortions.

The instrument now operates with: (1) a new Data Acquisition System capable of measuring full spectra for each detector and with EPICS-based process control, (2) one T0 and a frame-definition chopper providing wavelength-band selection and 15 Hz effective operation, (3) a 15 meter  $m = 3$  supermirror guide system with measured neutron gain factor  $> 6$  terminating 1 m (top) and 2 m (sides) from the sample position, (4) an incident flight pathlength of 25 m (up from 20 m) to reduce the moderator pulse-width contribution to peak shape resolution, and (5) no initial change in the L-CH4 moderator poisoning depth.

This work is funded by the U.S. Department of Energy under Contract W-31-109-ENG-38.

#### **WP28: Recent Technical Progress on High P-T Neutron Diffraction**

*Y. Zhao, L.L. Daemen, K. Lokshin, C. Pantea, J. Qian, S.C. Vogel, D.J. Williams, J. Zhang (Los Alamos National Laboratory)*

We will present the most recent progress made at LANSCE on High P-T Neutron Diffraction. We have developed a 500-ton toroidal press, TAP-98, to conduct simultaneous high pressure (up to 20 GPa) and high temperature (1700 K) neutron diffraction experiments. TAP-98 can be loaded into the HIPPO (High-Pressure and Preferred-Orientation Diffractometer) and we have performed high P-T



neutron diffraction experiments using HIPPO + TAP-98 for the first time in the run cycle of 2002. We have also developed a large crystal anvil cell, ZAP-01, to conduct experiments at high pressures and low temperatures. This cell can be used for integrated experimental techniques of neutron diffraction, laser spectroscopy, and ultrasonic interferometry. Most recently, construction of the new TAP-PLUS cell started, a 2000 ton press for neutron diffraction experiments which will run on a dedicated beam-line.

#### **WP29: Commissioning User-Ready Sample Environment Devices at ORNL**

*L. J. Santodonato (Spallation Neutron Source, Oak Ridge National Laboratory), G. B. Taylor (HFIR Center for Neutron Scattering, Oak Ridge National Laboratory, Oak Ridge, Tennessee 37831, USA)*

The first sample environment devices for the Spallation Neutron Source (SNS) have arrived, and we are already testing, debugging, and commissioning them for scientific research (presently at the High Flux Isotope Reactor (HFIR)). Scientific and technical teams from the HFIR and the SNS are collaborating on these efforts. Ultimately, we are working to establish a rigorous testing program to help both facilities maintain highly reliable sample environment inventories. These seemingly mundane tests also form a basis for more exciting endeavors such as prototype development, equipment upgrades, and the training of our growing technical teams. This poster highlights some of our recent efforts and results.

#### **WP30: Sample Environment Coordination at the NCNR**

*E. Fitzgerald, B. Clow, J. Leao, D. Dender (NIST Center for Neutron Research)*

The provision of sample environment for neutron scattering experiments is a multi-faceted exercise, the broad nature of which often goes unnoticed by guest researchers. This vital infrastructure is built upon knowledge and skills from physics, chemistry, electronics, machining, computer science, engineering, health physics, and management. By drawing on recent examples, we show how these multiple resources are brought to bear to ensure a smoothly functioning facility at the NIST Center for Neutron Research.

#### **WP31: Vibrational spectra of methyl derivatives of benzene selected as potential cold moderator materials**

*I. Natkaniec (Frank Laboratory of Neutron Physics, JINR, 141980 Dubna, Russia; H. Niewodniczanski*

*Institute of Nuclear Physics, PAS, 31-342 Krakow, Poland), K. Holderna-Natkaniec (Department of Physics, A. Mickiewicz University, 61-614 Poznan, Poland), J. Kalus (Institute of Physics, University of Bayreuth, D-95440 Bayreuth, Germany), I. Majerz (Faculty of Chemistry, University of Wroclaw, 50-383 Wroclaw, Poland)*

Vibrational spectra of selected methyl derivatives of benzene: toluene, *m*- and *p*-xylene, mesitylene (1,3,5-trimethylbenzene) and pseudocumene (1,2,4-trimethylbenzene), measured by inelastic incoherent neutron scattering (IINS) at 20 K, are compared with the amplitude weighted vibrational density of states calculated by the DFT quantum chemistry method. The IINS spectra were measured on the inverted geometry time-of-flight spectrometer NERA at the high flux pulsed reactor IBR-2 of the Joint Institute for Nuclear Research in Dubna. The calculation performed with the B3LYP/6-311++G\*\* basis set, gives quite satisfactory characteristics of internal modes, except for the frequencies of methyl librational modes. Internal barriers for methyl rotations of the investigated molecules are quite low, except for the two methyl groups which are connected to the neighboring carbon atoms of aromatic ring of pseudocumene molecule. The asymmetric molecules of toluene and *m*-xylene in solid phase form the crystals with low external barriers for methyl rotations. The mesitylene molecule contains the largest number of methyl groups around the aromatic ring with low internal rotational barriers. The external barriers caused by crystal packing significantly increase the frequencies of methyl librations in the low temperature phase III of mesitylene. The disordered phase II of solid mesitylene, which has low external rotational barriers of methyl, and additional density of states at low frequencies, caused by protonic glass state, is not stable at low temperatures. It is shown that mesitylene in solution with toluene, *m*-xylene or pseudocumene forms glassy solids, which are stable in the whole temperature range below the melting point. The IINS spectra of these glassy states also indicate relatively low barriers for methyl rotations, and additional density of states at low frequencies (boson peak) typical for disordered solids, which make these materials more preferable as potential solid moderators for very cold neutron sources.

#### **WP32: When Thin is Sexy – The Future of Neutron Reflectometry in Australia**

*M. James, A. Nelson, J. C. Schulz (Bragg Institute, Australian Nuclear Science and Technology Organisation, Australia)*

Neutron reflectometry is used to probe the structure



of surfaces, thin-films or buried interfaces as well as processes occurring at surfaces and interfaces. Applications cover adsorbed surfactant layers, self-assembled monolayers, biological membranes, electrochemical and catalytic interfaces, polymer coatings and photosensitive films. Contrast variation and selective deuteration of hydrogenous materials are important aspects of the neutron-based technique. Neutron reflectometry probes the structure of materials normal to the surface at depths of up to several thousand Å, with an effective depth resolution of a few Å.

Neutron reflectometry experiments have been performed by a number of Australian researchers at overseas facilities for more than a decade, however this capability has previously been absent in this country. We report instrument details as well as commissioning experiment results from Australia's first neutron reflectometer at the 10 MW HIFAR facility at Lucas Heights. This instrument has now become part of the AINSE User Program and is accepting beam time proposals from Australian and International researchers.

A neutron reflectometer has been recognised as one of the highest priority instruments to be constructed at the new 20 MW research reactor facility at Lucas Heights (due for completion in 2006). In this presentation we also report the design of the horizontal sample, time-of-flight reflectometer to be constructed at the new research facility.

#### **WP33: NPDF: A new high-resolution total scattering powder diffractometer**

*Th. Proffen (Los Alamos Neutron Science Center, Los Alamos National Laboratory)*

Knowing the atomic structure of materials usually means determining the crystal structure. However, many modern materials are complex, and their real structure often is deviated locally from the average crystal structure in significant ways. It is thus necessary to know the structure on various length scales, since properties are more directly governed by local atomic arrangements. But the conventional crystallographic approach cannot provide a complete picture; it has to be complemented by local probes such as the Pair Distribution Function (PDF) method.

The Neutron Powder Diffractometer NPD has recently been upgraded to become NPDF by adding a large number of detectors to the backscattering region of the instrument. The upgrade was funded by the National Science Foundation, Los Alamos National Laboratory, University of Pennsylvania and other academic institutions. On September 27<sup>th</sup>, 2002 the

shutter of NPDF opened for the first time. A standard data set suitable for PDF analysis can be obtained in only two hours. This puts NPDF at the cutting edge of local structure determination but also serve as development platform for this new structure analysis tool for disordered and nano-structured materials. The instrument is available to general users since the 2003 run cycle.

#### **WP34: A Time-of-Flight Ultra-Small-Angle Neutron Scattering Instrument Performance Gain Over Its Reactor-Based Analog**

*M. Agamalian (Oak Ridge National Laboratory), J. M. Carpenter (Oak Ridge National Laboratory; Argonne National Laboratory), K. C. Littrell (Argonne National Laboratory), A. Stoica, C. Rehm (Oak Ridge National Laboratory), P. Thiyagarajan (Argonne National Laboratory)*

We present the current version of the conceptual design of a Bonse-Hart Time-of-Flight Ultra-Small-Angle Neutron Scattering (TOF-USANS) Double-Crystal Diffractometer for use at the SNS 25 mm H<sub>2</sub>O or 60 mm H<sub>2</sub> moderator. This instrument consists of a 15 m-long supermirror neutron guide, 2D focused Si(2,2,0) bent pre-monochromator and Si(220) triple-bounce channel-cut crystals in a parallel double-crystal arrangement. The TOF technique allows the separation of seven wavelengths simultaneously satisfying the Bragg condition in the range,  $0.5 \text{ \AA} < \lambda < 3.7 \text{ \AA}$ , providing the opportunity to collect seven sets of USANS data at once. The smallest measurable scattering vector,  $Q_{\min}$ , decreases with the increase of the order of Bragg reflection and reaches the value  $Q_{\min} \approx 2 \times 10^{-6} \text{ \AA}^{-1}$  for the Si(14,14,0) reflection, about one order of magnitude smaller than for conventional reactor-based USANS instruments. The overall flux at the sample position is estimated to be as high as  $\sim 13000 \text{ n/(cm}^2 \text{ sec)}$  for the 25 mm H<sub>2</sub>O moderator and  $\sim 120000 \text{ n/(cm}^2 \text{ sec)}$  for the 60 mm H<sub>2</sub> moderator, the latter value being seven times higher than that achieved at the NIST reactor Bonse-Hart USANS, the world's best instrument of this type. Besides, the multi-wavelength performance of the TOF-USANS instrument allows variation of the Bonse-Hart collimation, which cannot be done at reactor-based USANS. This advantage gives the scattered intensity gain factor, which is proportional to the square width of the total Darwin plateau. The Bonse-Hart variable collimation gain factor depends of the order Bragg reflection; this factor calculated for the first Bragg peak is as high as  $\sim 19$  over the reactor-based analogue. Parallel measurements at different wavelengths may prove very helpful for diagnosing multiple and inelastic scattering in USANS experiments, as well as the

refraction effects. Moreover, time-of-flight operation is likely to reduce the background.

### **WP35: Neutron Polarization Evolution Calculations along the SNS Magnetism Reflectometer Beam Line**

*A. A. Parizzi, F. Klose (Spallation Neutron Source, Oak Ridge National Laboratory), V. Christoph (University of Applied Sciences, Dresden (Germany))*

In polarized neutron scattering instruments, most polarization devices apply magnetic fields of different space and time profiles for achieving the desired conditioning of the beam. Magnetic fields created at an individual device often impose fringe/stray fields onto other devices in the beam line, which may affect both their functionalities and the overall neutron polarization evolution.

For the SNS Magnetism Reflectometer, it is desirable that different sample environment magnets and different beam conditioning devices can be used in variable conditions. Spin polarizers and analyzers, broad-band spin flippers and other polarized neutron devices must be capable of working reliably in the vicinity of small magnetic fields generated for example by an iron-yoke electromagnet as well as in much larger magnetic fields created, for example, by a high-field superconducting magnet. The latter may not only impose relatively large stray fields along the beam path, but also produce relatively large field gradients.

In this paper, we present calculations treating the magnetic field interference between devices, the effect of sample environment magnets and the resultant polarization evolution of neutrons along the beam line. Calculations are presented for several polarized-beam set ups that will be adopted for different desired experimental conditions at the SNS Magnetism Reflectometer.

### **WP36: The Advanced Neutron Diffractometer / Reflectometer: a New CNBT Instrument at the NIST Center for Neutron Research**

*J. A. Dura, D. Pierce, C. F. Majkrzak (NIST Center for Neutron Research), K. V. O'Donovan, U. Perez-Salas (University of California—Irvine and NIST Center for Neutron Research)*

The Advanced Neutron Diffractometer / Reflectometer, AND/R, completed in July 2003, is the centerpiece of the Cold Neutrons for Biology and Technology, CNBT, program, funded by the NIH, National Center for Research Resources (NCRR). This instrument is dedicated to diffraction, reflectometry, and diffuse scattering measurement for research on

biological membranes and related materials.

It was modeled after and is located just upstream of the NG1 polarized beam reflectometer. Like the NG1 reflectometer, the AND/R has a horizontal scattering plane, which provides unrestricted access to higher scattering angles. Other features common to both instruments are the polarized beam capability to enable the use of magnetic reference layers for phase inversion of data, and a vertically focussing monochromator to increase the flux on the sample.

Additional features make the instrument well suited for both reflectometry and diffraction investigations of biological systems. First, the AND/R can operate using either a larger 2" pencil detector (increasing the flux at higher momentum transfer,  $Q$ ) or a 2-dimensional position sensitive detector (PSD). By simultaneously measuring non-specular scattering from large areas in reciprocal space, the PSD will make it much more efficient to obtain information on in-plane structures. Also, the sample tables will accommodate larger sample environments (up to 10.2" from tabletop to beam center and up to 1000 Lbs) or an Eulerian cradle (for diffraction experiments from single crystals). Optical benches, both inside and outside the shutter, and within the detector shielding, will make customization and upgrades of the neutron optical components simpler to implement. An increased number of motorized axes as well as additional supporting software provided by a dedicated programmer in the CNBT program will make this a more user friendly instrument.

In addition to serving the needs of the CNBT partners and collaborators, 25% of the time on this instrument is available to the general user community.

This material is based on work supported by the National Institutes of Health under grant no. 1 R01 RR14812 and The Regents of the University of California.

### **WP37: Developing ARCS: a status report on the wide Angular-Range Chopper Spectrometer at the SNS**

*D. L. Abernathy (Spallation Neutron Source, Oak Ridge National Laboratory), B. T. Fultz (California Institute of Technology)*

The U.S. Department of Energy has funded ARCS, a wide Angular-Range Chopper Spectrometer, to be constructed on beam line 18 at the Spallation Neutron Source. ARCS will be optimized to provide a high neutron flux at the sample and a large solid angle of detector coverage. The source-sample distance will be 13.6 m, and the secondary flight

path will be 3.0 m at all angles from  $-20^\circ$  to  $140^\circ$  horizontally and  $\pm 30^\circ$  vertically. The incident neutrons energy will vary between 10 and 1000 meV with a resolution of 2% or above at the elastic line. Combining the high flux from the SNS with a detector coverage of almost one-fourth of the possible solid angle will allow data collection rates roughly 10 to 100 times that currently possible at existing instruments.

The project is currently at its midpoint, and a number of technical and user oriented issues are being addressed in the course of turning the concept of the instrument into reality. For example, the detectors will be placed inside the same vacuum space as the sample and so have been extensively tested to prove the electronic design for operation in vacuum. Two different neutron chopper designs for blocking the prompt pulse of radiation from the target and moderator have been evaluated. Another issue that will have a great impact on the user experience at the instrument is the overall access and features around the sample region. Because of the unprecedented power of the SNS source, careful consideration of the shielding around the instrument is needed to minimize background while allowing for complex sample environment equipment.

#### **WP38: Progress on the New High Intensity Cold Neutron Spectrometer, MACS.**

*C. L. Broholm, T. D. Pike, P. K. Hundertmark (Johns Hopkins University; NIST Center for Neutron Research), P. C. Brand, J. W. Lynn, D. L. Pierce, J. Moyer, J. G. LaRock (NIST Center for Neutron Research), S. A. Smee, G. Scharfstein (Johns Hopkins University)*

A new high intensity neutron spectrometer is under development at the NIST Center for Neutron Research. The instrument will cover the energy transfer range from -10 to 17 meV with typical energy resolution 0.2 meV. The distinguishing feature of the Multi Axis Crystal Spectrometer is ultra high sensitivity to slowly propagating excitations in condensed matter. This is achieved by (1) Relaxing wave vector resolution transverse to the incident beam while maintaining high energy resolution (2) Increasing the solid angle of the detection system through multiple crystal analyzer channels. The instrument will be particularly well suited for mapping the wave vector dependence of neutron scattering at fixed energy transfer. For experiments that can use the full divergence of the incident beam and that benefit from all twenty detection channels the gain in sensitivity compared to a conventional cold neutron triple axis spectrometer will be at least two orders of

magnitude. MACS will therefore enable energy resolved neutron scattering experiments on a broad class of compounds early in the materials development cycle.

This poster reports on progress in the design of some of the intricate components of MACS that are crucial for enabling its performance. In particular we describe the mechanical design of the double crystal analyzer system that is key to increasing the solid angle of the detection system while maintaining the flexibility and high signal to noise ratio of a conventional triple axis spectrometer. A single stepping motor translates and rotates the two vertically focusing crystal assemblies of a detection channel and orients the blades of a coarse background suppressing collimator situated between them. We also describe the incident beam line that allows large solid angle access to the NIST cold source. It is based on a doubly focusing monochromator that translates along the white beam as the incident energy is varied. This approach enables a compact instrument and highly effective incident beam line shielding to improve the signal to noise ratio.

- (a) R. Hammond and J. D. Orndorff from Johns Hopkins University are also authors on this poster.  
(b) The MACS project is funded by NIST, NSF DMR-0116585, and JHU.

#### **WP39: Design of a Single Crystal Macromolecular Neutron Diffractometer at SNS**

*P. Thiyagarajan, Arthur Schultz (Intense Pulsed Neutron Source, Argonne National Lab), Christine Rehm, Jason Hodges, W.T. Lee (Spallation Neutron Source, Oak Ridge National Laboratory), Andrew Mesezar (Department of Medicinal Chemistry and Pharmacognosy, University of Illinois, Chicago)*

Neutron Macromolecular Crystallography (NMC) is able to accurately determine proton locations, protonation states and hydration, and hydrogen/deuterium exchange in macromolecular crystals even at a moderate resolution ( $2 \text{ \AA}$  to  $2.5 \text{ \AA}$ ). In order to exploit the high neutron flux that will become available by 2006 at the Spallation Neutron Source (SNS), and to leverage the enormous interest shown by the macromolecular crystallography community, it is proposed to develop a dedicated best-in-class high throughput and high resolution time-of-flight single crystal macromolecular neutron diffractometer (MaNDi) at the SNS. MaNDi has been designed to be able to collect a full hemisphere of Bragg data with a resolution of  $1.5$  to  $2 \text{ \AA}$  on a crystal with a lattice constant up to  $150 \text{ \AA}$  in a few days. A thorough evaluation of the instrument performance at different



moderators using analytical equations and Monte-Carlo simulations show that the decoupled hydrogen moderator at SNS would be the best choice for MaNDi. State-of-the-art neutron guides and optics will be used for efficient beam transport and optimization of collimation at the sample. To reduce the radiation damage and the instrument background a curved guide will be used to steer the beam gently so that the crystal will be out of line of sight of the moderator. The high throughput is accomplished by the use of a wide band width of cold neutrons (1.8 Å).

This work at IPNS was funded by the U.S. DOE, BES-Materials Science, under Contract W-31-109-ENG-38 to U. Chicago, and SNS funded by U.S. DOE, BES-Mat Sci. under contract DE-AC05-00OR22725UT-Battelle, LLC and ORAU.

#### **WP40: The effects of gravity on the operation of multiple confocal pinhole SANS instruments**

*K.C. Littrell (Intense Pulsed Neutron Source, Argonne National Lab)*

One of the most promising methods for increasing the flux on sample in broad-bandwidth Time-of-flight small angle scattering instruments while maintaining the ability to measure small minimum momentum transfers  $Q_{\min}$  is through the use of multiple, confocal “pinhole” apertures. Since the apertures themselves are wavelength independent, such an instrument would be expected to be wavelength independent as well. However, the effects of gravity produce a vertical dispersion of the neutron beam which can become significant compared to  $Q_{\min}$  as the overall length of the instrument increases or the size of the individual apertures or the detector pixel decreases. In this work, we extend the description of how to use material prisms to correct for this gravitational chromatic aberration for single pinhole instruments to encompass multiple-confocal pinhole geometries. A further concern is that when multiple apertures are separated by solid walls, these walls are invariably straight for ease of manufacturing, while the trajectory of the neutron is parabolic and wavelength-dependent, leading to a wavelength-dependent attenuation of the beam. We quantify this effect as a function of the vertical geometry of the pinholes.

#### **WP41: A Neutron Analyzer with Horizontal Focusing for Triple Axis Spectrometers**

*I. Zoto, E. Abdel-Raouf, S. Al-Ghamdi, Vemuru V. Krishnamurthy, G. J. Mankey (MINT Center, The University of Alabama, Tuscaloosa, Alabama 35487-0209), J. L. Robertson (Condensed Matter Sciences Division, Oak Ridge National Laboratory)*

Triple axis spectrometers have been extensively used

to study a variety of excitations in condensed matter. We report the design of the Bragg Angle Multi-crystal Analyzer (BAMA) for using with a triple axis spectrometer at the High Flux Isotope Reactor. BAMA will enable the measurements of spin dynamics in magnetic thin films and magnetic devices. A typical triple axis spectrometer contains one crystal as an analyzer, and there is no focusing of the scattered neutron beam. Recently horizontal focusing has been used in multi-crystal analyzers. There are two multi-crystal analyzers worldwide. One was developed by the Riso National Laboratory and is currently located at the Swiss Spallation Neutron Source. It is known by the acronym RITA for reinvented triple axis spectrometer. The other is used at the NIST Research Reactor in the spin-polarized triple axis spectrometer. Our design incorporates nine analyzer blades driven by individual motors. The motor interface for positioning the individual analyzer crystals is through an Ethernet controller. The design incorporates closed-loop picomotors manufactured by New Focus. The motors are designed as a micrometer drive for linear actuation and the analyzer blades are mounted directly to the micrometer screw to achieve angular control with a small linear translation. The picomotors are compact enough to be incorporated in a modular instrument design with nine 20 mm wide graphite blades. The computer code for driving the analyzer will be tested first with an optical analog using diffraction gratings and visible light from a light emitting diode. This project is funded by NSF DMR 02-81637 and DOE/EPSCoR DE-FG02-02ER45966.

#### **WP42: Rheo-SANS at the NCNR**

*L. Porcar, B.S. Greenwald (NIST Center for Neutron Research; University of Maryland, College Park), C.J. Glinka (NIST Center for Neutron Research), N. Wagner (University of Delaware, Newark, DE 19716), S.-M. Choi (Korea Advanced Institute of Science and Technology, Daejeon, Korea), J.C. Schultz (Australian Nuclear Science and Technology Organisation, NSW, Australia)*

Shear flow presents a great technological interest because shear-induced complex fluid phases have profound effects on industrial material processing. In order to correlate the unique flow properties exhibited by these complex fluids with their structural deformation, we have developed a device to perform simultaneous measurement of rheology and structure by Small Angle Neutron Scattering (SANS). Quartz and titanium Couette type flow cells have been designed to fit into a commercial rheometer. The setup allows scattering measurements from a range of configurations using both the so-called radial configuration, where the incident neutron beam is



parallel to the velocity gradient, to the tangential, where the incident neutron beam is parallel to the flow direction. Couette cells with gaps of 0.5 or 1 mm are available and can operate at temperatures ranging from  $-20\text{ }^{\circ}\text{C}$  to  $150\text{ }^{\circ}\text{C}$  with a solvent trap preventing sample evaporation. The apparatus allows many different rheological tests to be performed e.g., simple shear flow either at constant shear stress or constant shear rate, creep and creep recovery as well as amplitude oscillatory shear deformation, while simultaneously recording scattering data. To illustrate the performance of the equipment, we give a brief report of recent experiments carried out on colloidal suspensions and surfactant mesophases.

#### **WP43: Applications in Physics of the new Diffractometer HIPPO at LANSCE**

*D.J. Williams, S.C. Vogel (Los Alamos National Laboratory), M.A. Rodriguez, M.A. Mangan (Sandia National Laboratories, Albuquerque, NM 87123), M.E. Manley, E.J. Peterson (Los Alamos National Laboratory), J.L. Jones (The University of New South Wales, Sydney, Australia 2052), R.J. McQueeney (Los Alamos National Laboratory; Iowa State University), W. Palosz (Marshall Space Flight Center, AL 35812), B. Palosz (High Pressure Research Center, Polish Academy of Sciences, Warsaw, 01-142, Poland)*

The High-Pressure Preferred Orientation (HIPPO) neutron diffractometer is the first third-generation neutron time-of-flight powder diffractometer that was constructed in the United States. It utilizes extremely high neutron count-rates by virtue of a short (9 m) initial flight path viewing a high intensity water moderator and 1360  $^3\text{He}$  detector tubes covering  $4.5\text{ m}^2$  of detector area from  $10\text{ }^{\circ}$  to  $150\text{ }^{\circ}$  in scattering angles. HIPPO was designed and manufactured as a joint effort between LANSCE and the University of California with the goals of attaining world-class science and making neutron powder diffractometry an accessible and available tool to the national user community. On this poster, we give an overview of applications of HIPPO to physics-related investigations. Structural changes during charging and uncharging of a commercial Li-ion cell were studied as well as the crystal structure of highly textured magnetic and non-magnetic thin films consisting of Erbium (high Z) and hydrogen (low Z, deuterated for this study). Texture changes of piezo-electric materials with temperature and processing method were examined as well as the crystal structure of superconductors and pair-distribution function (PDF) on nanoparticle materials.

#### **WP44: Interaction of paraffin wax gels with random crystalline/amorphous hydrocarbon copolymers**

*R. K. Prud'homme (Department of Chemical Engineering, Princeton University, Princeton, NJ 08544), H. S. Ashbaugh (Los Alamos National Laboratory, Los Alamos, NM 87545), A. Radulescu, D. Schwahn, D. Richter, L. J. Fetters (Institut für Festkörperforschung, Jülich, Germany)*

The control mechanisms involved in the modification of wax crystal dimensions in crude oils and refined fuels are of joint scientific and practical interest. An understanding of these mechanisms allows strategies to be developed that lead to decreases in crude oil pour points or (for refined fuels) cold filter plugging points. The attainment of these goals involves the control and modification of wax crystals that spontaneously form in mixed hydrocarbon systems upon decreasing temperature. This work reports on the influence of random crystalline-amorphous block copolymers (ethylene-butene) upon the rheology of model oils. In a parallel fashion small-angle neutron scattering was exploited to gain microscopic insight as to how added poly(ethylene-butene) copolymers modify the wax crystal structures. The copolymers with different contents of polyethylene are highly selective with respect to wax crystal modification. Thus, the copolymer with the highest crystalline tendency is more efficient for the larger wax molecules while the less crystalline one is more efficient for the lower waxes.

#### **WP46: SANS method to study of mixture systems of surfactants SDS + TX-100 and CTAB + TX-100**

*A. Rajewska (Institute of Atomic Energy, 05-400 Swierk-Otwock, Poland; Joint Institute for Nuclear Research, LNP, 141980 Dubna, Moscow region, Russia), R. F. Bakeeva (Kazan State Technological University, Kazan, Russia)*

The mixing of amphiphiles in water may lead to the formation of mixed micelles which often present new properties with respect to the pure component solutions [1, 2]. Two mixture systems of classic surfactants: SDS (sodium dodecyl sulphate) + TX-100 (Triton-X-100) (anionic + non-ionic) and CTAB + TX-100 (cationic + non-ionic) in water solution were investigated for temperatures  $30\text{ }^{\circ}$ ,  $50\text{ }^{\circ}$ ,  $70\text{ }^{\circ}$  for compositions 1:1, 2:1, 3:1 with the time-of-flight small-angle neutron scattering (TOF SANS) spectrometer (YuMO) of the IBR-2 on pulsed neutron source [3] at FLNP, JINR in Dubna (Russia). Measurements have covered Q range from  $8 \times 10^{-5}$  to  $0.4\text{ \AA}^{-1}$ . The SANS measurements of aqueous solutions of nonionic / ionic surfactants have shown that the mixed micelles are formed. From the measured

dependence of the scattered intensity on the scattering angle, we derived the aggregation number and the electric charge of the mixed micelle at various compositions and ionic strengths.

- [1] Clint J., J. Chem.Soc., Faraday Trans., 1,1327 (1975); Moroi Y., Akisada H., et al., J. Colloid. Interface Sci., 61, 233 (1977);Corti M., Degiorgio V., et al., J. Phys. Chem., 86, 2533 (1982); Cantu L., Corti M., Degiorgio V., J. Phys.. Chem., 94, 793 (1990)  
[2] Rathman J., Scamehorn J. F., J. Phys. Chem., 88, 580 (1984); Treiner C.,Amar Khoida A., et al., J. Colloid Interface Sci., 128, 416 (1989)  
[3] Ostanievich Yu. M., Makromol. Chem. Macromol. Symp., 15, 91 (1988)

#### **WP47: Influence of chain stiffness on the properties of polyelectrolyte solutions**

*S. I. Yun, Y. B. Melnichenko, G. D. Wignall, K. Hong, J. Mays (Oak Ridge National Laboratory)*

Model systems for obtaining structural information on atomic-level interactions in polyelectrolyte solutions should incorporate primary features of the interactions of interest. For example, the effect of chain stiffness on polyelectrolyte conformation and counterion interactions can best be understood through the preparation of polyelectrolytes in which the same charge groups are attached to backbone structures of varying stiffness. For a ionizable group (sulfonate), the effect of chain stiffness can be elucidated through studies of poly(styrene sulfonate) (PSS) as a flexible example; poly(cyclohexadiene sulfonate) (PCHDS) as a “semiflexible” backbone structure. Small-angle neutron scattering (SANS) of PCHDS-h solutions have shown that the polyelectrolyte peak was observed to be much less pronounced and less dependent of polymer concentration compared to PSS. Finding peak position required working out an empirical procedure in order to subtract the contribution of excess scattering at small  $Q$ s. Preliminary data analysis shows that the peak position for solutions of PCHDS in  $D_2O$  scales with the polymer concentration (zero salt) with exponent  $\sim 0.1$  to be compared with the scaling predictions of 0.5 for flexible chains.

#### **WP48: Correction of tangential Couette SANS data**

*L. Porcar (NIST Center for Neutron Research; University of Maryland, College Park). W. A. Hamilton, P. D. Butler (Condensed Matter Sciences Division, Oak Ridge National Laboratory)*

In SANS Couette shear cell measurements conversion to an absolute scale for the radial scattering configuration can be done in the standard manner using the direct beam as a primary standard and then correct-

ing for sample and cell transmissions and the sample thickness (simply twice the Couette gap). Absolute calibration in the tangential geometry is more problematic – the geometrical limitations of asymmetries of sample path and absorption lead to clear asymmetries in the observed scattering patterns.

We recently found a simple and effective way to correct tangential scattering: from the tangential transmission we obtain an effective thickness consistent with the radial transmission and its known thickness [1]. However, even after these corrections, in some cases (usually for high scattering angles), a residual geometry dependent asymmetry is observed in our corrected tangential configuration scattering patterns because of neutrons scattered toward the cell axis traverse a significantly longer path through the sample fluid than those scattered away. As would be expected this effect is more pronounced for high sample absorption, scattering angle and sample annulus width.

To correct for this effect we propose to use a “sensitivity file” obtained from a mixture of heavy and light water matching the sample absorption in the same geometry tangential scattering configuration and thus subjecting evenly scattered incoherent neutrons to a similar absorption (re-scattering) geometry to that experienced in the sample. Furthermore, it is also possible to create a “calculated sensitivity” based on sample’s absorption and geometrical considerations which allow correction of the scattering asymmetry observed in the tangential configuration to a very good approximation. We will discuss the limits of validity of such approaches.

- [1] L. Porcar, W. A. Hamilton, P.D. Butler, and G.G. Warr, A new vapor barrier couette shear cell, for small angle neutron scattering measurements, Review of Scientific Instruments 73, 2345 (2002)

#### **WP49: Low Energy Excitation of Poly(methyl methacrylate)**

*M.-H. Kim, C.M. Brown (NIST Center for Neutron Research; Department of Materials Science and Engineering, University of Maryland)*

The relative contributions of poly(methyl methacrylate) side groups (ester, alpha-methyl, and main chain  $CH_2$ ) to the low energy Boson excitation were studied by isotopic substitution using the Fermi-Chopper Time-Of-Flight Neutron Spectrometer. The enhancement of the dynamic structure factor,  $S(Q, \omega)$  observed around 1.8 meV is dominated by the methyl vibration on the ester group ( $-COOCH_3$ ). The relative contributions follow the order  $-COOCH_3 > > -\alpha-CH_3 > -CH_2-$ .

**WP50: Effect of High Ionic Strength on Interfacial Properties, Lamellarity and Polydispersity of Unilamellar Vesicles Prepared By Extrusion**

*J. Pencer (Department of Chemical and Biomolecular Engineering, The Johns Hopkins University; NIST Center for Neutron Research), S. Krueger (NIST Center for Neutron Research), M. E. Paulaitis (Department of Chemical and Biomolecular Engineering, The Johns Hopkins University)*

Small-angle neutron scattering is used to determine the vesicle and bilayer form factors of DOPC vesicles prepared by extrusion in distilled water and 3 M NaCl. We find that vesicles prepared in the presence of 3 M NaCl exhibit a higher degree of multilamellarity and are significantly more polydisperse than those prepared in the absence of NaCl. Contrast variation studies are also performed, to observe possible NaCl induced changes to bilayer density. Finally, osmotic downshifts are performed to discern between inter and intravesicular correlations. Our observations are consistent with salt-induced attraction between DOPC bilayers. Since this result cannot be explained on the basis of charge screening, we discuss two other possible sources of attractive interactions, osmotic dehydration and charge fluctuations.

**WP51: Structural Studies of Single Bilayer Lipid Membranes on a Patterned Surface**

*G.S. Smith (HFIR Center for Neutron Scattering, Oak Ridge National Laboratory, Oak Ridge, Tennessee 37831, USA.), S.M. Baker (Harvey Mudd College, Dept. of Chemistry, Claremont, CA 91711), J. Tan (Harvey Mudd College, Dept. of Chemistry, Claremont, CA 91711; Columbia University, Applied Physics and Applied Mathematics Dept., New York, NY 10027-8351), T. McQueen (Harvey Mudd College, Dept. of Chemistry, Claremont, CA 91711), J. Majewski (Los Alamos Neutron Science Center, Los Alamos National Laboratory)*

One of the mechanisms by which proteins transport materials across living cell membranes is by forming pores in the lipid bilayer surrounding the cell. The pores consist of aggregates of protein molecules which form tubular structures which span the membrane. The transport through one of these pores may either be active, requiring an energy production reaction like the hydrolysis of ATP, or passive, where the molecule diffuses in the thermodynamically favorable direction. One clear requirement for the insertion and activation of the pores is a free membrane where the proteins can protrude from each surface. In this paper, we examine the utility of using templated surfaces as a means for creating regions of

unsupported lipid bilayer films. The templates with pores sizes on the order of tens of nanometers were prepared by phase segregation of diblock copolymers on a silicon oxide surface. The polymer templates were either coated with gold or reactively etched to the silicon surface to form hydrophilic (gold or silicon oxide, respectively) surfaces. Finally, we deposited bilayers of dimyrystoyl phosphatidylcholine on the templates either by a combination of Langmuir-Blodgett deposition and vesicle fusion or by vesicle fusion alone. We present neutron reflectometry and Atomic Force Microscopy measurements of these various samples and show that we have achieved the desired architecture over large areas of the substrate.

**WP52: Effects of Temperature and Salts on the Micelle Structure of Triblock Copolymer P84 in Aqueous Solutions**

*L. Guo, P. Thiyagarajan (Intense Pulsed Neutron Source, Argonne National Lab)*

We investigated the phase behavior of aqueous solutions of a triblock copolymer Pluronic P84 (EO19PO43EO19) at different copolymer and sodium carbonate concentrations and temperatures by using small angle neutron scattering (SANS). We obtained information on the shape and size of Pluronic P84 micelles, aggregation number and the volume fraction of the micelles. The results show that temperature and carbonate ion concentration have strong influence on the phase behavior of the triblock copolymer. The micelle aggregation number and size increase with polymer and carbonate ion concentrations as well as temperature. The CMT decreases with increasing temperature and carbonate ion concentration. At high temperatures and carbonate ion concentrations, spherical to cylindrical micelle transformation occurs. Phase separation is observed at sufficiently high temperatures and carbonate ion concentrations.

This work benefited from the use of the Intense Pulsed Neutron Source at Argonne National Laboratory funded by the Office of BES, US DOE under the contract # W-31-109-ENG-38. We thank Denis Wozniak at IPNS for his assistance with the SANS experiments.

**WP53: Annealing induced structural changes and microcracking in Mo-Mo<sub>5</sub>Si**

*X.-L. Wang (Spallation Neutron Source, Oak Ridge National Laboratory; Metals and Ceramics Division, Oak Ridge National Laboratory), J. H. Schneibel (Metals and Ceramics Division, Oak Ridge National Laboratory), Y. D. Wang, A. D. Stoica (Spallation Neutron Source, Oak Ridge National Laboratory), J.*



W. Richardson (*Intense Pulsed Neutron Source, Argonne National Lab*)

An outstanding issue in the processing of Mo-Mo<sub>3</sub>Si intermetallic composites is that microcracks develop after annealing at high temperatures [1], which significantly degrade the mechanical properties of the composite materials. The formation of microcracks is difficult to understand from the view point of differential thermal stresses that develop during cooling, which were estimated to be ~ 100 MPa for both phases. It is unlikely such a level of residual stress would cause microcracking at any stage during cooling. In order to determine the nature of microcracking in Mo-Mo<sub>3</sub>Si, we have conducted a systematic study of Mo-Mo<sub>3</sub>Si composites using a combination of *in situ* neutron diffraction, composition analysis, and scanning electron microscopy.

*In situ* neutron diffraction measurements at 1300 °C revealed a significant increase of the lattice parameter in the  $\alpha$ -Mo phase as a function of annealing time, whereas the lattice parameter of the Mo<sub>3</sub>Si phase shows a corresponding decrease. At the same time, the diffraction peak widths of both phases increased, unexpectedly, with increasing annealing time, giving evidence that plastic deformation occurred at high temperature. X-ray and neutron diffraction measurements made before and after annealing confirmed that the changes in lattice parameters are irreversible, i.e., due to plastic deformation. Because the as-cast materials were obtained off-equilibrium by fast cooling, the  $\alpha$ -Mo phase is known to be super-saturated with Si. The *in situ* neutron diffraction data therefore suggest that high-temperature plastic deformation during annealing was due to diffusion of Si atoms from  $\alpha$ -Mo to Mo<sub>3</sub>Si. This finding was corroborated by microscopy studies which demonstrated that the microcracks almost always started at the interface of  $\alpha$ -Mo and Mo<sub>3</sub>Si grains and grew into Mo<sub>3</sub>Si. Furthermore, crack density measurements via microscopy indicated that as the annealing time increased more cracks were formed. Based on these experimental observations, it is clear that microcracking in Mo<sub>3</sub>Si occurred at high temperature. Quite possibly, the diffusion of Si during high-temperature annealing created a highly inhomogeneous microstructure at the interface where cracks were initiated when the elastic energy exceeded the tensile limit of the Mo<sub>3</sub>Si phase.

This research was supported by the Division of Materials Science and Engineering, U.S. Department of Energy. Oak Ridge National Laboratory is managed by UT-Battelle, LLC, under contract DE-AC05-

00OR22725 with the US Department of Energy.

[1] J. H. Schneibel, C. T. Liu, D. S. Easton, and C. A. Carmichael, "Microstructure and mechanical properties of Mo-Mo<sub>3</sub>Si-Mo<sub>5</sub>SiB<sub>2</sub> silicides," *Mater. Sci. Eng. A261*, 78-83 (1999).

#### **WP54: Residual Stresses by Neutron Diffraction and Microstructural Characterisation by SANS of Materials and Components of Technological Interest**

*Massimo Rogante (Nuclear Engineering Laboratory, DIENCA, University of Bologna, Via dei Colli 16, 40136 Bologna; Rogante Engineering Office, Contrada San Michele, 61 / P. O. Box 189, 62012 Civitanova Marche, Italy)*

The adoption of neutron techniques, among the other non-destructive diagnostics, is becoming more and more relevant in studying materials and components of industrial interest. In this paper, neutron diffraction for Residual Stresses (RS) measurements and Small Angle Neutron Scattering (SANS) for microstructural characterisation—especially related to the precipitate distribution—are considered. The basic theoretical aspects and some industrial applications of each technique are reported. In particular, RS determination in weldings, in extruded specimens and in a component for nuclear/traditional energy industry is presented. SANS measurements are finally reported, concerning materials and components for energy and automotive industry.

#### **WP55: Neutron Residual Stress Measurements on Rail Sections for Different Production Conditions**

*V. Luzin (National Institute of Standards and Technology; State University of New York, Stony Brook, NY 11794-2275), J. Gordon (Volpe National Transportation Systems Center, Cambridge, MA 02142), T. Gnaupel-Herold (National Institute of Standards and Technology; University of Maryland, College Park), H.J. Prask (National Institute of Standards and Technology)*

Rail sectioning with subsequent neutron or synchrotron x-ray diffraction experiments is the most effective technique for assessment of the residual stresses in the rails. In this study we present the results of stress measurements performed on the BT8 diffractometer at the NIST Center for Neutron Research (NCNR) on rails that were produced under various conditions. Specifically, these are air-cooled, air-cooled and roller-straightened, head-hardened and head-hardened and roller-straightened. In addition, a head-hardened and roller-straightened rail was also studied after service to elucidate evolution of the service-induced residual stresses. Neutron



strain measurements with  $3 \times 3 \times 3 \text{ mm}^3$  spatial resolution were successfully employed for transversally-cut sections to verify the difference in the stress state depending on the production process. Although examination of slices allows determination of only two-dimensional stresses in the plane of the slice, additional measurements on obliquely-cut slices, which were also carried out, and utilization of FEM gives the possibility of reconstructing the full triaxial stress distribution. Together, these approaches provide a better understanding of rail fabrication and the possibility of improving the durability and safety of rails in the future.

**WP56: An analysis of copper precipitation in the thermally aged FeCu alloy using micro magnetic technique and SANS**

*D.G. Park (Korea Atomic Energy Research Institute, Yuseong P.O. Box 105, Daejeon, 305-600, Korea), M.N. Lee (Pohang University of Science and Technology, Materials Science and Engineering, Hyoja-Dong, Nam-Gu, Pohang, Kyungsangbuk-Do, 790-784, Korea), J.H. Kim, S.C. Kwon (Korea Atomic Energy Research Institute, Yuseong P.O. Box 105, Daejeon, 305-600, Korea), Y.M. Koo (Pohang University of Science and Technology, Materials Science and Engineering, Hyoja-Dong, Nam-Gu, Pohang, Kyungsangbuk-Do, 790-784, Korea), J.H. Hong (Korea Atomic Energy Research Institute, Yuseong P.O. Box 105, Daejeon, 305-600, Korea)*

In order to study the effect of the copper precipitate in the steel embrittlement under neutron irradiation, the characteristic of nano size defects were investigated in the thermal aged FeCu model alloys. The copper precipitation leads to a distortion of the crystal lattice surrounding the copper precipitates and yields internal micro-stress [1]. To verify the role of copper precipitation, microhardness test, stress related magnetic Barkhausen noise measurements and small angle neutron scattering (SANS) under magnetic field experiments were carried out. The results on precipitation composition, number density, size distribution and matrix composition obtained using high resolution TEM and SANS are compared and contrasted. The diameter of copper precipitates given by SANS varied from  $3 \sim 10 \text{ nm}$ , and increased continuously with aging time. For the thermally aged alloy, the most notable results include the clear observation of copper-rich precipitates, evidence for the retention of a significant copper fraction in solid solution at the peak of hardening, for a bimodal distribution of particle sizes in the averaged condition.

[1] I. Altpeter et al., Nucl. Eng. Design, 206 (2001) 337-350

**WP57: In situ deformation studies using HIPPO/CRATES**

*S.C. Vogel, T. Medina, E. Meyer, D.J. Williams (Los Alamos National Laboratory), T. Brissier (Los Alamos National Laboratory; HTW Saarbruecken, 66117 Saarbruecken, Germany), C. Hartig, J. Laakmann, O. Meyer, H. Mecking (TU Hamburg-Harburg, 21071 Hamburg, Germany)*

*In situ* neutron diffraction deformation studies of metals, alloys and composites using strain derived from peak-shifts are well established for more than two decades. However, the peak-shift measures by definition only the elastic strain. To obtain further insight into the deformation mechanisms which are active to achieve a given amount of plastic deformation, the texture is also an important quantity. The texture, or orientation distribution function (ODF), is accessible via peak intensity changes in a diffraction experiment. The texture changes are differently for instance for slip, twinning or grain boundary sliding, allowing differentiation between these mechanisms by a neutron diffraction experiment. Understanding of the deformation mechanisms is of fundamental interest for modeling of materials behavior. We describe the system HIPPO/CRATES which allows to study *in situ* both the anisotropic elastic strain evolution via the change in peak shift as well as the change in texture via the changes in peak intensity. CRATES, a load-frame for the High Pressure Preferred Orientation diffractometer HIPPO at LANSCE, allows to apply uni-axial stresses up to 100 kN in tension or compression to a specimen. It is equipped with rotation and translation stages for increase of pole figure coverage and alignment, respectively. HIPPO's large detector area allows to measure the full ODF with few sample rotations and provides anisotropic elastic strain information for 20 to 100 different diffraction vectors. First results from an investigation of metals with a hexagonal close packed crystal structure (Mg and Zr alloys) are presented.

**WP58: Second Generation Neutron Residual Stress Mapping Facility at ORNL**

*C. R. Hubbard, M.C. Wright, S. Spooner, E. A. Payzant, S. Craig, A. Stoica (Oak Ridge National Laboratory)*

The replacement of the beryllium reflector at the High Flux Isotope Reactor (HFIR) at Oak Ridge National Laboratory (ORNL) presented an opportunity to make major upgrades of beam tubes, shutters, shielding, neutron optics and instrumentation. The upgrade of the Neutron Residual Stress mapping Facility (NRSF) at HFIR is one of the major instrument upgrades taking advantage of this special opportunity. The NRSF upgrade aims to return to

operation an improved world class strain mapping and research instrument at HFIR, a high flux steady state reactor, and reintegrating it into the Residual Stress User Center suite of instruments used to study residual stress and materials behavior using neutron diffraction as well as laboratory and synchrotron x-ray diffraction.

The upgrades of NRSF aim to greatly improve the system's capabilities and create a second generation strain mapping facility. The upgrades include utilizing: (a) the new larger and higher flux beam at HB-2; (b) a new multiwafer Si, doubly focusing, two crystal monochromator which yields a choice of wavelengths (from 0.145 nm to 0.227 nm) and supports horizontal bending of the monochromator to achieve optimal focusing; (c) two new very stable high precision goniometers, one of which is capable of quite large specimens while the other will enable strain tensor and highly textured specimen studies; and (d) an array of seven 40 x 100 mm active area 1-D position sensitive detectors. The flux on specimen is predicted to be of the order of  $10^8$  neutrons/cm<sup>2</sup>/sec. Estimates of the various gains indicate that approximately a 10-fold improvement in strain measurement capability will be achieved.

As of March 1st we have initiated radiological tests of the shielding and expect in April and May to complete the installation and launch commissioning of the new facility. User access to this instrument is via the High Temperature Materials Laboratory User Program (<http://html.ornl.gov/>). The results of monochromator tests, calibration of the instrument, and initial performance tests will be highlighted.

Research sponsored by the Assistant Secretary for Energy Efficiency and Renewable Energy, Office of FreedomCAR and Vehicle Technologies, as part of the High Temperature Materials Laboratory User Program, Oak Ridge National Laboratory, managed by UT-Battelle, LLC, for the U.S. Department of Energy under contract number DE-AC05-00OR22725.

#### **WP59: Comprehensive analysis of spin dynamics in stripe-ordered $\text{La}_{2-x}\text{Sr}_x\text{NiO}_4$**

*H. Woo (Physics Department, Brookhaven National Laboratory; ISIS, Rutherford Appleton Laboratory), J. M. Tranquada (Physics Department, Brookhaven National Laboratory), A. T. Boothroyd (University of Oxford, U. K.), K. Nakajima (University of Tokyo, Japan), T. G. Perring, C. Frost (ISIS, Rutherford Appleton Laboratory), P. G. Freeman, D. Prabhakaran (University of Oxford, U. K.), K. Yamada (University of Tokyo, Japan)*

The nature of the magnetic excitations in stripe-

ordered nickelates and cuprates is a topic of considerable current interest. Here we will present measurements of spin waves in  $\text{La}_{2-x}\text{Sr}_x\text{NiO}_4$  ( $x = 0.275$  and  $1/3$ ). The data, collected on the MAPS spectrometer at ISIS, provide a comprehensive mapping of the spin excitations throughout the two-dimensional Brillouin zone. We analyze the results using linear spin-wave theory [1], and show that the data provide a clear choice between two alternative models for effective exchange coupling through the charge stripes. The success of semi-classical spin-wave theory for describing excitations in stripe-ordered nickelates contrasts with its failure in the recently studied case of  $\text{La}_{1.875}\text{Ba}_{0.125}\text{CuO}_4$  [2].

HW and JMT are supported by the Office of Science, U.S. DOE under Contract No. DE-AC02-98CH10886.

[1] Boothroyd et al. Phys. Rev. B 67, 100407(R) (2003).

[2] Tranquada et al., cond-mat/0401621.

#### **WP60: Structure and Dynamic of the Superionic Conductor $\text{AgI-Ag}_2\text{S-AgPO}_3$ , measured by HIT-II at KENS and MARI at ISIS.**

*E. Kartini (R & D Center for Materials Science and Technology, National Nuclear Energy Agency, Tangerang 15314, Indonesia), M. Arai, H. Iwase (Neutron Science Laboratory, KEK, Tsukuba, Japan), K. Itoh (Kyoto University Research Reactor Institute, Kumatori-cho, Japan), S Bennington (ISIS, Rutherford Appleton Laboratory), M.F. Collins (Department of Physics and Astronomy, McMaster University, Hamilton, ON, Canada), S.J. Kennedy (Bragg Institute, Australian Nuclear Science and Technology Organisation, Australia)*

Superionic conducting glasses are of considerable technological interest because of their use in batteries, displays, sensors and fuel-cells. One of the main scientific challenges is to explain how the disordered structure of the mixture is related to the high ionic conductivity that can be achieved at ambient temperature. This work presents the relation between the ionic conductivity on the superionic glasses  $\text{AgI-Ag}_2\text{S-AgPO}_3$  and the appearance of a prepeak at low  $Q \sim 0.6-0.9 \text{ \AA}^{-1}$  in the structure factor  $S(Q)$  measured by a time-of flight HIT-II instruments at KENS, Japan and the existence of Boson Peaks at low  $E \sim 2.5 \text{ meV}$  in the dynamic structure factor  $S(Q,E)$  measured by the time-of flight MARI instrument at ISIS, UK. These materials exhibited good conductivity at ambient temperatures. With increasing mol % of  $\text{AgI} + \text{Ag}_2\text{S}$ , the results show (i) rapidly increasing conductivity (ii) slowly decreasing glass transition temperature (iii) increasing intensity and decreasing

Q of the prepeak (iv) increasing the intensity and decreasing energy of the Boson peak. There is a strong correlation between the ionic conductivity and the existence and intensity of both the prepeak and the Boson peak.

#### **WP61: Quantum momentum distribution and kinetic energy in solid $^4\text{He}$**

*S. Diallo, H. R. Glyde (Department of Physics and Astronomy, University of Delaware, Newark, DE 19716), R. T. Azuah (Department of Materials Science and Engineering, University of Maryland; NIST Center for Neutron Research)*

We present measurements of neutron scattering from solid  $^4\text{He}$  at high momentum transfer. The solid is held close to the melting line at molar volume  $21.0 \text{ cm}^3/\text{mol}$  and temperature  $T = 1.6 \text{ K}$ . From the data, we determine the shape of the momentum distribution,  $n(\mathbf{k})$ , of atoms in the solid and the leading Final State contribution to the scattering. We show that  $n(\mathbf{k})$  in this highly anharmonic, quantum solid differs significantly from a Gaussian. The  $n(\mathbf{k})$  is more sharply peaked with larger occupation of low momentum states than in a Maxwell-Boltzmann distribution, as found in liquid  $^4\text{He}$  and predicted qualitatively by Path Integral Monte Carlo calculations. The atomic kinetic energy is  $\langle K \rangle = 24.25 + I - 0.2 \text{ K}$ . If  $n(\mathbf{k})$  is assumed to be Gaussian, as is usually the practice, a  $\langle K \rangle \sim 10\%$  smaller is obtained.

#### **WP62: Effect of the metal-insulator transition on oxygen phonons in Ca-doped $\text{YBa}_2\text{Cu}_3\text{O}_6$**

*S. Chang (Ames Laboratory), R. J. McQueeney (Ames Laboratory; Iowa State University), P. Dai (Oak Ridge National Laboratory; University of Tennessee, Knoxville), F. Dogan (University of Missouri - Rolla), F. R. Trouw (Los Alamos National Laboratory)*

High-temperature superconductors are based on antiferromagnetic insulating materials caused by strong electronic correlations. Doping charge carriers (holes) into this system creates a two-dimensional correlated metallic state in the  $\text{CuO}_2$  plane that becomes superconducting at low temperatures. The development of the metallic state with hole doping and the metallic state itself still remain poorly understood. Inelastic neutron scattering measurements of the lattice dynamics show evidence of strong and unusual electron-lattice coupling in many high- $T_c$  compounds with the primary effect being the large softening of oxygen optical phonons in the energy range from 55-80 meV. Here we present the phonon density-of-states as a function of hole doping in  $\text{YBa}_2\text{Cu}_3\text{O}_6$  obtained from inelastic neutron scattering experiments. The holes were introduced via the

systematic replacement of Y by Ca ( $\text{Y}_{1-x}\text{Ca}_x\text{Ba}_2\text{Cu}_3\text{O}_6$ ), where the Ca concentrations were chosen to straddle the metal-insulator transition (MIT) at  $x \sim 0.2$ .

Changes in the oxygen phonon modes at higher energies arising from electron-phonon coupling (55-80 meV) are well separated from any introduced Ca modes ( $< 40 \text{ meV}$ ), similar to the unambiguous experiments LSCO where holes are introduced by Sr doping. In addition, Ca doping has the advantage of avoiding new oxygen phonon states, as happens when holes are introduced by increasing the oxygen content. We see clear changes in the phonon density-of-states when doping across the MIT, which we attribute to coupling of holes to oxygen phonons.

#### **WP63: Neutron Investigation of Low Temperature Magnetization Steps in CMR Manganites**

*F.M. Woodward, J.W. Lynn (NIST Center for Neutron Research), M.B. Stone, P. Schiffer (Department of Physics and Materials Research Institute, Pennsylvania State University, University Park, PA 16802), D.N. Argyriou (Hahn-Meitner-Institut Berlin), L.C. Chapon (ISIS, Rutherford Appleton Laboratory), J.F. Mitchell (Materials Science Division, Argonne National Laboratory)*

The doped manganite  $\text{Pr}_{0.7}(\text{Ca}_x\text{Sr}_{1-x})_{0.3}\text{MnO}_3$  ( $x = 0.0, 0.7, 0.75$ ), shows anomalous steps in bulk magnetization and resistivity as a function of applied field for  $T < 2 \text{ K}$ , both in powdered and single crystal samples. Neutron diffraction was used as a probe to investigate the nature of these steps. Ferromagnetic and antiferromagnetic intensity as a function of field were measured in a single crystal sample at  $T = 2 \text{ K}$ . On increasing the field from the virgin state the antiferromagnetic phase abruptly disappears at  $H = 1.75 \text{ T}$ , with a concomitant increase in the ferromagnetic intensity. Once the transition occurs, the system remains fixed in the new state when the field is returned to zero. Details of the magnetic and crystallographic structures as a function of field will be presented.

#### **WP64: Distortions and orientations of fulleride ions in $\text{K}_4\text{C}_{60}$ , $\text{Rb}_4\text{C}_{60}$ and $\text{Cs}_4\text{C}_{60}$**

*N. M. Nemes (NIST Center for Neutron Research; Department of Materials Science and Engineering, University of Maryland), Gy. Klupp, G. Oszlanyi, K. Kamaras (Research Institute for Solid State Physics and Optics, Hungarian Academy of Sciences, P. O. Box 49, H-1525 Budapest, Hungary), C. Brown (NIST Center for Neutron Research; Department of Materials Science and Engineering, University of Maryland), J. Leao (NIST Center for Neutron Research)*

$\text{A}_4\text{C}_{60}$  compounds ( $\text{A} = \text{K}, \text{Rb}, \text{Cs}$ ) are good candi-



dates for the Mott-Jahn-Teller insulating state. We have previously shown that in these materials a splitting of vibrational lines occurs on cooling, the transition temperature depending on the counterion. We will now present new low temperature neutron diffraction, inelastic neutron scattering and near-IR data on  $K_4C_{60}$ ,  $Rb_4C_{60}$  and  $Cs_4C_{60}$  to prove that the splitting of the vibrational and electronic excitations is not coupled to a structural phase transition; rather, the driving force behind this change is an interplay between the molecular Jahn-Teller effect and the crystal potential. Between room temperature and 5 K,  $Cs_4C_{60}$  is orthorhombic while  $K_4C_{60}$  and  $Rb_4C_{60}$  are tetragonal; their low-temperature vibrational spectra are, however, identical. Since the molecular point group compatible with the crystal structure is the same in both space groups, the picture we suggest is orientational order in  $Cs_4C_{60}$  and static disorder in  $K_4C_{60}$  and  $Rb_4C_{60}$  between the two standard orientations. With increasing thermal energy, the molecules start to rotate and induce a dynamic disorder. When the time scale of the rotation reaches that of the measurement, the apparent symmetry changes from biaxial to uniaxial. We will discuss this point by comparing our results to methods with different time constants (NMR and ESR).

#### WP65: Proton Tunneling in Supercritical Water

*G.F. Reiter (Physics Department, University of Houston), J.C. Li (Physics Department, University of Manchester), J. Mayers, T. Abdul-Redah (ISIS, Rutherford Appleton Laboratory), P. Platzman (Bell Labs-Lucent Technologies)*

Neutron Compton Scattering measurements can give a detailed measurement of the momentum distribution of light ions in solids and liquids. We present the momentum distribution in ice, room temperature water, supercritical water, and confined supercritical water. While the ice and room temperature water data can be interpreted in terms of nearly harmonic potentials, the supercritical water data shows clear evidence of tunneling, apparently along the bond, over distances of about 0.3 Å. Confinement by hydrophobic surfaces of C60 reduces slightly that distance. The data is consistent with vapor phase at the hydrophobic surfaces, and inconsistent with ice phase formation. The strong anharmonicity makes classical simulations of dubious value in describing supercritical water. We interpret the data in terms of 'inherited tunneling' from the motion transverse to the bond.

#### WP66: Deep Inelastic Neutron Scattering from water in the 1-40 eV energy range employing the Resonance Detector Spectrometer configuration

*R. Senesi, C. Andreani, A. Filabozzi (Universita degli Studi di Roma Tor Vergata, V. Ric. Scientifica 1 00133 Roma Italy; INFN UdR Roma Tor Vergata), G. Gorini (Universita degli Studi di Milano-Bicocca, Dipartimento di Fisica; Istituto Nazionale per la Fisica della Materia), S. Nufri (Universita degli Studi di Roma Tor Vergata, V. Ric. Scientifica 1 00133 Roma Italy; INFN UdR Roma Tor Vergata), E. Perelli-Cippo (Universita degli Studi di Milano-Bicocca, Dipartimento di Fisica; Istituto Nazionale per la Fisica della Materia), A. Pietropaolo (Universita degli Studi di Roma Tor Vergata, V. Ric. Scientifica 1 00133 Roma Italy; INFN UdR Roma Tor Vergata), N. Rhodes, E. M. Schooneveld (ISIS, Rutherford Appleton Laboratory), M. Tardocchi (Istituto Nazionale per la Fisica della Materia; Universita degli Studi di Milano-Bicocca, Dipartimento di Fisica)*

The Resonance Detector Spectrometer configuration has recently been revised on the VESUVIO inverse geometry spectrometer at ISIS spallation source. It appears as the most promising approach for electron Volt neutron spectroscopy due to its effectiveness in detecting neutron up to 70 eV final energy. We employed this experimental configuration on VESUVIO spectrometer for Deep Inelastic Neutron Scattering measurements from a water sample. This has been done in order both to test the behavior of the detection system and to derive the single proton wave vector distribution and mean kinetic energy, at two different thermodynamic conditions, up to final neutron energies of about 37 eV. The results have been compared with those obtained through a simultaneous measurement on VESUVIO, carried out in the standard Resonance Filter Spectrometer configuration. These measurements provide a further confirmation of the effectiveness of the Resonance Detector Spectrometer configuration for electron Volt neutron spectroscopy on inverse geometry instruments operating at pulsed neutron sources.

#### WP67: Crystal structure and phase transition of $K_{0.2}(NH_4)_{0.8}Cl$ mixed salt at low and high temperature

*G. Batdemberel (Mongolian University of Science and Technology, Ulaanbaatar, Mongolia; Darmstadt University of Technology, Darmstadt, Germany), A.N. Skomorokhov (Institute for Physics and Power Engineering, Obninsk, Russia; Darmstadt University of Technology, Darmstadt, Germany), L. Smirnov, A.I. Beskrovny (Joint Institute for Nuclear Research, Dubna, Russia), H. Fuess (Darmstadt*



*University of Technology, Darmstadt, Germany), D. Sangaa (National University of Mongolia, Ulaanbaatar, Mongolia), Sh. Chadraabal (Mongolian University of Science and Technology, Ulaanbaatar, Mongolia)*

Have been carried out the crystal structure studies of  $K_{0.2}(NH_4)_{0.8}Cl$  at room temperature by x-ray and neutron diffraction techniques. It was established that the  $K_{0.2}(NH_{0.8})Cl$  compound has CsCl structure with the Pm3m space group. By using of the x-ray powder diffraction determined lattice parameters, K, N, Cl atom positions and the thermal factors. From the neutron powder diffraction data determined hydrogen atom position. High-resolution differential calorimetric analysis observed phase transition points at the low temperature  $T = 232$  K and at the high temperatures  $T = 425$  K, 458 K, 478 K, 513 K and 573 K. On diffractograms obtained at 232 K temperature appeared along with CsCl structural reflections the low intensity peaks corresponding to superstructure and if in diffraction data Rietveld refinement procedure to be accounted these superstructure reflections the essential CsCl structure transforms to the tetragonal setting distorted by C3v symmetry. At the high temperature points: 425 K, 458 K, 478 K, 513 K and 573 K except the CsCl structure peaks have been observed the low intensity diffraction peaks with a monoclinic symmetry and at the point 478 K occurred a transition of the CsCl structure to the NaCl structure with Fm3m space group.

#### **WP68: Vibrational Entropy of Dissolving Ag in Al**

*T. Swan-Wood, M. Kresch, J. Lin, M. McKerns, B.*

*Fultz (California Institute of Technology)*

There is an unusually strong increase with temperature of the solubility of Ag in fcc Al. This phenomena is not unique to the Al-Ag system and is seen in many binary alloys, particularly those where the impurity has a mass ratio of at least 3 to that of the matrix atom. We hypothesize that low-frequency resonance modes associated with massive solute atoms make a large contribution to the vibrational entropy of mixing. Inelastic neutron scattering spectra were measured on LRMECS at the IPNS from Al, Al-7 at. % Ag, Al-60 at. % Ag, and a 2-phase region (Al-7 at. % Ag and Al-60 at % Ag) at room temperature. Phonon density of state (DOS) curves were obtained by correcting for multi-phonon scattering, Debye-Waller effects, and the thermal factor. The difference in phonon scattering efficiencies of Al and Ag (neutron-weighting) is not large, but we developed methods for correcting this neutron weighting through computer simulations of the lattice dynamics. The phonon DOS from the Al-7 % Ag alloy showed a large resonance mode at low energies. This

resonance mode made a significant contribution of  $0.160 \pm 0.006 k_B/\text{atom}$  to the vibrational entropy of the alloy compared to fcc Al, a significant fraction of the total neutron-weight-corrected entropy of mixing of  $0.09 \pm 0.01 k_B/\text{atom}$ , but there is also a stiffening of some of the vibrational modes. The hcp phase, 60 % Ag, showed a large softening of its phonon DOS compared to Al-7 % Ag. A full correction for the neutron weighting is not possible, but assuming it is not large we deduce a vibrational entropy for Al-60 % Ag that is  $1.35 k_B/\text{atom}$  larger than for fcc Al. Vibrational entropy makes a large contribution to the thermodynamics of phase stability in the Al-Ag system. The mass and probably the size of Ag atoms may be responsible for some of the trends.

#### **WP69: Neutron Diffraction Study of Phase Transformations and Mechanical Properties in Ni[AlFe] Alloys**

*L. Yang (Dept. of Chemical and Materials Engineering, University of Cincinnati, Cincinnati, OH 45221-0012; Spallation Neutron Source, Oak Ridge National Laboratory), X.-L. Wang (Spallation Neutron Source, Oak Ridge National Laboratory; Metals and Ceramics Division, Oak Ridge National Laboratory), J. A. Fernandez-baca (Condensed Matter Sciences Division, Oak Ridge National Laboratory), A. D. Stoica (Spallation Neutron Source, Oak Ridge National Laboratory), C. T. Liu (Metals and Ceramics Division, Oak Ridge National Laboratory), J. W. Richardson (Intense Pulsed Neutron Source, Argonne National Lab)*

Phase transformations in NiAl alloys are complex and have been a subject of extensive experimental and theoretical studies. The martensitic transformation in NiAl alloys involves the formation of long period stacking orders, which can be either B2-2M(3R, L10) or B2-17M(7R) depending on the composition. When magnetic transitional atoms (e.g., Fe, Mn) are added, various types of magnetic properties appear due to the competition of ferromagnetic and antiferromagnetic interactions. The study by Morito et al. [1,2] on Ni50[AlxMn50-x] shows a continuous martensitic transformation of B2-10M-14M, and a magnetic phase transition from a paramagnetic to an antiferromagnetic and finally to a spin glass state. It is not yet clear whether or how the martensitic and magnetic phase transformations are related.

Our interest in Ni[AlFe] alloys was prompted by a recent systematic study that reported an unusual softening behavior in mechanical properties [3]. First-principle calculations revealed that when Fe atoms are added, a localized moment of  $2.4 \mu_B$  develops at the Fe site. The calculations further

suggest that the magnetic interactions enlarge the atomic size of the Fe atom, which lead to the increase of the lattice parameter and hence the softening effect. If these explanations hold, magnetic interactions may be explored as a new mechanism to alter the mechanical property of metallic materials, which would open up a new way in the design of metallic materials for structural applications.

We have carried out preliminary characterizations of Ni[AlFe] alloys. Magnetic susceptibility measurements confirmed that when Fe replaces Al, a localized moment develops. Upon cooling, a paramagnetic to ferromagnetic transformation was observed, and the system goes to a spin-glass state below 12 K. Neutron diffraction data collected at High Flux Isotope Reactor showed an intensity gain at low temperatures, which followed a Q-dependence reminiscent of magnetic scattering. Meanwhile, high-resolution powder diffraction data collected at IPNS revealed extra Bragg peaks below 20 K. Upon warming up, these extra peaks disappear at temperatures above 50 K. While the experimental data are still being analyzed, the thermal hysteresis and Q-dependence of the extra peaks suggest that they came from a martensitic phase transformation. More systematic studies are underway to determine the structure and the nature of phase transformations in Ni[AlFe] alloys and their relationship with the usual mechanical properties.

This research was supported by Division of Materials Sciences and Engineering, Office of Basic Energy Sciences, U.S. Department of Energy under Contract DE-AC05-00OR22725 with UT-Battelle, LLC.

[1] S. Morito, K. Otsuka, *Mat. Sci. Engr.*, A208, 1996, 47-55

[2] S. Morito, T. Kakeshita, K. Hirata and K. Otsuka, *Acta Mater.*, 46, 1998, 5377-5384

[3] C.T. Liu, C.L. Fu, L.M. Pike, and D.S. Easton, *Acta Mater.*, 50, 2002, 3205-3212

#### **WP70: PDF analysis of local distortions in $Ti_2Sb$ and $CeTe_3$**

*H. J. Kim, X. Qiu, S. J. L. Billinge (Department of Physics & Astronomy, and Center for Fundamental Materials Research Michigan State University, East Lansing, Michigan 48824), S. Derakhshan, A. Assoud, E. Dashjav, H. Kleinke (Department of Chemistry University of Waterloo, Waterloo, ON, Canada N2L 3G), C. Malliakas, T. Kyratsi, M. G. Kanatzidis (Department of Chemistry, and Center for Fundamental Materials Research Michigan State University, East Lansing, Michigan 48824), P.J. Chupas, C.P. Gray (State University of New York, Stony Brook, NY 11794-2275), P.L. Lee (Advanced*

*Photon Source, Argonne National Laboratory, Argonne, IL)*

Recent years have seen enormous progress in developing novel electronic materials. Mounting evidence suggests that structures, defects, and interactions on nanometer length-scales are intimately connected to their remarkable properties. Therefore, precisely resolving these structures is inevitable for the ultimate understanding of the properties of the materials and it requires advanced local techniques such as atomic Pair Distribution Function (PDF) analysis. Local distortions in two materials,  $Ti_2Sb$  and  $CeTe_3$ , are investigated using PDF analysis. The single crystal x-ray study on a new binary antimonide  $Ti_2Sb$  suggests a new type of distortion in the Ti square planar nets. The PDF analysis on this system verifies that Ti nets deform to squares and rhombs in order to enhance Ti-Ti bonding. Formation of 1:1:7 superstructure on a layered chalcogenide  $CeTe_3$ , also known as a charge-density wave material, is observed by the single crystal x-ray and TEM studies. The chemical, physical, and electronic properties of this material are largely decided by Te square nets whose average Te-Te bond ( $\sim 3.1$  Å) is larger than the normal covalent Te-Te bond ( $\sim 2.8$  Å). The PDF measurements suggest that local structural distortions occur in the Te square nets forming short bonds around 2.8 Å resulting in a 1:1:7 superstructure.

#### **WP71: Acoustic Mode Confinement in Nano-Crystalline Yttria**

*M.P. Hehlen, F.R. Trouw, J.T. Mang (Los Alamos National Laboratory), R.M. Laine (University of Michigan, Ann Arbor, MI 48109)*

Nano-crystalline cubic yttria ( $Y_2O_3$ ) was prepared by liquid-feed flame spray pyrolysis. The mean particle diameter was 21 nm as determined by small-angle x-ray scattering and assuming polydisperse spheres. Inelastic neutron scattering from nano-crystalline and coarse-grained  $Y_2O_3$  at 15 K was measured with an incident energy of 90 meV ( $\Delta E/E \sim 6\%$ ) on the Pharos spectrometer at LANSCE. The phonon density of states (PDOS) of both the nano-crystalline and the coarse-grained  $Y_2O_3$  exhibits a number of well resolved peaks in the 15-75 meV range that are in agreement with optical phonons observed by Raman scattering and infrared absorption. Relative to coarse-grained  $Y_2O_3$ , the PDOS of nano- $Y_2O_3$  is substantially enhanced in the 5-30 meV range by a broad asymmetric band peaking at 10 meV. This additional phonon density is due to acoustic modes becoming confined on the length scale of the nano-particles. The confined acoustic modes are analyzed using a model of homogeneous, elastic spheres as well as

molecular dynamics calculations.

#### **WP72: SANS Data Reduction and Analysis Using ISAW**

*A. Chatterjee (Intense Pulsed Neutron Source, Argonne National Lab), R. Mikkelsen, D. Mikkelsen, M. Miller, B. Serum, C. Bouzek (University of Wisconsin-Stout), J. Hammonds, T. Worlton, J. Tao (Intense Pulsed Neutron Source, Argonne National Lab)*

Small-angle neutron scattering (SANS) instruments probe sizes and shapes on length scales of  $\sim 0.5 - 100$  nm. A wide range of systems that include biological, chemical, solid-state can be studied using SANS. Typically, these instruments use low-angle forward scattering techniques and have area detectors the data from which is reduced to produce scattering intensity,  $I(q)$ . A number of steps precede the calculation of  $I(q)$  like calculation of the beam center, sensitivity of the detector pixels, transmission coefficients etc. Integrated Spectral Analysis Workbench (ISAW) is a software package developed at IPNS to reduce, analyze and visualize neutron scattering data. It has recently started supporting the upgraded small-angle neutron scattering instrument (SAND) at IPNS. ISAW provides a collection of scripts and wizards that do all the steps in the SAND data treatment. The scripts and wizards make use of java operators in ISAW. To process multiple runs, ISAW provides a script that processes files in a batch mode. The  $q$  bins can be 1 or 2 dimensional with a resolution that can be set in the scripts. A number of viewers that come with ISAW can be used to look at the reduced files and the output from some viewers of data collected on SAND will be presented.

#### **WP73: SPICE – Spectrometer Instrument Control Environment**

*M.D. Lumsden, J.L. Robertson, M. Yethiraj (HFIR Center for Neutron Scattering, Oak Ridge National Laboratory, Oak Ridge, Tennessee 37831, USA.)*

We have developed a LabVIEW-based data acquisition system for neutron scattering instruments with initial implementation on the triple-axis spectrometer. The software is written with a modular framework to allow easy expansion to handle different instruments, commands, and user interfaces. At the core of the software is a command-line parsing engine which sequentially executes commands from an execution stack. Commands can be added to the execution stack via by directly typing into the command line, from the included graphical user interface or from web-based interfaces. The hardware interface layer is based on object-oriented programming concepts

allowing easy addition and removal of hardware. Flexibility is achieved through an alias structure, the ability to write lists of commands into a macro, the ability to produce custom scans, and full scripting through an ActiveX interface with Python. User downloadable executables allow monitoring of the instrument status remotely and basic data analysis and visualization. The triple-axis version of SPICE incorporates a full UB-matrix implementation which can handle general crystal symmetry and movements out of the scattering plane. This program has been successfully running the HB1A, HB1 and HB3 triple-axis spectrometers at the High-Flux Isotope Reactor for over 1 year and is being extended to operate the powder diffractometer and wide-angle neutron diffractometer (WAND).

#### **WP74: New Software for Single Crystal, Time-of-Flight Neutron Scattering Instruments**

*Dennis Mikkelsen (University of Wisconsin-Stout), Arthur Schultz (Argonne National Laboratory), Peter Peterson (Oak Ridge National Laboratory), Ruth Mikkelsen (University of Wisconsin-Stout), Thomas Worlton, John Hammonds, John Cowan, Martha Miller (Argonne National Laboratory), Chris Bouzek, Michael Miller (University of Wisconsin-Stout)*

Single crystal time-of-flight neutron scattering experiments provide information about three dimensional regions in reciprocal space. A new set of software tools for single crystal diffractometers has been developed. The software includes components for instrument calibration, data visualization, finding and indexing peaks, fitting orientation matrices and peak integration. The instrument calibration software adjusts multiple instrument parameters to minimize the sum squared differences between calculated peak positions and measured peak positions in reciprocal space, for a known sample. User friendly “wizards” guide the user through the data reduction process. This software is currently in use at the single crystal diffractometer at IPNS and can process single crystal data from NeXus files. This software was developed in the context of the Integrated Spectral Analysis Workbench (ISAW) project at the Intense Pulsed Neutron Source Division of Argonne National Laboratory, with support from the National Science Foundation.

#### **WP75: DANSE – distributed data analysis for neutron scattering**

*M.M. McKerns, M.A.G. Aivazis, T.M. Kelley, S.J. Kim, B. Fultz (California Institute of Technology)*

The DANSE system will merge the various computational tasks of neutron scattering into a unified, component-based runtime environment. Standard



components will implement data analysis, visualization, modeling, and instrument simulation for all major areas of neutron scattering. A core technology of DANSE is an open source software framework that supports the components and mediates their interactions. Within the DANSE environment, users will be able to mix and match different software components without compilation, and execute calculations seamlessly across distributed resources. DANSE will provide tools to help instrument scientists and expert users migrate their existing routines (written in any of a number of languages) to components, and an interface that allows new and casual users to access a stock set of standard analysis applications or configure their own new computing procedures for novel experiments. The modular structure of DANSE parallels the steps of data analysis performed by scientists, thus making it a natural environment for creating flexible computing procedures. DANSE will lower barriers to sharing software, and extend the experimentalist's toolkit with capabilities of analysis and interpretation such as high-performance simulations (band structure, molecular dynamics, etc.), co-analysis of data from multiple experiments, and real-time feedback for experiment control.

#### **WP76: NCNR reflectometry software**

*P.A. Kienzle (NIST Center for Neutron Research; University of Maryland, College Park), K.V. O'Donovan (NIST Center for Neutron Research; University of California at Irvine)*

At the NCNR we have been developing a graphical user interface (GUI) for our data reduction and analysis tools. We support the reduction of raw data for monochromatic source neutron and x-ray reflectometry for NCNR data formats. For analysis we use a multi-layer model evaluated using the Parrat formalism. Interfaces are approximated by a series of layers, which allows the interface effects to be computed accurately even for very broad interfaces. Arbitrary constraints between the parameters for the different layers can be programmed by the user. We support polarized beam data, allowing us to reduce and analyze magnetic as well as nuclear effects on reflectivity.

The GUI for reduction strives to be flexible while conveniently supporting the common operations required for selection and manipulation of the data. The GUI for analysis is distinct from others in that it allows direct manipulation of the scattering length density profile rather than entering layer parameters by hand. Our software is based on an underlying scripting language (Tcl/Tk) with direct access available within the program. For those cases where the GUI

has not anticipated the needs of the user, the user is free to modify data from the console without abandoning the entire GUI. Thus our software is suited both to the new user performing standard measurements as well as the expert user performing new types of measurements on our instruments.

Since the introduction of our software at the NCNR, the benefits have been great. Data reduction tasks that used to take hours can now be done in minutes. The results are more reliable since the data is in view at every step in the transformation, which makes instrumental errors easier to detect. Training time for new users is considerably reduced, leading to a more pleasant experience for our users and freeing time for our support staff.

#### **WP77: The State of NeXus**

*P.F. Peterson (Spallation Neutron Source, Oak Ridge National Laboratory)*

During the course of the last year, the NeXus data format for neutron and x-ray scattering has undergone several changes which improve usability and increase the number of applications available. The NeXus International Advisory Committee has been formed, with representation from eleven facilities around the world, including all the US neutron scattering facilities. This committee is charged with providing formal ratification for the instrument components, defined in XML. I will present recent changes to the abstract programmer's interface (API), enhanced data browsing and validation utilities, and a selection of software that is NeXus aware.

#### **WP78: Neutron spin echo study of AOT reverse micelles with application to metallic nanoparticle synthesis and compressible fluids**

*Christopher L. Kitchens and Christopher B. Roberts (Department of Chemical Engineering, Auburn University, AL 36830), Dobrin Bossev (University of Maryland, College Park; National Institute of Standards and Technology)*

The common surfactant, AOT (Sodium bis-2-ethylhexyl-sulfosuccinate), forms thermodynamically stable water-in-oil microemulsions containing self-assembled spherical reverse micelles. The reverse micelles consist of a small water pools encased in an AOT surfactant monolayer and dispersed within a bulk organic fluid. The nanometer sized water core acts as a "nanoreactor" for aqueous phase reactions, eg. metallic nanoparticle synthesis within the micelle cores. It has been demonstrated that the metallic nanoparticle growth rate and the average particle size synthesized are influenced by the size of the reverse micelle,



represented by  $W$  where  $W = [H_2O]/[AOT]$  and the thermophysical properties of the bulk alkane solvent, specifically the solvent interactions with the surfactant tails. Studies of reverse micelle dynamics in solution have shown that adjustable parameters such as the bulk solvent properties and  $W$  influence the intermicellar exchange rate. In this work, we propose to use Small Angle Neutron Scattering (SANS) correlated with Neutron Spin Echo (NSE) Spectroscopy to study reverse micelle dynamics as a function of the bulk d-alkane solvent and the size of the reverse micelles. NSE offers the unique ability to perform dynamic measurements of thermally induced shape fluctuation in the AOT surfactant monolayer, however the time averaged, static SANS measurements are necessary to obtain pertinent information from the dynamic system, specifically the bending elastic modulus and saddle-splay elastic modulus.

**W2-A, Mechanical Behavior and Residual Stress, Chair: Henry Prask (NIST), Room 1123 Blue**

**W2-A1 (13:30) Residual Stress and Texture in Engineering Materials (Invited)**

*J. H. Root (National Research Council, Chalk River, Ontario, Canada)*

Because neutrons penetrate easily through many engineering materials, neutron diffraction can often be applied to determine distributions of stress or crystallographic texture, non-destructively, inside intact engineering components. Experimental knowledge obtained by neutron diffraction has refined ideas about the deformation of polycrystalline materials and validated simulations of material behaviour during processing, service and failures. This knowledge has proven to be of great interest to various industries, because it can address issues of safety, regulations, competitiveness and market penetration. In parallel, neutron diffraction measurements of residual stress and texture have opened new opportunities for fundamental materials science, attracted a new user community to the sphere of neutron scattering and stimulated the development of new neutron instruments and methods. This presentation will provide some illustrations of residual stress and texture studies at Chalk River Laboratories, where materials science and engineering projects occupy more than one third of available neutron beam time. We shall consider the state of the art, as practised at neutron facilities worldwide, and list some of the experimental and scientific challenges in this field.

**W2-A2 (14:00) The use of neutron diffraction and polycrystal plasticity modeling to understand deformation in hexagonal metals.**

*D. W. Brown, M. A. M. Bourke, W.R. Blumenthal, S.C. Vogel, C. N. Tome (Los Alamos National Laboratory), T. M. Holden (Northern Stress Technologies), K. Conlon (Chalk River), S.R. Agnew (University of Virginia)*

Due to the high crystallographic symmetry of body-centered and face-centered cubic metals, plastic deformation is relatively simple because one unique slip mode can provide arbitrary deformation. This is not true in lower symmetry hexagonal metals, where prismatic and basal slip (the usual favored modes) are insufficient to provide arbitrary deformation. Often, either pyramidal slip and/or deformation twinning must be activated to accommodate the imposed plastic deformation. The varied difficulty of activating each of these deformation mechanisms results in highly anisotropic yield surface and subsequent mechanical properties. Further, the incipient activity of each deformation mode may be manipulated through control of the crystallographic texture, opening new opportunities for the optimization of mechanical properties for a given application. This talk will highlight studies done by several researchers at the neutron scattering center at Los Alamos over the past two years focused on the combined use of neutron diffraction measurements and computational modeling to understand micro-mechanical deformation mechanisms in hexagonal metals, in particular Be, Mg, Ti, and Zr.

**W2-A3 (14:15) Residual stresses in cold-drawn eutectoid wires**

*J. Ruiz-Hervias (NIST Center for Neutron Research; Departamento de Ciencia de Materiales, Universidad Politecnica de Madrid. c/ Profesor Aranguren s/n, E-28040 Madrid (SPAIN)), V. Luzin, H. Prask, T. Gnaeupel-Herold (NIST Center for Neutron Research), M. Elices (Departamento de Ciencia de Materiales, Universidad Politecnica de Madrid. c/ Profesor Aranguren s/n, E-28040 Madrid (SPAIN))*

Textures and residual stresses have been determined in cold-drawn eutectoid steel wires (pearlitic microstructure composed of ferrite and cementite phases) by neutron diffraction using the BT8 diffractometer at the NIST Center for Neutron Research (NCNR). Samples corresponding to different stages in the drawing process, and consequently subjected to different plastic deformation were examined. The wire sizes ranged from 10.5 to 5.2 mm diameter and all had the same composition (plain carbon steel with 0.8% C). Stress profiles along three principal direc-

tions (axial, radial and hoop) were obtained for the ferrite phase for all the samples with spatial resolution through the wire diameter better than 1 mm. The gauge volume for the radial and hoop components was  $0.5 \times 15 \times 0.5 \text{ mm}^3$ , whereas for the axial component it was  $1 \times 1 \times 1 \text{ mm}^3$ . Different reflections had to be used because diffraction peak intensity was significantly diminished in certain directions due to texture. The results are consistent with earlier measurements, but are the first which examine residual stress evolution for different processing stages in commercial wires.

#### **W2-A4 (14:30) Residual Stress Determination in Thermally Sprayed Metallic Coatings by Neutron Diffraction**

*W. Wagner, T. Keller (Paul Scherrer Institut, 5232 Villigen-PSI, Switzerland), N. Margadant (EMPA Swiss Federal Laboratories for Materials Testing and Research, Thun, Switzerland), T. Pirling (Institut Laue Langevin)*

Thermally sprayed coatings are nowadays widely applied in industrial technology for surface protection or improvement of surface properties for specific applications. Among others, residual stresses often play a crucial role in the performance and lifetime of such coatings and therefore, their determination is of general interest.

The present study investigates metallic NiCrAlY deposits (chemical composition 67wt. % Ni, 22wt. % Cr, 10wt. % Al, 1wt. % Y) on steel substrates. Neutron diffraction was used to obtain spatially resolved strain and stress profiles in the deposits and the underlying steel substrates. For the neutron diffraction measurements special emphasis was given to a high spatial resolution when entering the surface and crossing the interface to the substrate. Samples of four different spray techniques were analyzed: atmospheric and water-stabilized plasma spraying (APS and WSP), flame spraying (FS) and wire arc spraying (WAS). The results are quantitatively compared with the average in-plane residual stress determined by complementary mechanical profilometry (bending tests). While the stress profiles from the surface to the interface in the deposits are similar for all investigated spray techniques, their absolute values and gradients vary strongly. This is attributed to different quenching stresses from the impinging particles, different thermal histories the deposit/substrate systems undergo during the spraying and subsequent cooling, and also to different coating properties. In the WSP- and WAS-deposits, a gradient in the stress free lattice parameter was observed. Crack formation is found to be a dominant

mechanism for stress relaxation in the surface plane.

#### **W2-B, Lipids and Micelles, Chair: Shenda Baker (Harvey Mudd), Room 2100/2/4 Red**

##### **W2-B1 (13:30) Surface constraints and membrane phase miscibility gaps (Invited)**

*W. A. Hamilton (Condensed Matter Sciences Division, Oak Ridge National Laboratory), L. Porcar (NIST Center for Neutron Research), G.S. Smith (Condensed Matter Sciences Division, Oak Ridge National Laboratory)*

In many surfactant membrane systems the competition between intrinsic curvature and membrane composition leads to large miscibility gaps in which membrane phases of very different geometries coexist in the bulk. Depending on the phase geometries we would expect the bulk equilibrium balance to be affected by the ordering potential exerted by a proximate surface. In this work we consider a situation in which the effect should be relatively strong: when one of the coexisting phases, the so-called  $L_3$  “sponge”, is a manifestly isotropic convolution of membranes for which any accommodation to a flat surface will represent a significant distortion, whereas for the other, a regularly stacked  $L_\alpha$  lamellar phase, it should not. Using neutron reflectivity and “Near-Surface” SANS (NS-SANS) we have tracked a temperature driven  $L_3$  to biphasic  $L_3 + L_\alpha$  transition in an AOT membrane solution near the quartz surface of a reflection geometry sample cell. The NR signal allows us to probe the membrane conformation to a depth of order 1000 Å, a relatively few membrane separations from the solid-solution interface (the expected range of any ordering potential), while the NS-SANS signal allows simultaneous monitoring of “bulk” phase behavior corresponding to the surface signal to depths of tens of  $\mu\text{m}$ . While these are static measurements, we note that these phases are to some extent stabilized by hydrodynamic fluctuations. These have well known structural consequences in the bulk, such as logarithmic correction of the scaling of characteristic lengths with respect to dilution. In the vicinity of the surface these fluctuation modes will be inhibited, narrowing their spectrum, so the surface may be expected to frustrate these membrane phases dynamically as well as geometrically.

\* Research sponsored by the U.S. Department of Energy under contract DE-AC05-00OR22725 with ORNL managed by UT-Battelle, LLC.

##### **W2-B2 (14:00) Structural Characterization and Solution Behavior of Polymerized Rod-like Surfactant Micelles**

*Michael J. Gerber, Lynn M. Walker (Department of*

*Chemical Engineering, Center for Complex Fluids Engineering, Carnegie Mellon University, Pittsburgh PA)*

The polymerization of elongated micellar structures offers a novel approach to the production of high aspect ratio, water-soluble amphiphilic nanorods. A cationic surfactant is used as a template to polymerize a vinyl-containing counterion, cetyltrimethylammonium 4-vinylbenzoate (CTVB) based on procedures presented by Kline (Kline, S. R., *Langmuir* 15:2726 1999). The surfactant-polyacid aggregate that forms results in high aspect ratio nanoparticles. In this work, the influence of initiator concentration on particle length and structure is characterized. Small angle neutron scattering and light scattering are combined to characterize the dimensions and the solution behavior of the polymerized aggregates. Scattering provides evidence that the aggregates have a net negative charge, explaining their solubility and stability. NMR studies reinforce this observation and indicate that the surfactant is able to dissociate while the polymerized counterion is trapped in the aggregate. Finally, GPC of the polymer extracted from the aggregates indicates that approximately 2 chains are immobilized in each aggregate. Results demonstrate our ability to control aggregate dimensions and properties. This procedure offers an inexpensive and simple approach to generate nanorods with a diameter of 4nm and aspect ratios ranging from 20 to 60.

#### **W2-B3 (14:15) Formation of Lipid Membranes Assembled on Ordered Nanocomposite and Nanoporous Silica Thin-Films: A Neutron Reflectivity Study**

*D. A. Doshi, A.M. Dattelbaum, E.B. Watkins, J. Majewski, A.P. Shreve (Los Alamos National Laboratory), A.N. Parikh (University of California-Davis)*

Ordered nanocomposite and nanoporous silica thin-films are promising platforms for supporting lipid membrane architectures that mimic biological systems. In this study we have systematically investigated the viability and the interfacial characteristics of phospholipid membranes formed on ordered silica thin-films using neutron reflectivity. The non-destructive nature and long penetration depth of neutrons (compared to x-rays) makes neutron reflectivity an ideal technique to study the soft silica film-membrane and membrane-water interfaces. Silica thin-films used here were prepared via an evaporation induced self-assembly process, which involves the hierarchical organization of organic surfactant and inorganic silica building blocks. POPC (1-Palmitoyl-2-Oleoyl-sn-Glycero-3-Phosphocholine) lipid mem-

branes were then deposited on the silica thin-film surfaces by vesicle fusion. The nature of the silica thin-film surface was found to be critical for the vesicle fusion process. In case of vesicle fusion on a self-assembled nanocomposite silica film, where the templating surfactant is present, a low-density lipid membrane was formed. When the templating surfactant was removed via photo-calcination, a densely packed lipid bilayer formed on the surface. The silica surfaces were also modified with a self-assembled silane monolayer prior to lipid membrane formation. A detailed analysis of all the thin-film/lipid membrane interfaces and structures formed will be presented.

#### **W2-B4 (14:30) Neutron Spin-Echo Study of Dynamics of Hydrophobically Modified Polymer Doped Surfactant Bilayers**

*R. K. Prud'homme (Department of Chemical Engineering, Princeton University, Princeton, NJ 08544-5263), B.-S. Yang (Bristol-Myers Squibb, One Squibb Drive, New Brunswick, NJ 08903), J. Lal (Intense Pulsed Neutron Source, Argonne National Laboratory, Argonne, IL 60439), M. Mihailescu, M. Monkenbusch, D. Richter (Institut fur Festkorperforschung-Forschungszentrum Julich D-52425 Julich, Germany), J. S. Huang (Department of Chemical Engineering, Princeton University, Princeton, NJ 08544-5263), J. Kohn (Department of Chemistry, Rutgers University, Piscataway, NJ 08854), W. B. Russel (Department of Chemical Engineering, Princeton University, Princeton, NJ 08544-5263)*

We characterize the effect of adsorbed hydrophobically modified polymers (hm-polymers) on the dynamics of surfactant bilayers by small-angle neutron scattering (SANS) and neutron spin-echo (NSE) spectroscopy. Two kinds of hm-polymers, (a) hydrophobically modified poly(acrylate) (hmPAA) with tetradecyl ( $C_{14}$ ) sidegroups randomly grafted to the poly(acrylate) backbone and (b) poly(PEG<sub>6k</sub>-lysine-stearylamine) (hmPEG) with equally spaced hydrophobes, are added to bilayers of penta(ethylene glycol) dodecyl ether ( $C_{12}E_5$ ) and hexanol. Both bare and polymer doped membrane exhibit a stretched exponential relaxation in the form of  $I(\mathbf{q}) \equiv S(\mathbf{q}) \exp(-\Gamma_q t)^{2/3}$ , where  $S(\mathbf{q})$  is the static structure factor and  $\Gamma_q$  is the relaxation rate. The relaxation rate depends subtly on the surface-coverage of polymer. At high surface coverage, polymer slows down the relaxation by 20 %; whereas at low surface coverage, polymer enhances the rate relative to the bare membranes. Hindered flow of solvent through the adsorbed polymer layer at high coverage appears to explain retardation. The



faster dynamics at low polymer coverage may be due to stiffening of the membrane or lateral diffusion of the dilute adsorbed polymer chains. The  $\mathbf{q}$  range covered by the static and dynamic measurements coincide. The slowest relaxation rate occurs at length scales (i.e.,  $\mathbf{q}$  vectors) of the diffraction peak corresponding to interlamellar spacings. The quality of the NSE data available invites the development of new theories of the dynamics of lamellar phase liquid crystalline fluids.

## W2-C, Cobaltates, Chair: James Jorgensen (ANL), Auditorium

### W2-C1 (13:30) Structural and Physical Properties of the $\text{Na}_x\text{CoO}_2$ system (Invited)

*Y. S. Lee (Massachusetts Institute of Technology)*

Sodium cobalt oxide,  $\text{Na}_x\text{CoO}_2$  (with  $x \sim 0.7$ ), has received considerable attention due to its unusual thermal electric properties. Recent studies have revealed anomalous non-Fermi liquid behavior in transport properties which point to the importance of strong correlations. Interest in this material escalated with the discovery of superconductivity in  $\text{Na}_x\text{CoO}_2 + y\text{H}_2\text{O}$  when the sodium concentration is reduced to about 0.3 and water is intercalated between the layers. We have developed a novel electrochemical de-intercalation method and have used this to successfully produce single crystal samples of  $\text{Na}_x\text{CoO}_2$  with a wide range of compositions ( $x = 0.3$  to 0.75). We have performed scattering experiments on both hydrated superconductors and non-hydrated samples. We will discuss our results and how they relate to our measurements of the physical properties in this interesting class of materials.

### W2-C2 (14:00) Crystal structure of $\text{Na}_x\text{CoO}_2$ ( $x$ from 1 to 0.3) at room temperature

*Q. Huang (NIST Center for Neutron Research), M.L. Foo (Department of Chemistry, Princeton University, Princeton NJ), J.W. Lynn (NIST Center for Neutron Research), H.W. Zandbergen (National Centre for High Resolution Electron Microscopy, Technical University Delft, The Netherlands), B. Toby (NIST Center for Neutron Research), R.J. Cava (Department of Chemistry, Princeton University, Princeton NJ)*

The crystal structure of  $\text{Na}_x\text{CoO}_2$  ( $x$  from 1 to 0.3) has been studied using the neutron powder diffraction technique. The structure consists of layers of edge-shared  $\text{CoO}_6$  octahedra in a triangular lattice (hexagonal lattice  $a_H \sim 2.85$  and  $c_H \sim 10.8$  Å), with Na ions occupying ordered or disordered positions in the interleaving planes that form by four different Na

ions order/disorder configurations. For  $x = 1$  the Na ions are completely ordered and fully occupy the  $2d$  ( $2/3, 1/3, 1/4$ ) site of a  $P6_3/mmc$  symmetry. At  $x = 0.5$  the Na ions occupy the  $2a$  and  $2b$  sites of  $Pnmm$  symmetry ( $a_o \sim 1.73a_H, b_o \sim 2a_H, c_o \sim c_H$ ), forming zigzag chains. In the range of  $x$  between 1 and 0.75, the Na ions randomly occupy the  $2b(0, 0, 1/4)$  and  $2c(2/3, 1/3, 1/4)$  sites of  $P6_3/mmc$  symmetry and the occupancy at the  $2c$  site increases with  $x$  increasing. For  $x$  between 0.75 and 0.5 and between 0.5 and 0.3, the Na randomly occupy the  $2b(0, 0, 1/4)$  and  $6h(2x, x, 1/4)$  sites in  $P6_3/mmc$  and the occupancy at the  $6h$  site decreases with decreasing  $x$ . Structural parameters as a function of  $x$  indicate slope changes at  $x = 0.75$ .

### W2-C3 (14:15) Crystal Structure of the Sodium Cobaltate Deuterate Superconductor

#### $\text{Na}_x\text{CoO}_2 \cdot 4x\text{D}_2\text{O}$ ( $x = 1/3$ )

*M. Avdeev, J.D. Jorgensen, D.G. Hinks, J.C. Burley, S. Short, P.W. Barnes (Materials Science Division, Argonne National Laboratory)*

Neutron and x-ray powder diffraction have been used to investigate the crystal structures of a sample of the newly-discovered superconducting sodium cobaltate deuterate compound with composition  $\text{Na}_{0.31(3)}\text{CoO}_2 \cdot 1.25(2)\text{D}_2\text{O}$  and its anhydrous parent compound  $\text{Na}_{0.61(1)}\text{CoO}_2$ . The deuterate superconducting compound is formed by coordinating four  $\text{D}_2\text{O}$  molecules (two above and two below) to each Na ion in a way that gives Na-O distances nearly equal to those in the parent compound. One deuteron of the  $\text{D}_2\text{O}$  molecule is hydrogen bonded to an oxygen atom in the  $\text{CoO}_2$  plane and the oxygen atom and the second deuteron of each  $\text{D}_2\text{O}$  molecule lie approximately in a plane between the Na layer and the  $\text{CoO}_2$  layers. This coordination of Na by four  $\text{D}_2\text{O}$  molecules leads to ordering of the Na ions and  $\text{D}_2\text{O}$  molecules. The sample studied here, which has  $T_c = 4.5$  K, has a refined composition of  $\text{Na}_{0.31(3)}\text{CoO}_2 \cdot 1.25(2)\text{D}_2\text{O}$ , in agreement with the expected 1:4 ratio of Na to  $\text{D}_2\text{O}$ . The crystal structure of the intermediate monolayer hydrate is discussed.

### W2-C4 (14:30) Spin structure and dynamics in the half-doped $\text{La}_{1.5}\text{Sr}_{0.5}\text{CoO}_4$ (Invited)

*I. A. Zaliznyak, J. M. Tranquada, G. Gu (Physics Department, Brookhaven National Laboratory), R. W. Erwin (National Institute of Standards and Technology), Y. Moritomo (Center for Integrated Research in Science and Engineering (CIRSE), Nagoya University, Nagoya 464-8601, Japan)*

Magnetic order and spin dynamics in the charge-ordered phases of the doped, strongly correlated transition metal oxides such as superconducting



cuprates, magnetoresistive manganites, etc., are at the focus of the modern condensed matter research. The interplay of charge, spin and/or orbital degrees of freedom in these systems results in non-trivial ground states and leads to many fascinating physical properties, such as a magnetic field driven metal-insulator transition, etc. In order to understand the relative importance of the various interactions it is imperative to explore the properties of different materials in the strongly correlated oxides family. Here we report a study of the charge and spin order and the spin dynamics in the half-doped cobaltate,  $\text{La}_{1.5}\text{Sr}_{0.5}\text{CoO}_4$ , by elastic and inelastic neutron scattering. We find a short-range correlated, glassy charge order (CO) which occurs at a very high temperature,  $T_c = 825(25)$  K. It is of the checkerboard type, which is not unexpected at half doping, and is essentially two-dimensional. This ordering does not seem to depend on the spin order, which is incommensurate and occurs only below  $T_s \sim 30$  K. The spin system, on the contrary, is essentially defined by the charge-ordered ground state, where  $\text{Co}^{3+}$  ions are in the  $S = 1$ , intermediate spin (IS) state. As a result, these ions seem to be quenched to the  $S^z = 0$  state at low  $T$  by the strong single-ion anisotropy, and do not participate in the static magnetic ordering. However, they bridge the magnetic  $\text{Co}^{2+}$  ions and introduce a diagonal, frustrating coupling between them. Peculiar coupling of the  $\text{Co}^{2+}$  and  $\text{Co}^{3+}$  spin systems leads to a very unusual spin dynamics, where a well-defined 2D spin waves with bandwidth  $\Delta_{\text{sw}} \sim 15$  meV are followed by a broad continuum scattering at  $E > 20$  meV.

**W2-D, Low Dimensional Magnetism, Chair:  
Stephen Nagler (ORNL), Room 2101/3/5 Green**

**W2-D1 (13:30) Spin Echo Study of the Dynamics of Spin Ice (Invited)**

**G. Ehlers** (Spallation Neutron Source, Oak Ridge National Laboratory), **J. S. Gardner** (Physics Department, Brookhaven National Laboratory; NIST Center for Neutron Research), **N. Rosov** (NIST Center for Neutron Research), **W. Häußler** (Institut Laue Langevin), **S. T. Bramwell**, **J. Lago** (Department of Chemistry, University College London, 20 Gordon Street, London WC1H 0AJ, UK)

Neutron spin echo measurements have been performed at NIST and at ILL on the spin ice related materials  $\text{Ho}_{2-x}\text{Y}_x\text{Ti}_2\text{O}_7$  ( $0 \leq x \leq 1.8$ ) to study the spin relaxation processes in the paramagnetic phase ( $T > 1$  K) [1]. A cross-over from a thermally activated single-ion process to a temperature independent quantum mechanical process occurs at  $T \approx 15$  K in samples with moderate magnetic dilution ( $x \leq 1.1$ ).

However in very dilute samples  $x \geq 1.6$  another, faster relaxation process appears at relatively high temperature (up to at least  $T \approx 55$  K). Our neutron data will be discussed in relation to complementary a.c. susceptibility and  $\mu\text{SR}$  results.

[1] G. Ehlers, A. L. Cornelius, M. Orendac, M. Krajnakova, T. Fennell, S. T. Bramwell, and J. S. Gardner, *J Phys: Condens. Matter* **15**, L9 (2003).

**W2-D2 (14:00) Spin-waves in antiferromagnetic Kagome lattice**

**K. Matan** (Department of Physics, MIT), **D. Grohol**, **D. Nocera** (Department of Chemistry, MIT), **S. -H. Lee** (National Institute of Standards and Technology), **S. Nagler** (HFIR Center for Neutron Scattering, Oak Ridge National Laboratory, Oak Ridge, Tennessee 37831, USA.), **Y. S. Lee** (Department of Physics, MIT)

We have used inelastic neutron scattering to study spin-waves in single crystal samples of the antiferromagnetic kagome lattice compound,  $\text{KFe}_3(\text{OH})_6(\text{SO}_4)_2$ . The  $5/2$   $\text{Fe}^{3+}$  spins on the kagome lattice order three dimensionally for temperatures below the Neel temperature,  $T_N = 65$  K. Spin-waves were measured at  $T = 10$  K, much lower than  $T_N$ . We have observed a novel weakly dispersive “zero-energy mode”, which is a consequence of the geometrical frustration. A spin Hamiltonian, which includes nearest-neighbor, second-nearest-neighbor interactions, easy-plane and easy-axis anisotropies, provides a good fit to our spin-wave data. We will discuss the implications of our results for the physics of the ideal kagome lattice.

**W2-D3 (14:15) Spin, orbital, and lattice couplings in a geometrically frustrated magnet  $\text{CdV}_2\text{O}_4$**

**Z. Zhang**, **A. Visinoinu**, **D. Louca** (Department of Physics, University of Virginia), **Y. Qiu**, **S. Park** (NIST Center for Neutron Research), **T. Proffen**, **J. Thompson** (Los Alamos National Laboratory), **S.-H. Lee** (NIST Center for Neutron Research)

The microscopic properties of the vanadate spinels are distinctly different from those of the chromates due to the intrinsic orbital degeneracy of the vanadium ion. We studied a vanadate compound,  $\text{CdV}_2\text{O}_4$ , to investigate how the orbital degree of freedom couples to the lattice and spin.  $\text{CdV}_2\text{O}_4$  undergoes a cubic-to-tetragonal transition at 87 K and a magnetic long range order at 35 K. This contrasts with the chromates where a tetragonal distortion and a magnetic long range order occurs simultaneously due to a spin-lattice coupling. We have performed neutron diffraction and inelastic neutron scattering measurements on a powder sample of  $\text{CdV}_2\text{O}_4$ . Upon cooling, the Q-lineshape of the inelastic scattering

intensity changes from symmetric in the cubic phase to asymmetric in the tetragonal phase. This indicates that the vanadate becomes a system of weakly coupled straight chains in the tetragonal phase. We will discuss implication of the results to the interplay between the orbital, spin and lattice degrees of freedom in the vanadates.

#### **W2-D4 (14:30) Cooperative ordering of gapped and gapless spin networks in $\text{Cu}_2\text{Fe}_2\text{Ge}_4\text{O}_{15}$**

*T. Masuda (Condensed Matter Sciences Division, Oak Ridge National Laboratory), B. Grenier (DRFMC/SPSMS/MDN Centre d'Etudes Nucleaires), A. Zheludev (Condensed Matter Sciences Division, Oak Ridge National Laboratory), S. Imai, K. Uchinokura (Department of Advanced Materials Science, the University of Tokyo), E. Ressouche (DRFMC/SPSMS/MDN Centre d'Etudes Nucleaires), S. Park (NIST Center for Neutron Research)*

The unusual magnetic properties of a novel low-dimensional quantum ferrimagnet  $\text{Cu}_2\text{Fe}_2\text{Ge}_4\text{O}_{15}$  are studied by neutron scattering and bulk methods. The crystal structure of this material contains chains of  $\text{Fe}^{3+}$  ions intercalated by paired  $\text{Cu}^{2+}$  sites. The magnetic susceptibility in the high temperature region is described by the simple sum of classical  $S = 5/2$  spin chains and  $S = 1/2$  quantum dimers. In the 3D ordered state neutron diffraction reveals strongly reduced moments on  $\text{Cu}^{2+}$  and large moments on  $\text{Fe}^{3+}$ , respectively. The observed linear relation between  $m_{\text{Cu}}$  and  $m_{\text{Fe}}$  is consistent with the  $\text{Cu}^{2+}$ -spins being bound in a gapped spin-singlet state. Low-energy spin excitations up to 10 meV energy transfer are studied by cold neutron inelastic scattering. The measured dispersion relation can be understood as that of  $\text{Fe}^{3+}$  spin chains with effective inter-chain coupling. A combination of experimental technique reveals that the material can be described in terms of two subsystems with distinct energy scales. Magnetic ordering in this case is a cooperative phenomenon caused by interactions between these two units.

This work was carried out under DOE Contract No. DE-AC05-00OR22725.

#### **W2-D5 (14:45) Dynamics of a Z2xZ2 invariant (non-Haldane) $S = 1$ quantum chain**

*A. Zheludev (Condensed Matter Sciences Division, Oak Ridge National Laboratory), L.-P. Regnault (MDN/DRFMC/SPSMS CEA-Grenoble, France), M. Hagiwara (RIKEN, Waco, Japan), T. Masuda (Condensed Matter Sciences Division, Oak Ridge National Laboratory)*

Integral antiferromagnetic spin chains are best known for having an exotic spin liquid ground state

and the Haldane gap in the magnetic excitation spectrum. Considerably less attention has been given to a *different* spin liquid realized in integral spin chains with alternating exchange interactions. In practice, the two ground states and the corresponding excitation spectra are notoriously difficult to distinguish, due to the fact that they only differ in topological "hidden" spin correlators.

We present two series of inelastic neutron scattering experiments on a bond-alternating S-1 quantum spin chain compound NTENP. In the first series of measurements [1] we exploit the Hohenberg-Brinkman 1st moment sum rule to directly measure the *distribution of exchange energies* in the ground state. The results allow us to unambiguously identify NTENP as a Z2xZ2 invariant (non-Haldane) spin liquid. We then proceed to study the spin dynamics in NTENP in strong external magnetic fields [2]. At  $H_c = 11$  T we observe a closing of the spin gap and a field-induced *Bose-condensation of magnons*. Surprisingly, the high-field state is very similar to that of a classical one-dimensional magnet. The excitation spectrum consists of a doublet of conventional spin-wave-like excitations. Such behavior is in stark contrast with that previously seen in the Haldane-gap antiferromagnet NDMAP in similar conditions [3]. Here the high-field phase is a quantum spin solid characterized by a *triplet* of coherent breather excitations.

- [1] A. Zheludev, T. Masuda, B. Sales, D. Mandrus, T. Papenbrock, T. Barnes, S. Park, cond-mat/0310741.
- [2] M. Hagiwara, L.-P. Regnault and A. Zheludev, to be published (2004)
- [3] A. Zheludev et al., cond-mat/0308545; Phys. Rev. B 68, 134438 (2003); Phys. Rev. Lett. 88, 077206 (2002), and references therein.

#### **W2-D6 (15:00) Bound spinons in an antiferromagnetic $S = 1/2$ chain with a staggered field (Invited)**

*M. Kenzelmann (Department of Physics & Astronomy, Johns Hopkins University; NIST Center for Neutron Research), Y. Chen (Los Alamos National Laboratory), C. Broholm (Department of Physics & Astronomy, Johns Hopkins University; NIST Center for Neutron Research), D. Reich (Department of Physics & Astronomy, Johns Hopkins University), C.D. Batista (Los Alamos National Laboratory), Y. Qiu, S. Park (Department of Materials Science and Engineering, University of Maryland)*

Strongly-correlated charge and spin degrees of freedom can lead to cooperative many-body states which are believed to have wide implications for the macroscopic properties of complex solids. The emergent character of such states can give rise to

non-linear excitations which are very different from those in more conventional systems like the Fermi liquids or ordered magnetic structures. We have recently studied the antiferromagnetic  $S = 1/2$  chain in high uniform and staggered fields using various cold neutron scattering techniques. We have found that the spinon excitations bind under the influence of the staggered field and appear as well-defined excitations in the neutron spectra. This is in stark contrast to broad neutron scattering spectra observed from  $S = 1/2$  chains in zero field. In the long wavelength limit, the experiments are in excellent quantitative agreement with predictions of soliton and breather excitations of the quantum sine-Gordon model. On finite length scales, we find that a mapping of the Hamiltonian to a gas of interacting fermions with spin explains the dispersion of the observed excitations surprisingly well.

**W3-A, Breakout Sessions, Chair: Shenda Baker (Harvey Mudd)**

**W3-A1: Breakout Session: Perspectives for Neutron Scattering of Biomembrane Systems**

*M. Loesche, S. H. White, D. J. Tobias, J. K. Blasie*

Neutron scattering of biological systems has for some time been under represented in this country. Consequently, there is a noticeable gap in the levels of activity in this area between the US and other world regions. The CNBT (“Cold Neutrons in Biology and Technology”) initiative aims at closing this gap by promoting structural characterization of biomembrane systems using a concerted approach that involves neutron and x-ray scattering, high-performance computing, and NMR spectroscopy. With the advent of the AND/R, a new neutron spectrometer at NCNR’s NG-1 guide which is geared toward reflectometry and diffraction studies of membranous systems, US neutron science is on the leap back to making an impact on biology-related problems. This is also important in view of the SNS coming on-line in a few years, an event which will provide a dramatic boost to neutron-related science in a much broader context. We will discuss perspectives and opportunities of the CNBT in membrane science, aiming at potential outside users from the life science and biotech communities.

**W3-A2: Breakout session on Use of Depleted U Targets at Low and Medium Power Spallation Source**

*Jim Rhyne (LANL/LANSCE) and Ray Teller (ANL/IPNS)*

The development of cubic uranium metallic phases creates the possibility of the use of these materials in medium power spallation neutron sources allowing

an increase of perhaps 70-80 % in neutron production per proton. The purpose of this session is to: 1) present the case of the use of these materials; 2) to assess the interest within the community to develop a new generation of U targets; and 3) initiate a discussion about the issues that would arise should such a development be deemed worthwhile.

**W3-A3: Breakout Session on the SNS Magnetism Reflectometer**

*F. Klose (Spallation Neutron Source, Oak Ridge National Laboratory)*

This session will review the progress in design, the status of procurements and the planned scientific program of the SNS Magnetism Reflectometer. The Instrument Advisory Team of the instrument and other interested scientists are welcome to attend.

**W3-A4: Breakout Session: Portable software for neutron scattering**

*T. G. Worlton (Intense Pulsed Neutron Source, Argonne National Lab), D. J. Mikkelsen (University of Wisconsin-Stout), P.F. Peterson (Spallation Neutron Source, Oak Ridge National Laboratory)*

Development of portable software for neutron scattering will facilitate use of neutron facilities by visiting scientists. Adoption of a NeXus data format for storage and interchange of data can help make this possible, but work on file definitions for some neutron instruments is still incomplete. Tools such as ISAW and NXvalid can be used as a tools to examine, visualize, and analyze data from NeXus files and are currently being used at LANSCE and IPNS. Scientists from Argonne, Los Alamos, SNS, and the University of Wisconsin-Stout are collaborating on specifications for NeXus files which will contain all the information needed for visualization and analysis. In this session we will discuss information which should be stored in NeXus files and tools which can be used to read, visualize, reduce, and analyze the data.

**W3-A5: Breakout Session on Doing Science with Neutron Scattering Data**

*B. Fultz (California Institute of Technology), X-L. Wang ( Spallation Neutron Source, Oak Ridge National Laboratory)*

The purpose of this breakout session is to describe today’s software for the analysis of neutron scattering data, describe new developments, and seek viewpoints on future needs. The focus of the session will be on the science enabled by software, with less emphasis on specific software packages or software engineering. For example, the leaders may steer the discussion towards how new computing resources for simulations, modeling, and visualization enable new



experiments, or elevate the sophistication of experiments possible today.

The session will be divided into one-hour sub-sessions on the topics below. Each will begin with a scheduled 12-15 minute presentation. “Flash presentations” follow—attendees who prepare 2-3 viewgraph transparencies prior to the session will be given 3-5 minutes for a brief presentation. Open discussion will follow the flash presentations.

3-4 PM Diffraction and Engineering Diffraction (Simon Billinge and Ersan Ustundag)

4-5 PM SANS and Reflectometry (Paul Butler and Paul Kienzle)

5-5:30 PM Inelastic Scattering (Frans Trouw and Brent Fultz)

### **W3-A6: Breakout Session on Sample Environment at Neutron Scattering Facilities**

*K. J. Volin (Intense Pulsed Neutron Source, Argonne National Lab), D. C. Dender (NIST Center for Neutron Research), J. S. Fieramosca (Intense Pulsed Neutron Source, Argonne National Lab), L. J. Santodonato (Spallation Neutron Source, Oak Ridge National Laboratory)*

Sample environment staff from some of the major US neutron scattering facilities will make presentations and facilitate open discussion on topics relevant to the use of sample environment for neutron scattering experiments. Presentations will be made on: a prototype system called the Fast Exchange Refrigerator for Neutron Science (FERNS) [1], a modular system that combines familiar cryogenic technology with more recent automation technology; modifying existing sample environment equipment beyond its originally designed operating parameters to accommodate newer and more demanding scientific studies; and pitfalls and successful strategies to employ when contracting for new equipment. Lessons learned during the performance of neutron scattering experiments using a variety of sample environments will also be presented and discussed, including experiences with equipment, operations, and procedures and how these experiences changed the way sample environments are handled.

[1] A collaborative effort with R. Weber and J. Rix of Containerless Research, Inc., conducted under a Department of Energy Small Business Innovation Research grant.

### **W3-A7: Breakout session on the Fermi Chopper spectrometers for the SNS**

*D. Abernathy (Spallation Neutron Source, Oak Ridge National Laboratory), B. Fultz (California Institute*

*of Technology), B. Gaulin (Department of Physics and Astronomy, McMaster University, Hamilton, ON, Canada), G. Granroth (Spallation Neutron Source, Oak Ridge National Laboratory), S. Nagler (Condensed Matter Sciences Division, Oak Ridge National Laboratory)*

The ARCS and SEQUOIA spectrometers are the wide angle and high resolution Fermi chopper spectrometers planned for the SNS. This breakout session will provide the IDT's, and other interested parties, with updates on the design and procurements of the two spectrometers. Furthermore the community will have the opportunity to share their preferences on several design issues. Specifically we will discuss requirements for sample access and the optimization of chopper slit packages.

### **W3-A8: Breakout session for VISION, an neutron vibrational spectrometer for SNS**

*J.Z. Larese (Chemistry Department, University of Tennessee; Oak Ridge National Laboratory), B.S. Hudson (Chemistry Department, Syracuse University), L.L. Daemen (LANSCE, Los Alamos National Laboratory)*

At this breakout discussion we will discuss the VISION project, a neutron vibrational spectrometer for the SNS. We encourage all interested participants of the ACNS to attend. At the breakout session we will provide information on the purpose, performance and status of the VISION project in the form of a short presentation. VISION has been designated by SNS as one of the viable instruments for inclusion in the first target station instrument suite. We will follow the informational segment with a town meeting or round table discussion to address community inclusion, outreach and participation by members of the neutron community. We will close with a brief team meeting to discuss and develop a strategy to move the project into the next (design and engineering) phase and to discuss funding and technical issues that are relevant to the project at the time of the ACNS meeting. Several members of the VISION team will be called upon to give a brief highlight of the types of science possible with such an instrument. There is a need in the United States for a state-of-the-art neutron scattering instrument for vibrational spectroscopy to investigate the structure and dynamics of condensed matter systems by the simultaneous use of elastic diffraction and moderate resolution (1-2%  $\Delta E/E$ ) inelastic scattering over a broad energy transfer range. The use of neutron vibrational spectroscopy (NVS) is growing at a significant rate in Europe thanks to the second-generation instrument TOSCA at ISIS, the spallation neutron source at the Rutherford-Appleton Laboratory in England. We



propose to design a next generation, time of flight (TOF) spectrometer named, VISION, which is not an acronym, to investigate a vast array of molecular dynamics and structure. Under optimal conditions this instrument will - have a throughput two orders of magnitude greater than TOSCA –currently the best instrument in the field; - cover an energy transfer range of 0-500 meV (0-4000  $\text{cm}^{-1}$ ); - have a 1-2 % energy resolution while simultaneously enabling diffraction studies for structural characterization; - offer a wide range of sample environments (low temperature, high-pressure, flow cell, thermal analysis, etc). Our approach will incorporate neutron techniques developed during the decade since TFXA and TOSCA were first designed and built. This includes improved supermirror technology, parametrically matched crystal analyzer–helium gas detectors, efficient electronics for high rate data acquisition, high-performance data analysis algorithms, novel moderator concepts, as well as the use of (by now) well-developed Monte Carlo software for neutron optics and instrument design and optimization. The flux available at SNS will enable for the first time time-resolved vibrational measurements at a neutron source. Proposals to form an Instrument Design Team (IDT) and a subsequent proposal describing the scientific background for VISION have been presented to the Spallation Neutron Source (SNS) Experimental Facilities Advisory Committee (EFAC) and have been positively received. (EFAC has enthusiastically endorsed the science case presented by the IDT and a beamline position for installation and construction of VISION has been identified by SNS.) We are confident that VISION's broader impact will be that an entirely new segment of users will be brought into the U.S. neutron community. This is exemplified by the extraordinary expansion in recent years of the community of scientists in the United Kingdom and the European Union using TOSCA at ISIS. Indeed, TOSCA is now routinely oversubscribed by a factor of 1.5 to 2. The demand for beam time is so great that only a few days per year are available to investigate novel applications. Furthermore, the VISION instrument will introduce a new generation of students and researchers to the use of neutron vibrational spectroscopy in the study of new materials and a wide range of engineering problems, especially those materials that have interesting structure and dynamics on the nanometer length scale and topics of commercial importance. VISION will substantially expand the range and flexibility of neutron investigations in in the United States. It will open new and fruitful directions for studies of atomic and molecular dynamics and structure in condensed matter.

### **W3-A9: Breakout Session on Detectors and SCD for SNS**

*Christina Hoffmann (SNS, Oak Ridge National Laboratory), R. Bau, T. F. Koetzle and A. J. Schultz*

A best-in-class single-crystal diffractometer (SCD) utilizing the time-of-flight Laue technique is under development for the Spallation Neutron Source (SNS). The 2 MW SNS, currently under construction in Oak Ridge, TN, USA, is scheduled to begin operation in 2006. Because sample volumes will approach those of typical “x-ray crystals,” SNS SCD promises to revolutionize the application of single-crystal neutron diffraction as we know it, particularly from the viewpoint of the practicing synthetic chemist. The instrument will be specifically optimized for high-throughput on samples with moderate-size unit cells, up to ca. 50 Å on edge. Provision is also intended for the measurement of diffuse scattering and for the production of polarized beams to facilitate the study of magnetic structures. The authors are executive officers of the Instrument Development Team (IDT) for the SCD, which will be operated in a broadly based user mode.

We want to invite the IDT and interested researchers to participate in this breakout session to voice the user community's future needs for single-crystal neutron diffraction. The session will provide an opportunity to actively define an instrument that is optimized for the community's needs. It will also be an opportunity to update the user community on recent instrument design studies and developments. Progress has been made on development of polarized neutron options for white beam single-crystal diffraction, on neutron detector design concepts, and on evaluation of options for neutron beam focusing.

### **W3-A10: Breakout Session on HYSPEC: A Novel Direct Geometry Polarized Beam Inelastic Instrument for the SNS**

*M. Hagen (Spallation Neutron Source, Oak Ridge National Laboratory), S. M. Shapiro I. A. Zaliznyak (Brookhaven National Laboratory)*

HYSPEC is a direct geometry inelastic scattering spectrometer for single crystal and polarized neutron studies at the SNS. The instrument combines time-of-flight spectroscopy and focusing Bragg optics to enhance the monochromatic neutron flux on small samples. It is a moderate resolution instrument optimized for an incident energy range of 3.6–60 meV. HYSPEC will be designed to do polarized neutron studies using a Heusler crystal monochromator and supermirror bender analyzers for the polarization analysis of the scattered neutrons. There will be presentations describing the instrument design

and estimated performance along with the important simulations aimed at keeping the background to a minimum. This breakout session will serve as an IDT Meeting, but is open to all who have an interest in learning about HYSPEC and have the desire to use a polarized beam inelastic scattering instrument.

## Thursday

**Morning Visit to the NIST Center for Neutron Research (Buses depart the Inn at 8:30)**

# Author Index

## A

Abdel-Raouf, E: WP41  
Abdul-Redah, T: M3-D2, WP65  
Abernathy, DL: W3-A7, TP66, WP37  
Agamalian, M: M2-C4, WP34  
Agnew, SR: W2-A2  
Aivazis, MAG: TP73, WP75  
Al-Ghamdi, S: WP41  
Alcantar, NA: T1-B3  
Alessi, ML: MP12  
Alexandrov, YuA: TP43  
Allen, A: T2-B1  
Allen, AJ: T2-B2  
Allis, Damian: MP9  
Allis, DG: WP23  
Amis, EJ: M4-D1  
Amos, K: TP41  
Ando, Y: MP39  
Andreani, C: MP17, WP66  
Angelopoulos, Marie: M2-B5  
Ankner, JF: M2-C5  
Arai, M: M4-A5, WP60  
Argyriou, DN: WP63  
Arif, M: M4-B3  
Arleth, L: M2-B2  
Armstrong, TR: TP15  
Arnold, T: TP14, WP11  
Aronson, MC: TP58  
Arrott, AS: T1-C4  
Ashbaugh, HS: T1-A2, WP44  
Ash, BJ: WP22  
Ashish, : WP3  
Assoud, A: WP70  
Avdeev, M: W2-C3  
Azuah, RT: TP69, WP61

## B

Bakeeva, RF: WP46  
Baker, SM: WP51  
Balsara, NP: **M2-B1**, MP26  
Bao, W: M4-A4, T2-D2  
Bau, R: W3-A9  
Barbier, J: T3-A2  
Barilo, SN: TP60  
Barker, JG: M2-B6, M2-C4, T2-B2, T3-B3, TP36  
Barnes, PW: W2-C3, TP13  
Baronov, S: WP23  
Barrera, GD: M3-D5  
Batdemberel, G: WP67  
Batista, CD: W2-D6  
Bauer, ED: T2-D3  
Baxter, DV: T1-D1  
Beise, EJ: M4-B2

Benesi, AJ: TP8  
 Benmore, CJ: T2-C5, MP15, TP49, TP70  
 Bennett, KA: T3-C6  
 Bennington, S: WP60  
 Benson, ML: M3-A5, MP31, MP32  
 Berk, NF: M3-B3, WP4  
 Berliner, R: T2-B3, TP24  
 Berlinsky, AJ: MP46  
 Beskrovny, AI: WP67  
 Billinge, SJL: MP38, WP70  
 Birgeneau, RJ: M3-C1, TP55, TP56  
 Black, DJ: WP7  
 Black, TC: M4-B3  
 Blasie, JK: **T1-B1**, W3-A1  
 Bleuel, M: M2-C3  
 Blumenthal, DK: WP5  
 Blumenthal, WR: W2-A2  
 Boatner, LA: M3-C6  
 Boerio-Goates, J: TP64  
 Bonn, D: TP56  
 Boothroyd, AT: WP59  
 Borchers, JA: M2-A3, M2-A5, T2-C1, MP43  
 Bossev, DP: MP1, **M3-B5**, M4-D1, MP2, WP78  
 Boukari, H: TP46  
 Bourke, MAM: T3-C2, W2-A2, TP12, WP17  
 Bouzek, C: TP71, WP72, WP74  
 Bowman, JD: T1-D3  
 Braden, DA: MP9, WP23  
 Bramwell, ST: W2-D1  
 Brand, PC: TP19, TP30, WP38  
 Briber, RM: W1-A1, MP22, MP24, MP23, WP13, WP8  
 Brissier, T: WP57  
 Britten, JF: T3-A2  
 Brockner, C: TP30  
 Broholm, CL: M3-C4, MP35, TP53, W2-D6, WP38  
 Broussard, LJ: MP18  
 Brown, CM: MP49, MP5, TP18, TP22, TP8, WP19, WP23, WP49,  
 WP64  
 Brown, DW: M3-A5, T3-C2, W2-A2, MP29, MP30, MP32  
 Brown, SP: M4-A3, WP5  
 Buchanan, MV: TP33, WP9  
 Buchanan, RA: M3-A5, MP30, MP32  
 Bud'ko, SL: T1-C3  
 Bugaev, V: MP36  
 Burley, JC: W2-C3  
 Burnham, C: M4-C3  
 Burns, R: WP19  
 Butler, PD: M4-D4, MP6, MP10, TP33, WP48, WP9  
 Buyers, WJL: TP56  
 Bychkov, GL: TP60

## C

Caliskan, GH: M3-B4, MP3, MP50, WP8  
 Cameron, JM: T1-D1



Caneba, GT: M2-B6  
Canfield, PC: T1-C3  
Cappelletti, RL: TP4  
Carey, MJ: M2-A5  
Carneim, RD: TP15  
Carpenter, JM: **T1-D5**, T2-C2, TP21, WP34  
Carvalho, LB: MP48  
Casson, J: TP47  
Castellan, JP: MP46  
Cava, RJ: W2-C2  
Chadraabal, Sh: WP67  
Chakoumakos, B: MP40  
Chanaa, S: TP14  
Chang, S: WP62  
Chapon, LC: WP63  
Chatterjee, A: TP70, TP71, WP72  
Chatterji, T: T3-A4, TP61  
Chen-Mayer, HH: T2-C2  
Chen, C: T3-B1  
Chen, JJ: T2-B2  
Chen, Sow-Hsin: M4-C1  
Chen, WC: T2-C1  
Chen, Y: **M4-A4**, W2-D6  
Cheong, S-W: M3-C2, M3-C4, TP54, TP63  
Chernenkov, YuP: TP60  
Chiarelli, P: TP47  
Chien, CL: M2-A2  
Chi, Lisheng: WP12  
Choi, BH: TP29  
Choi, S-M: WP42  
Choi, YH: TP29  
Choo, H: M3-A5, T3-C2, MP29, MP30, MP31, MP32  
Cho, Sj: TP29  
Chowdhuri, Z: T3-B1, MP3, TP4  
Christen, DK: M4-A5  
Christianson, AD: T2-D2, T2-D3  
Christoph, V: WP35  
Chung, Brian: T3-B5  
Chupas, PJ: T3-A6, WP70  
Chupp, TE: MP18  
Cianciolo, TV: T1-D3  
Cicerone, MT: M3-B4, MP50  
Ciezak, JA: MP5  
Ciezak, Jenn: MP9  
Clarke, S: TP14  
Clausen, B: WP17  
Clausen, KN: T1-A4  
Clemens, D: T2-C7  
Clow, B: TP28, WP30  
Cole, DR: M4-C2  
Collins, MF: TP17, WP60  
Conlon, K: W2-A2  
Cook, RE: TP14  
Cooper, M: T1-D3  
Cooper, RL: MP18, TP74

Copland, E: WP15  
Copley, JRD: MP36, MP46, TP64, TP66  
Coulter, KP: MP18  
Cowan, JA: T2-B6, WP74  
Craig, S: WP58  
Crawford, MK: TP64  
Criswell, L: T3-B4  
Crow, L: TP74  
Crowe, S: M4-A5  
Cubitt, R: M4-A3  
Cummins, P: MP27  
Curtis, JE: T2-A3, WP21

## D

Dabkowska, HA: MP46, T3-A2  
Dadmun, MD: M2-B3, M4-D2, MP13, WP16  
Daemen, LL: M3-D4, W3-A8, MP30, T2-B5, TP9, TP14, TP40, WP10,  
WP28  
Dai, P: M4-A1, T3-A3, MP39, TP67, WP62  
Darling, T: M3-C7  
Dashjav, E: WP70  
Dattelbaum, AM: W2-B3  
Daud, SofianM: M3-B2  
David, SA: MP29  
Daymond, MR: M3-A5, MP31, MP33, TP39  
De Lurgio, PM: TP38  
Deb, PK: TP41  
Delaire, O: M3-A3, MP44  
Dender, DC: TP28, W3-A6, WP24, WP30  
Derakhshan, S: WP70  
Derenchuk, VP: T1-D1  
Dewey, MS: M4-B2, MP18, TP42  
Dewhurst, CD: M4-A3  
Diallo, S: WP61  
Diama, A: T3-B4  
Diat, O: MP20  
Dimeo, RM: M2-D2, T3-B4, MP49, TP69  
Dmowski, W: M3-C7  
Dogan, F: WP62  
Dolgos, M: WP18  
Donner, W: MP48  
Dosch, H: MP36  
Doshi, DA: W2-B3  
Doucet, M: TP72  
Douglas, JF: T3-B2  
Doyle, J: T1-D3  
Drew, AJ: M4-A3  
Drews, AR: M2-C4  
Dufour, C: M2-A3  
Dumesnil, K: M2-A3  
Dura, JA: TP25, WP36  
Durham, WB: T3-C6  
Dzhosyuk, SN: **M4-B5**

## **E**

Eckert, J: **M3-D1**, M3-D4, TP40, WP10  
Edwards, L: TP39  
Egami, T: M3-C7  
Egelstaff, PA: TP49  
Egres, RG: MP28  
Ehlers, G: **W2-D1**  
Eklund, PC: M4-C5  
Elashvili, I: M3-B1  
Elices, M: W2-A3  
Epand, RM: T1-B2  
Erwin, RW: M3-C2, M3-C6, W2-C4  
Eykens, R: TP42

## **F**

Faller, R: MP51  
Fan, Lixin: TP45  
Faraone, Antonio: M4-C1  
Farinelli, MJ: TP14  
Fedeyko, JM: MP7  
Fei, X: TP42  
Felcher, GP: M2-A2  
Feng, H: MP22  
Feng, Z: MP29  
Fernandez-baca, JA: T3-A3, WP69  
Fernandez-Garcia, J: M4-C4  
Fetters, LJ: WP44  
Fieramosca, JS: W3-A6, TP26  
Filabozzi, A: WP66  
Fink, Charles: TP38  
Fischer, JE: M2-B4, WP14  
Fisher, BM: M4-B2  
Fisher, RA: TP64  
Fisk, Z: TP58  
Fitzgerald, E: TP28, WP30  
Flippen, R: TP64  
Foecke, TJ: T3-C3  
Foo, ML: W2-C2  
Forgan, EM: M4-A3  
Frazier, L: WP11  
Freedman, SJ: MP18  
Freeman, PG: WP59  
Frick, B: TP61  
Frielinghaus, H: M4-C2  
Frost, C: WP59  
Fuess, H: WP67  
Fuhrmann, D: T3-B4  
Fujikawa, BK: MP18  
Fujita, M: M4-A2  
Fultz, BT: M3-A3, MP44, T2-D5, TP73, W3-A5, W3-A7, WP37, WP68,  
WP75  
Furdyna, JK: MP43  
Furrer, A: TP60

## G

Gaehler, R: M2-C3  
Gangoda, M: M3-B4, MP50  
Garamus, V: TP37  
Garcia-Sakai, V: T3-B1  
Garcia, A: MP18  
Gardner, JS: MP40, T2-D2, W2-D1  
Garlea, E: MP30  
Garlea, VO: M3-A2, T1-C3, TP50, TP51  
Gaulin, BD: MP46, W3-A7  
Gauthier, M: MP24  
Gauthier-Picard, P: TP20  
Geelan, M: TP9  
Gehring, PM: M3-C3, M3-C5  
Gentile, TR: M4-B2, T2-C1  
Georgiev, PA: M4-C4  
Georgii, R: T2-C4  
Gerber, MichaelJ: W2-B2  
Ghazi, H: T3-A2  
Ghosh, VJ: TP23  
Gibson, WM: T2-C2  
Giebultowicz, TM: M2-A4  
Gilardi, R: M4-A3  
Gilbert, EP: TP59, WP19  
Gilliam, DM: TP42  
Glanville, YJ: MP49  
Glinka, CJ: M2-B4, M2-C2, M2-C4, MP21, MP27, T2-C6, WP13, WP42  
Glyde, HR: WP61  
Gnaupel-Herold, T: T3-C3, W2-A3, WP55  
Gog, T: T1-B4  
Goka, H: M4-A2  
Goldberger, J: TP7  
Goldfarb, D: M2-B5  
Goossens, DJ: T3-A5, TP57  
Gopalakrishnan, V: M4-D5  
Gordon, J: WP55  
Goremychkin, EA: T2-D3  
Gorini, G: MP17, WP66  
Goukassov, A: TP60  
Gourieux, T: M2-A3  
Granroth, GE: TP66, W3-A7  
Gray, CP: WP70  
Greedan, JE: T3-A2, WP12  
Greenblatt, M: M2-D5  
Greene, GL: T1-D3, TP42  
Greenwald, BS: MP28, WP42  
Greer, SC: MP12  
Gregory, R: MP3  
Gregory, RB: M3-B4, MP50  
Gregurick, SK: MP11, T2-A2  
Grenier, B: W2-D4, TP53  
Greven, M: MP37, MP47  
Grohol, D: W2-D2  
Gschneidner Jr, KA: TP51



Gu, B: M4-D4  
Gudkov, V: M4-B4  
Gu, GD: M4-A2, W2-C4  
Guo, L: M2-B6, TP45, WP52  
Gupta, K: MP2  
Gurney, BA: M2-A5  
Guthrie, M: TP49  
Guttmann, M: MP40  
Gu, X: T3-B3

## H

Hadzi, D: M3-D4  
Haese-Seiller, M: T2-C4, WP26  
Hagen, M: W3-A10  
Hagiwara, M: W2-D5  
Hamilton, WA: M4-D4, T1-B3, **W2-B1**, WP48  
Hammonds, JP: TP70, TP71, WP72, WP74  
Hammouda, B: MP27, TP58  
Hansen, FY: T3-B4  
Haravifard, S: MP46  
Harden, James: T3-B5  
Hardy, WN: TP56  
Harlow, RL: TP64  
Harpham, MR: MP25  
Harris, AB: **T1-C1**  
Harrison, N: MP35  
Harrison, NM: TP54  
Hartig, C: T2-C8, WP57  
Hartl, M: M3-D4, WP10  
Hartman, MR: T2-B3  
Hasan, ZM: TP63  
Head-Gordon, T: T2-A4  
He, B: T1-A3  
He, D: M2-D5  
Heffner, RH: M3-C7  
Hehlen, MP: WP71  
He, J: MP40  
Heller, WT: TP33, WP5, WP7, WP9  
Hemley, RJ: **M2-D3**, M2-D5  
Hennion, B: M3-C6  
Hennion, M: M2-A3  
Hersman, FW: **M4-B1**  
Herwig, KW: M4-C6, T3-B4, MP25  
Hettinger, JD: TP68  
Hiera, KJ: T2-C5  
Hilger, A: MP16  
Hinde, R: WP11  
Hinks, DG: W2-C3  
Hiraka, H: M3-C3  
Hjelm, RP: M2-B2  
Hobbie, EK: M2-B4  
Hodges, J: WP39  
Hodges, JP: TP34

Ho, DL: M2-B4, T3-B3, MP12, WP13, WP14  
Hoffmann, A: MP43  
Hoffmann, C: TP74, W3-A9  
Holden, TM: W2-A2  
Holderna-Natkaniec, K: WP31  
Holt, SA: M3-B2  
Homouz, D: MP45  
Honda, Z: TP53  
Hong, GP: TP29  
Hong, JH: WP56  
Hong, K: WP47  
Hong, KS: M3-C7  
Hormadaly, J: TP64  
Horsewill, AJ: M2-D2  
Horton, DJ: T3-C4  
Howard, CA: MP42  
Huang, C-Y: MP21  
Huang, JG: MP31  
Huang, JS: W2-B4  
Huang, JY: MP31  
Huang, Q: W2-C2, TP4, TP64  
Hubbard, CR: T3-C2, MP29, MP30, WP58  
Hudson, BS: MP5, MP9, W3-A8, TP16, TP40, WP23  
Huffman, PR: M4-B3, T1-D3  
Hundertmark, PK: WP38  
Huq, A: WP27  
Hura, G: T2-A4  
Hur, N: M3-C2  
Hu, Tengjiao: M2-B5  
Hu, Z: M2-B2  
Hwang, PJ: TP62  
Hwang, SR: MP18  
Häussler, W: W2-D1

## I

Ijiri, Y: **M2-A1**  
Imai, S: W2-D4  
Iniguez, J: **M3-D6**  
Iolin, E: WP25  
Islam, MF: WP14  
Isnard, O: TP6  
Itoh, K: TP17, WP60  
Iwase, H: WP60

## J

Jacobson, DL: M4-B3, TP19  
James, M: T3-A5, WP32  
Jenkins, T: MP9, WP23  
Jeong, I-K: M3-C7  
Jeon, JW: T3-C2  
Jin, R: TP67  
Jones, CY: M2-D4, TP19, TP2, TP51, WP15  
Jones, GL: MP18

Jones, JL: WP43  
Jones, Ronald: M2-B5  
Jorgensen, JD: W2-C3

## **K**

Kacman, P: M2-A4  
Kaiser, H: WP6  
Kakurai, K: TP57  
Kalus, J: WP31  
Kamaras, K: WP64  
Kamath, SK: M2-B3, M4-D2  
Kamitakahara, WA: WP20  
Kamiyama, T: TP17  
Kampmann, R: T2-C4, WP26  
Kanatzidis, MG: WP70  
Kang, H: MP39  
Karen, P: T3-A1, TP13, TP7  
Kartini, E: TP17, WP60  
Kastner, MA: TP55  
Katsaras, J: MP21  
Katsumata, K: TP53  
Keegan, N: M3-B2  
Keller, T: W2-A4  
Kelley, TM: T2-D5, MP44, TP73, WP75  
Kennedy, SJ: T1-D2, WP60  
Kent, MS: T1-B4  
Kenzelmann, M: M3-C4, **W2-D6**  
Kepa, H: M2-A4  
Keppens, V: TP66  
Kern, S: T2-D4  
Khaykovich, B: TP55  
Kienzle, PA: WP76  
Kim, HC: MP23  
Kim, HJ: WP70  
Kim, H-Ch: MP22  
Kim, JH: WP56  
Kim, M-H: M2-C4, T2-C6, WP49  
Kim, SB: M3-C4  
Kim, SJ: WP75  
Kim, YJ: TP29  
Kintzel, Jr, EJ: M4-C6  
Kirby, BJ: MP43  
Kiriluk, KG: M4-B2  
Kiryukhin, V: M3-C2  
Kisliuk, A: M3-B4, MP50  
Kitchens, CL: WP78  
Kjær, K: MP51  
Klann, RT: TP38  
Klarstrom, DL: M3-A5, MP32  
Kleinke, H: WP70  
Klose, F: W3-A3, WP35  
Klug, DD: TP49  
Klupp, Gy: WP64  
Kneller, LR: TP69

Koetzle, TF: T2-B6, W3-A9  
Kohlbrecher, J: M3-A4  
Kohn, J: W2-B4  
Kolesnikov, AI: **M4-C3**  
Koo, YM: WP56  
Kozlowski, P: TP16  
Kozlowski, T: T1-D4  
Kramer, D: T1-A4  
Kresch, M: WP68  
Kresch, MG: M3-A3, MP44  
Krishnamurthy, LN: M4-D3  
Krishnamurthy, VV: T1-A3, WP41  
Krist, Th: T2-C3  
Krueger, JK: WP3, WP7  
Krueger, S: **M3-B1**, T1-B2, T2-A2, MP11, MP2, TP46, WP4, WP50, WP8  
Kudryashov, V: T2-C4, WP26  
Kuhl, TL: T1-B3, MP51  
Kulkarni, A: T3-C5  
Kuo, RC: MP31  
Kurita, Y: MP39  
Kuzmanovic, DA: M3-B1  
Kwon, SC: WP56  
Kyratsi, T: WP70  
Kögerler, P: TP50

## **L**

Laakmann, J: WP57  
Ladanyi, BM: MP25  
Lago, J: W2-D1  
Lai, K-C: MP24  
Laine, RM: WP71  
Lakey, JH: M3-B2  
Lal, J: M2-C3, W2-B4  
Lamberty, A: TP42  
Landee, CP: TP48  
Lander, GH: T2-D4  
Langan, P: **T2-A1**  
Lang, E: TP38  
Lan, Y: WP23  
Larese, JZ: W3-A8, TP14, TP40, WP11  
LaRock, JG: WP38  
Lashley, JC: T2-D5  
Lavelle, C,: T1-D1  
Lawrence, JM: T2-D3  
Lawson, A: TP9  
Lawson, AC: T2-D5  
Lay, M: M2-B3, M4-D2  
Lay, MA: MP13  
Lea, C: WP6  
Leao, JB: TP18, TP22, WP24, WP30, WP64  
Lee, CH: TP29  
Lee, J-K: M3-C7  
Lee, JS: TP29  
Lee, MN: WP56



Lee, PL: TP64, WP70  
Lee, S-H: M3-C2, M3-C3, M4-A4, W2-D2, W2-D3, MP46  
Lee, SL: M4-A3  
Lee, VY: MP22  
Lee, WT: M2-A2, WP39  
Lee, YS: **W2-C1**, W2-D2, TP55  
Leheny, R: T3-B5  
Lehmann, E: T1-A4  
Letzring, HF: MP30  
Leuschner, MB: T1-D1  
Levinger, NE: MP25  
Lewis, P: T1-D4  
Liang, L: M4-D4  
Liang, R: TP56  
Liaw, PK: M3-A5, T3-C2, T3-C4, MP29, MP30, MP31, MP32  
Lieutenant, K: T2-C7  
LI, JC: M3-D2, WP65  
Li, JF: M3-C5  
Li, L: MP34  
Lim, WL: MP43  
Lin-Gibson, S: MP10  
Lin, E: M2-B5  
Ling, CD: MP41  
Lin, J: WP68  
Lin, Z: MP23  
Lising, LJ: MP18  
Littrell, KC: M2-C3, TP44, WP34, WP40  
Liu, CT: WP69  
Liu, L: M4-C1  
Liu, X: MP43  
Livescu, V: TP12  
Livingston, RA: T2-B1, TP5, TP8  
Li, W-H: TP62  
Li, Y: TP63, WP27  
Llobet, A: T2-D2, TP11  
Lobanov, MV: M2-D5  
Lobo, RF: **M2-D1**, MP7, TP2  
Loesche, M: W3-A1  
Lofland, SE: TP68  
Lograsso, TA: M3-A2, TP51  
Loizou, E: MP10  
Lokshin, K: WP28  
Lokshin, KA: M2-D5  
Lone, MA: T1-D1  
Loong, C-K: M4-C3  
Lorenzo, JE: M4-A4  
Louca, D: T3-A6, W2-D3  
Loutfy, RO: M4-C3  
Lufaso, MW: TP10, TP13  
Lumsden, MD: TP67, WP73  
Lutterotti, L: T2-C8  
Luzin, V: T3-C6, W2-A3, MP34, WP55  
Lynn, GW: TP33, WP9  
Lynn, JW: M3-C4, T2-D2, T3-A6, TP58, TP63, W2-C2, MP47, TP30,  
TP62, TP64, TP68, WP38, WP63

## M

Maat, S: M2-A5  
Majerz, I: WP31  
Majewski, J: T1-B3, T1-B4, W2-B3, TP47, MP51, WP51  
Majkrzak, CF: M2-A4, M3-B3, T2-C1, WP36, WP4  
Major, J: MP36  
Maliszewskyj, NC: TP72  
Malliakas, C: WP70  
Malwitz, M: MP10, MP6  
Mamontov, E: TP6  
Mancini, DC: M2-B6  
Mandrus, D: MP40, TP66, TP67  
Mandrus, DG: TP65  
Mangan, MA: WP43  
Mangin, Ph: M2-A3  
Mang, JT: WP71  
Mang, PK: MP37, MP47  
Mankey, GJ: T1-A3, WP41  
Manley, ME: WP43  
Mao, H-K: M2-D3, M2-D5  
Mao, WL: M2-D5  
Maple, MB: **T2-D1**  
Maranas, JK: **T3-B1**  
Margadant, N: W2-A4  
Marmotti, M: T2-C4  
Martin, JD: **T2-B4**  
Martínez-Iñesta, MM: M2-D1  
Mason, TE: **W1-A3**  
Masuda, T: W2-D4, W2-D5  
Matan, K: W2-D2  
Maxey, ER: T2-C2, T3-C4, WP27  
Mayers, J: M3-D2, WP65  
Mays, J: WP47  
McDaniel, SM: T3-C6  
McGillivray, DJ: WP4  
McGregor, DS: TP38  
McKerns, MM: TP73, WP68, WP75  
McLain, SE: MP15, TP49, WP18  
McLaughlin, JC: TP5  
McMorrow, DF: TP50  
McQueeney, RJ: T2-D4, **T2-D5**, WP43, WP62  
McQueen, T: WP51  
Mecking, H: WP57  
Medina, T: TP9, WP57  
Mehta, R: M2-B3, M4-D2, WP16  
Melnichenko, YB: M4-C2, WP47  
Mesecar, Andrew: WP39  
Mesot, J: M4-A3, **W1-A2**  
Metting, CJ: TP68  
Meyer, E: WP57  
Meyer, HO: T1-D1  
Meyer, O: WP57  
Mezei, F: T1-D4, T2-C3, T2-C7  
Micklich, BJ: TP21

Middleton, CT: WP23  
Migliori, A: T2-D5  
Mignot, JM: T2-D2  
Mihailescu, M: M3-B3, W2-B4  
Mikkelson, DJ: TP70, TP71, W3-A4, WP72, WP74  
Mikkelson, RL: TP70, TP71, WP72, WP74  
Mikula, P: WP25  
Mildner, DFR: T2-C2  
Miller, CE: MP51  
Miller, M: WP72, WP74  
Miller, ME: T2-B6, T2-C2  
Miller, M: WP74  
Miller, RD: MP22, MP23  
Mitchell, JF: T3-A6, WP63  
Modi, N: WP7  
Mo, H: T3-B4  
Mojet, B: WP10  
Monkenbusch, M: W2-B4  
Moodenbaugh, AR: TP7  
Mook, HA: **M4-A1**, TP65  
Moravsky, AP: M4-C3  
Moreno, NO: T2-D2, T2-D3  
Moritomo, Y: W2-C4  
Morosan, E: T1-C3  
Morrison, I: M4-C4  
Morrison, MM: MP30  
Moss, SC: **M3-A1**, MP36  
Motahari, SM: MP33  
Moyer, J: M2-C4, WP38  
Mumm, HP: MP18  
Murbach, M: TP30  
Myles, DAA: TP33, WP9

## **N**

Naday, Istvan: TP38  
Nagler, SE: TP50, TP65, TP66, TP67, W2-D2, W3-A7  
Nair, S: M2-D2  
Nakajima, K: WP59  
Nakotte, H: T2-D4  
Nann, H: T1-D1  
Narayanan, RA: WP22  
Narehood, DG: M4-C5  
Natkaniec, I: WP31  
Necker, CT: T2-C8  
Neiser, R: MP34  
Nelson, A: WP32  
Nemes, NM: T2-B1, TP5, WP64  
Neumann, DA: M2-D2, M3-D3, T2-B1, T3-B4, MP36, TP18, TP22, TP5,  
WP21  
Neumeier, JJ: MP41  
Nico, JS: M4-B2, MP18, TP42  
Niedermayer, C: , TP50  
Nieh, M-P: MP21  
Nikles, DE: T1-A3

Noakes, DR: T1-C4  
Nocera, D: W2-D2  
Nossal, R: TP46  
Notardonato, W: TP12  
NPDGamma Collaboration: M4-B1  
Nufris, S: WP66

## O

O'Brien, CP: M2-B3  
O'Donovan, KV: M2-A5, T2-C1, MP43, WP36, WP76  
Ohwada, K: M3-C3  
Okorokov, A: WP26  
Oldfield, E: WP6  
Osborn, R: **M2-C1**, T3-A6  
Oszlanyi, G: WP64  
O'Connell, C: M3-B1

## P

Pagliuso, PG: T2-D2, T2-D3  
Paliwal, A: MP1  
Palosz, B: WP43  
Palosz, W: WP43  
Pang, J: T3-C2  
Pantea, C: WP28  
Parikh, AN: W2-B3  
Parise, J: M2-D3  
Parizzi, AA: WP35  
Park, DG: MP32, WP56  
Park, JS: M3-C7  
Park, SY: M3-C2, M4-A4, W2-D3, W2-D4, W2-D6, MP30, TP63  
Passell, L: TP23  
Paulaitis, ME: MP1, MP2, WP50  
Paul, DMcK: M4-A5  
Pauwels, J: TP42  
Payzant, EA: TP15, WP58  
Pecharsky, AO: TP51  
Pecharsky, VK: TP51  
Peets, D: TP56  
Pencer, J: T1-B2, MP2, TP1, WP50  
Penin, N: T3-A2  
Penttila, S: T1-D4  
Peral, I: M2-D1, M2-D4, M3-B4, M4-C6, T3-B1, MP3, TP2, MP50, WP15  
Perelli-Cippo, E: MP17, WP66  
Perez-Salas, UA: WP4, WP8, WP36  
Perring, TG: M4-A2, WP59  
Persechini, A: WP7  
Peters, J: T2-C7  
Peterson, EJ: WP43  
Peterson, P: WP74  
Peterson, PF: W3-A4, WP77  
Peterson, VK: MP4  
Phair, JW: TP8  
Pheiffer, S: TP72



Piao, M: T1-A3  
Pierce, DL: WP36, WP38  
Pietropaolo, A: MP17, WP66  
Pike, TD: TP19, WP38  
Pirling, T: W2-A4  
Pittman, Jr, C: MP14  
Pivovar, AM: T2-A3  
Plakhty, VP: TP60  
Platzman, P: M3-D2, MP45, WP65  
Podlesnyak, A: TP60  
Polachowski, S: M2-C2  
Porcar, L: M4-A5, M4-D4, T1-A3, W2-B1, MP10, MP28, MP6, WP42,  
WP48  
Pozzo, DC: MP19  
Prabhakaran, D: WP59  
Prabhu, VM: **M4-D1**  
Prask, H: W2-A3  
Prask, H-J: T3-C3, MP34, WP55  
Prince, T: TP19  
Proffen, TE: M2-D1, M3-C7, MP38, W2-D3, TP11, TP15, WP18, WP33  
Prokes, K: T2-D2  
Prud'homme, RK: T1-A2, W2-B4, WP44  
Purwanto, A: TP17

## Q

Qian, J: WP28  
Qiu, X: MP38, WP15, WP70  
Qiu, Y: M4-A4, W2-D3, W2-D6, MP46, TP50, TP64, TP69

## R

Radaelli, PG: TP54  
Radulescu, A: WP44  
Raebiger, J: M2-C2  
Rajaram, R: T2-D4  
Rajewska, A: WP46  
Ramakrishnan, S: M4-D5  
Ramanujachary, KV: TP68  
Ramirez-Cuesta, AJ: M3-D5, WP11  
Ramirez-Cuesta, T: TP14  
Rangan, P: WP8  
Rappl, TJ: M2-B1, MP26  
Ratcliff II, W: M3-C2, TP54, TP63  
Rathod, CR: TP12, WP17  
Refson, K: TP54  
Regnault, LP: T3-A4, W2-D5, TP53  
Rehm, C: M2-C5, WP34, WP39  
Reich, DH: MP35, W2-D6  
Reichert, H: MP36  
Reiter, GF: M3-D2, MP45, WP65  
Ressouche, E: W2-D4  
Rhodes, N: MP17, WP66  
Rhyne, JJ: MP43, TP11, W3-A2  
Richardson, JW: T2-C2, T3-C4, WP27, WP53, WP69

Richter, D: W2-B4, WP44  
Rinckel, T: T1-D1  
Riseborough, PS: T2-D3  
Rix, JE: T2-C5, TP27  
Roberts, CB: WP78  
Roberts, J: TP9  
Robertson, JL: MP36, MP48, WP41, WP73  
Robertson, RGH: MP18  
Robinson, J: TP47  
Robinson, RA: T1-D2, TP57, TP59  
Rodriguez, E: TP11  
Rodriguez, JA: MP36  
Rodriguez, MA: WP43  
Rogan, RC: MP33  
Rogante, M: WP54  
Roh, JH: M3-B4, MP3, MP50  
Root, JH: **W2-A1**  
Rosenkranz, S: M2-C1, T3-A6  
Rosov, N: M3-B5, M4-D1, T3-B1, W2-D1  
Ross, DK: M4-C4  
Rowe, JM: **M1-B2**  
Rubatat, L: MP20  
Ruiz-Hervias, J: W2-A3  
Rusevich, L: WP25  
Rush, JJ: TP6  
Russell, TP: MP8  
Russel, WB: W2-B4  
Russina, M: T1-D4  
Russo, D: T2-A4

## **S**

Sackett, DL: TP46  
Sackmann, E: WP26  
Saibal B, : TP32  
Sakuma, T: TP17  
Saleh, TA: M3-A5, T3-C2, MP31, MP32  
Sales, BC: TP65  
Sampath, S: MP34  
Sangaa, D: WP67  
Sankowski, P: M2-A4  
Santhosh, PN: TP7  
Santodonato, LJ: W3-A6, TP27, WP29  
Santoro, A: TP19  
Sarraf, J: M4-A4  
Sarraf, JL: T2-D2, T2-D3  
Sasaki, DY: T1-B4  
Satija, S: T1-B4  
Schadler, L: WP22  
Scharfstein, G: WP38  
Scherer, G: T1-A4  
Schiffer, P: WP63  
Schlagel, DL: TP51  
Schmidt, G: MP10, MP6  
Schmidt, M: TP54

Schneibel, JH: WP53  
Schoenborn, BP: T2-A1  
Schoen, K: M4-B3  
Schoen, KP: TP35  
Schooneveld, EM: MP17, WP66  
Schreyer, A: WP26  
Schultz, AJ: T2-B6, T2-C2, W3-A9, WP39, WP74  
Schulz, JC: WP19, WP32, WP42  
Schwahn, D: WP44  
Schwartz, F: T2-A2  
Schweizer, K: M4-D5  
Scierka, S: T3-B3  
Seeger, PA: TP40  
Senesi, R: MP17, WP66  
Seong, BS: TP29  
Serum, B: WP72  
Shannon, N: T3-A4  
Shapiro, SM: M3-C6, TP23, TP53, W3-A10  
Shaw, WJ: WP4  
Sherstobitova, E: TP52  
Shim, CM: TP29  
Shin, EJ: TP29  
Shirane, G: M3-C1, M3-C3, M3-C5  
Shiryaev, SV: TP60  
Shmalo, S: TP12  
Short, S: W2-C3, WP15  
Shreve, AP: W2-B3  
Siewenie, JE: T2-C5, MP15  
Sipatov, AY: M2-A4  
Skipper, NT: MP42  
Skomorokhov, AN: WP67  
Smee, SA: WP38  
Smeibidl, P: TP55  
Smirnov, L: WP67  
Smith, GS: T1-B3, TP74, W2-B1, WP51  
Snow, WM: M4-B3, T1-D1, T1-D3, TP42  
Sokolov, AP: M3-B4, MP3, MP50  
Sokolov, D: TP58  
Sokol, PE: M4-C5, MP49  
Soles, CL: T3-B2  
Somasundaran, P: MP27  
Soriano, S: M2-A3  
Speakman, SA: TP15  
Spooner, S: WP58  
Stare, J: M3-D4  
Stassis, C: M3-A2, T1-C3, TP50, TP51  
Sternstein, SS: WP22  
Stevens, RW: TP64  
Stock, C: **M3-C1**, M3-C5, TP56  
Stoica, A: WP34, WP58  
Stoica, AD: M3-A5, T3-C4, WP53, WP69  
Stone, MB: MP35, WP63  
Streule, S: TP60  
Strobl, M: MP16, WP25  
Strzalka, J: T1-B1

Stuhr, U: TP31  
Stull, JT: WP7  
Stunault, A: M2-A3  
Sung, L: T3-B3  
Sun, JR: TP62  
Sun, Y: MP31  
Surendra S, : TP32  
Svitelskiy, O: M3-C6  
Swainson, IP: T3-A2, WP12  
Swan-Wood, TL: M3-A3, WP68

## **T**

Takata, S: T2-A3  
Tangeman, JA: T2-C5  
Tan, J: WP51  
Tao, J: WP72  
Tao, JZ: TP70  
Tardocchi, M: MP17, WP66  
Taub, H: T3-B4  
Taylor, GB: WP29  
Taylor, SS: WP5  
te Velthuis, SGE: MP43  
Teller, R: W3-A2  
Terashita, H: MP41  
Thirumalai, D: WP8  
Thiyagarajan, P: M2-B6, M4-C3, TP38, TP45, WP22, WP34, WP39, WP52  
Thomas, JJ: T2-B2  
Thompson, AK: M4-B2, MP18  
Thompson, H: MP42  
Thompson, J: W2-D3  
Thompson, JD: T2-D3  
Tian, H: T3-C4  
Tirumala, VR: M2-B6  
Tobias, DJ: W3-A1, WP21  
Toby, BH: TP19, W2-C2  
Toghiani, H: MP14  
Tokura, Y: T3-A3  
Tome, CN: W2-A2  
Tomioka, Y: T3-A3  
Toomey, RG: T1-B3  
Toperverg, B: WP26  
Torbet, J: WP6  
Torikachvili, MS: TP57  
Toulouse, J: M3-C6  
Tranquada, JM: M4-A2, W2-C4, WP59  
Treimer, W: MP16, WP25  
Trehella, J: WP5, WP7  
Trouw, FR: T2-D3, TP47, WP62, WP71  
Trull, C: MP18  
Tsao, FC: TP62  
Tulk, CA: M2-D3, TP49  
Tung, C-S: WP7  
Turnbull, MM: TP48



Turner, J: WP18  
Turner, JFC: MP15, TP49

## U

Uchinokura, K: W2-D4  
Udovic, TJ: M3-D3, TP18, TP22, TP4, TP6  
Uefuji, T: M4-A3  
Urban, VS: TP33, WP9  
Urquidi, J: TP49  
Ustundag, E: T3-C1, MP33

## V

Vaidyanathan, R: TP12, WP17  
Vajk, OP: M3-C4, MP47  
Vaknin, D: T1-C2, TP50  
Van Gestel, J: TP42  
Varkey, SP: TP2  
Verdal, N: TP16  
Viehland, D: M3-C5  
Vigil, D: WP5  
Visinoiu, A: W2-D3  
Vlachos, D: MP7  
Vogel, SC: T2-C8, T2-B5, TP9, W2-A2, WP28, WP43, WP57  
Vokhmyanin, AP: TP52  
Volin, KJ: W3-A6  
Volkman, UG: T3-B4  
Volksen, W: MP23  
Volz, H: TP9  
Von Dreele, RB: T2-C8  
Vorderwisch, P: MP35, TP55

## W

Wada, N: WP20  
Waddington, ED: T3-C6  
Wagner, NJ: M4-D3, MP28, WP42  
Wagner, W: M3-A4, W2-A4, TP31  
Wakimoto, S: M3-C1, TP55  
Walker, LM: MP19  
Walker, LM: W2-B2  
Wang, H: M2-B4, TP47, WP14  
Wang, W: M4-D4  
Wang, X: T2-B6  
Wang, X-L: M3-A5, T3-C4, W3-A5, WP53, WP69  
Wang, YD: T3-C4, WP53  
Wasse, JC: MP42  
Watkins, EB: TP47, W2-B3  
Weber, JKR: T2-C5, TP27  
Wenk, HR: T2-C8  
Werner, SA: M4-B3, TP35  
Weygand, M: MP51  
White, SH: M3-B3, W3-A1  
Wick, C: M3-B1

Wiebe, CR: T3-A2  
Wiest, JM: T1-A3  
Wietfeldt, FE: M4-B2, MP18  
Wignall, GD: M4-C2, TP33, WP47, WP9  
Wilemsk, G: T1-A1  
Wilkerson, JF: MP18  
Williams, DJ: T2-B5, T2-C8, TP9, WP28, WP43, WP57  
Willumeit, R: TP37  
Wilson, C: MP40  
Wilson, S: TP67  
Winey, KI: M2-B4, WP14  
Withers, RL: T3-A5  
Withnall, R: WP23  
Wietfeldt, FE: TP42  
Wojowicz, T: MP43  
Woodfield, BF: TP64  
Woodruff, T: TP12  
Woodson, SA: WP8  
Woodward, FM: TP48, WP63  
Woodward, PM: **T3-A1**, TP13, TP7  
Woodward, R: TP59  
Woo, H: M4-A2, WP59  
Woo, W: MP29  
Worcester, D: WP6  
Worlton, TG: W3-A4, TP70, TP71, WP72, WP74  
Wozniak, Denis: TP38  
Wrenn, C: TP30  
Wright, MC: WP58  
Wu, J: M2-B2  
Wu, W-l: M2-B5, T3-B2  
Wyslouzil, BE: **T1-A1**

## **X**

Xia, X: M2-B2  
Xu, G: M3-C5, M4-A2  
Xu, GY: M3-C3  
Xu, J: WP10  
Xu, Ting: MP8

## **Y**

Yamada, K: M4-A2, M4-A3, **M4-A6**, TP55, WP59  
Yang, B: MP30, MP31  
Yang, B-S: W2-B4  
Yang, CC: TP62  
Yang, FY: M2-A2  
Yang, L: WP69  
Yardimci, Hasan: T3-B5  
Yaron, PN: TP14  
Ye, F: T3-A3  
Ye, S: T1-B1  
Yethiraj, M: M4-A5, TP65, WP73  
Yildirim, T: M3-D3  
Yim, H: T1-B4

Yodh, AG: WP14  
Yong, G: M3-C6  
Yoonessi, Mitra: MP14  
Youngman, R: T2-C2  
Yu, DH: TP59  
Yue, B: MP21  
Yun, Seok-II: MP24  
Yun, SI: WP47

## **Z**

Zaliznyak, IA: MP35, **W2-C4**, TP23, W3-A10  
Zandbergen, HW: W2-C2  
Zanotti, J-M: M4-C3  
Zarestky, JL: M3-A2, T1-C2, T1-C3, TP50, TP51  
Zhang, J: T1-A4, WP28  
Zhang, R: MP27  
Zhang, Y: TP64  
Zhang, Z: W2-D3  
Zhao, JK: TP37  
Zhao, Y: M2-D5, WP28  
Zheludev, A: W2-D4, W2-D5, TP53  
Zhong, Z: M3-C5  
Zhou, J: T2-A2, MP11  
Zhou, Q: MP27  
Zhou, W: M2-B4, WP14  
Zhu, AJ: WP22  
Zhu, F: M2-A2  
Zoto, I: WP41  
Zukoski, C: M4-D5

# METAL TECHNOLOGY, INC.

173 Queen Ave. SE • Albany, OR 97322 USA

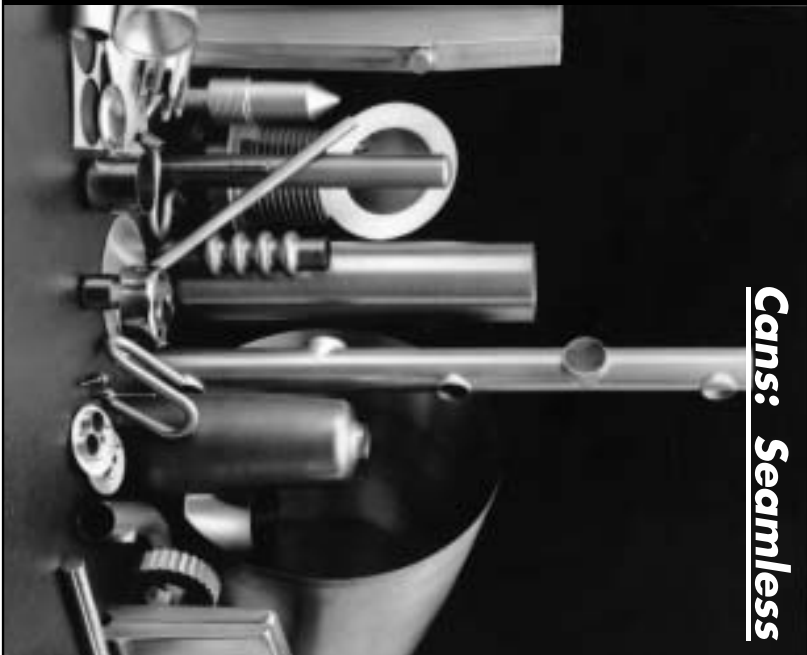
Phone: (800) 394-9979 • Fax: (541) 928-0596

E-mail: [sales@mtialbany.com](mailto:sales@mtialbany.com)

URL: [www.mtialbany.com](http://www.mtialbany.com)

## METAL TECHNOLOGY, INC.

- *Parts manufacturer* specializing in Tantalum, Vanadium, Columbium (Niobium), Molybdenum, Titanium, Zirconium & their alloys.
- *Cost-cutting techniques:* deep draw (ratios 20:1 & up), CNC precision turning & milling, spinning, stamping, forging, tube bending, fabrication & welding.
- *State-of-the-art machinery* to manufacture to your specs, including: acid-resistant vessels & liners; tubing (wall thicknesses: .005–.25", lengths to 3' & diameters to 16"); nozzles; cones; missile parts; valves; high-temp manifolds; fasteners; & expansion joints.
- *Meets Mil-I-45208 & Mil-Q-9858.*
- *30-years experience with reactive metals.*



Cans: Seamless

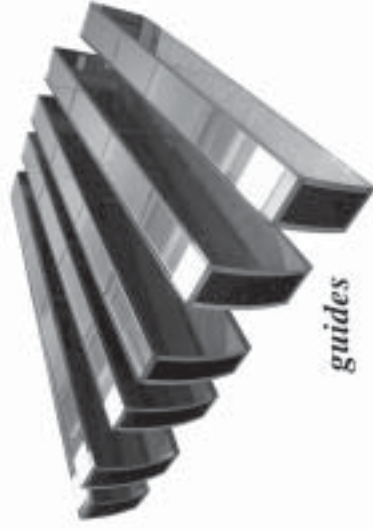


---

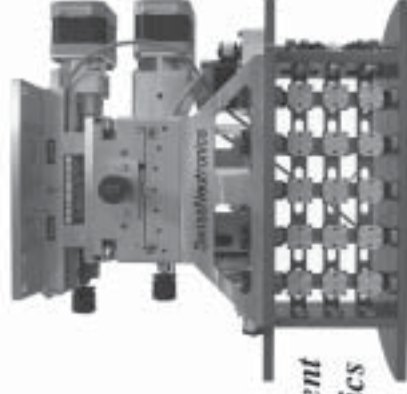
# SwissNeutronics

Neutron Optical Components  
& Instruments

Brühlstrasse 28, CH-5313 Klingnau, Switzerland  
phone: +41 56 245 0202, fax: +41 56 245 0204  
tech@swissneutronics.ch, www.swissneutronics.ch



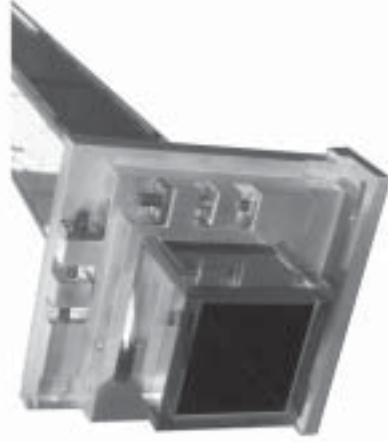
*guides*



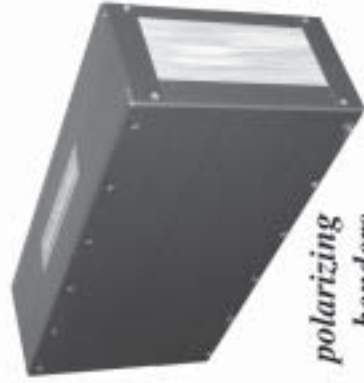
*instrument  
mechanics*

*from ideas...*

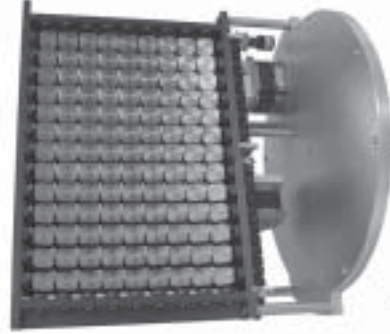
*...to solutions*



*focussing guides*



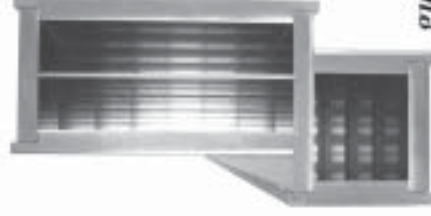
*polarizing  
benders*



*monochromators/analyzers*



*monochromator  
shields*



*guide  
switches*

---



[Neutronguide.com](http://Neutronguide.com)

Neutronguides, Supermirrors,  
Vacuum Systems, Special  
Devices

# NTK

**Neutronentechnische Komponenten GmbH**

Since more than two decades NTK has produced a wide variety of guides and neutron reflecting structures. NTK guides are installed at many neutron sources around the world. We have made any type of guide necessary between a neutron source and an experiment:

- Straight guides for thermal neutrons
- Curved guides for cold neutrons
- Single channel guides
- Multi-channel guides for a short length of direct sight
- Beam benders
- Conical guides for focussing neutrons
- Beam splitters and deviators
- Vacuum-tight guides
- Guides in vacuum housings
- A „twisted“ guide for a reflectometer at FRM-II

Our guides are made from borated float glass and coated with natural nickel, Ni-58 or with super-mirror. The geometrical precision is  $1 - 2/100$  mm, the angular deviations from the ideal surface less than  $1 - 2 \times 10^{-4}$  radian.

Please contact us

NTK  
Neutronentechnische Komponenten GmbH  
Oststraße 5  
D - 86825 Bad Wörishofen  
Germany  
Tel. 0049-8247-31335  
Fax 0049-8247-9636950



**TOOLS FOR DISCOVERY**

**wiener**

Plein & Baus Elektronik

Werk 52

Industrie-  
elektronik

Nach-  
marken

Regelung  
SICOM

**CAEN**  
**wiener**



**Crates**

- VME
- NIM
- CAMAC
- VXI



**LV Power Supplies**

- Modular
- Floating



**Controllers**

- PCI to CAMAC
- PCI to VME
- VME to CAMAC interface



**Backplanes**

- Standard
- Custom

**CAEN & WIENER**

Several years of partnership  
at your service

**WIENER, Plein & Baus, Ltd.**

300 E. Auburn Ave., Springfield, OH 45505

937-324-2420 / [www.wiener-us.com](http://www.wiener-us.com)





**International Conference on Neutron Scattering ICNS2005  
NEUTRONS FOR STRUCTURE AND DYNAMICS—A NEW ERA**



**International Advisory Committee**

Gabriel Aeppli	UK
Fabrizio Barrochi	Italy
Alexander Beloshkin	Russia
Mark Daymond	UK
GR Desiraju	India
Yasuhiko Fuji	Japan
Albert Furrer	Switzerland
Jose C Gomez-Sal	Spain
J Rolando Gonzalez	Argentina
Julia Higgins	UK
Tom Holden	Canada
Jim Jorgensen	USA
Kazu Kakurai	Japan
Don Kearley	Netherlands
Gerry Lander	Germany
Chang-Hee Lee	Korea
Wen-Hsien Li	Taiwan
Thom Mason	USA
Joel Mesot	Switzerland
Dan Neumann	USA
John Parise	USA
Winfried Petry	Germany
Adrian Rennie	Sweden
Dieter Richter	Germany
Vladimir Sachdevsky	Czech Republic
Andrzej Szylka	Poland
Peter Timmins	France
Jill Trethewe	USA
Andrew Venter	South Africa
Christas Vetter	France
Chick Wilson	UK

**Sydney Convention & Exhibition Centre**  
Sydney | Australia | 27 November – 2 December 2005

**[www.icns2005.org](http://www.icns2005.org)**

[icns2005@ausconvservices.com.au](mailto:icns2005@ausconvservices.com.au)

**Call for Papers Available – December 2004**

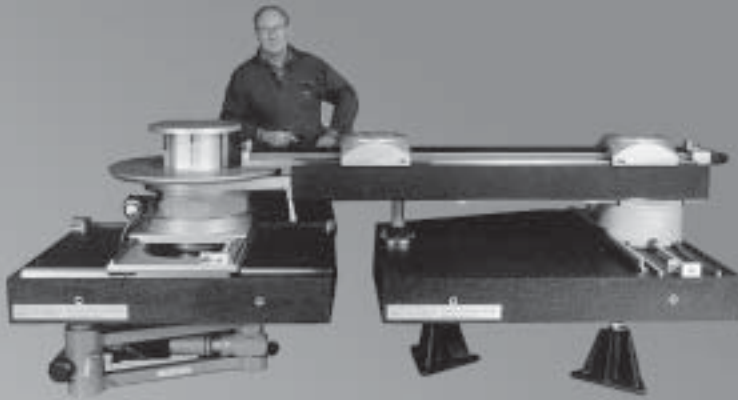
**Topics to be covered include:**

- 1.** Condensed Matter Physics
- 2.** Condensed Matter Chemistry
- 3.** Structure (including glasses and liquids); Dynamics
- 4.** Magnetism
- 5.** Materials Science
- 6.** Soft Condensed Matter
- 7.** Life and Biological Sciences
- 8.** Industrial and Medical Applications
- 9.** Earth Sciences
- 10.** Advanced Neutron Sources
- 11.** Neutron Instrumentation and Techniques

**Organising Committee**

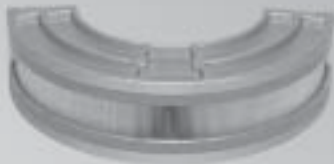
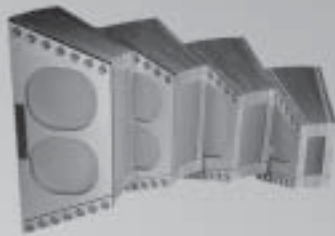
**Chair:** Brendan Kennedy, University of Sydney | **Secretary:** Rob Robinson, Bragg Institute  
**Treasurer:** Walter Kalceff, University of Technology Sydney | **Programme Committee Chair:** Evan Gray, Griffith University  
**Publications Committee Chair:** Stewart Campbell, UNSW@ADFA  
**Committee Member:** Dennis Mather, Australian Institute of Nuclear Science and Engineering

**[www.icns2005.org](http://www.icns2005.org)**

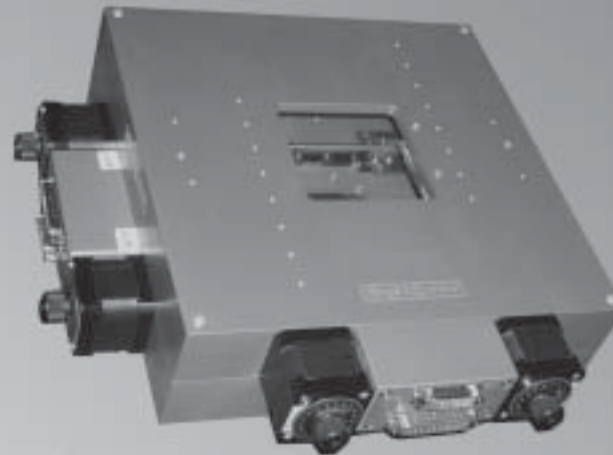


Custom  
Design

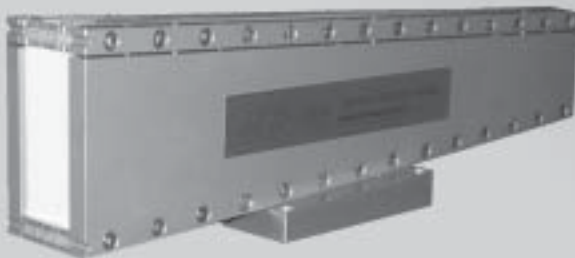
# Instrumentation for Neutrons



**Collimators**



**Precision  
Slits**



For more info:

[info@jjxray.dk](mailto:info@jjxray.dk)

+45 4776 3003

***JJ X-Ray***  
*Danish Science Design*

[www.jjxray.dk](http://www.jjxray.dk)

# Neutron Scattering Guide Systems & Instrumentation

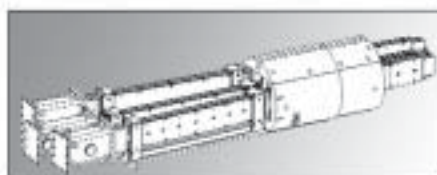
## MIRROTRON LTD

Partners in Neutron Science

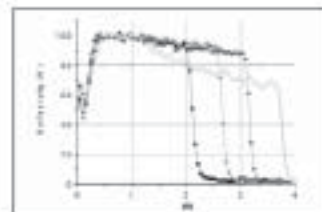
# Kurt J. Lesker Company



Custom Housing & Shutter Manufacturing



Neutron Guide Design/Modeling



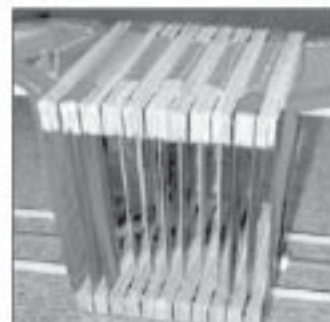
Excellent Supermirror Reflectivities  
100% Parts QC on Reactor



Multi-Blade & Multi-Disc  
Neutron Velocity Selectors



Single & Multi-Disc Choppers  
High Reliability Mag-Lev Bearings



Neutron Spin Flippers  
& Various H<sup>2</sup>-2D Detectors

Gary Smith: USA  
1.800.245.1656  
412.233.4200  
neutron@lesker.com

Gyorgy Kaszas: Hungary  
kaszas@ns.kfkipark.hu

# SERVING RESEARCH

Conception

Design

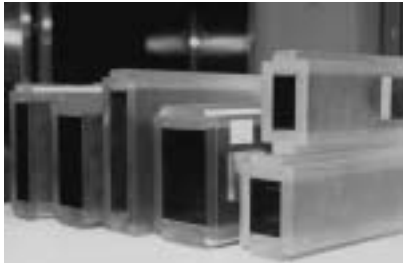
Manufacturing

Installation

## CILAS neutron guides systems:

- all shape of neutron guides
- coatings from  $m=1$  up to  $m=4$
- neutron guides substrate adapted for very high neutron flux
- adapted mechanic for long term stability

## long term stability neutron guides



## GMI spectrometers program:

- neutron optical components (diaphragm, monochromator)
- adjusting and positioning devices (goniometer, translation, rotation)
- complete instruments (reflectometers, triple axes, HRPD, ...)
- engineering (new design, improvement)

## powerfull tools for your research



## References:

ILL, LLB, NIST, HFIR, SNS, BNL, LANL, PSI, KFA, HMI, HANARO, KAERY,  
DEMOKRITOS, ESRF, ...

CILAS - Compagnie Industrielle des Lasers - 8, Avenue Buffon -BP6319- 45063 ORLEANS - FRANCE

Tél.: +33 2 38 64 59 12

Fax : +33 2 38 64 59 07

[nguide@cilas.com](mailto:nguide@cilas.com)



## Radial cavity – the cost efficient 2D analysis

- ▶ Proven technology, improved design
- ▶ needs less supermirror coating than benders
- ▶ keeps the original flight path
- ▶ divergence larger than  $5^\circ$

## Polarize and collimate within a few cm!

- ▶ solid state technique
- ▶ bender: for polarization and analysis  
use deflected or transmitted beam
- ▶ collimator: absorbing or reflecting + absorbing walls  
collimations down to  $0.8^\circ$

High quality products from the spin off company  
of the Hahn-Meitner-Institut Berlin

nob neutron optics berlin GmbH,  
Krumme Str. 64, 10627 Berlin, Germany  
Tel: +49-30-3101 7962, Fax: +49-30-3101 7963  
email: [info@neutronopticsberlin.com](mailto:info@neutronopticsberlin.com)





